# Méthodes cinétiques atomistiques

Normand Mousseau

Professeur de physique
Université de Montréal

Directeur de l'Institut de l'énergie Trottier
Polytechnique Montréal

Îstres, Juillet 2019

## In collaboration with

Gerard Barkema (Utrecht)
Eduardo Machado-Charry (CEA)

Laurent Karim Béland (UdeM)
Peter Brommer (UdeM)
Fedwa El-Mellouhi (Qatar)
Simon Gelin (UdeM)
Jean-François Joly (UdeM)

Charlotte Becquart (Lille)
Christophe Domain (EDF)
Romain Candela (Lille)
Anne Hémeryck (Toulouse)

Cosmin Marinica (CÉA)
Pascal Pochet (CÉA)

Laurent Lewis (UdeM)
Sami Mahmoud (UdeM)
Gawonou T'Souaglo (UdeM)
Oscar Restrepo (UdeM)
Michaël Trochet (UdeM)

Nicolas Salles (Toulouse)
Antoine Jay (Toulouse)
Nicolas Richard (CEA)

# With the support of

Natural Science and Engineering Research Council of Canada (NSERC)
Fonds de recherche du Québec - Nature et technologies
Canada Research Chair Foundation
Canadian Foundation for Innovation

Computer Time : Calcul Québec / Compute Canada

YAHOO! Travel

N Quebec

NUNAVUT

Salluit

Kangiqsujuaq

Hudson Bay

Inukjuak

Kuujjuaq

Kuujjuarapik

Chisasibi

QUEBEC

Eastmain

Waskaganish

Matagami

Rouyn-Noranda

Dolbeau

Jonquière

Chicoutimi

Baie-St.-Paul

Québec

Cap-de-la-Madeleine

Trois-Rivières

Laval

Montreal

Ottawa

ONTARIO

U.S.

80°

70°

60°

55°

50°

45°


NEWFOUNDLAND

Atlantic Ocean

Mutton Bay

St. Johns

NEW BRUNSWICK

P.E.I.

Fredericton

NOVA SCOTIA

0 100 200 mi

0 100 200 km

INSTITUT
DE L'ÉNERGIE
**TROTTIER**

Foundation familiale
**Trottier**
Family Foundation

## Mission:

La formation d'une nouvelle génération d'ingénieurs, de scientifiques et d'innovateurs ayant une compréhension systémique et transdisciplinaire des enjeux énergétiques;

La recherche de solutions durables qui permettront d'assurer l'avenir énergétique, en appuyant la génération de connaissances et l'innovation dans le domaine énergétique afin d'aider à relever les défis auxquels la société fera face au cours des prochaines décennies;

La diffusion des connaissances liées à l'énergie pour ainsi contribuer à hausser le niveau des débats sociaux sur les questions énergétiques.


NORMAND MOUSSEAU
AU BOUT DU
pétrole
TOUT CE QUE VOUS DEVEZ SAVOIR
SUR LA CRISE ÉNERGÉTIQUE
MULTIMONDES


NORMAND MOUSSEAU
L'AVENIR DU QUÉBEC PASSE PAR
l'indépendance
énergétique
ÉDITIONS
MULTIMONDES


Normand Mousseau
LA RÉVOLUTION DES
Gaz de
schiste
ÉDITIONS
MULTIMONDES

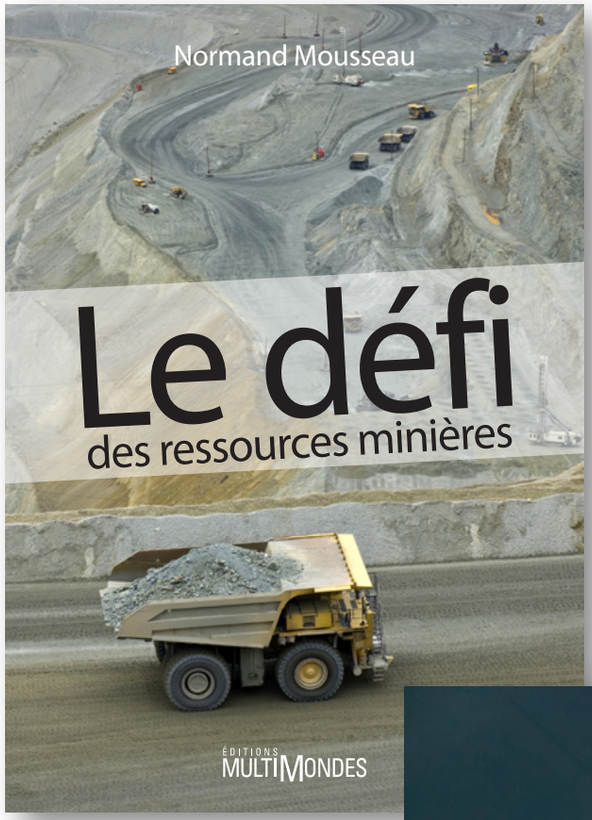
Normand Mousseau
Le défi
des ressources minières
ÉDITIONS
MULTIMONDES

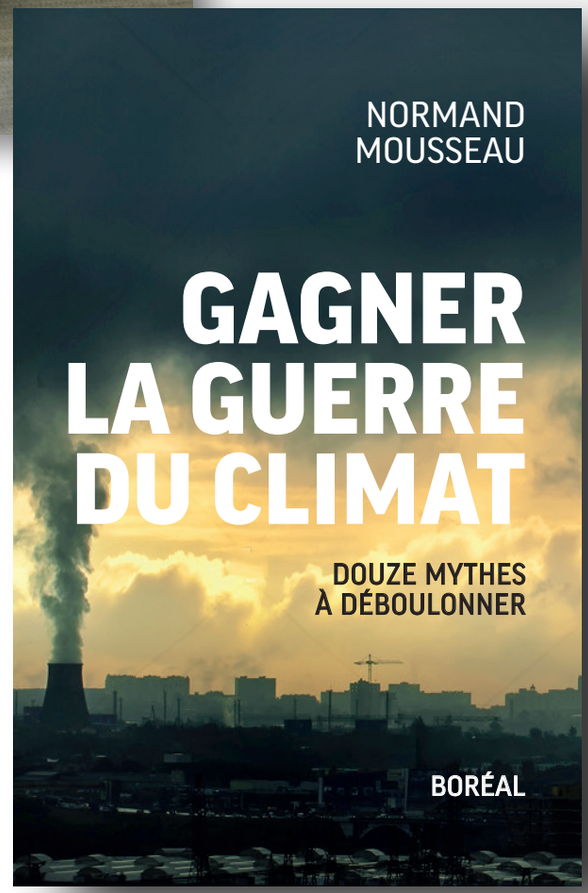
NORMAND
MOUSSEAU
GAGNER
LA GUERRE
DU CLIMAT
DOUZE MYTHES
À DÉBOULONNER
BORÉAL

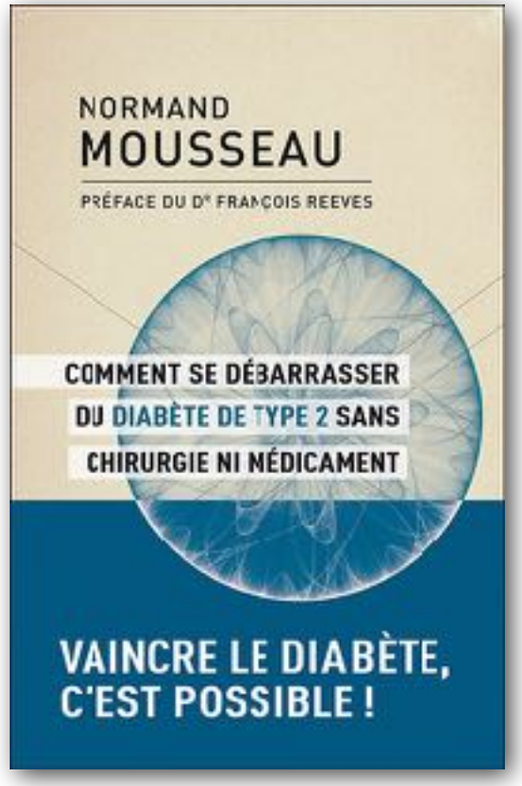
NORMAND
MOUSSEAU
PRÉFACE DU Dr FRANÇOIS REEVES
COMMENT SE DÉBARRASSER
DU DIABÈTE DE TYPE 2 SANS
CHIRURGIE NI MÉDICAMENT
VAINCRE LE DIABÈTE,
C'EST POSSIBLE !

Commission sur les enjeux énergétiques du Québec

# MAÎTRISER NOTRE AVENIR ÉNERGÉTIQUE

Pour le bénéfice économique, environnemental et social de tous

Roger Lanoue
Normand Mousseau

Coprésidents

# LE CLIMAT L'ÉTAT ET NOUS

Repenser l'action publique en environnement

The Transition Accelerator

L'Accélérateur de transition

# METTRE LE CANADA SUR LA VOIE D'UN AVENIR À FAIBLES ÉMISSIONS DE CARBONE

## Concevoir et mettre en œuvre des trajectoires de transition


Carleton University

CRC IN GOVERNANCE FOR SUSTAINABLE DEVELOPMENT

James Meadowcroft, PhD.
Professor and Canada Research Chair in Governance for Sustainable Development,
Department of Political Science & School of Public Policy and Administration,
Carleton University, Ottawa, ON

University of Calgary
CESAR Canadian Energy Systems Analysis Research

David B. Layzell, PhD, FRSC.
Professor and Director, Canadian Energy Systems Analysis Research (CESAR) Initiative,
Department of Biological Sciences,
University of Calgary, Calgary, AB

Université de Montréal
IET Institut de l'énergie Trottier

Normand Mousseau
Professeur, Université de Montréal
Directeur académique,
Institut de l'énergie Trottier
Polytechnique Montréal

# How does ciment microstructure evolve?

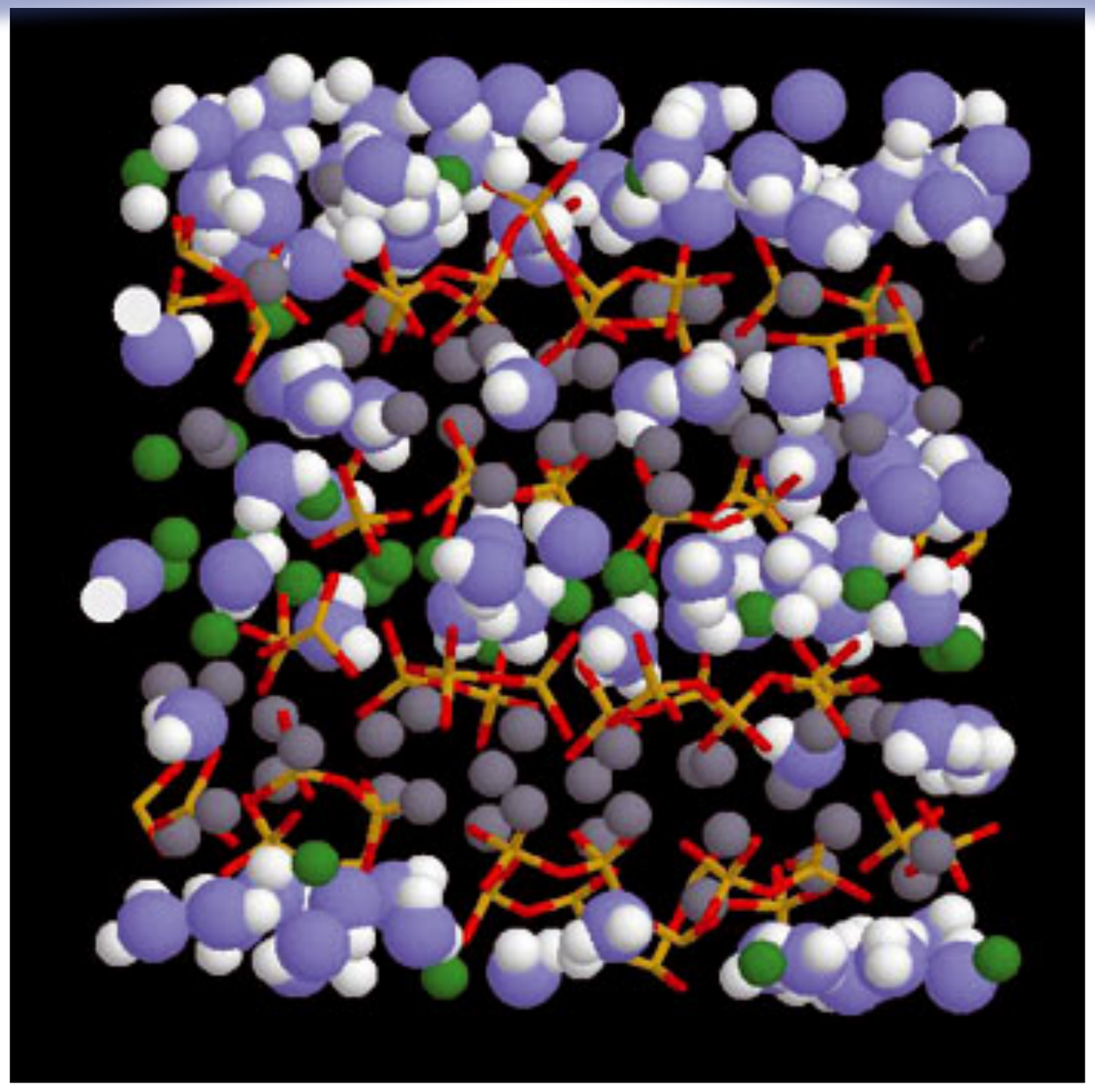

R. Pellenq

# What is the microscopic origin of metal dusting?

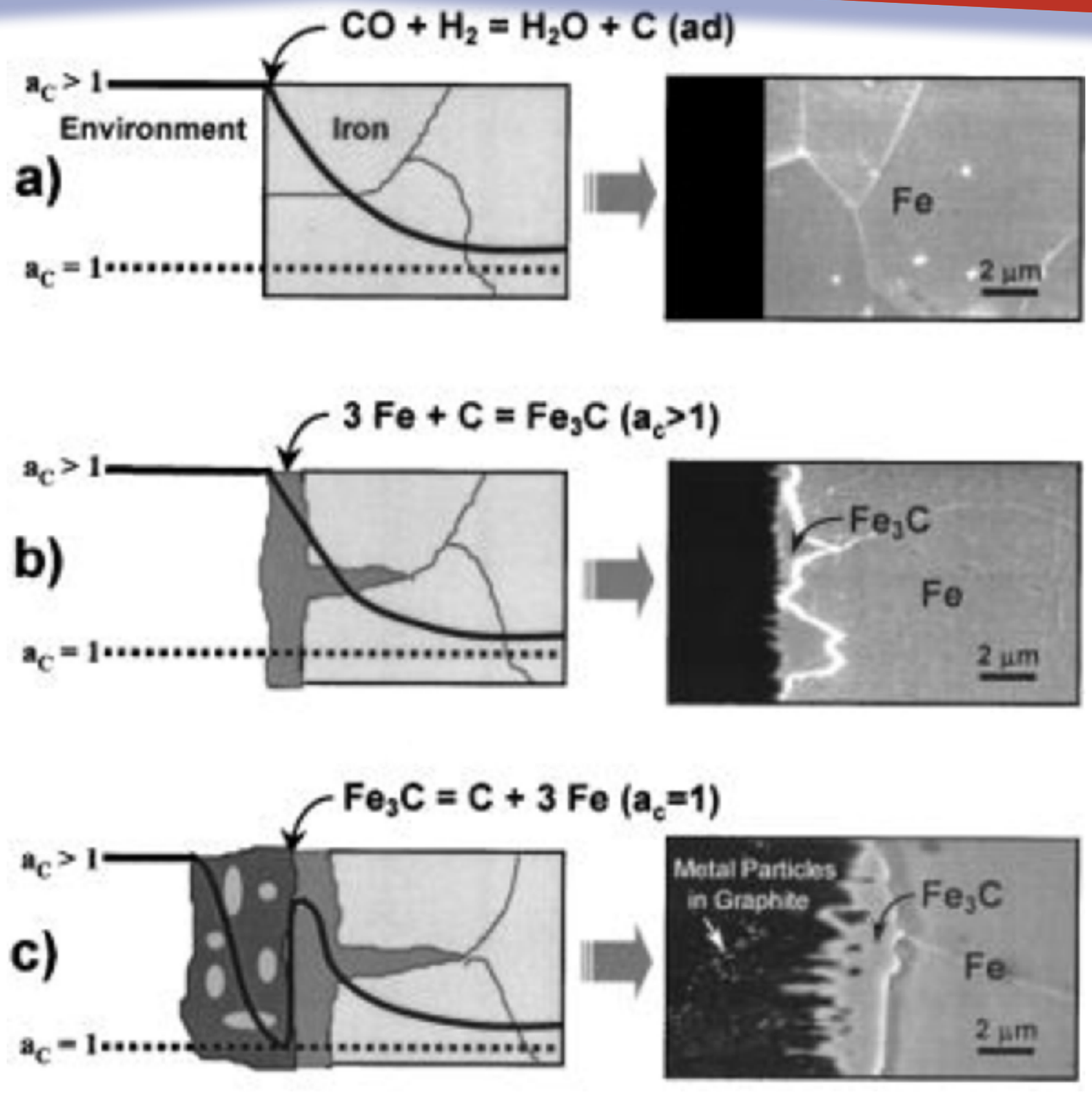


Chun *et al.*, J. Electrochem. Soc. (2002)

# kinetics of point defects

Accumulation of point defects and their complexes in irradiated metals as studied by the use of positron annihilation spectroscopy

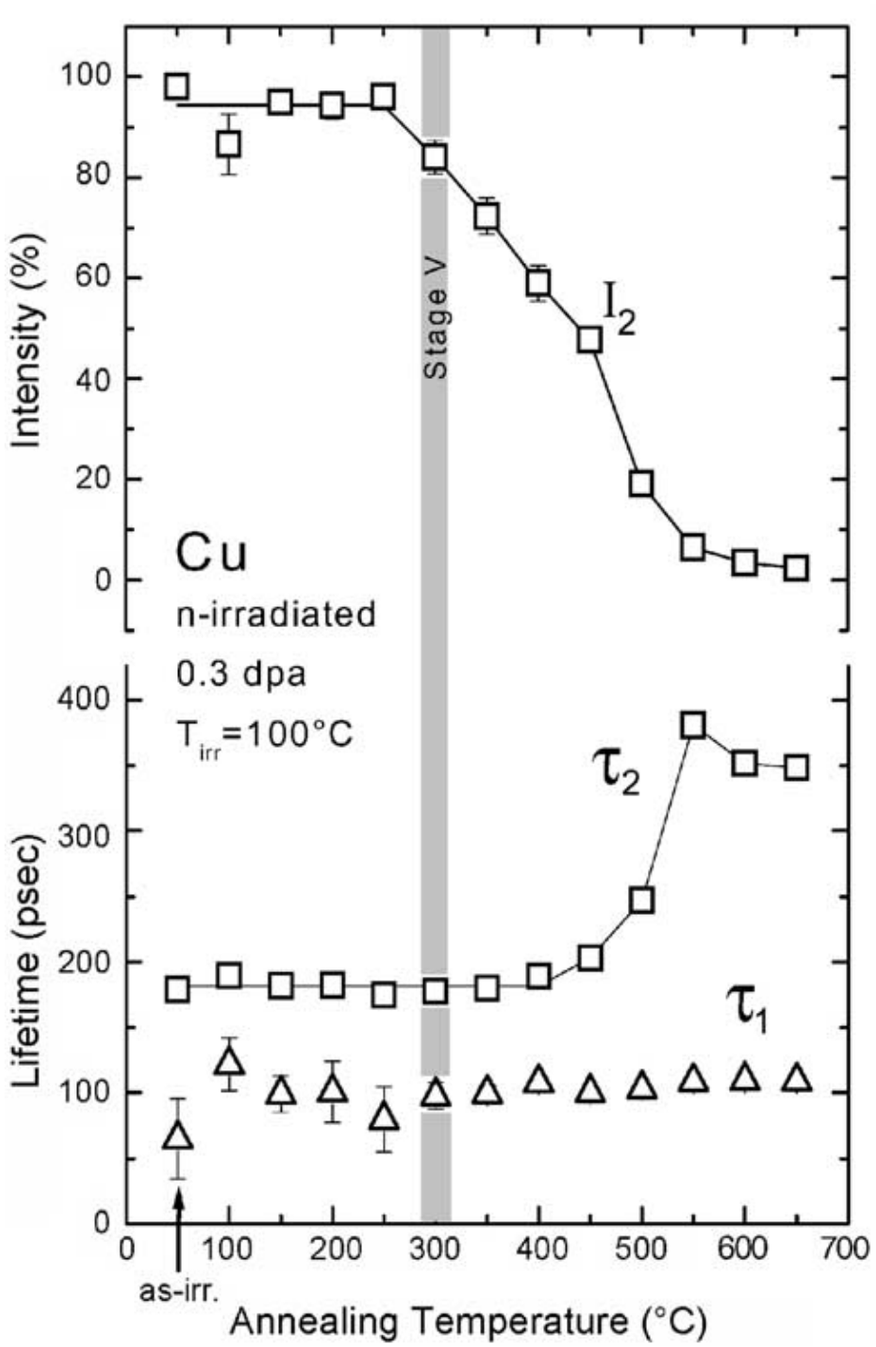


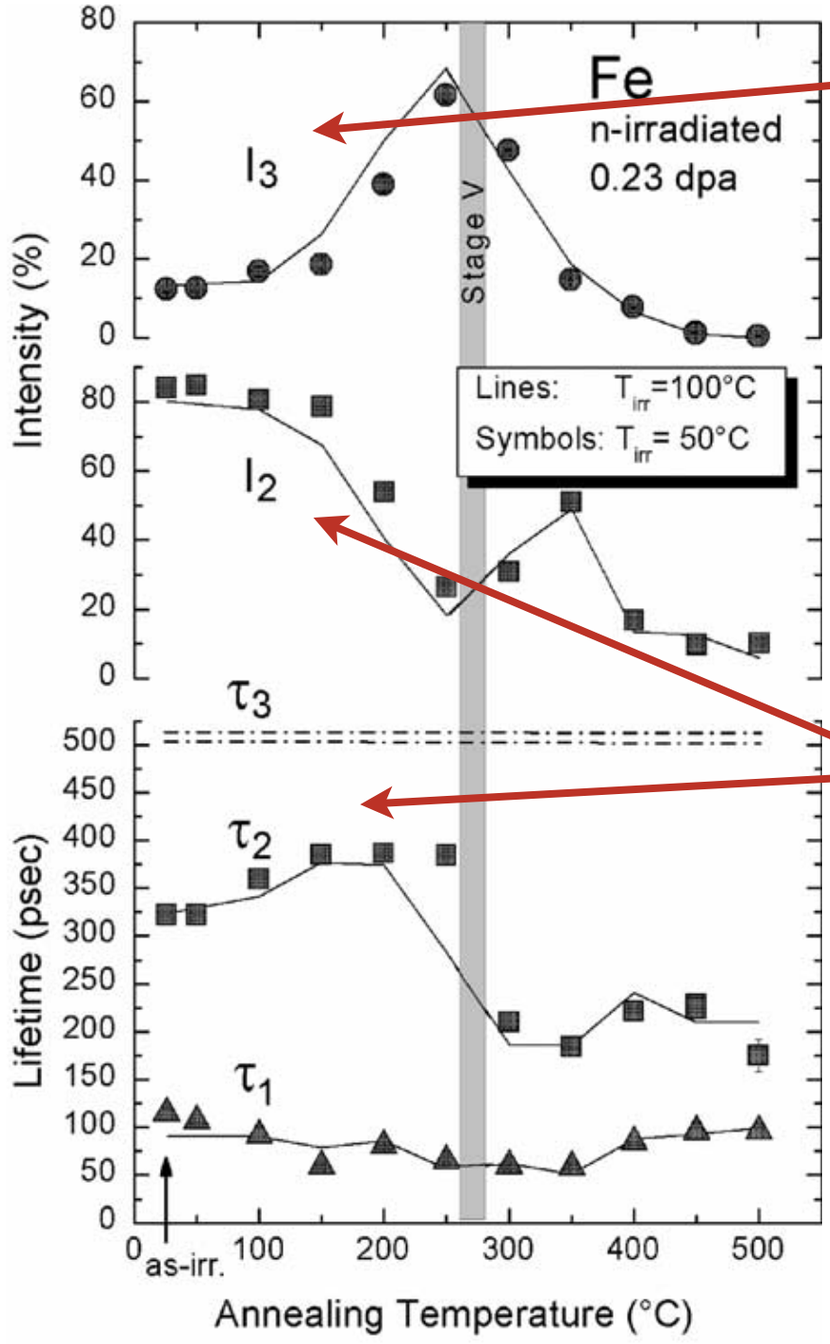


40-50 vacancies

9-14 vacancies

M. Eldrup and B.N. Singh, Journal of Nuclear Materials **323** (2003) 346–353.

# Growth of nanostructures

Growth of Ge on Si leading to the formation of pyramids through Asaro-Tiller-Grinfeld instability.

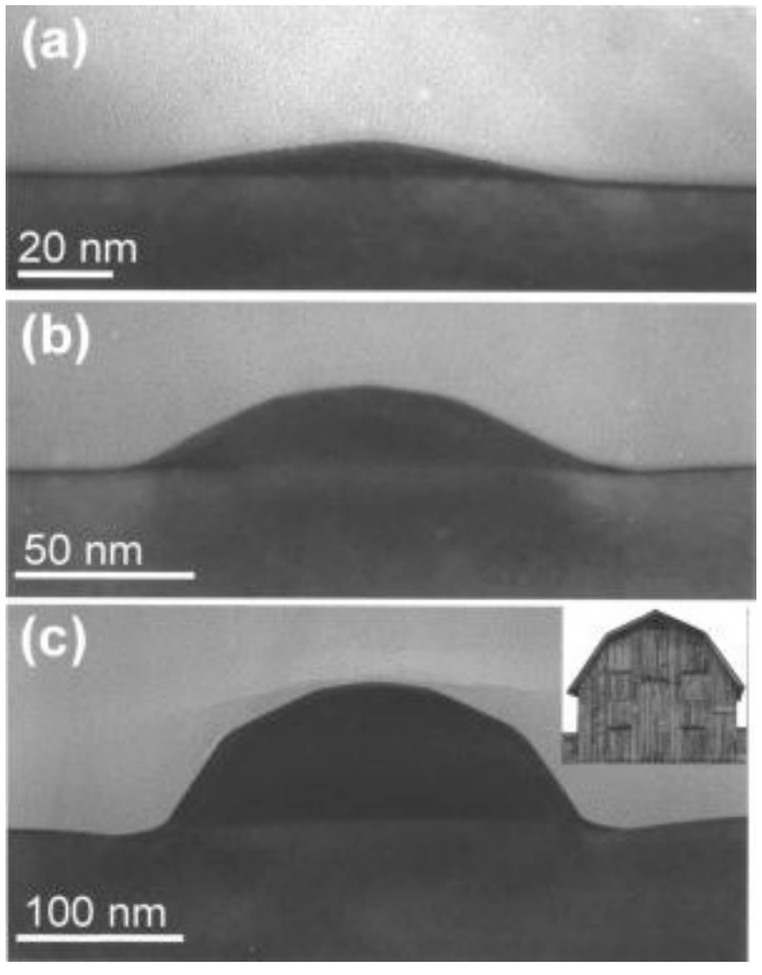


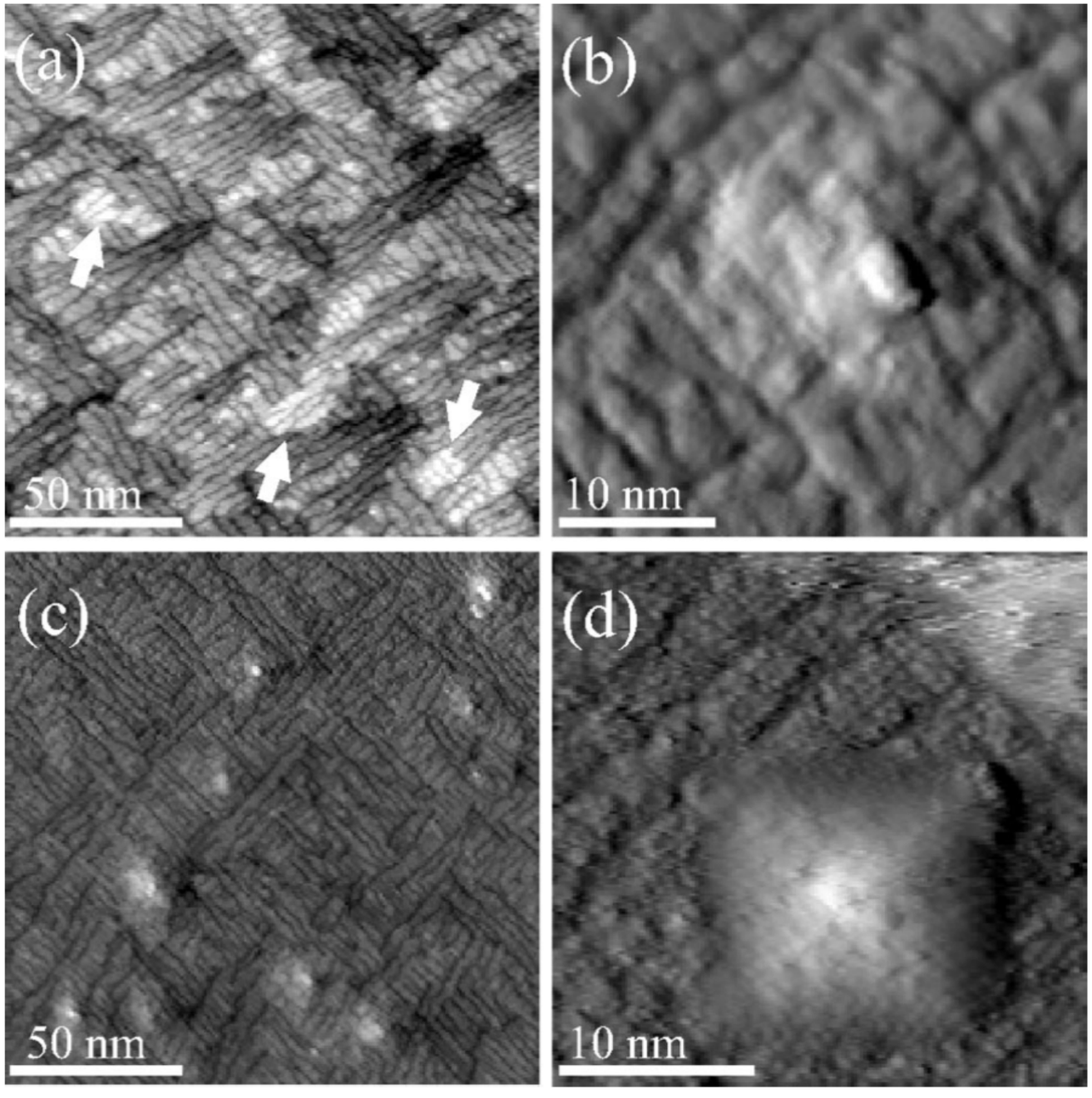


A. Vailionis, B. Cho, G. Glass, P. Desjardins, D. G. Cahill, and J. E. Greene, Phys. Rev. Lett. 85, 3672 (2000).

# Kinetics of disordered systems

How do glasses relax at low T?

What are the defects?

What is the impact of impurities (e.g.: H in Si)

How do we understand the Si/$SiO_2$ interface?

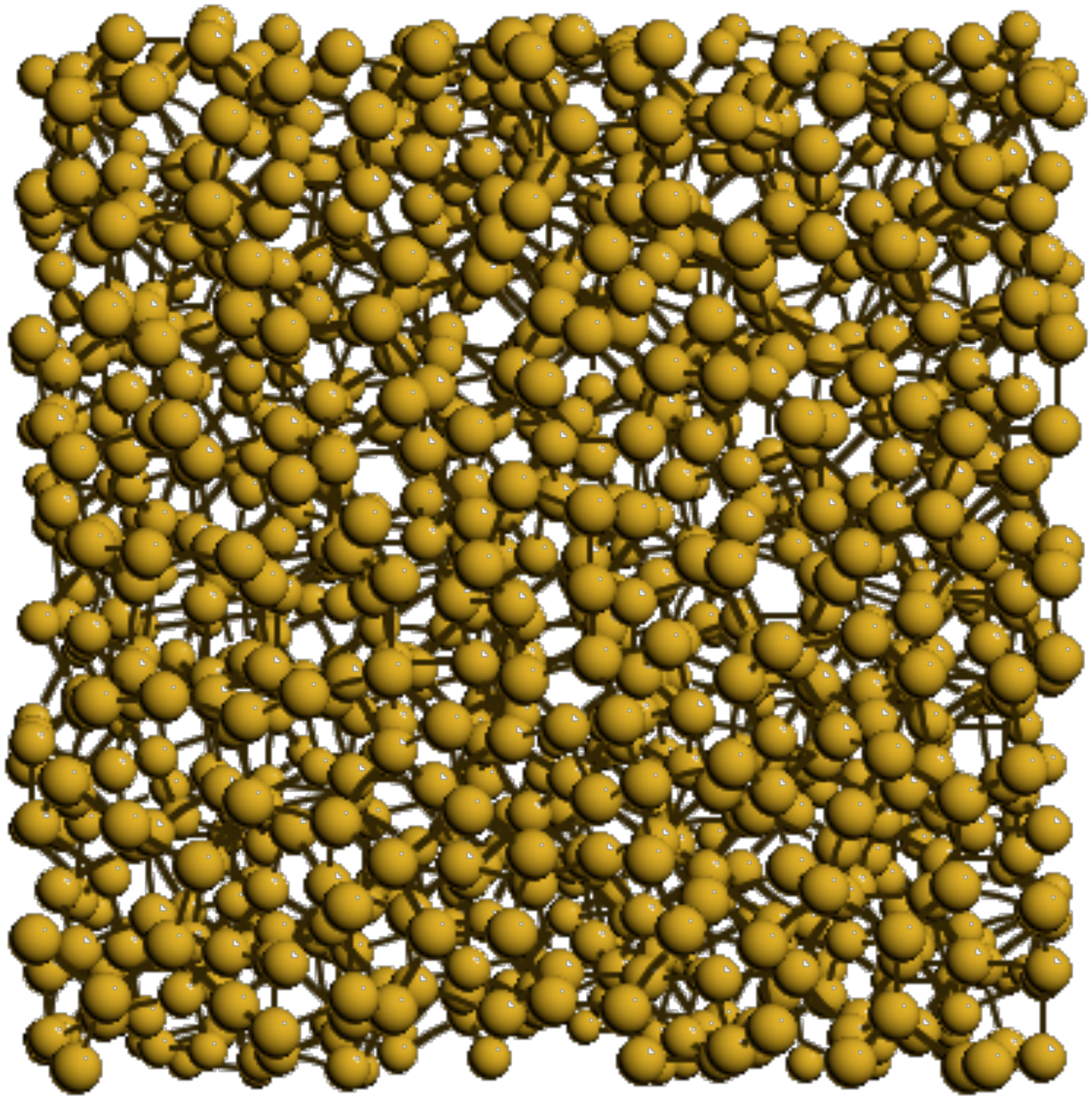

# Outline

**1.** The challenge of simulating over multiple time scales. Energy landscapes. The transition state theory. Brief overview of various methods for breaching these time scales.

**2.** Basic concepts. Searching for saddle points. Sampling the energy landscape : the activation-relaxation technique (ART nouveau)

**3.** Accelerated MD approaches. Basic concepts kinetic Monte Carlo. Limits.

**4.** Off-lattice kinetic Monte Carlo methods. The kinetic Activation-Relaxation Technique. Topological analysis. Constructing an event catalog. Handling flickers. Limitations of current accelerated methods. Extending to large systems. Coming developments.

# The challenges

- Thermodynamics
- Kinetics

# Thermodynamics

We need to sample correctly the phase space

- access all relevant points in phase space
- establish their relative probability or, better, their absolute probability

# Kinetics

We need to establish the dynamical evolution of the system

- focus on out-of-equilibrium property
- describe accurately the dynamical relation between points in phase space

# The challenges

**Equilibrium/Quasi-equilibrium systems**

- Defects
- Polymers
- Multiphase materials

Difficult to identify the states, to establish their relative weight

**Out-of-equilibrium processes**

- Growth processes
- Self-Assembly
- Chemical reactions
- Glasses

What is the right initial point? How to find the pathways? How to access the right time scale?

# Energy landscapes

Atoms vibrate at $10^{12}$ Hz

The evolution can occur on any scale

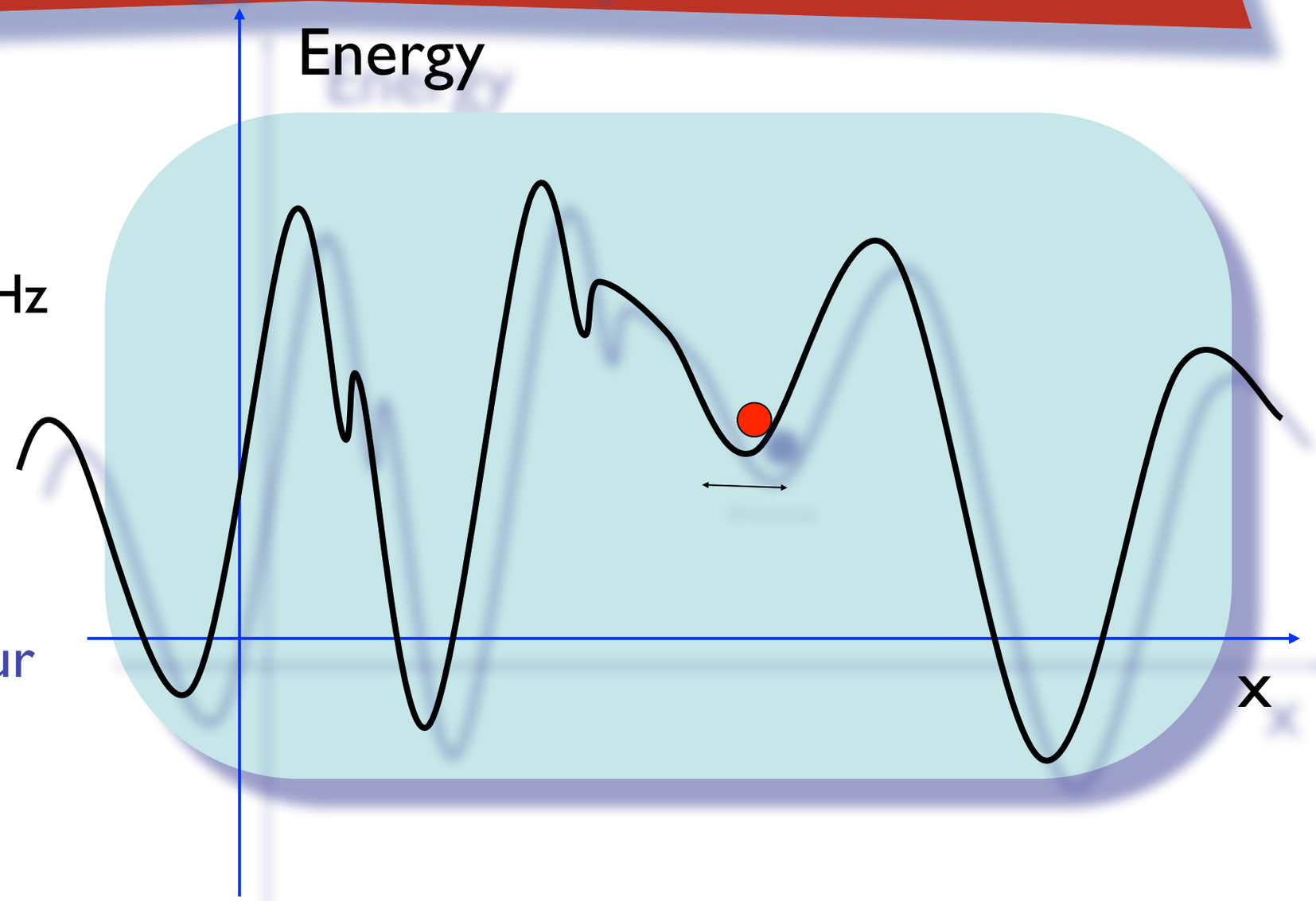


Generic problem:

How to explore the space of variables of a high dimensional cost function?

# Sampling states : discrete systems

In case of discrete systems, it can be easy to identify basic mechanisms:

| | | |
|---|---|---|
| Spin networks | $\Rightarrow$ | Spin flip |
| Adatom at surface | $\Rightarrow$ | Atomic jump (too simple, but we will get back to it) |

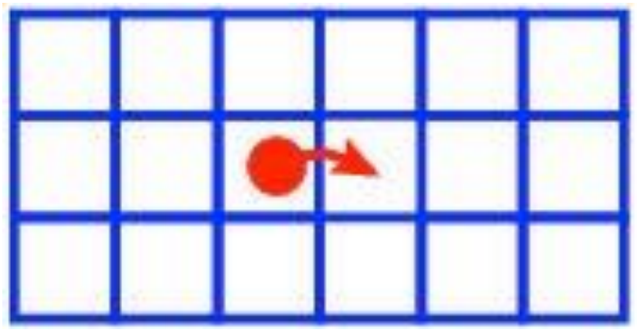

Once barriers are known, it is possible to accelerate the dynamics

| | | |
|---|---|---|
| Swendsen and Wang | $\Rightarrow$ | Flip of spin clusters |
| Voter, Barkema *et al.* | $\Rightarrow$ | Rare event dynamics |

Can we do the same thing for continuous systems ?

# But surfaces are not always symmetrical nor discrete

# Standard approaches (at atomic scale)

**Molecular dynamics**

**Monte Carlo**

What are they?
What are their differences/ similarities?

Ensemble?

# (Free) Energy landscapes

Let us go back to the landscape

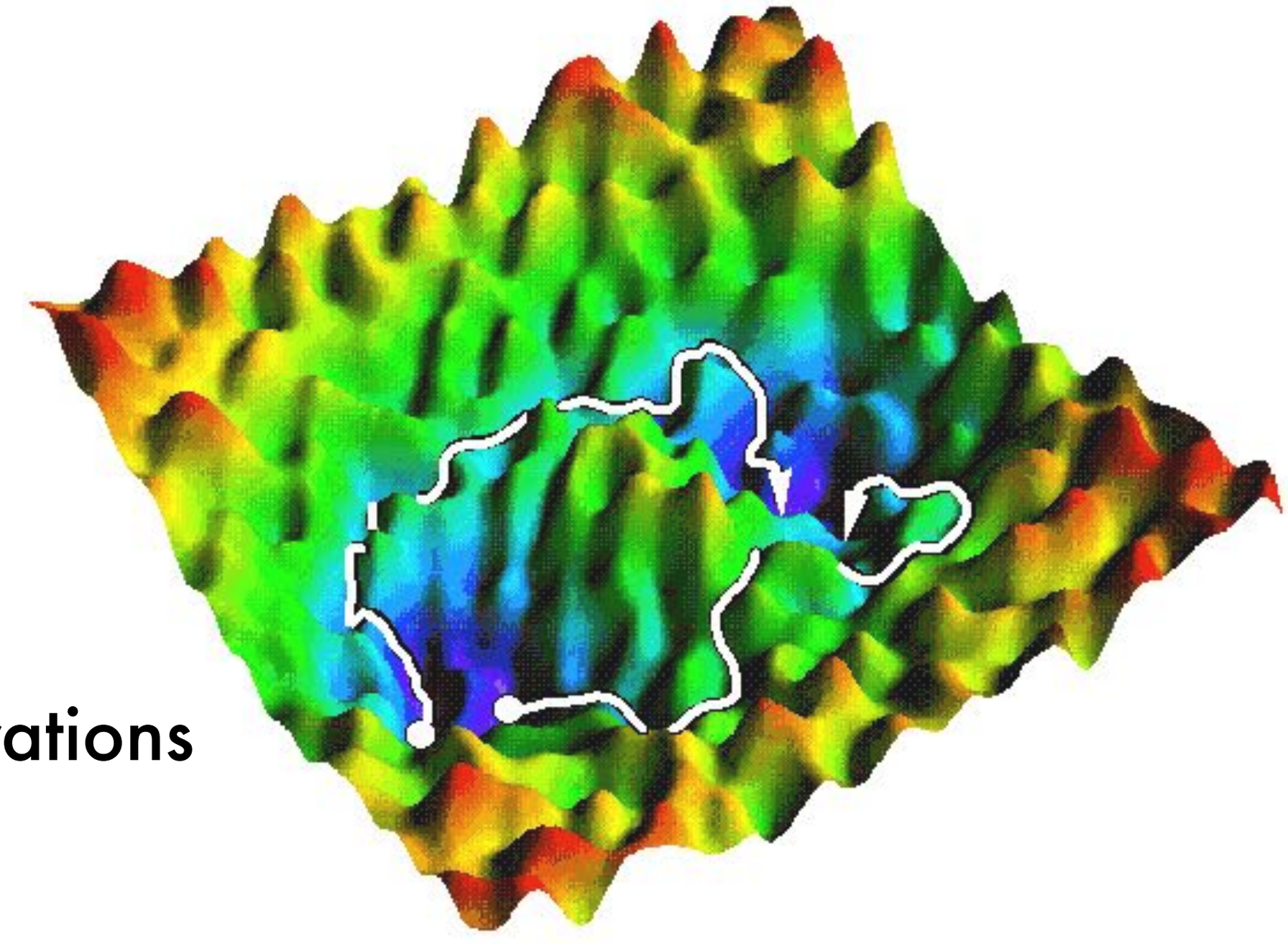

- entropy
- state
- thermal vibrations

# Transition State Theory

TST Escape rate is the equilibrium flux through the dividing surface

$\Delta W = W_{bas} - W_{sad}$

The rate is

$$k = \kappa \cdot k_{\mathrm{TST}}$$

with

$$k_{\mathrm{TST}} = \nu e^{-\Delta W / k_B T}$$

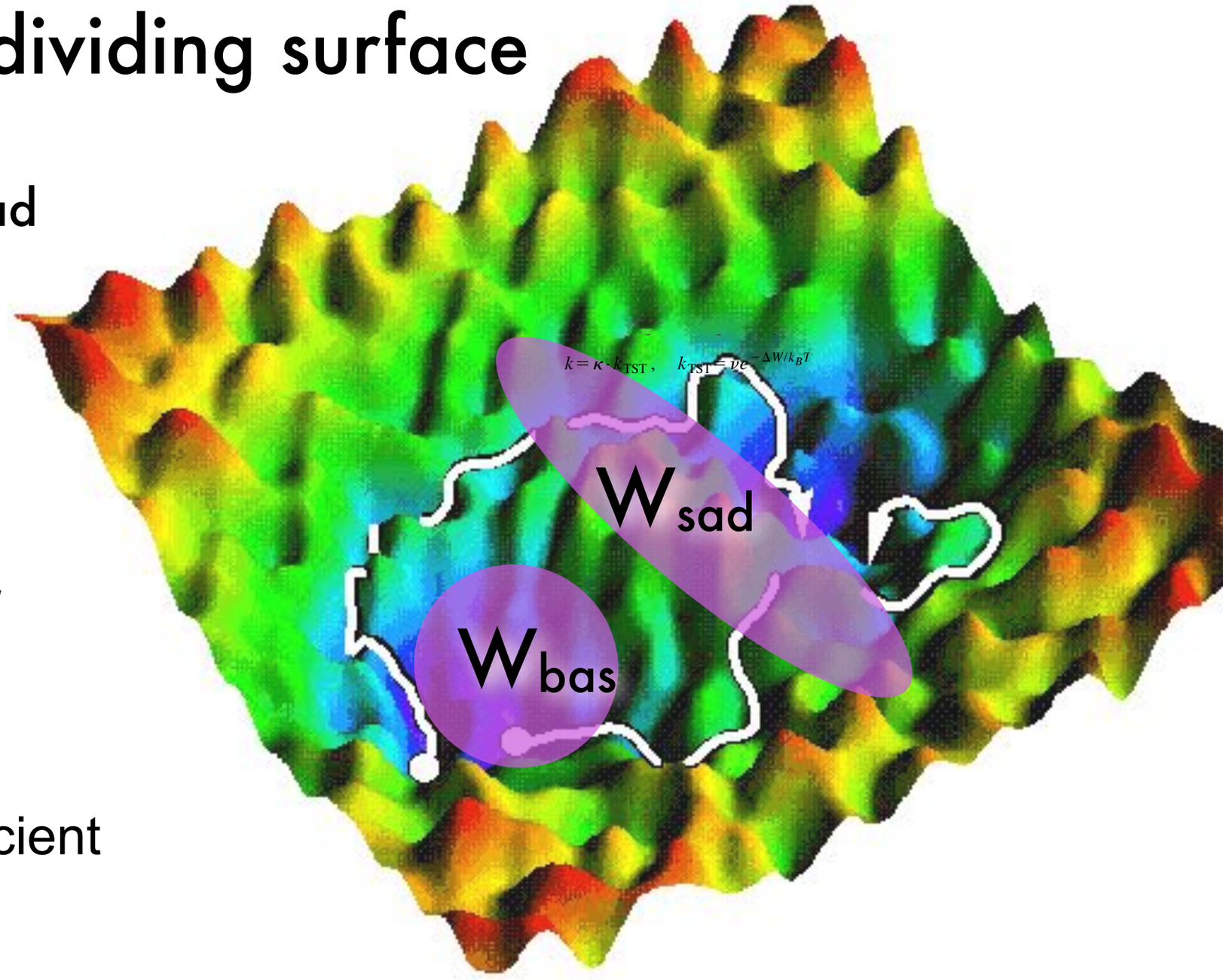


k : Crossing rate

$\kappa$ : Transmission coefficient

$\nu$ : Attempt frequency

$\Delta W$ : Activation energy

Marcelin (1915), Eyring and Wigner (1930s)

# Transition State Theory

The attempt frequency is defined as

$$\nu = \left[\frac{k_B T}{2\pi m}\right]^{1/2} \left[\int_{\text{well}} \exp\{-[W(x) - W(x_m)]/k_B T\} dx\right]^{-1}$$

Where *W(x)* is the potential of mean-force

$$W(x) = \int_{x_m}^{x} \langle f(\lambda) \rangle_{\lambda = x'} dx'$$

where the averaged over the force is taken along the reaction pathway defined by the reaction coordinate λ

# Transition State Theory

If we define

$$W(x) \simeq \alpha \frac{x^2}{2} - \beta \frac{x^3}{3}$$

with $W(x_m) = 0$ and $\Delta W = W(x_b) - W(x_m)$, we obtain

$$\nu(T) = \nu(0) \sqrt{\frac{\Delta E - T\Delta S}{\Delta E}}$$

If the barrier is simple and chosen correctly, $\kappa \approx 0.5$, we can ignore it and write the rate as :

$$\Gamma \simeq \nu e^{-\Delta W / k_B T} = \Gamma_0 e^{-\Delta E / k_B T}$$

with

$$\Gamma_0 = \nu e^{\Delta S / k}$$

# Transition State Theory

While the transmission coefficient is given by

$$\kappa = \left\langle \Theta[x(+t) - x_b] - \Theta[x(-t) - x_b] \right\rangle_{t \gg \tau_{\text{vib}}}$$

# Computing the pre-factor : The harmonic approximation

We have seen that the transition rate is given by

$$\Gamma = \Gamma_0 e^{-\Delta E/k_B T}$$

where

$$\Gamma_0 = \nu e^{\Delta S/k}$$

In the harmonic approximation, the entropy is related to the phonon frequencies and the prefactor becomes:

$$\Gamma_0 = \frac{\prod_i^{3N} \nu_i^{\min}}{\prod_i^{3N-1} \nu_i^{\mathrm{sad}}}$$

# Computing the pre-factor : A constant value

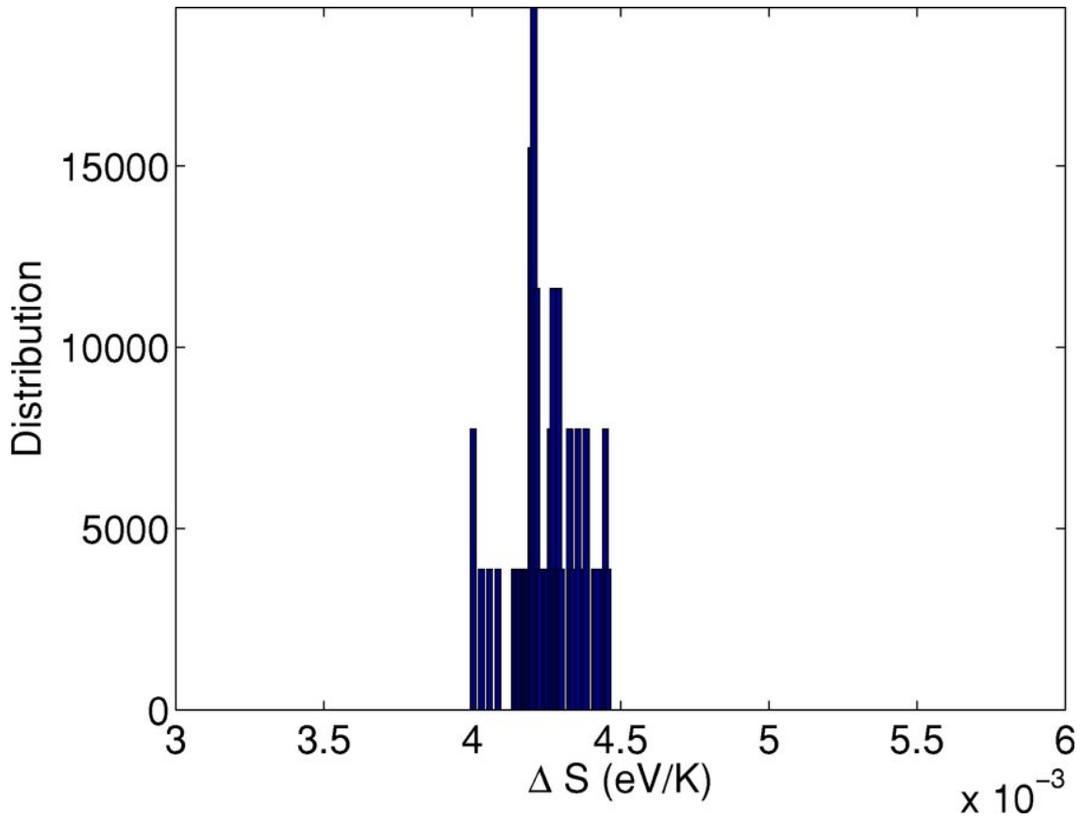


Amorphous silicon

FIG. 9. Distribution of the entropy barrier at the saddle point evaluated in the harmonic limit, for 50 different events selected at random.

Francis Valiquette and Normand Mousseau, Phys. Rev. B 68, 125209 (2003)

# TST : The simplified version

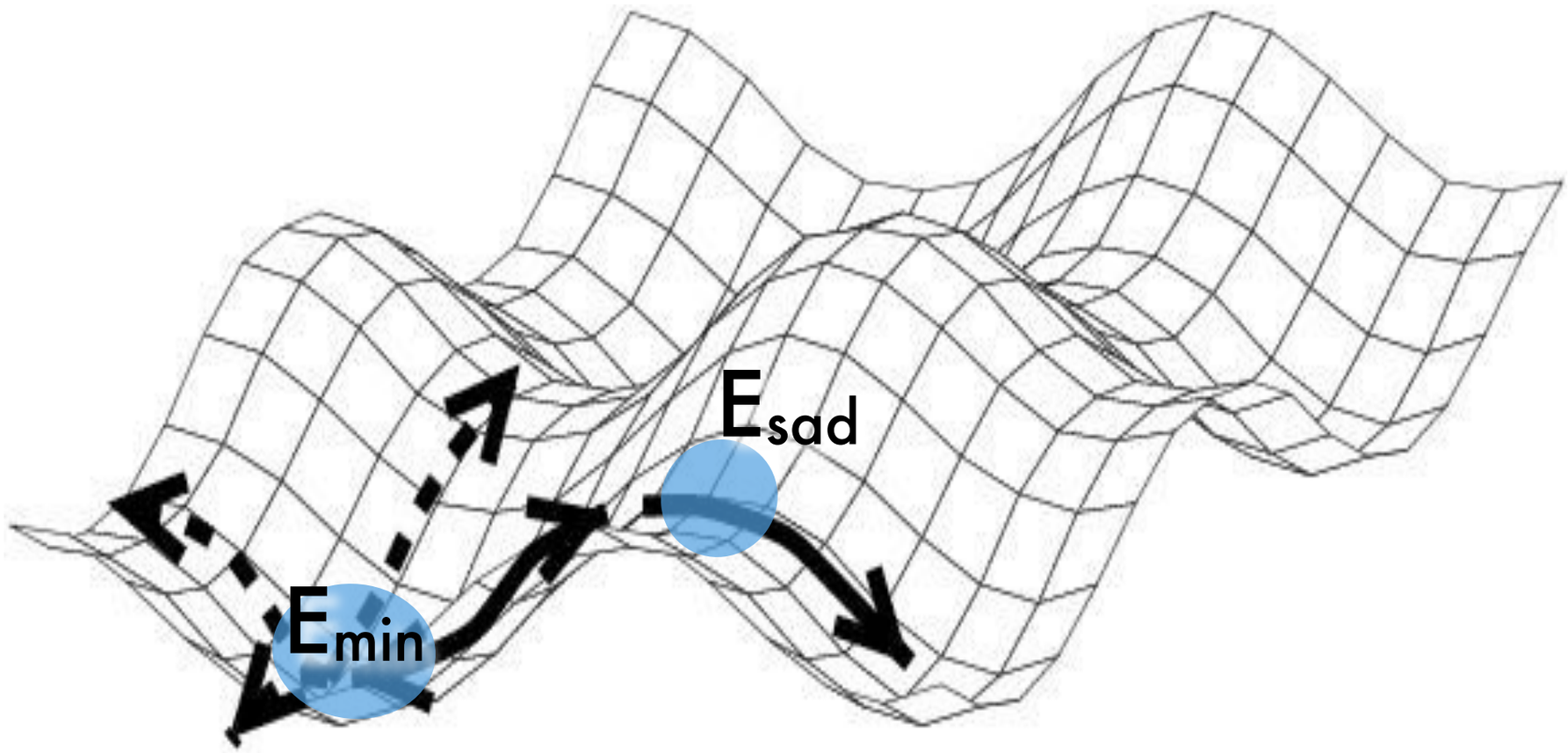


$$\Gamma = \Gamma_0 e^{-\Delta E / k_B T}$$

# TST: Approximations

$$\Gamma = \Gamma_0 e^{-\Delta E / k_B T}$$

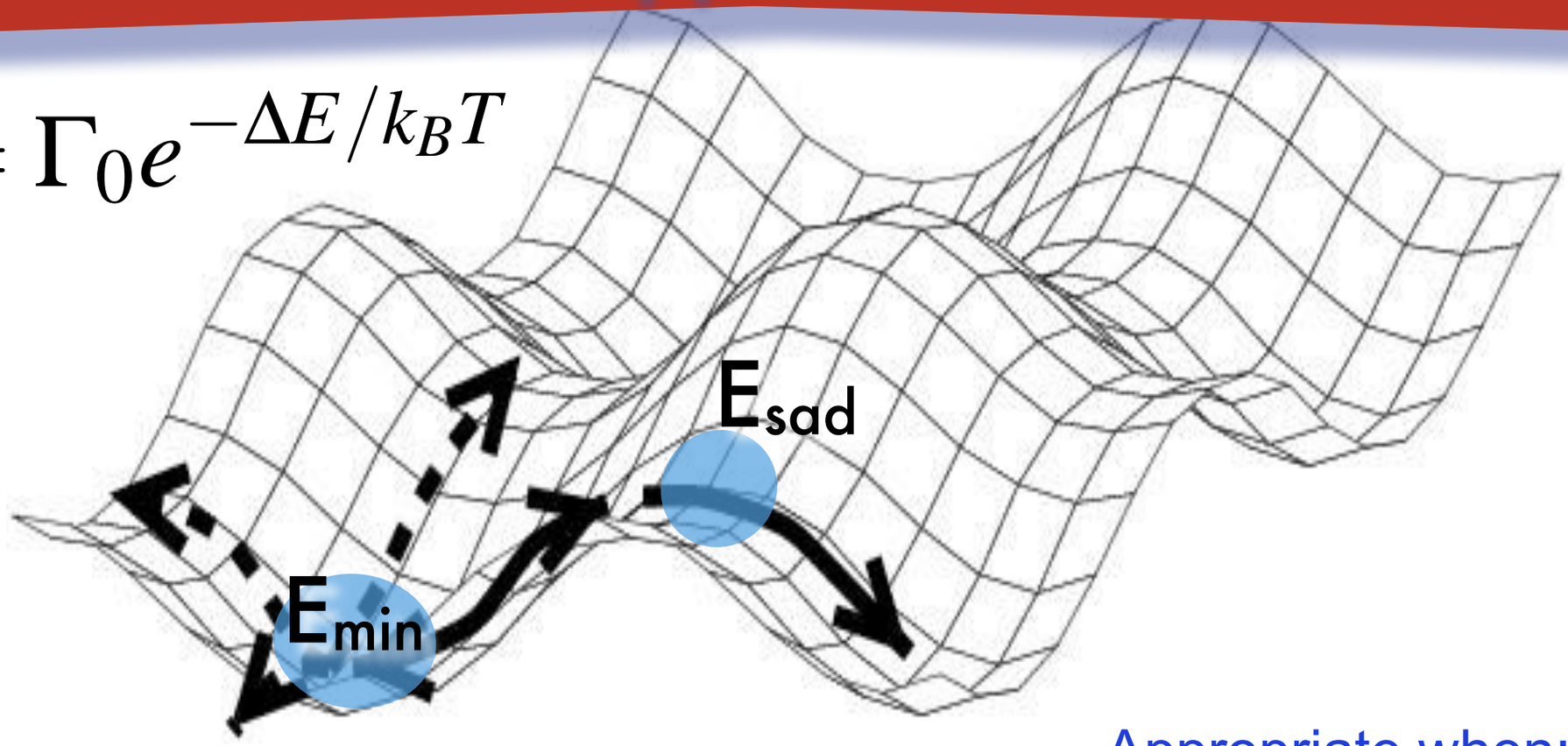


we need to know:

1. Knowledge of saddle points
2. Prefactor

Appropriate when:

1. Uncorrelated jumps
2. High barriers wrt $k_B T$
3. No diffusive mechanisms

Prefactor approximation

1. Homogeneous
2. Well-separated pathways

# Failures

## Inverse Meyer-Neldel behavior for activated processes in model glasses

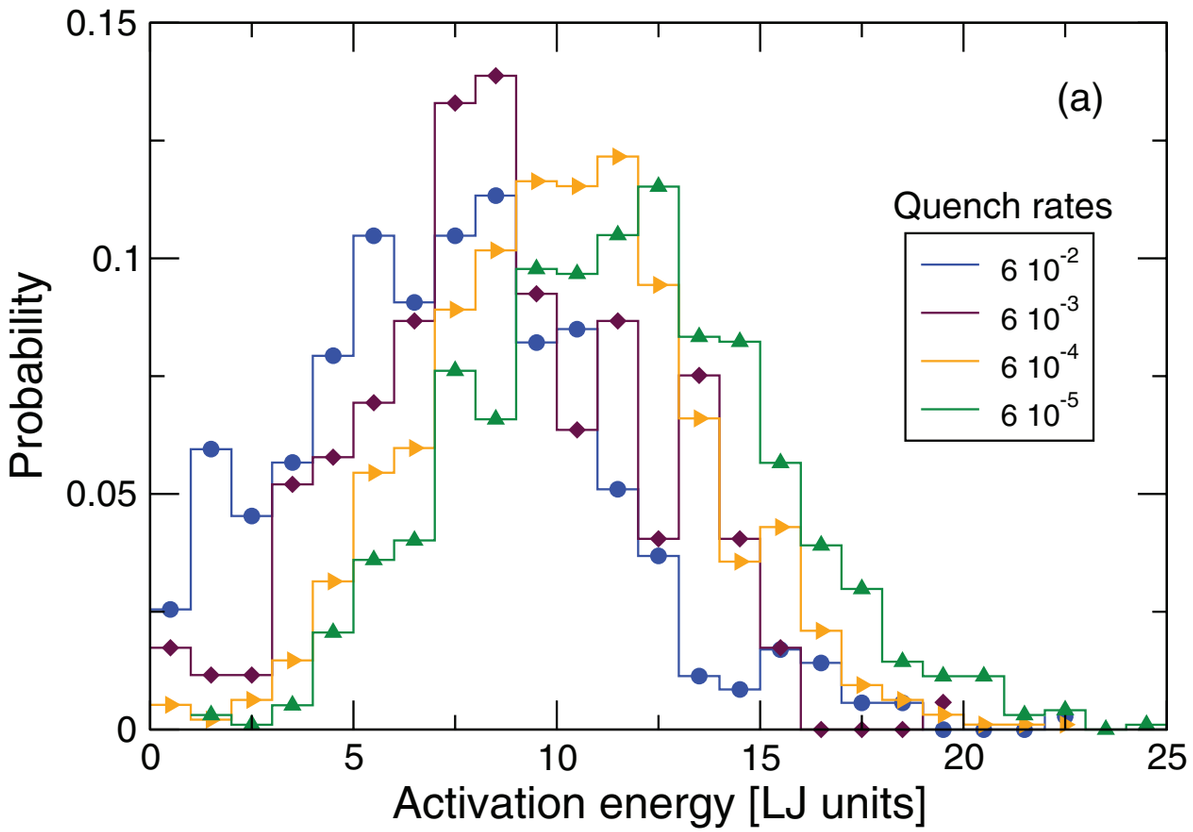


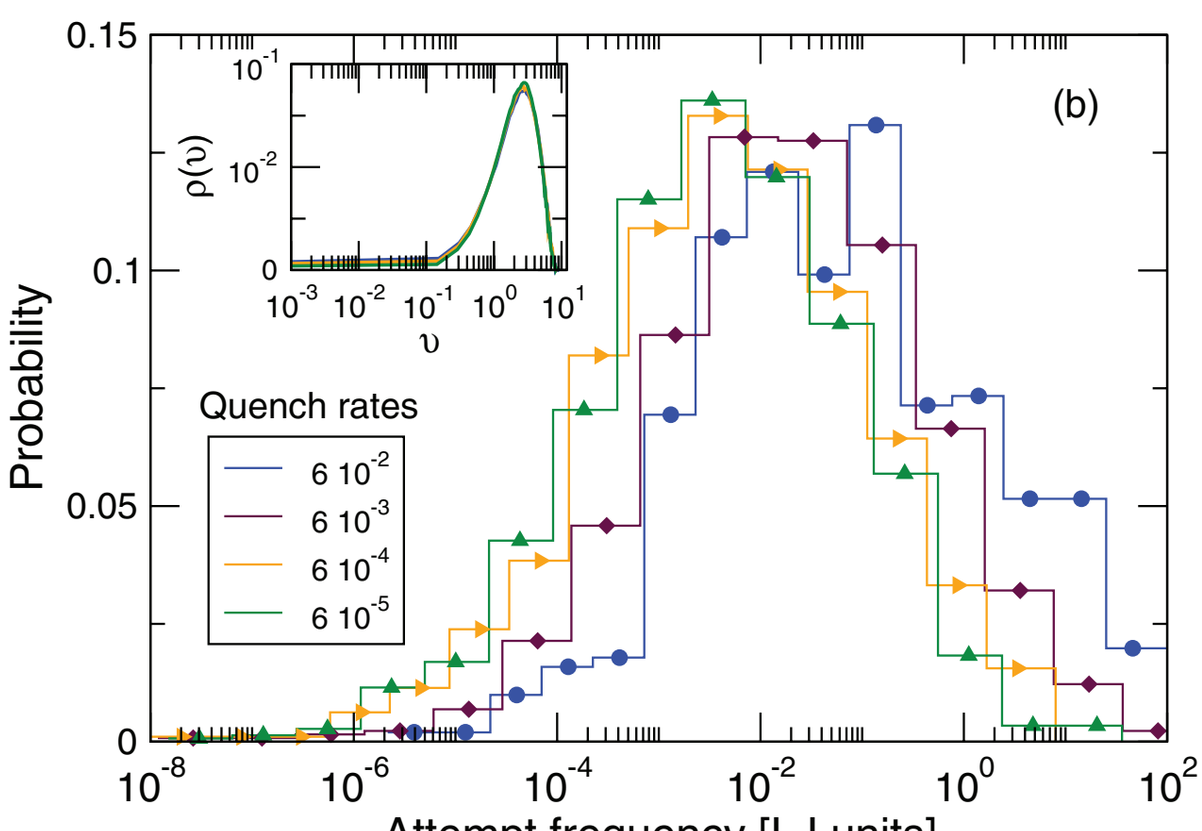


Pawel Koziatek, Jean-Louis Barrat, Peter Derlet, and David Rodney
Phys. Rev. B 87, 224105 (2013

# TST

**Beyond trivial results as a function of temperature**

**For thermodynamics : need entropy of each state + state**

**For kinetics : even with constant prefactors, competing phenomena, may lead to complex changes**

# Many methods have been proposed

There are many approaches to increase the efficiency of sampling the phase space of slow systems :

- parallel tempering
- entropic sampling
- transition path sampling
- hyper molecular dynamics
- temperature-assisted dynamics
- biased methods such as Laio and Parrinello

The methods have provided important results. There are still problems with complex materials with continuous distribution of barriers

# Replica-exchange MD

1. launch $n$ molecular dynamical simulations in parallel, at $n$ different temperatures
2. at regular intervals, try an exchange of configurations between two adjacent temperatures using a Metropolis accept-reject criterion

$$p(i,j) = \min\left\{1.0,\ \exp\left[\frac{1}{kBT_i} - \frac{1}{kBT_j}\right](E_i - E_j)\right\}$$

REMD accelerates sampling (in some cases) for the cost of losing dynamical information.

REMD still provides thermodynamical information

# Accelerating time
# Part 2

# Outline

**1.** The challenge of simulating over multiple time scales. Energy landscapes. The transition state theory. Brief overview of various methods for breaching these time scales.

**2.** Basic concepts. Searching for saddle points. Sampling the energy landscape : the activation-relaxation technique (ART nouveau)

**3.** Accelerated MD approaches. Basic concepts kinetic Monte Carlo. Limits.

**4.** Off-lattice kinetic Monte Carlo methods. The kinetic Activation-Relaxation Technique. Topological analysis. Constructing an event catalog. Handling flickers. Limitations of current accelerated methods. Extending to large systems. Coming developments.

# Transition State Theory

$\Delta W = W_{bas} - W_{sad}$

The rate is

$$k = \kappa \cdot k_{TST}$$

with

$$k_{TST} = \nu e^{-\Delta W / k_B T}$$

k : Crossing rate

$\kappa$ : Transmission coefficient

$\nu$ : Attempt frequency

$\Delta W$ : Activation energy

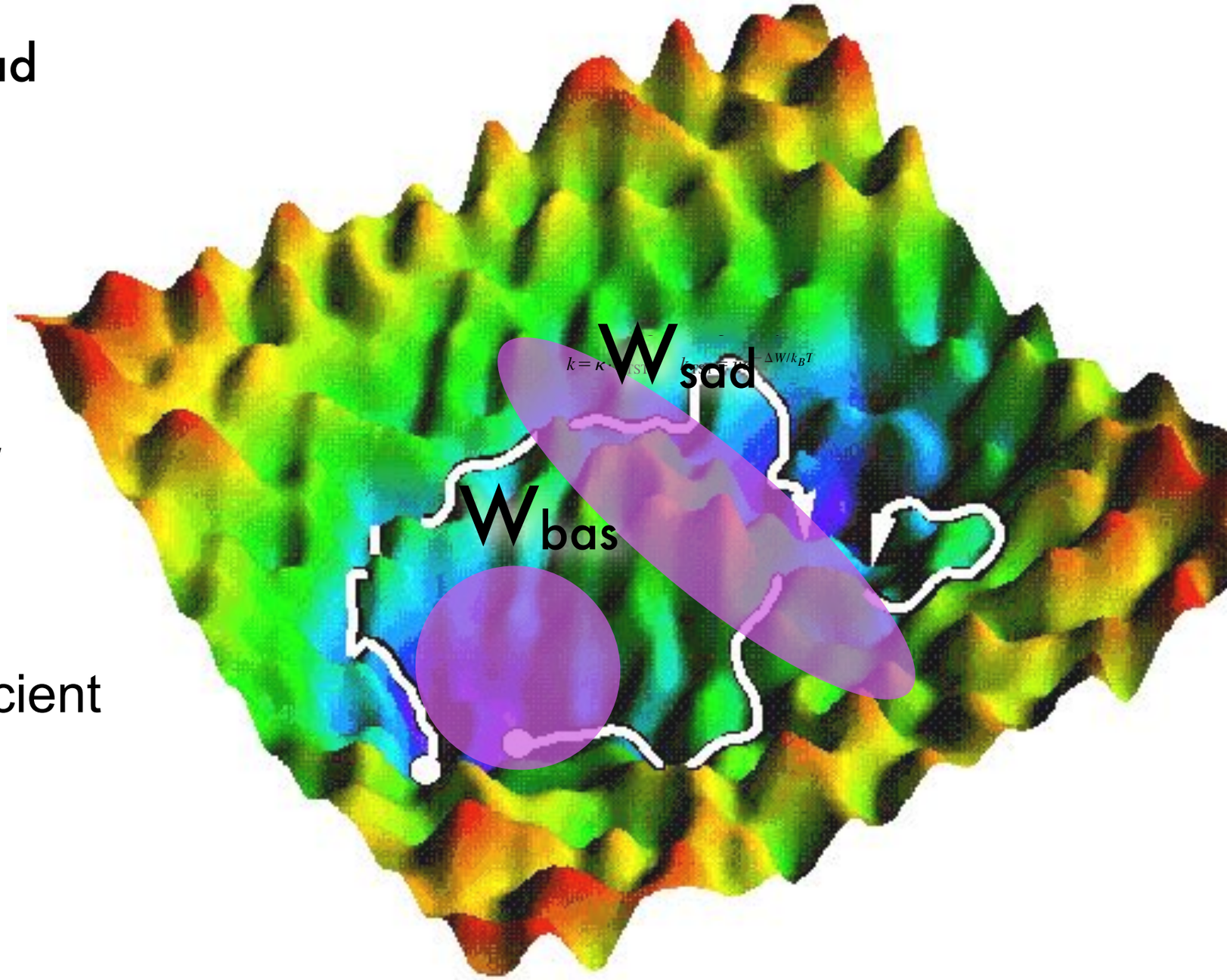


Marcelin (1915), Eyring and Wigner (1930s)

# Transition State Theory

The law of compensation or the Meyer-Neldel Rule:

W. Meyer and H. Neldel, Z. Tech. Phys (Leipzig )12, 588 (1937).

Cu on Cu (EAM) with two mechanisms:

- Jump
- Exchange

(Feibelman, end of 1980's)

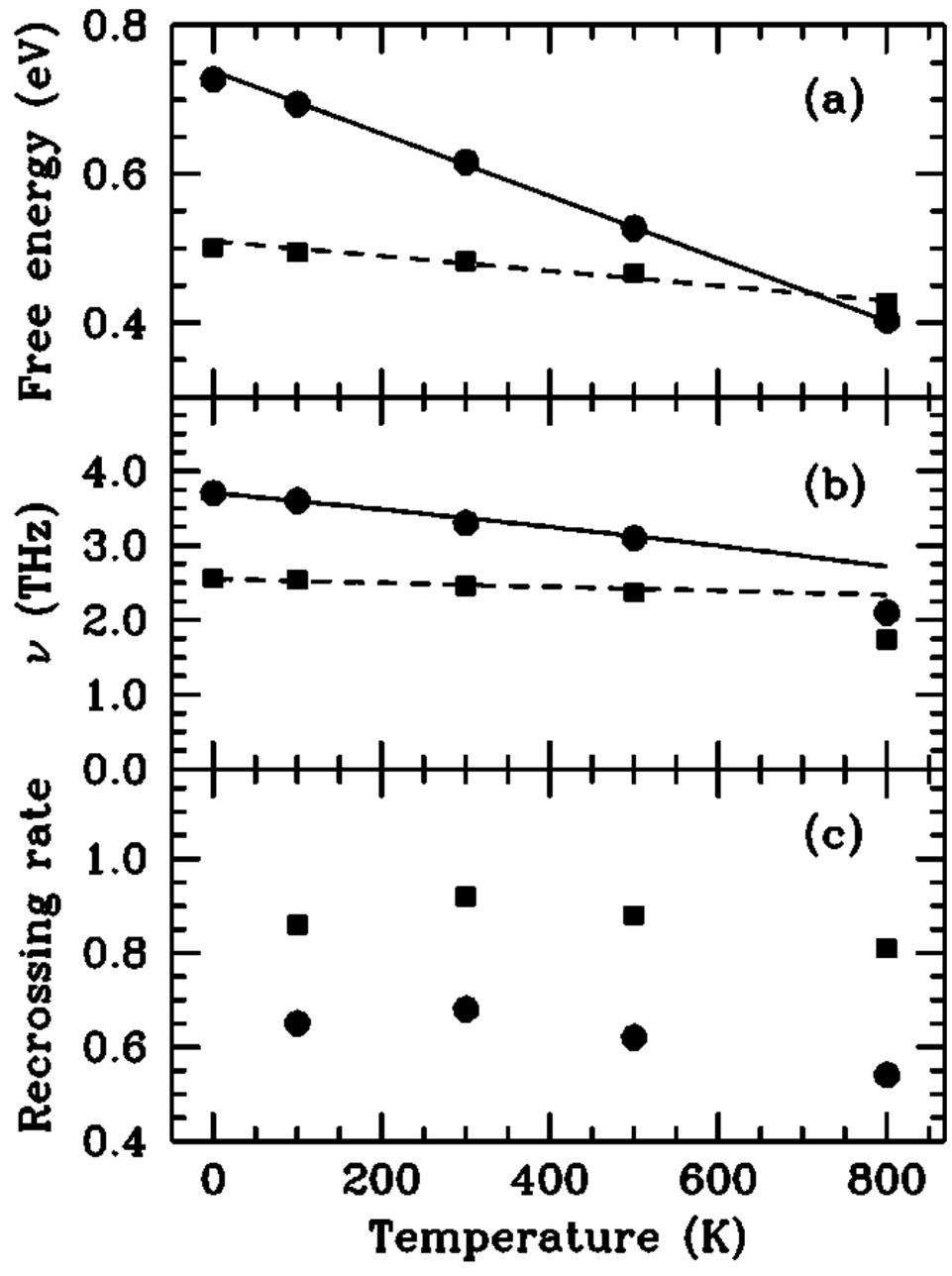


Boisvert, Mousseau and Lewis, PRB **58,** 12667 (1998)

# Transition State Theory

TABLE I. Comparison between TI and MD results for the jump ($J$) and exchange ($X$) diffusion activation barriers $\Delta E$ (in eV) and rate prefactors $\Gamma_0$ (in THz); also given are the entropy $\Delta S$ (in $k_B$) and the static energy barrier, $\Delta E(0)$. Estimated errors are given in parenthesis.

| | $\Delta S$ | $\Delta E$ | $\Delta E$ | $\Delta E(0)$ | $\ln \Gamma_0$ | $\ln \Gamma_0$ |
|---|---|---|---|---|---|---|
| | (TI) | (TI) | (MD) | | (TI) | (MD) |
| $J$ | 1.1(0.2) | 0.51(0.02) | 0.49(0.01) | 0.50 | 2.9(0.2) | 3.0(0.2) |
| $X$ | 4.9(0.6) | 0.74(0.02) | 0.70(0.04) | 0.73 | 6.5(0.6) | 6.1(0.7) |

Boisvert, Mousseau and Lewis, PRB **58,** 12667 (1998)

# Simplifying the search

Reduce phase space to trajectories between minima going through saddle points

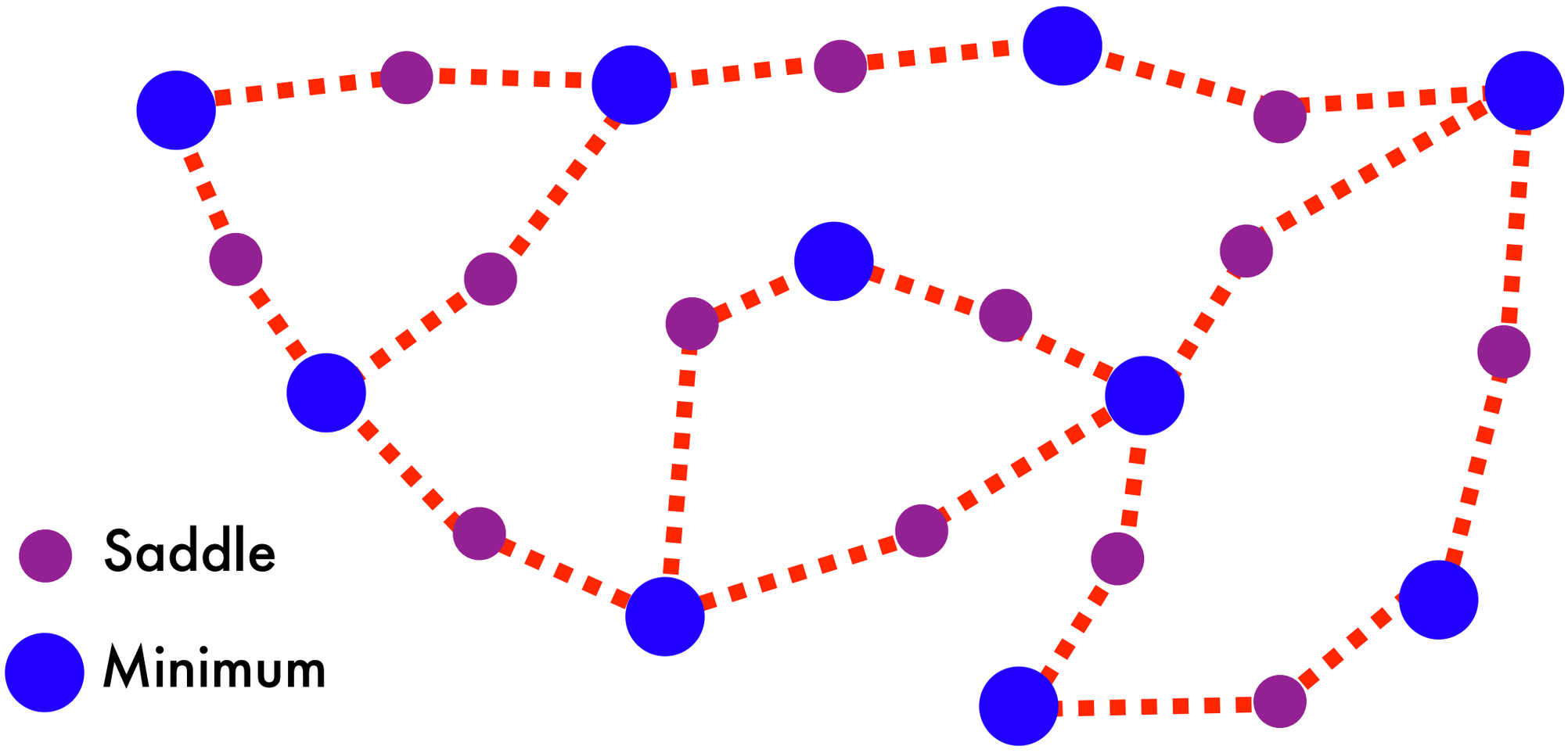

# A few definitions...

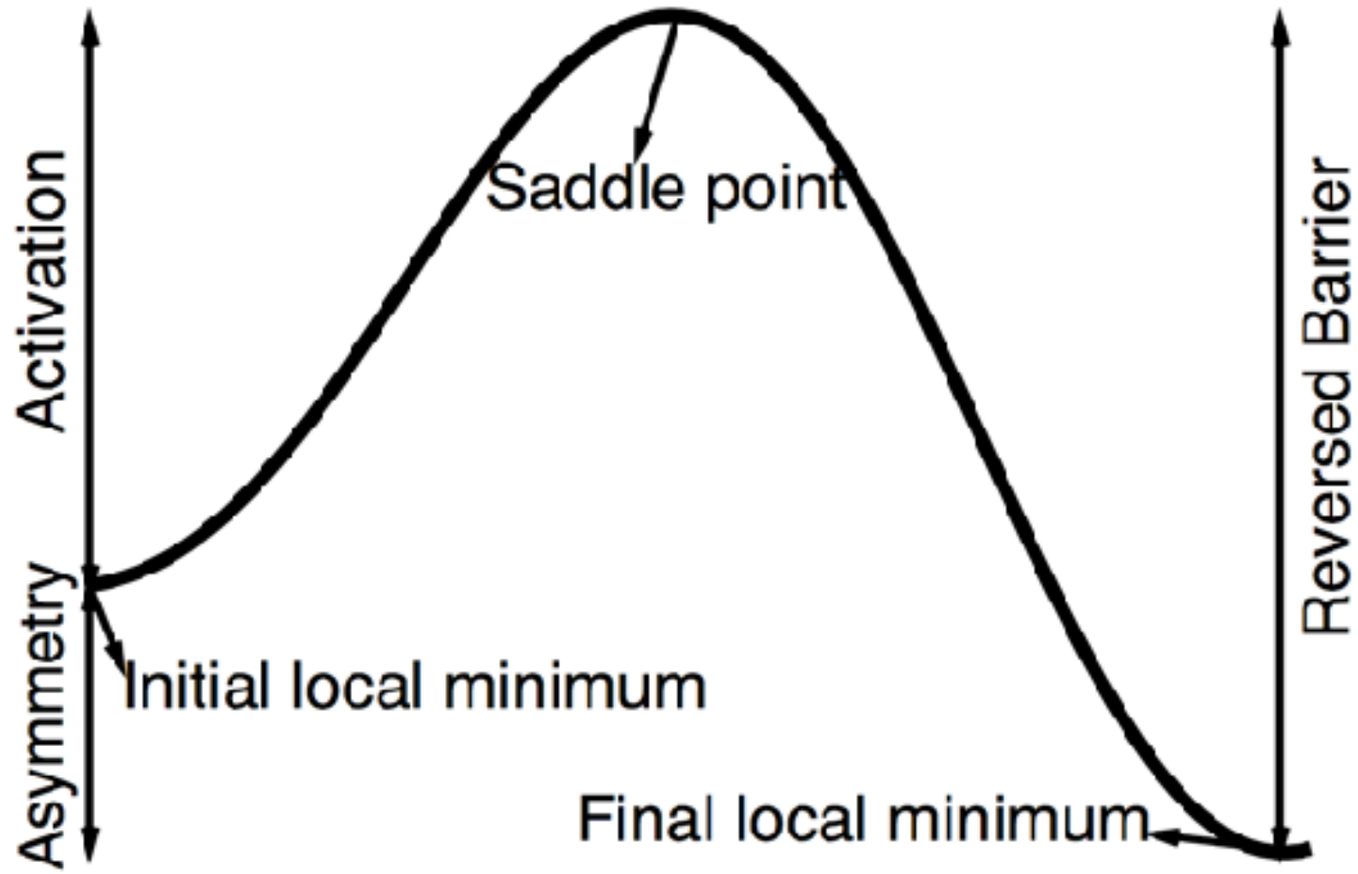

# Example: Finding barriers with ART nouveau

The activation-relaxation technique is defined in three steps.

1) Leave the harmonic basin;
   threshold determined by value of lowest curvature

2) Push the configuration up along the corresponding direction;
   energy is minimized in the perpendicular hyperplane;
   can converge to the saddle point with any desired precision

3) Minimize the energy;
   bring the configuration into a new minimum

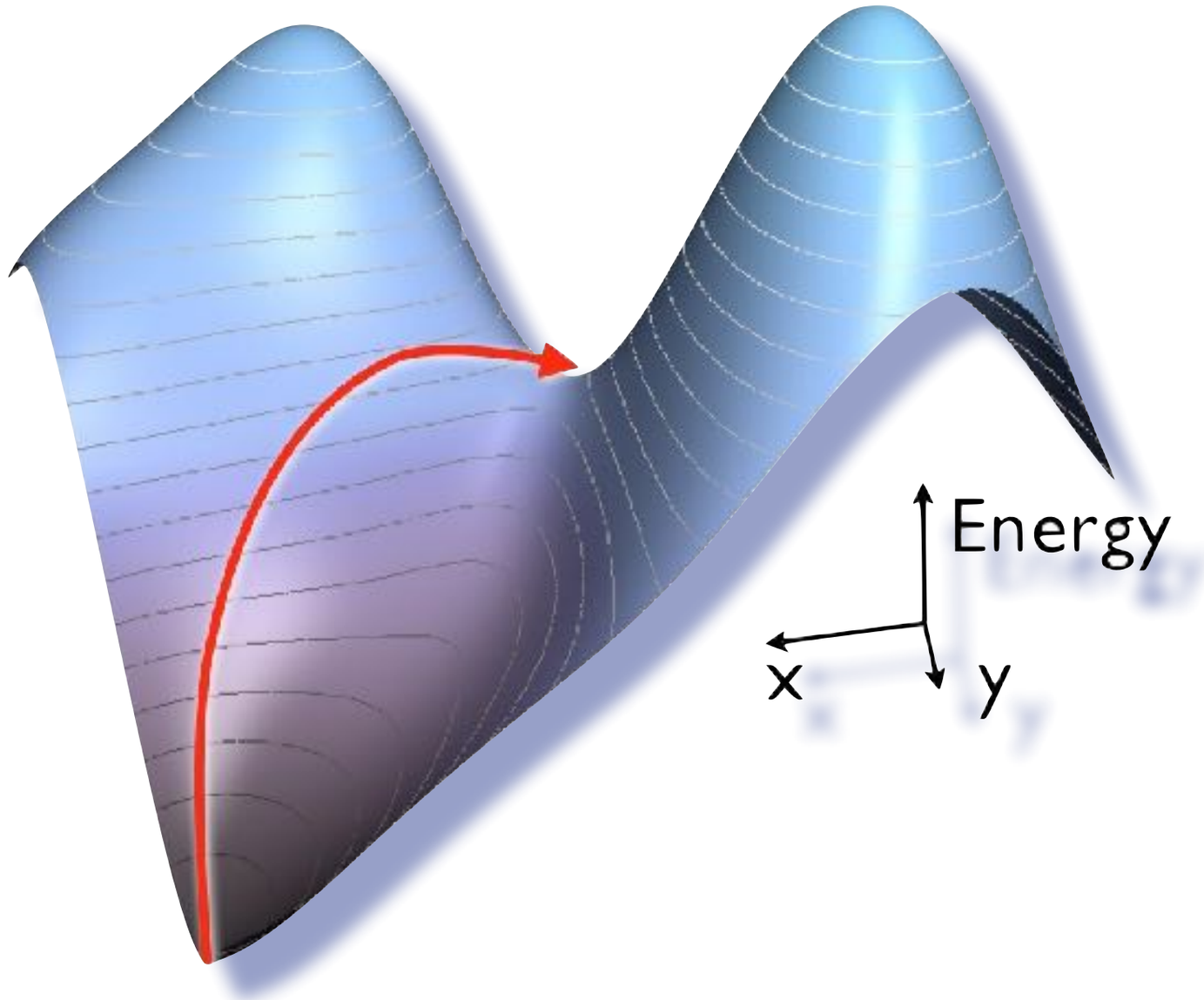


*Barkema & Mousseau, Phys. Rev. Lett. 77 (1996);*
*Malek & Mousseau, Phys. Rev. E 62 (2000);*

# Generating an event

ART nouveau can be used to identify barriers

1. Start from a local minimum

2. Select the atom in the center of the local topological region; displace this atom and its neighbours slowly.

3. Follow this direction until an eigenvalue become negative.

4. Push along the corresponding eigenvector until total force is zero. (Saddle point)

5. Converge to a new minimum (event).

6. Assign the event to the atom that has moved most.

7. Repeat, from (2) a desired number of times.

8. Move to the next atom and start at (2)

# Lanczos

The Hessian matrix is defined as

$$H_{i\alpha,j\beta}[\mathbf{q_0}] = \frac{\partial^2 E[\mathbf{q}_0]}{\partial q_{i\alpha}\partial q_{j\beta}},$$

It is possible to extract its lowest eigenvalue and corresponding eigenvector through an iterative process first proposed by Lanczos. We first generate a random vector $\mathbf{u_0}$ and compute $\mathbf{u_1}$ from:

$$\mathbf{H}\mathbf{u}_0 = a_0\mathbf{u}_0 + b_1\mathbf{u}_1$$

and, iterating:

$$\mathbf{H}\mathbf{u}_1 = a_1\mathbf{u}_1 + b_1'\mathbf{u}_0 + b_2\mathbf{u}_2,$$

Because the Hessian is symmetric:

$$\mathbf{u}_1 \cdot (\mathbf{H}\mathbf{u}_0) = \mathbf{u}_0 \cdot (\mathbf{H}\mathbf{u}_1)$$

So that $b_1'=b_1$ giving the relation:

$$\mathbf{H}\mathbf{u}_k = a_k\mathbf{u}_k + b_k\mathbf{u}_{k-1} + b_{k+1}\mathbf{u}_{k+1}$$

Closing can be done simply as :

$$\mathbf{H}\mathbf{u}_{l-1} = a_{l-1}\mathbf{u}_{l-1} + b_{l-1}\mathbf{u}_{l-2}$$

# Lanczos

And, in the end, we only have to diagonalize:

$$\mathbf{T}_l = \begin{pmatrix} a_0 & b_1 & 0 & \cdots & 0 \\ b_1 & a_1 & b_2 & \cdots & 0 \\ 0 & b_2 & a_2 & \cdots & 0 \\ 0 & \ddots & \ddots & \cdots & 0 \\ 0 & & b_{l-2} & a_{l-2} & b_{l-1} \\ 0 & & 0 & b_{l-1} & a_{l-1} \end{pmatrix}$$

Because of the properties of linear algebra, the lowest eigenvalue (and its corresponding eigenvector) comes out exponentially fast from the Lanczos aglorithm. By reusing the final eigenvector as $\mathbf{u_0}$, only a matrix of 12x12 is sufficient to obtain the desired vector and eigenvalue, irrespective of the system's size.

Moreover, the Hessian does not have to be computed directly, only the forces are needed:

$$\mathbf{H}[\mathbf{q}_0]\mathbf{u} = -\frac{\mathbf{f}(\mathbf{q}_0 + \delta_L \mathbf{u}) - \mathbf{f}(\mathbf{q}_0 - \delta_L \mathbf{u})}{2\delta_L} + O\left(\delta_L^3\right)$$

# Details of the algorithm

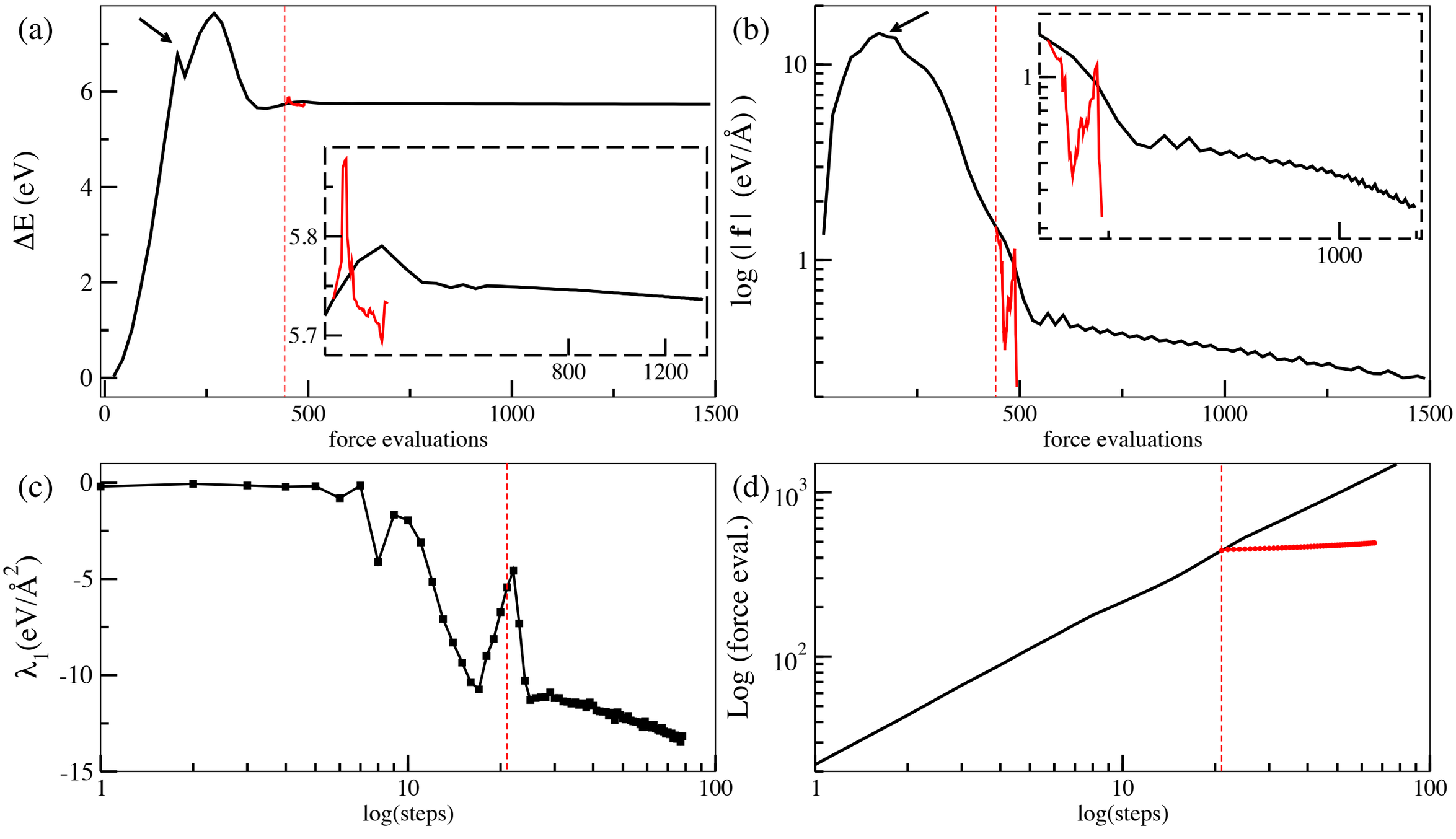


E Machado-Charry, LK Béland, D Caliste, L Genovese, NM and P Pochet, J. Chem Phys. (2011).

# Features of ART

not sensitive to the real space complexity of activated jump nor the height of the activation energy barrier, which can be very high

not biased toward pre-determined

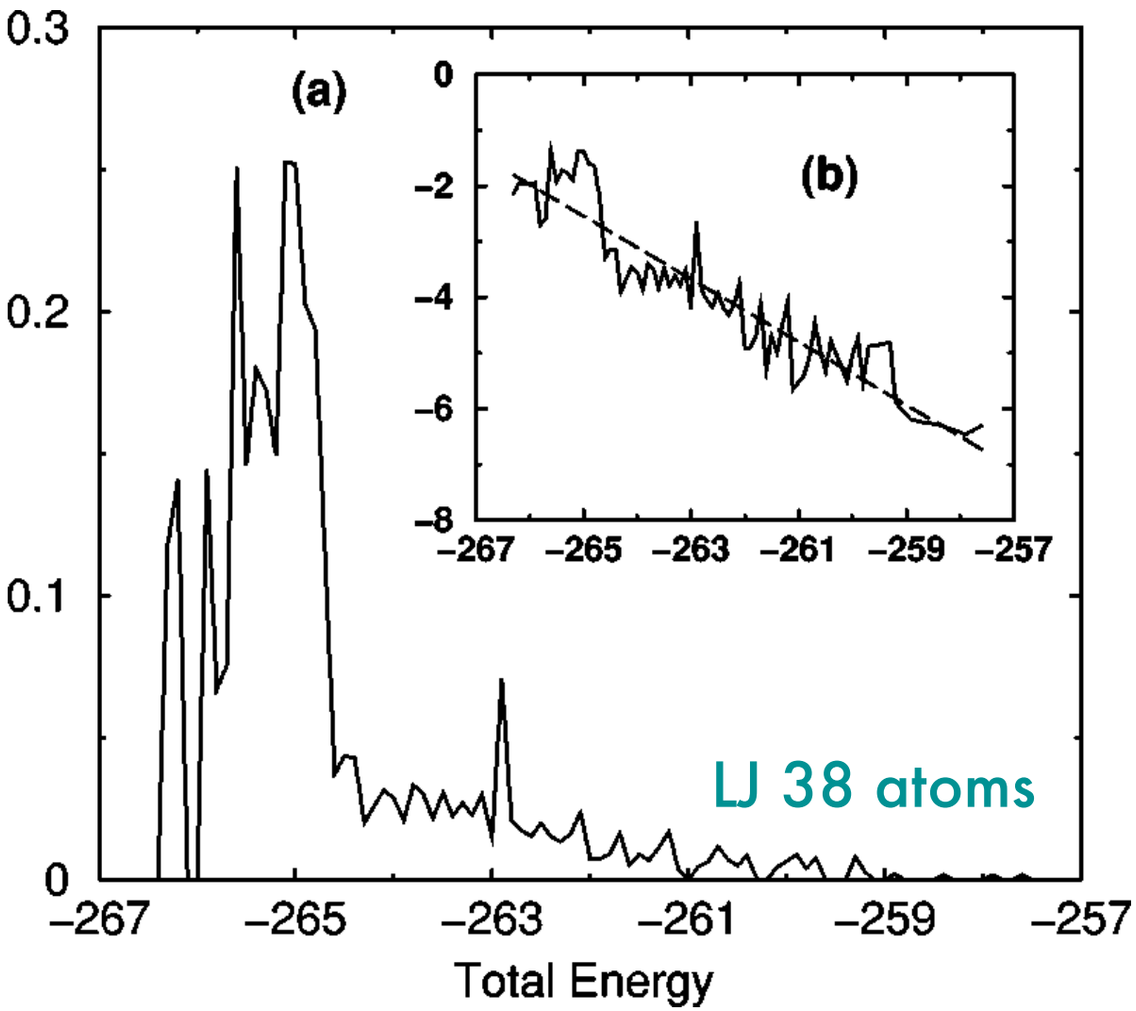


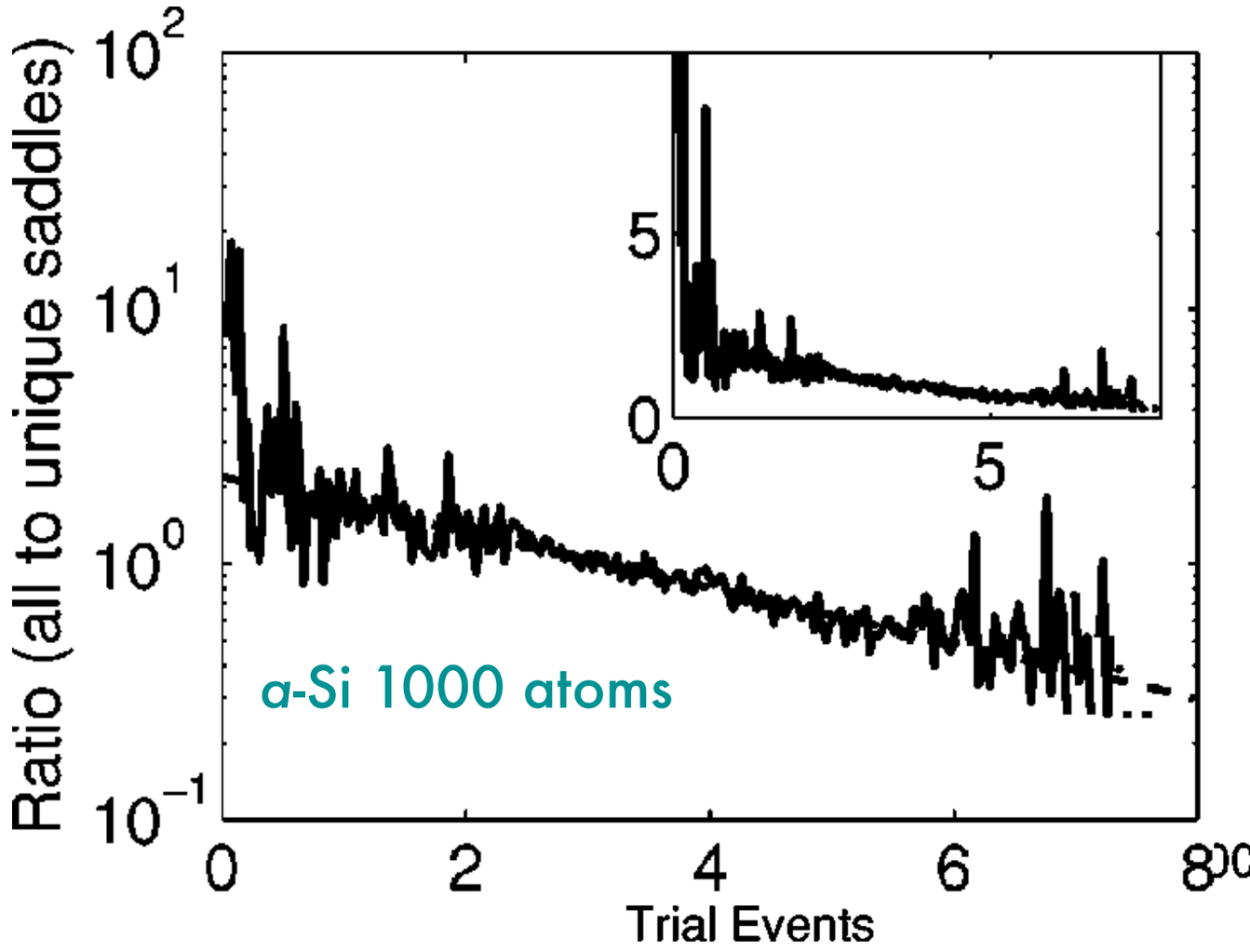


very efficient numerically

seems to sample all classes of events (ergodic)

events are reversible

# Comparison with other methods

| Algo. | ART nouveau | | | | ARTn (Olsen) | | Dimer method | | Improved dimer | | GSM |
|---|---|---|---|---|---|---|---|---|---|---|---|
| Ref. | | | | | [33] | | | | [34] | [35] | [6] |
| System | *a-Si* | $V_{Si}$ | $C_{20}$ | SiC | Pt(111) | Pt(111) | Pt(111) | Pt(111) | $C_6H_{10}$ | $PHBH/H_2O$ | $VO_x/SiO_2$ |
| BC | Bulk | Bulk | Isol.e | Surf. | Surf. | Surf. | Surf. | Surf. | Isol. | Sol. | Isol. |
| Pot. | SW | DFT | DFT | DFT | Morse | Morse | Morse | Morse | DFT | QM/MM | DFT |
| Method | | PBE | LDA | PBE | | | | | B3LYP | AM1 | B3LYP |
| DOF | 3000 | 12[1] | 60 | 222[1] | 3 | 525 | 3 | 525 | 48 | 144 | 12[1] |
| $\langle f \rangle$ | 235 | 210 | 322 | 262 | 145 | 372 | 204 | 335 | 384[2] | 425[3] | 330 |
| $\langle f \rangle_s$ | 670 | 302 | 718 | 728 | 145 | 2163 | 204 | 2148 | - | - | - |
| A/S | 2.72 | 79/78 | 434/201 | 134/75 | - | - | - | - | - | - | - |


E Machado-Charry, LK Béland, D Caliste, L Genovese, NM and P Pochet, J. Chem Phys. **135**, 034102, 11 pp., (2011).

E Cances, F Legoll, M-C Marinica, F Minoukadeh, and F Willaime, J. Chem. Phys. **130**, 114711 (2009).

# C20 - BigDFT + ART nouveau

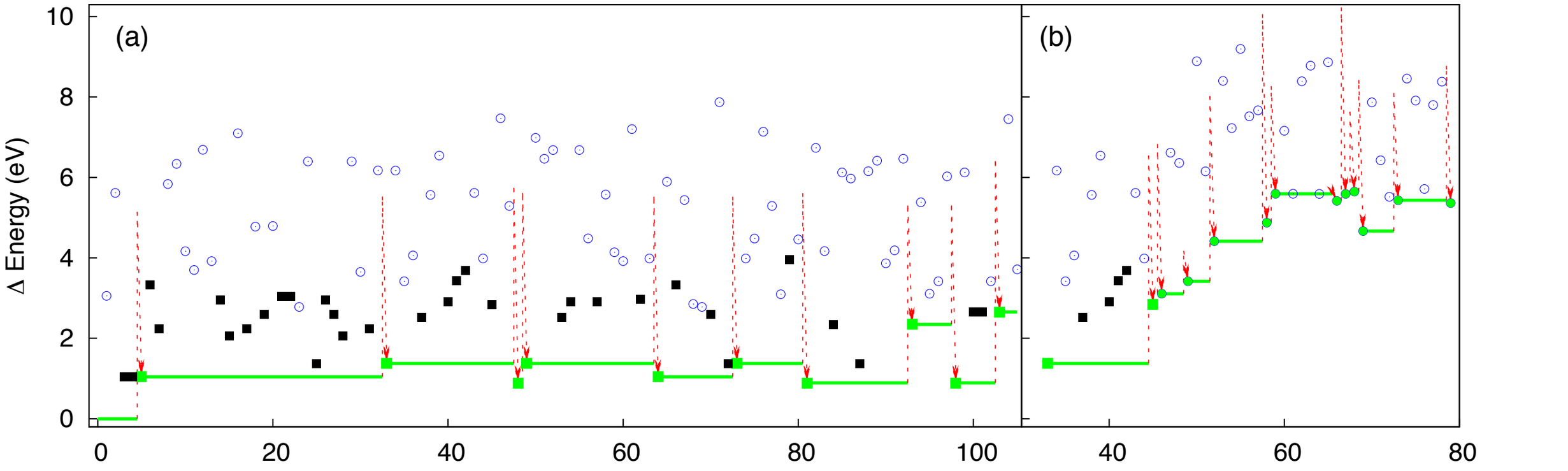


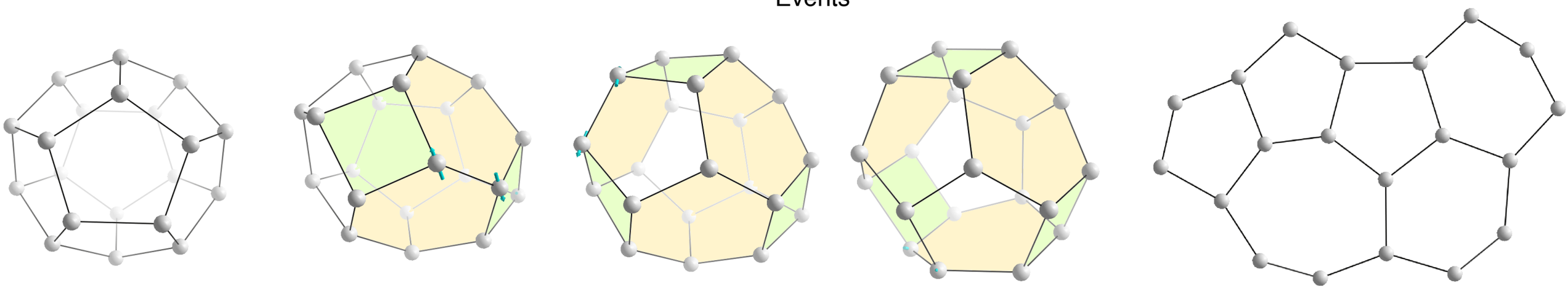

(a)ΔE=0.0 eV (b)ΔE=1.04 eV (c)ΔE=1.37 eV (d)ΔE=0.89 eV (e)ΔE=5.36 eV

E Machado-Charry, LK Béland, D Caliste, L Genovese, NM and P Pochet, J. Chem Phys. **135**, 034102, 11 pp., (2011).

# Systematic study of interstitials in Iron

- Interstitial-type defects formed by the clustering of self-interstitials produced under irradiation have rather peculiar properties in α-iron by comparison with other body centered cubic (BCC) metals

- In α-iron isolated self-interstitial atoms (SIA) have a rather large migration energy, about 0.3 eV.

- Nanometer size clusters – or dislocation loops – have either ⟨111⟩ or ⟨100⟩ orientation in Fe.

- The structure of interstitial clusters with intermediate size is largely unknown although they play a key role in the loop growth mechanism.

- The barrier height is such that MD can easily get trapped into specific minima, and not sample all mechanisms.

M.-C. Marinica, F. Willaime and N. Mousseau, PRB (2011)

# Systematic study of interstitials in Iron

- Ackland-Mendelev potential
- ART nouveau
- 1024 atoms
- 50 trajectories which are stopped after 2000 successful activation events (each taking less than a week)

# Mono-interstitials in Iron

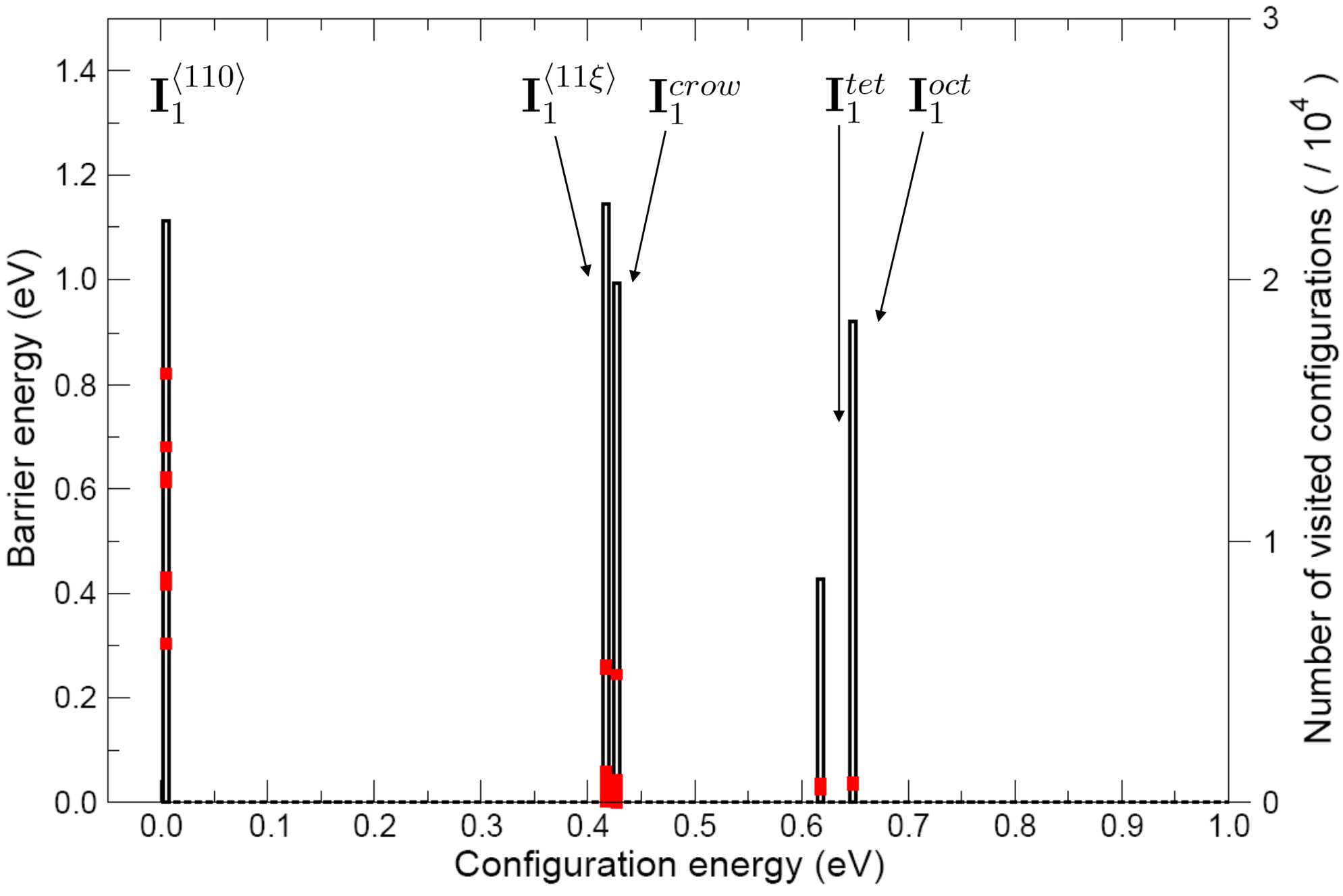

# Di-interstitials in Iron

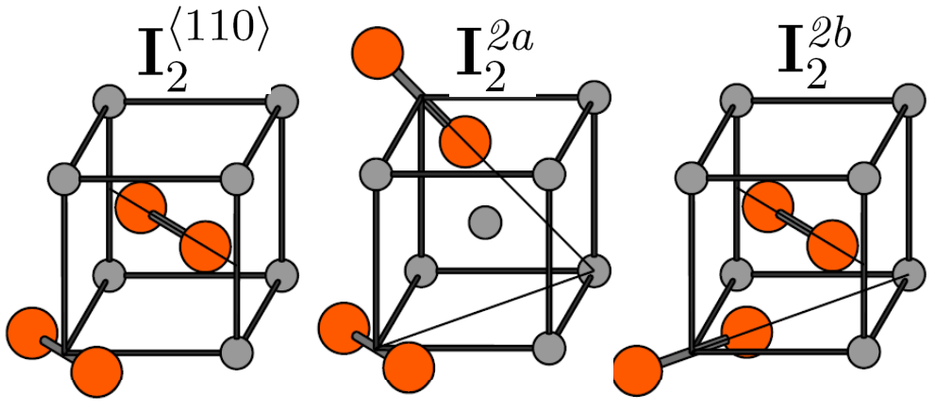


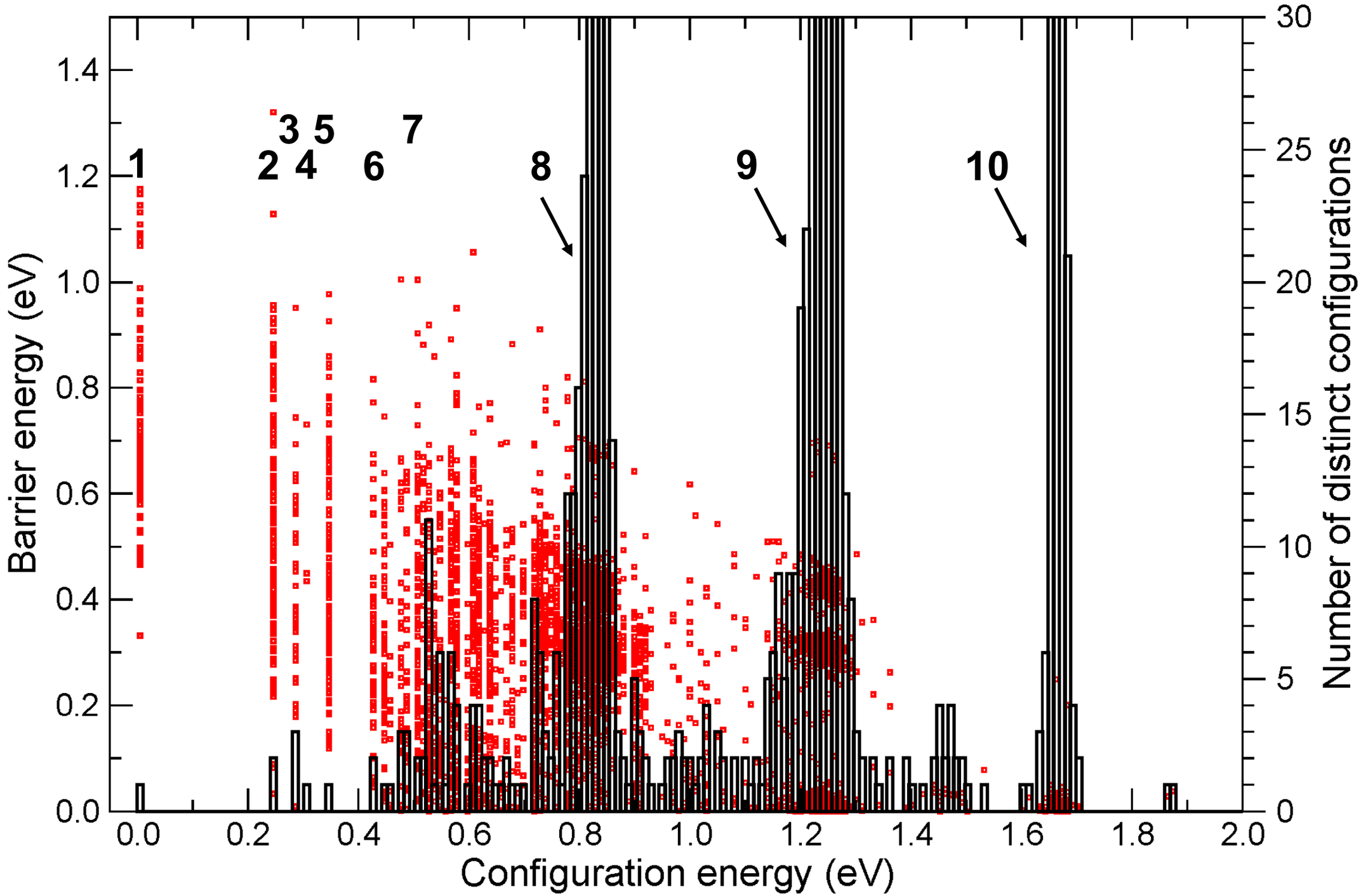

# The three lowest-energy saddles for $I_2$

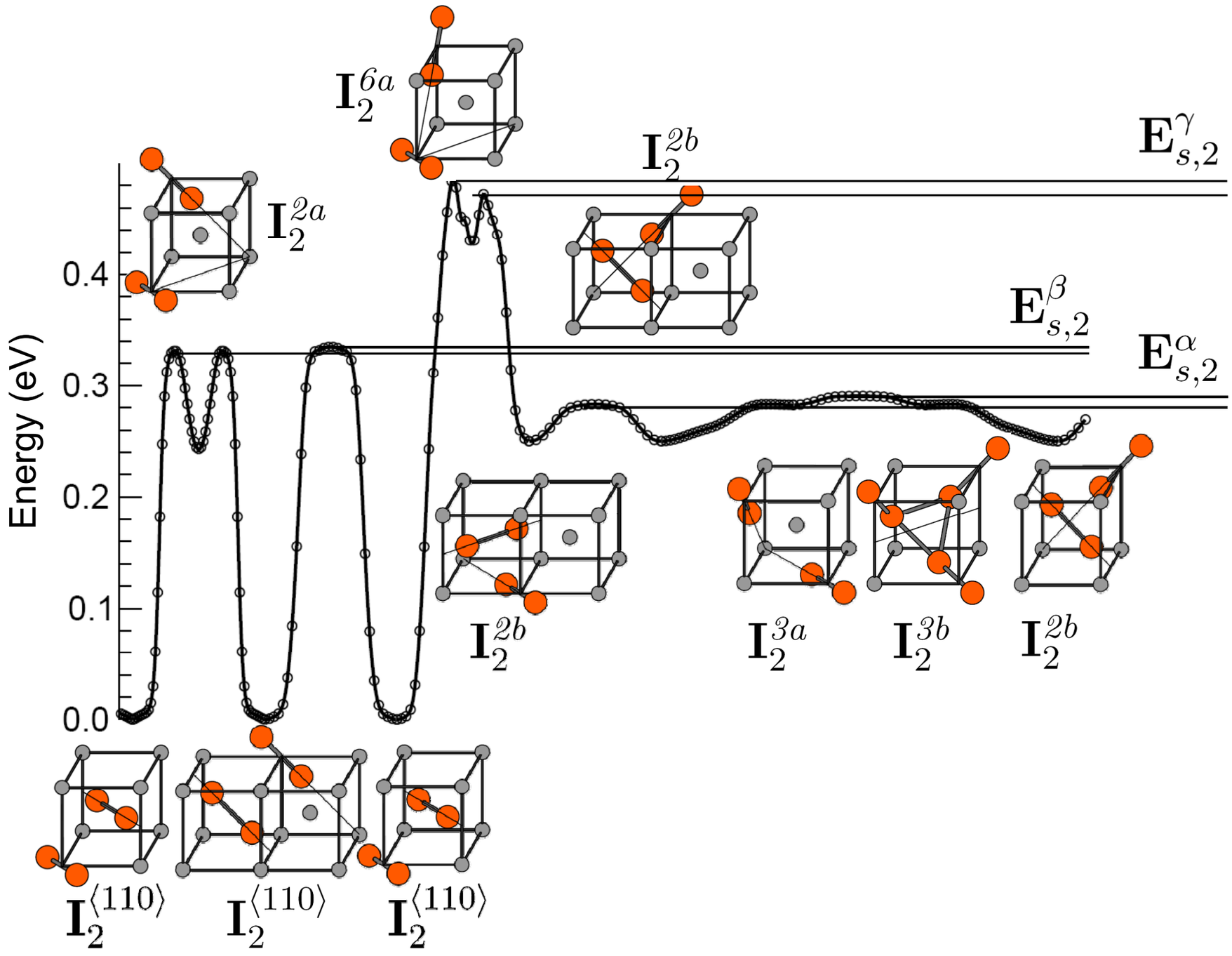

# $I_4$ in Iron

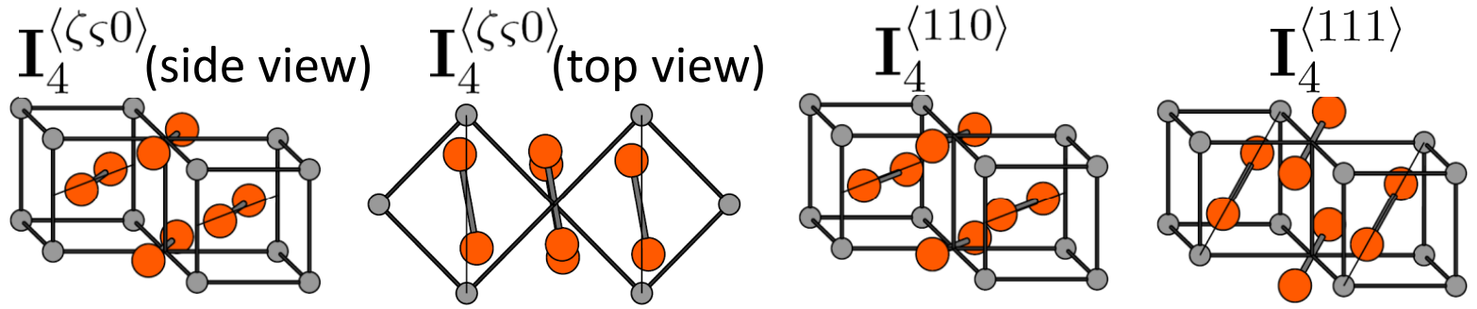
$\mathbf{I}_4^{\langle\zeta\varsigma 0\rangle}$(side view)
$\mathbf{I}_4^{\langle\zeta\varsigma 0\rangle}$(top view)
$\mathbf{I}_4^{\langle 110\rangle}$
$\mathbf{I}_4^{\langle 111\rangle}$

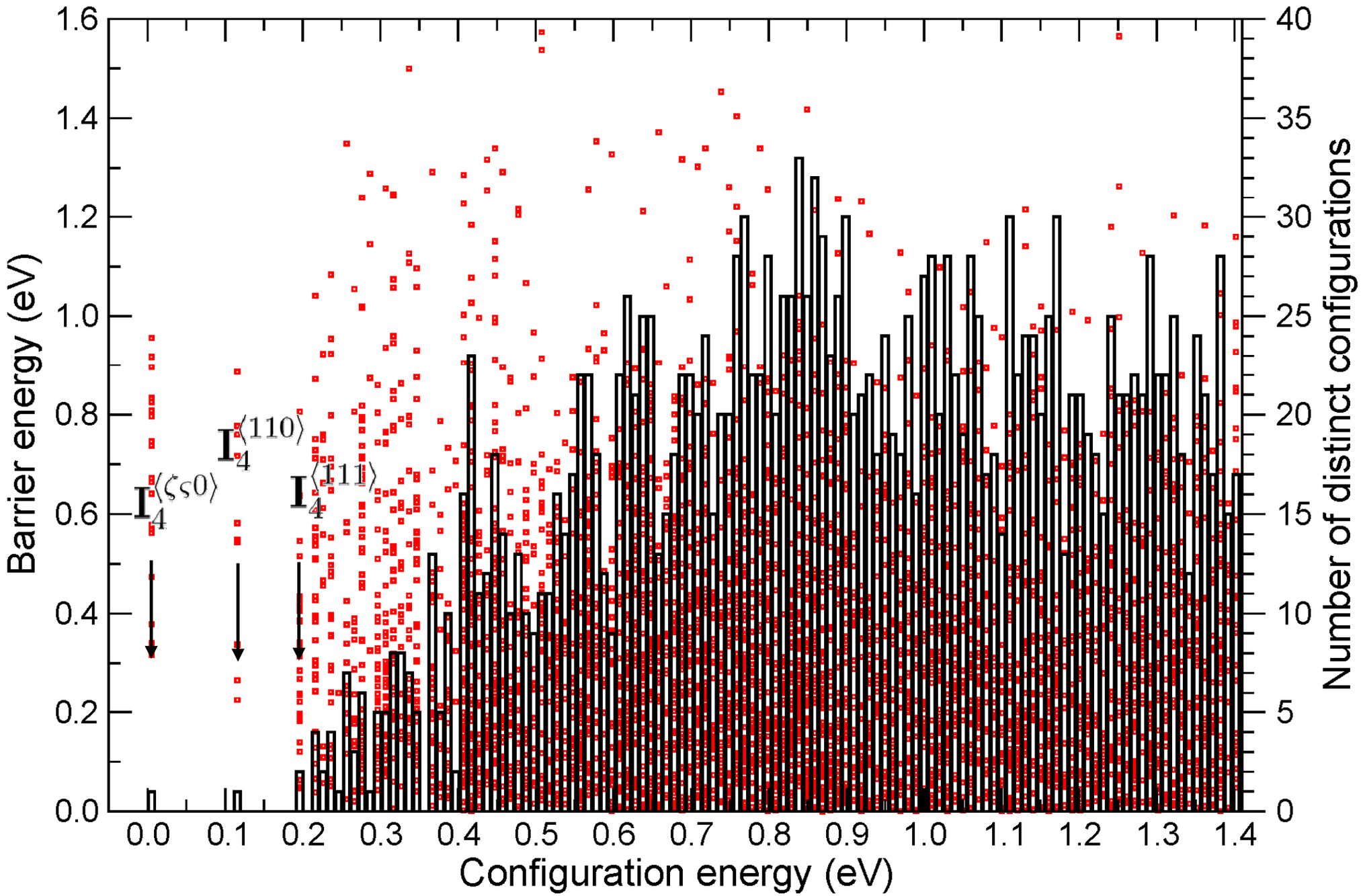
Barrier energy (eV)
Number of distinct configurations
Configuration energy (eV)
$\mathbf{I}_4^{\langle\zeta\varsigma 0\rangle}$
$\mathbf{I}_4^{\langle 110\rangle}$
$\mathbf{I}_4^{\langle 111\rangle}$
0.0
0.2
0.4
0.6
0.8
1.0
1.2
1.4
1.6
0
5
10
15
20
25
30
35
40
0.0
0.1
0.2
0.3
0.4
0.5
0.6
0.7
0.8
0.9
1.0
1.1
1.2
1.3
1.4

# Transition pathways for $I_4$

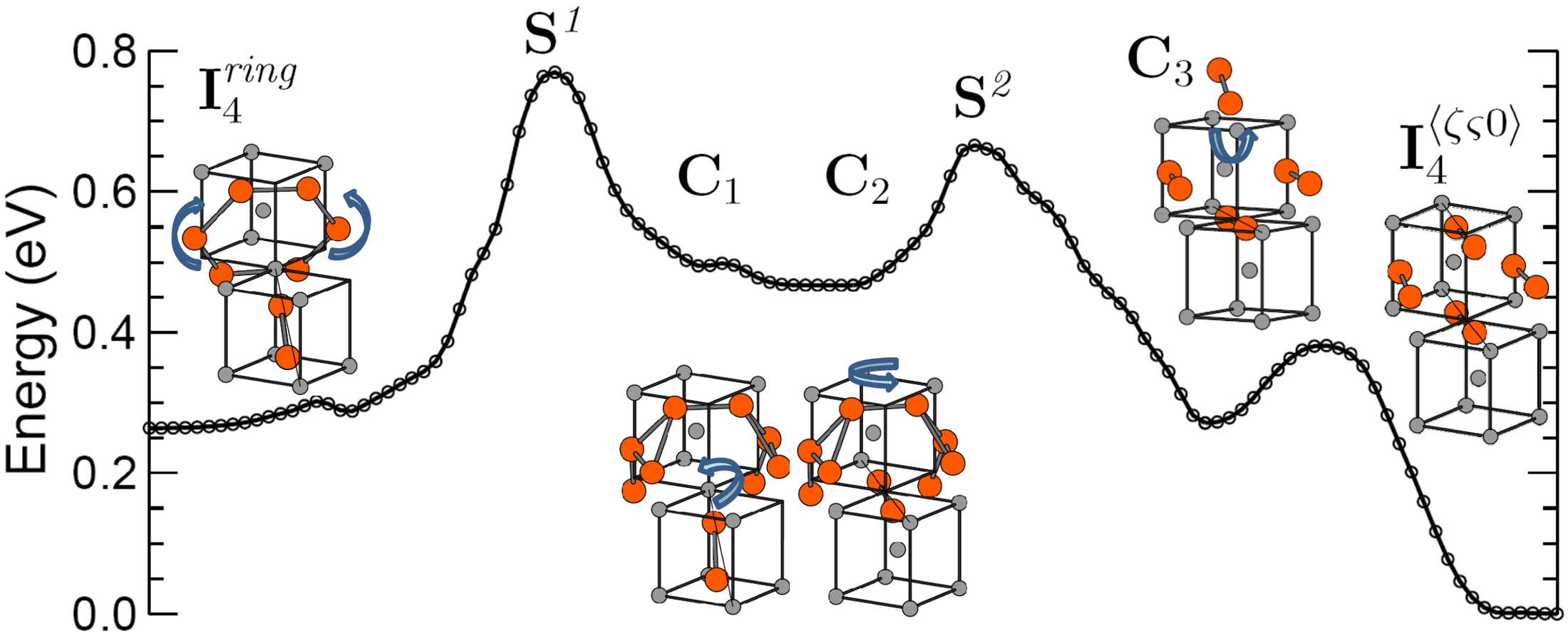


Transition pathway for the unfaulting mechanism of the ring configuration of the tetra-interstitial, $I_{ring}$, into the most stable configuration, $I_{\langle\zeta\varsigma 0\rangle}$.

# Systematic study of interstitials in Iron

- The number of bound configurations increases rapidly with cluster size, exceeding 400, 1100 and 1500 distinct bound configurations for $I_2$, $I_3$ and $I_4$
- lead to the appearance of a quasi-continuous band of states at relatively low energy above the ground state – at 0.42 eV, 0.23 eV, 0.20 eV for $I_2$, $I_3$ and $I_4$
- For $I_3$ and $I_4$, migration is more complicated and takes place via a series of jumps between configurations with relatively energies (0.3 eV or more).

M.-C. Marinica, F. Willaime and N. Mousseau, PRB (2011)

# Application to protein folding: B domain of protein A

Fast folder - used by Fersht as a way to make contact between simulation and experiment
(Sato *et al*, PNAS 2004)

60 residues

ART-OPEP
600 K
20 000 steps
(5-6 weeks on a single processor)

Jean-François St-Pierre, Ph. Derreumaux and NM, J. Chem. Phys. (2008)

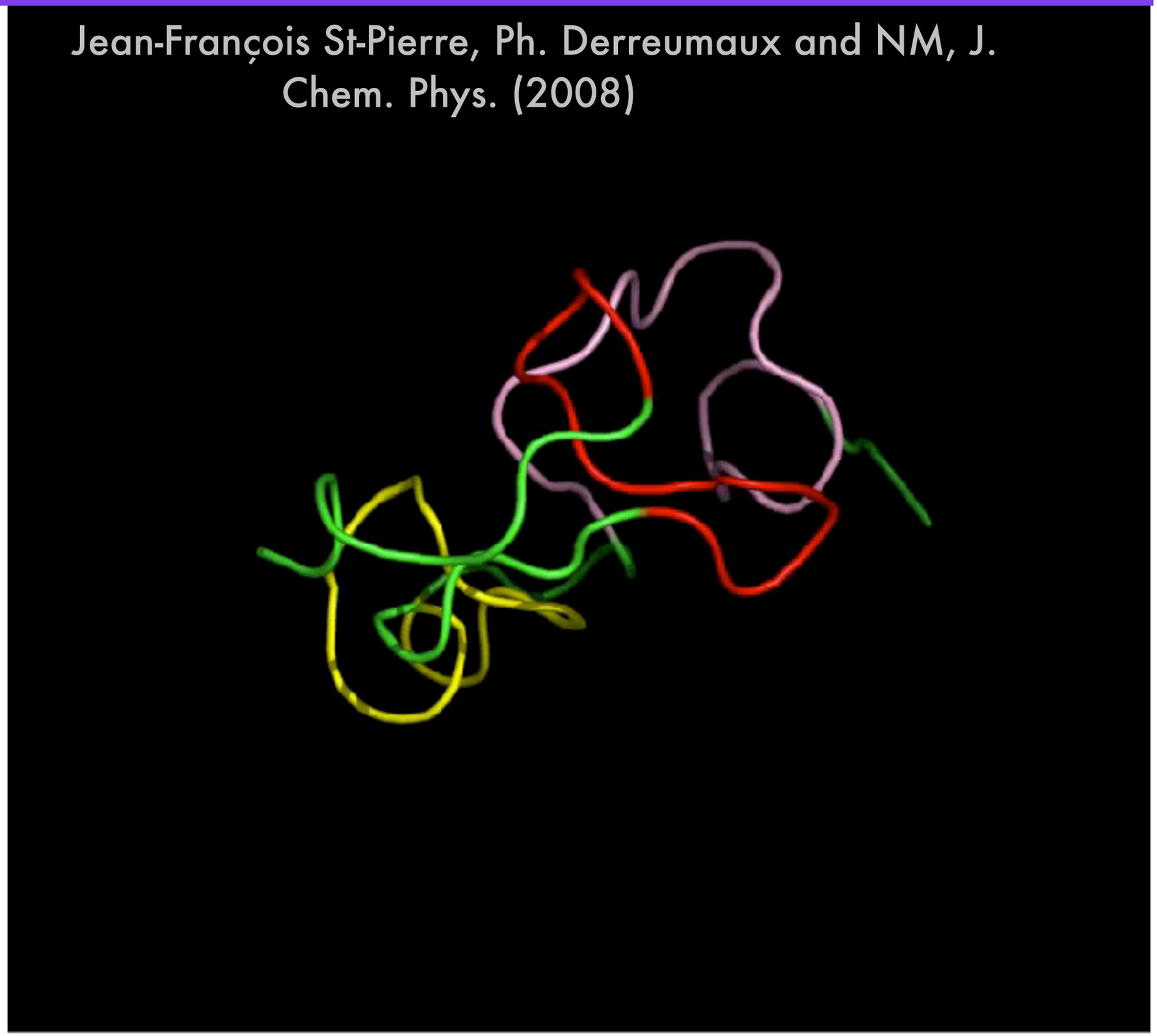

# Two differents folding paths (among many)

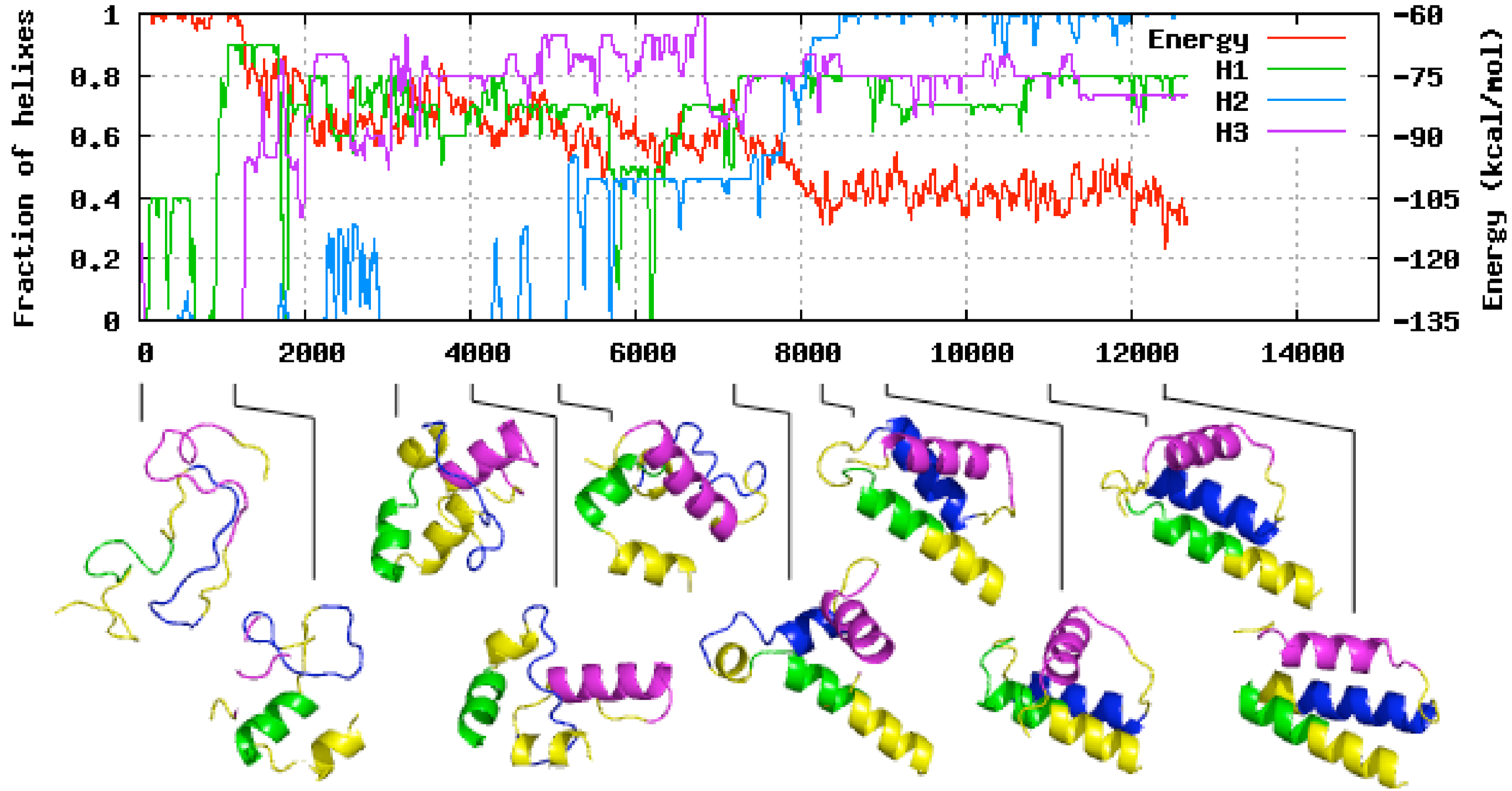

# The low-energy structures of protein A

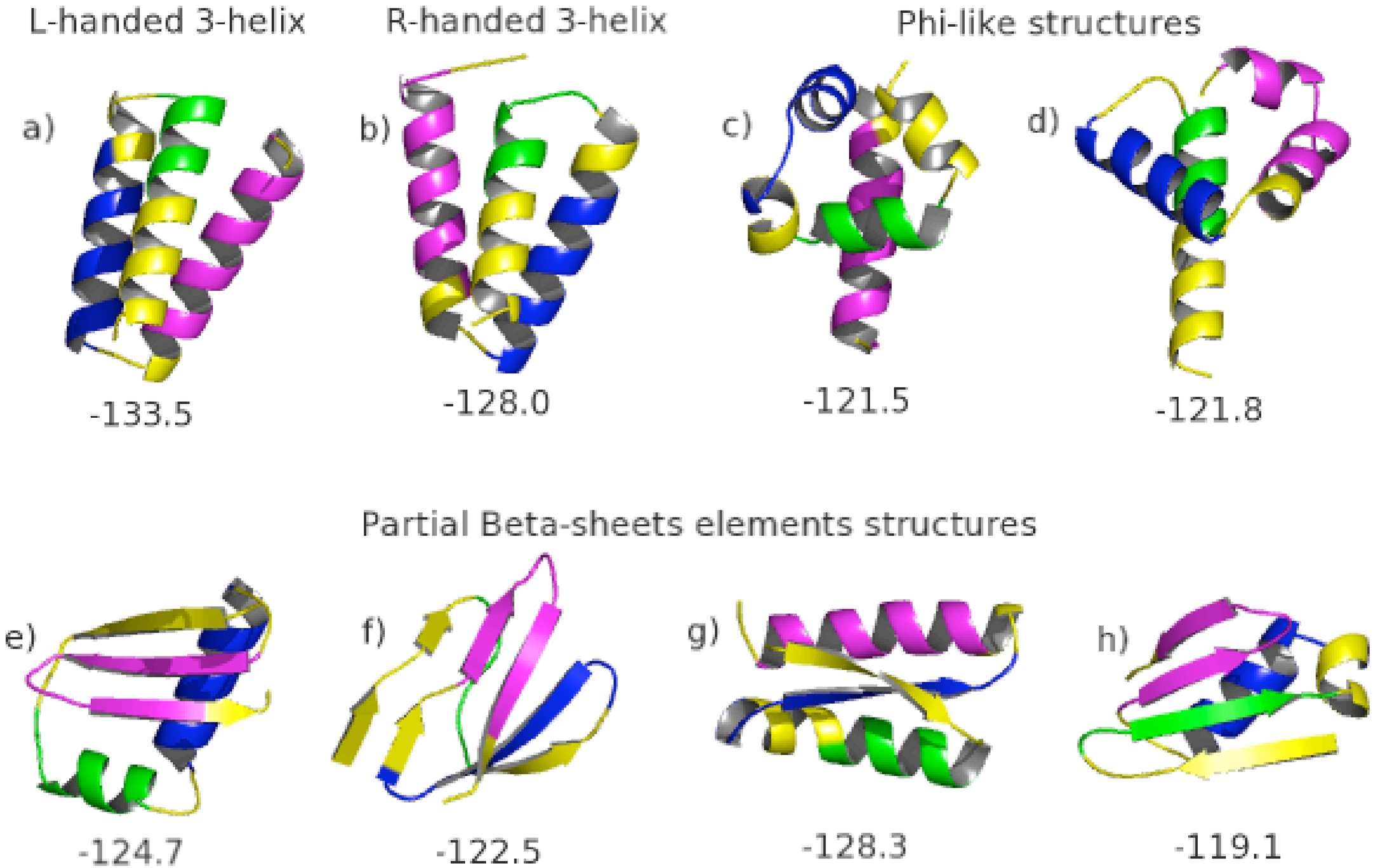

# Multiscale simulations

**Lilianne Dupuis et NM, Journal of Chemical Physics 136, 035101 (2012)**
**Lilianne Dupuis et NM, Journal of Physics: Conference Series 341, 012015 (2012).**

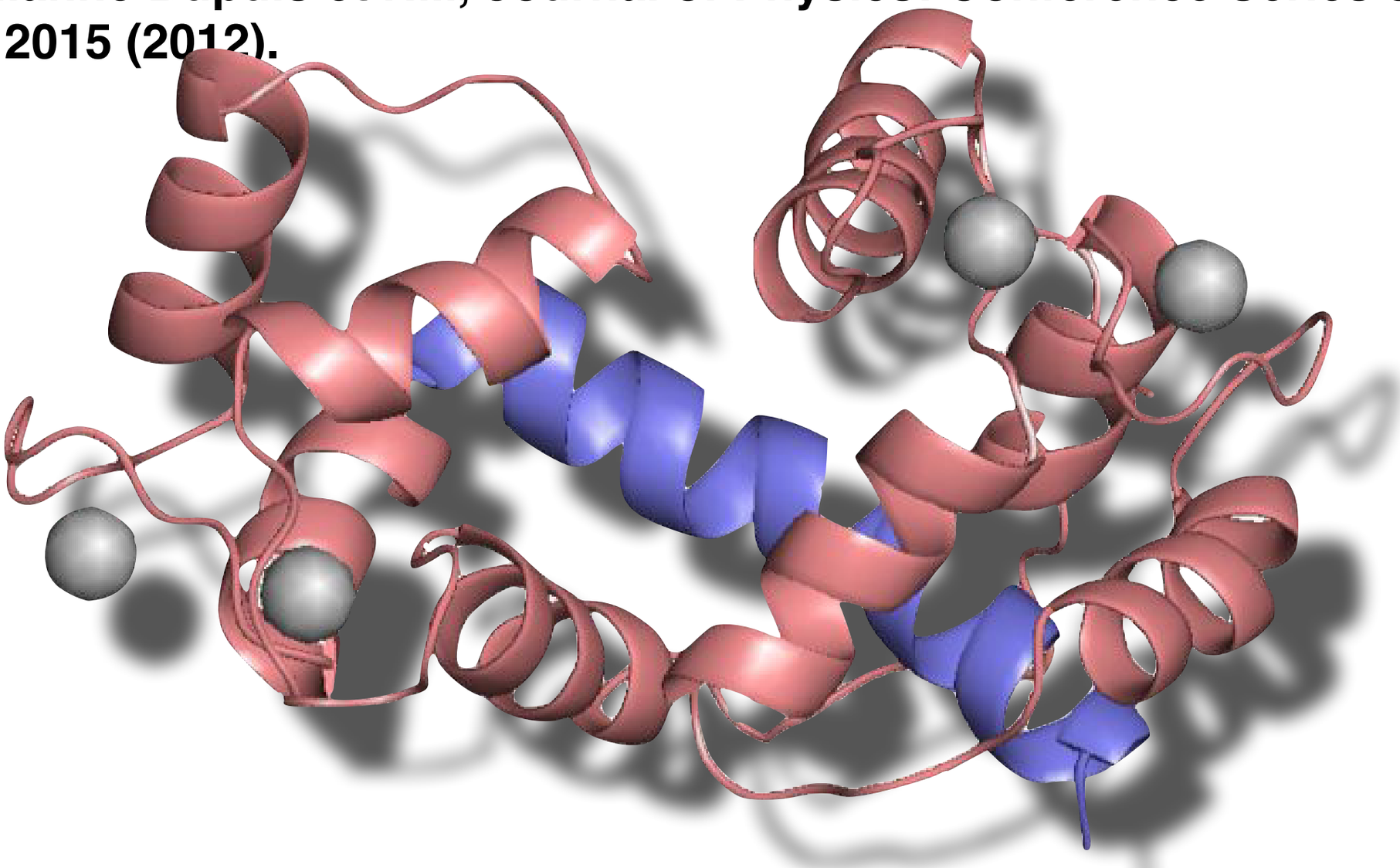

# Extended OPEP

- Implicit solvent force field

- **EOPEP Development**
  - hydrogen bonds MC-SC
  - all atom (core: F, M, etc)
  - Calibrated on protein A and Calmodulin
  - Used unmodified on troponin C and protein G
  - TRP : 12b, 18v, 30t

**Comparisons with CHARMM19/EEF1**

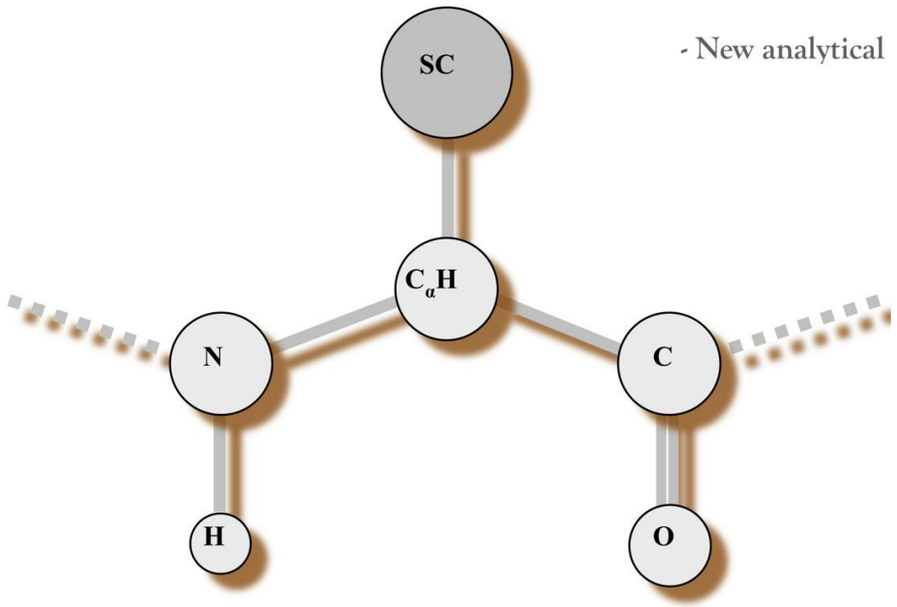


- New analytical

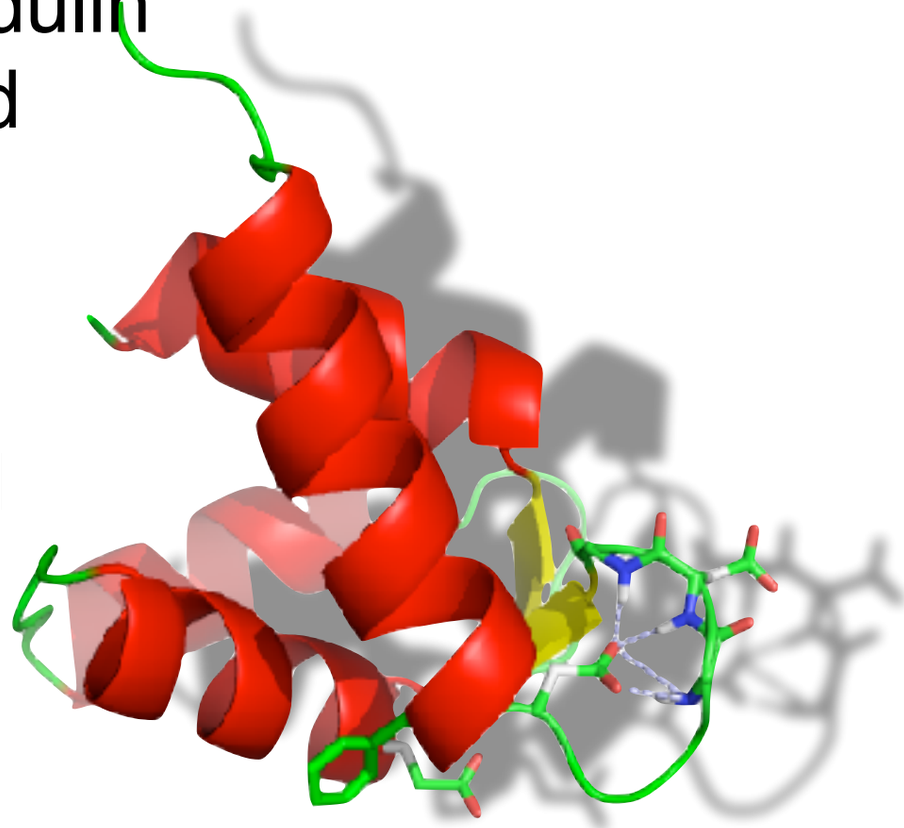

# Test : Protein A

24 simulations protein A A, 60 résidus

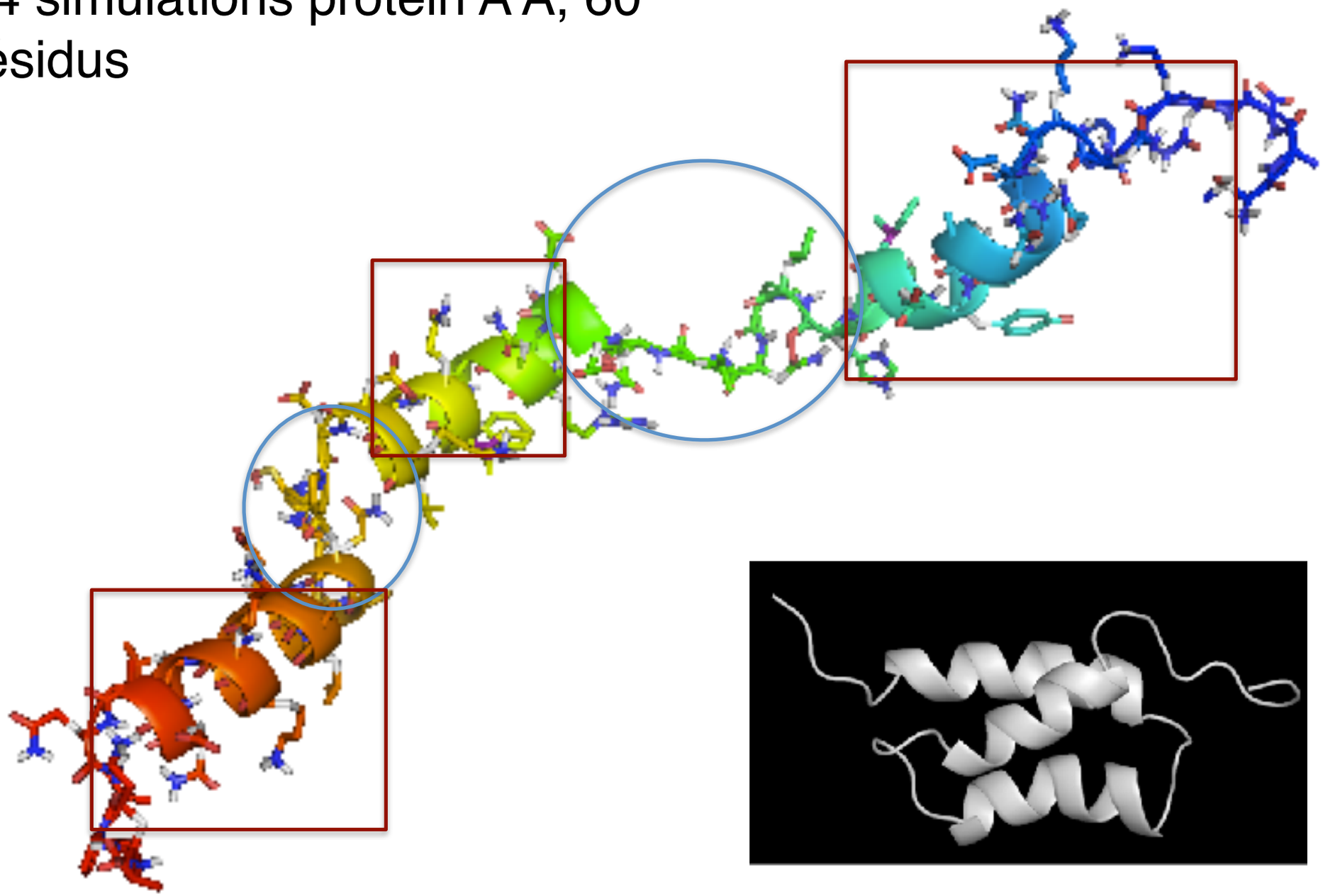



1BDC.pdb

# Test : Protein A

Protéine A, 60 résidus

# Test : Protein A

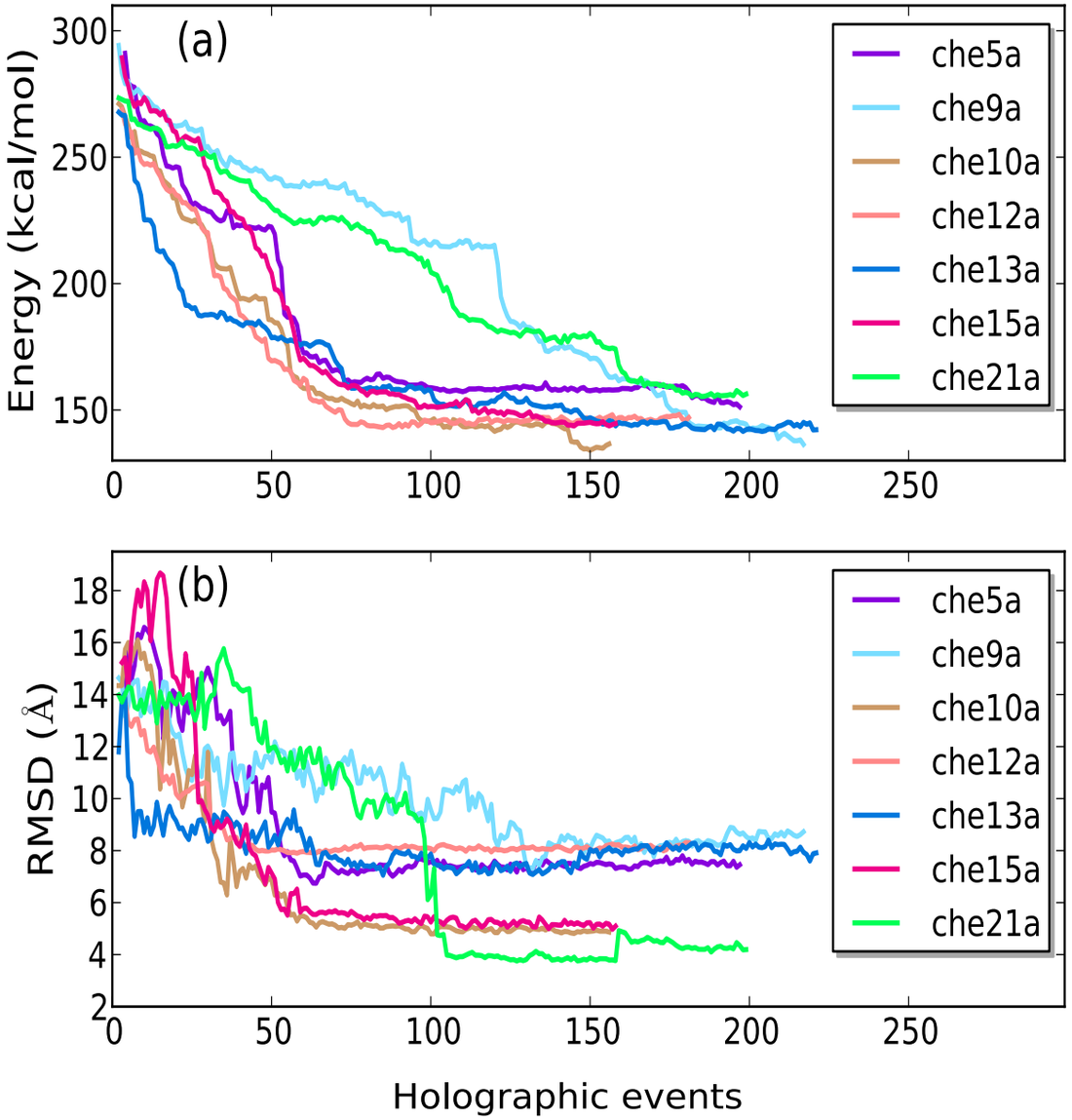


**Fermeture protéine A avec CHARM19/EEF1**

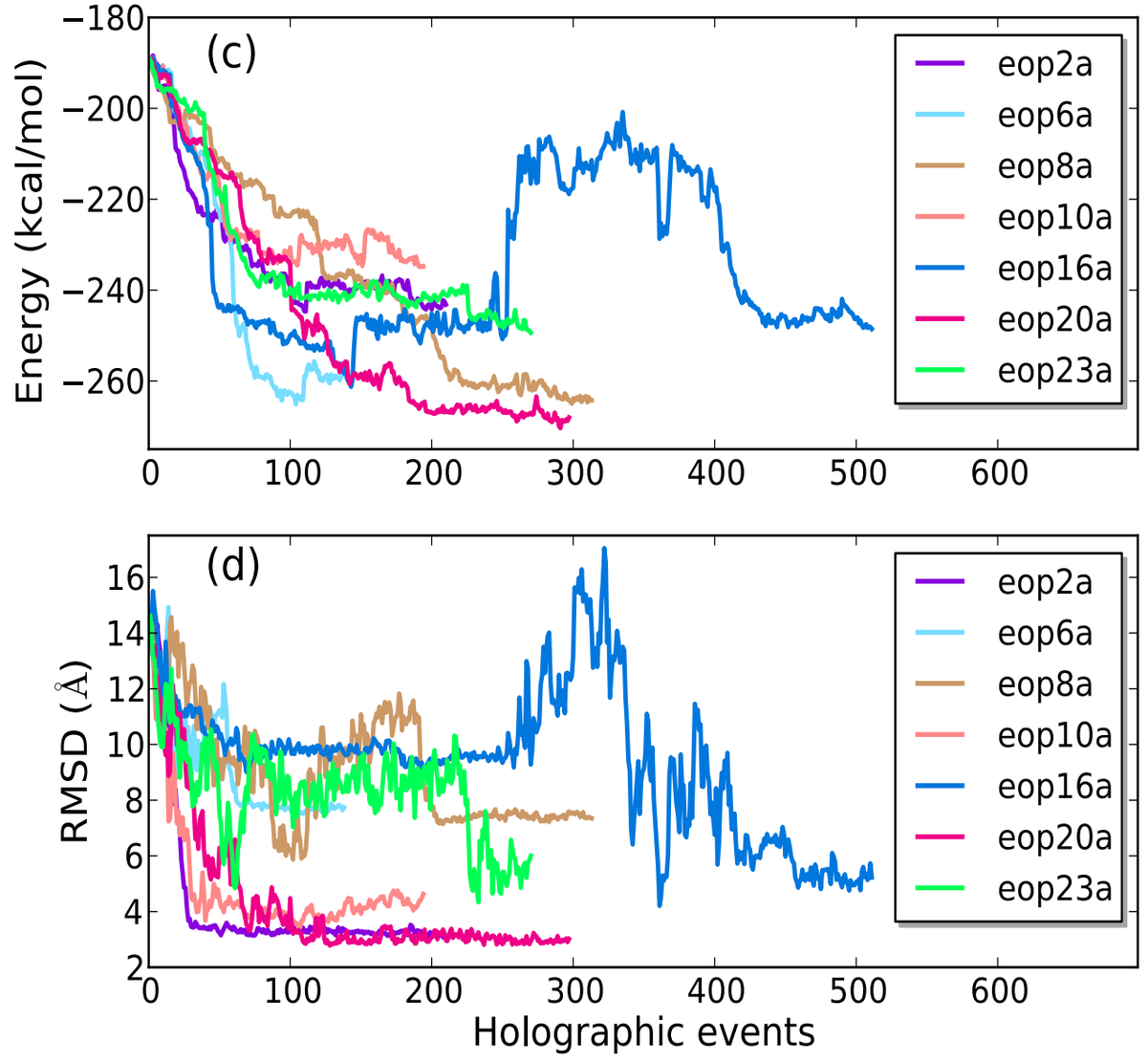


**Fermeture protéine A avec EOPEP**

# Test : Protein A

Tableau 4.II – Mean RMSD between events : statistics for a few simulation examples

| Protein model | Forcefield | Sim | mean RMSD at saddle all events | at min all events | mean RMSD at saddle accepted only | at min accepted only |
|---|---|---|---|---|---|---|
| Protein A | CHARMM19 | 5 | 2.29 | 2.39 | 1.27 | 1.28 |
| Protein A | CHARMM19 | 16 | 2.93 | 2.96 | 0.96 | 0.77 |
| Protein A | EOPEP | 1 | 4.13 | 4.38 | 1.11 | 1.03 |
| Protein A | EOPEP | 20 | 3.10 | 3.25 | 1.16 | 1.09 |
| Protein G | CHARMM19 | 2 | 2.24 | 2.03 | 1.26 | 0.98 |
| Protein G | CHARMM19 | 11 | 2.07 | 1.94 | 1.12 | 0.95 |
| Protein G | EOPEP | 2 | 2.74 | 2.66 | 1.25 | 0.83 |
| Protein G | EOPEP | 14 | 1.93 | 1.52 | 1.19 | 0.69 |

# Application to EF-hand proteins

Calmodulin Nt, 76 R

1CFD.pdb

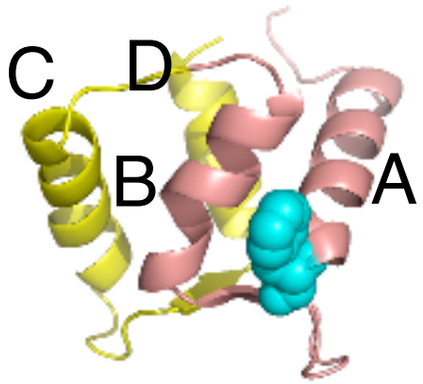


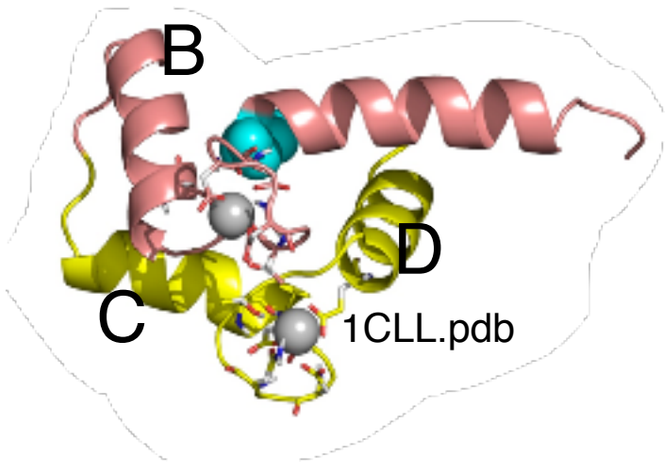


Troponin C bound to its target

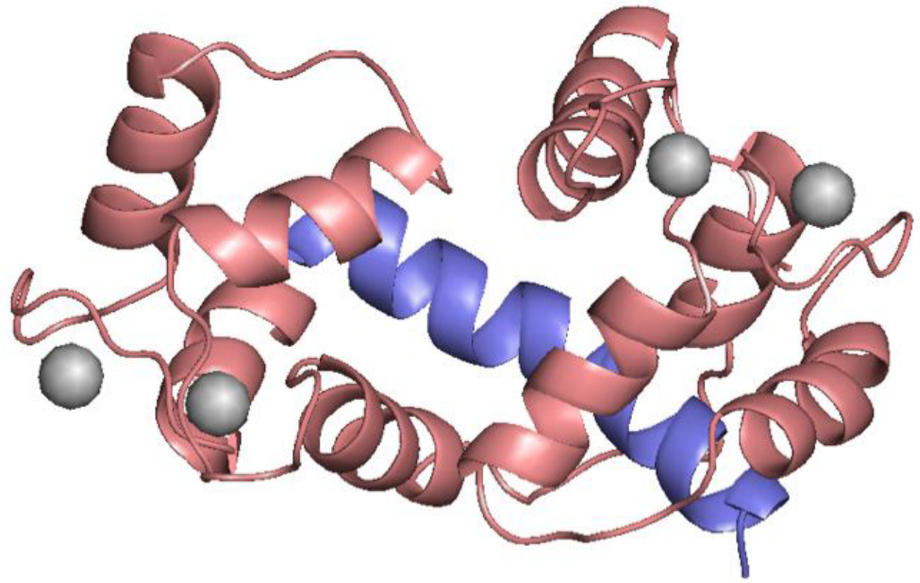

```
CaM NT
EFhand1          ADQLTEEQIAEFKEAFSLFDKDGDGTITTKELGTVMRSL
EFhand2            GQNPTEAELQDMINEVDADGNGTIDFPEFLTMMARKM
TpC NT
EFhand1  ASMTDQQAEARAFLSEEMIAEFKAAFDMFDADGGGDIKSTELGTVMRMLG
EFhand2            QNPTKEELDAIIEEVDEDGSGTIDFEEFLVMMVRQMKEDA
```

- All previous folding simulations of EF-hand proteins were biased

# X. Grabarek's hypothesis

- β-sheet that links the two-loops central zone stabilised the closed structure
- In the loop NT region, oxygen-carrying residues are very flexible and will capture $CA^{+2}$.
- This restructures the central zone in order to allow helices A & B into a perpendicular position.
- Residu GLU in position 12 moves closed and binds $CA^{+2}$.

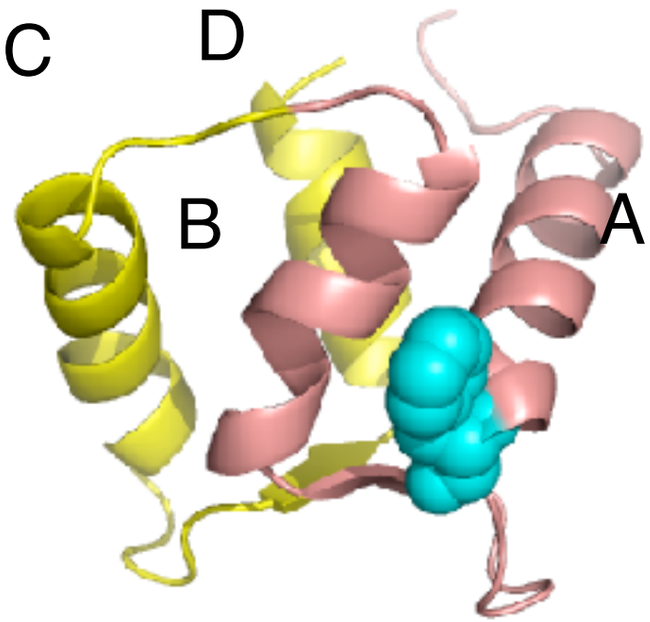

# Calmodulin closure

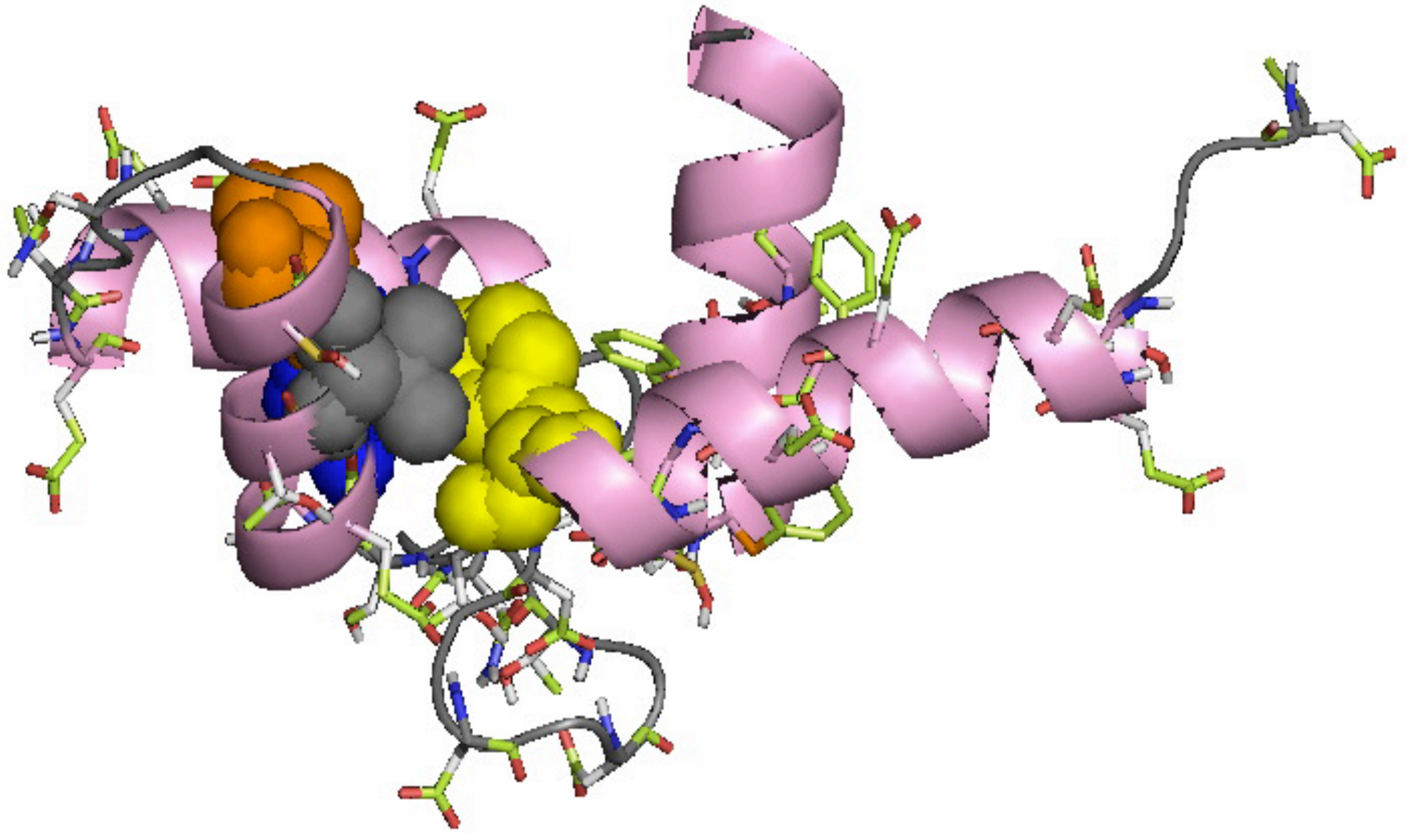

# Closing of calmodulin

EOPEP

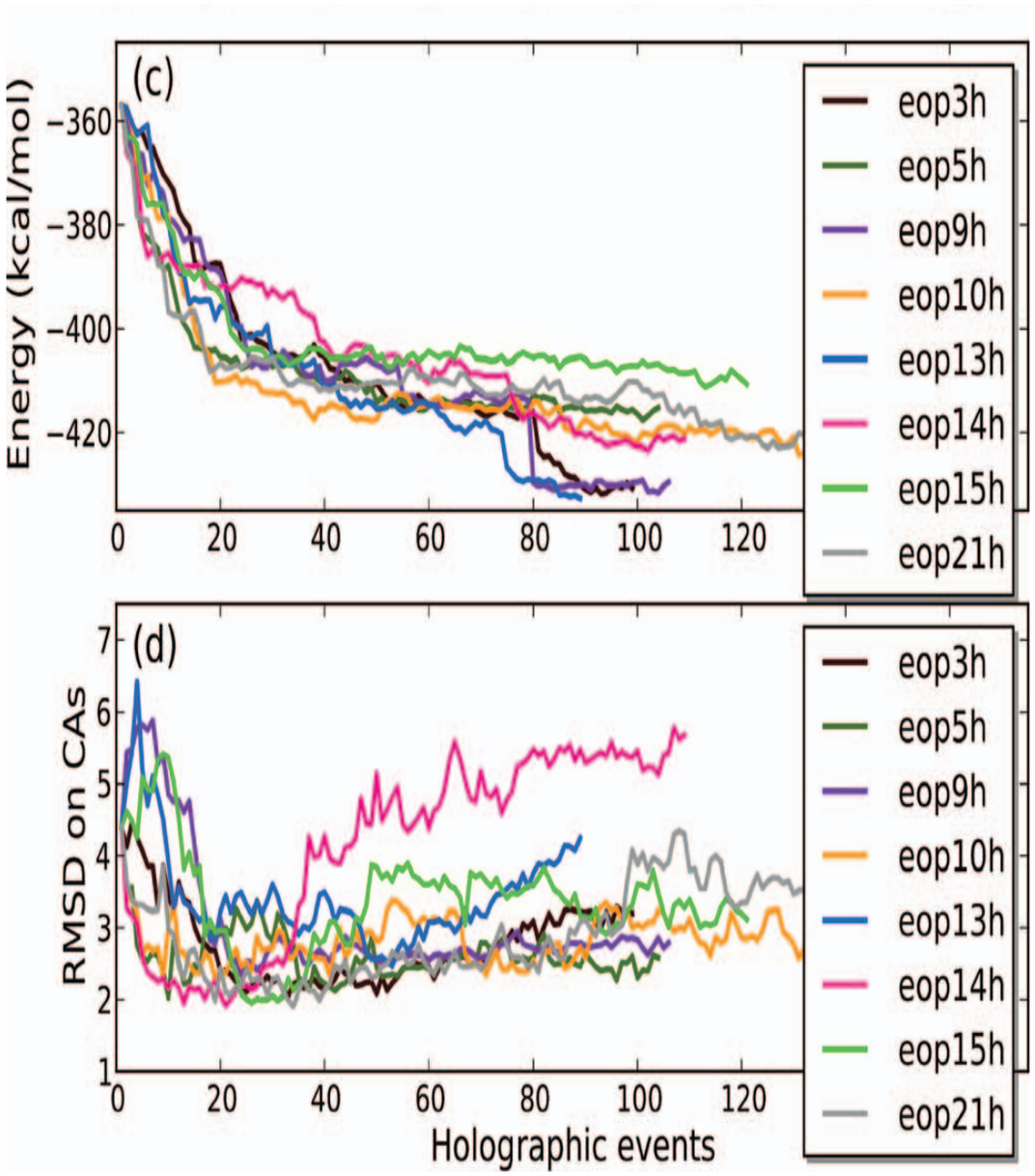


CHARMM19/EEF1

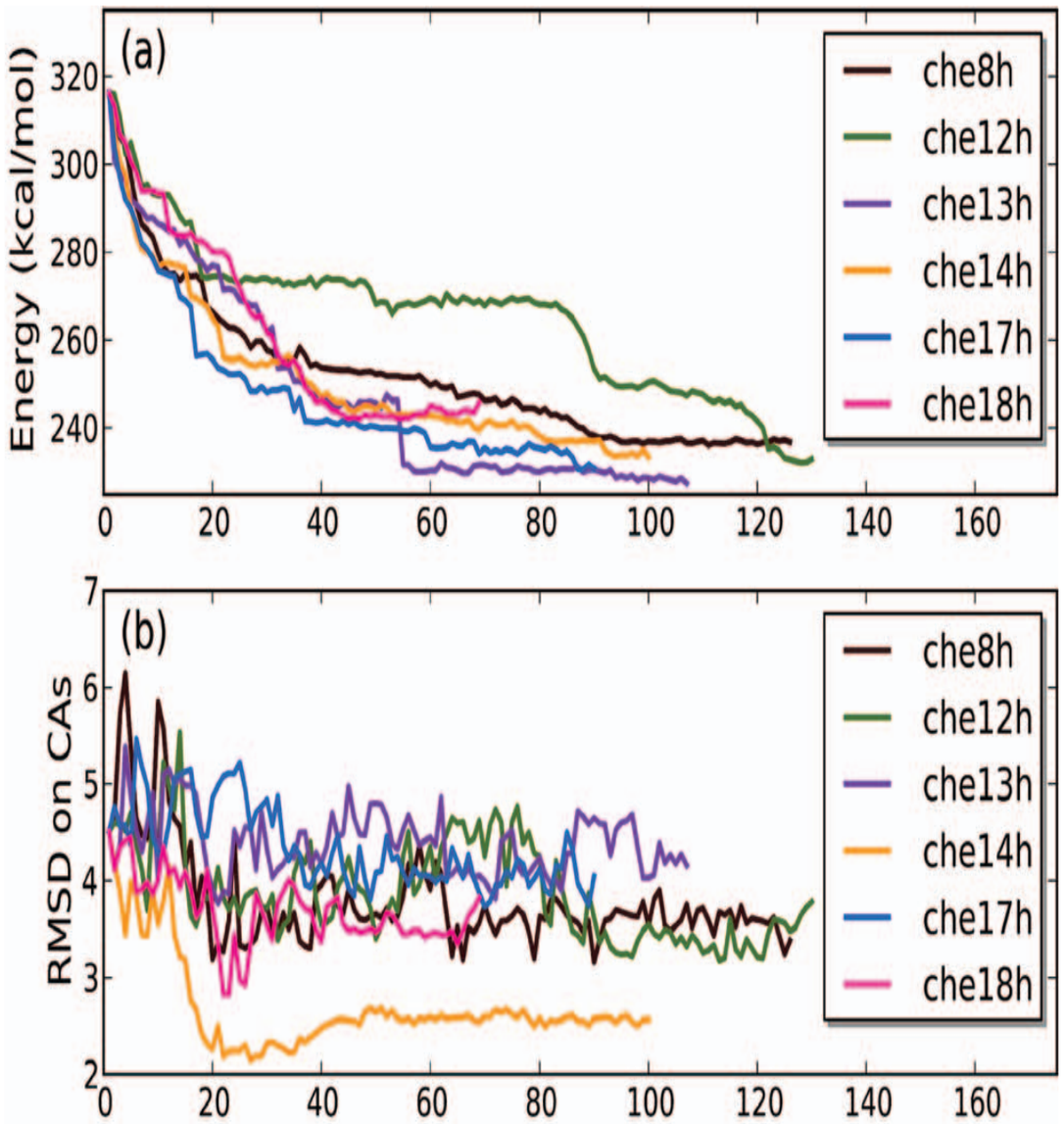

# Closing steps

1. Residues bound with $CA^{+2}$ are freed

2. Consolidation/élongation of the loop-binding β-sheet, which increases teh space between helices A and B

3. PHE19 side chains is expelled form the hydrophobic core transiting through VAL35

   CAM: 5, 4 and 5 cas at $T_{300k}$

   11/24 à ay $T_{900k}$

   17/24 including intermediate states

   TPC: PHE29, VAL45: 8/24 à 300K

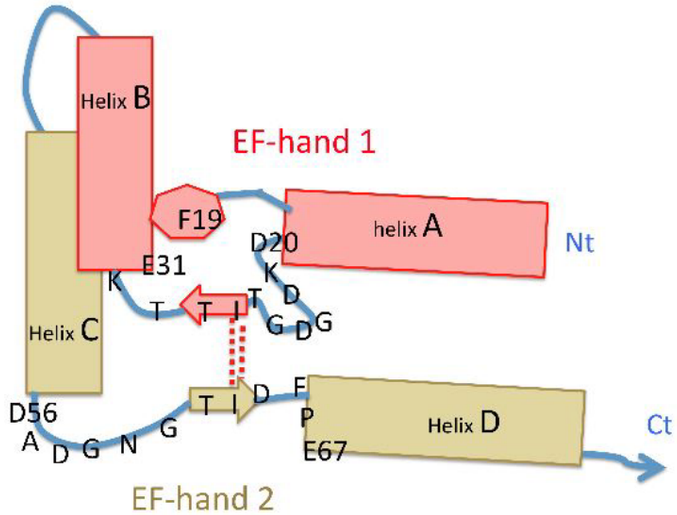


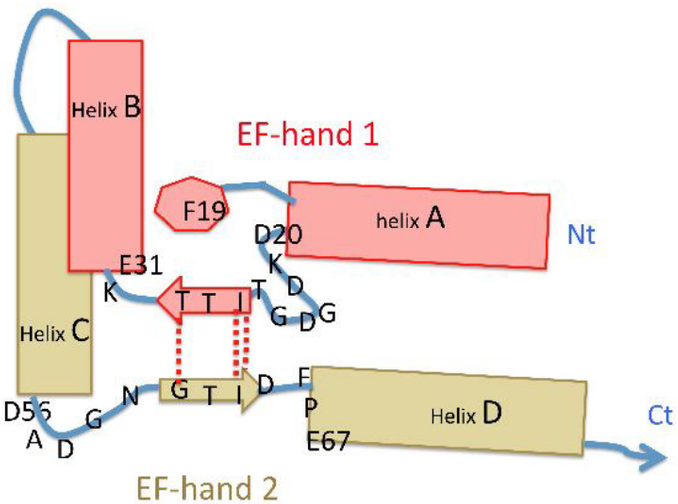


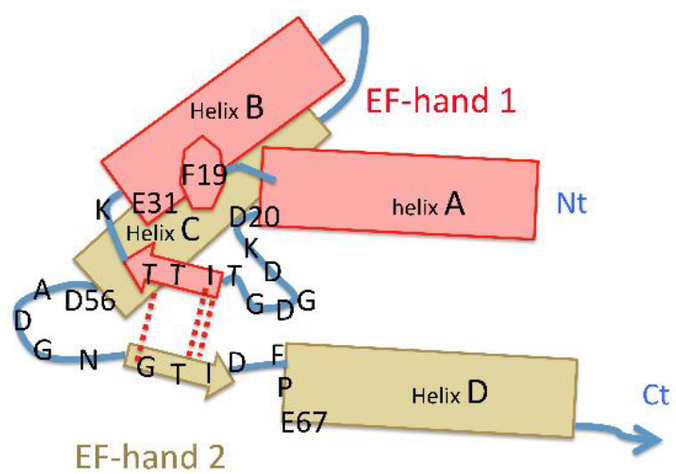

# Conclusions : EF-hands

Simulations of the open model for the NT domains of Calmodulin and Tropnonin C have managed to fold into the closed structures allowing us to identify:

- Specific intermediate steps
- the importance of a number of residues
- An intermediate state
- an irreversible sequence that suggests the opening requires the introduction of $CA^{+2}$ ions

# Some applications of ART nouveau

Ab initio calculation of defects diffusion mechanisms in Silicon, GaAs

El-Mellouhi and NM - PRB (2004, 2005), J. Appl. Phys.(2006); Malouin, PRB (2007)

Amorphous silicon - structure, relaxation and activated mechanisms

Barkema, Song and NM - PRL (1996,1998), PRE (1998), PRB (2000, 2001,2003)

Amorphous gallium arsenide - structural properties

Lewis and NM - PRL (1997), PRB (1997), Barkema and NM, JPhys:CondMatt (2004)

Interstitials in Fe

M.-C. Marinica, F. Willaime and N. Mousseau, PRB (2011)

Silica glass - structural properties, activated mechanisms

Barkema, de Leeuw - NM - JCP (2000)

Lennard-Jones clusters and glasses

Brébec, Limoge, Malek and NM, PRB (2000), Def. Diff. Forum (2001)

Protein folding

Derreumaux, Wei and NM - J. Mol. Graph. (2001), JCP (2003), Proteins (2004);
St-Pierre, Derreumaux and NM (2008)

Protein aggregation

Boucher, Derreumaux, Melquiond, Santini and NM - JACS (2004), Biophys. J., Structure (2004), JCP (2005), Accounts Chem. Res.(2005), Proteins(2006), JCP (2006,2007)

# Available

ART nouveau - via gitlab.com

# Accelerating time
# Part 3

# Outline

**1.** The challenge of simulating over multiple time scales. Energy landscapes. The transition state theory. Brief overview of various methods for breaching these time scales.

**2.** Basic concepts. Searching for saddle points. Sampling the energy landscape : the activation-relaxation technique (ART nouveau)

**3.** Accelerated MD approaches. Basic concepts kinetic Monte Carlo. Limits.

**4.** Off-lattice kinetic Monte Carlo methods. The kinetic Activation-Relaxation Technique. Topological analysis. Constructing an event catalog. Handling flickers. Limitations of current accelerated methods. Extending to large systems. Coming developments.

# Accelerated molecular dynamics

## Hyperdynamics (1997)

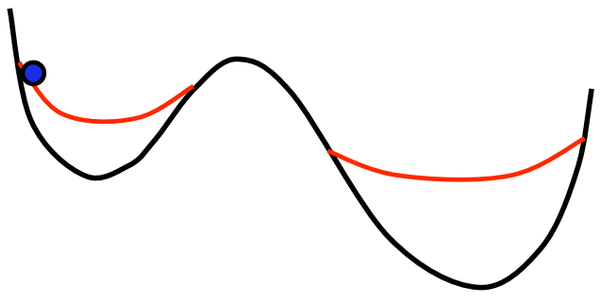

## Parallel Replica Dynamics (1998)

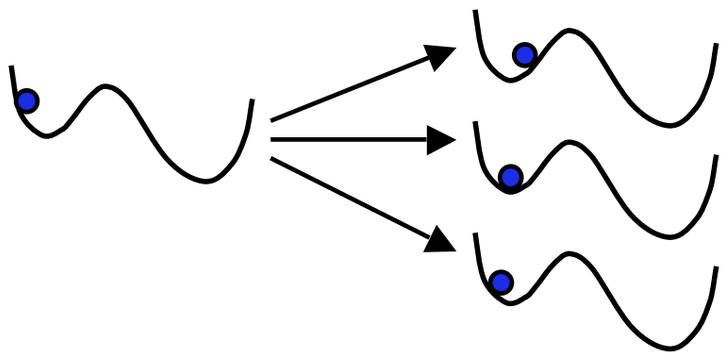

## Temperature Accelerated Dynamics (2000)

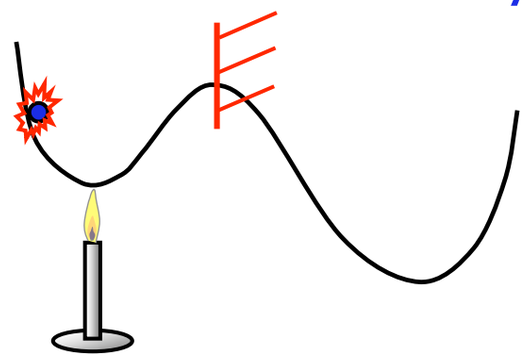

**Properly-obeyed probability**

**Activation-Relaxatoin Technique**

(Vocks, 2005)

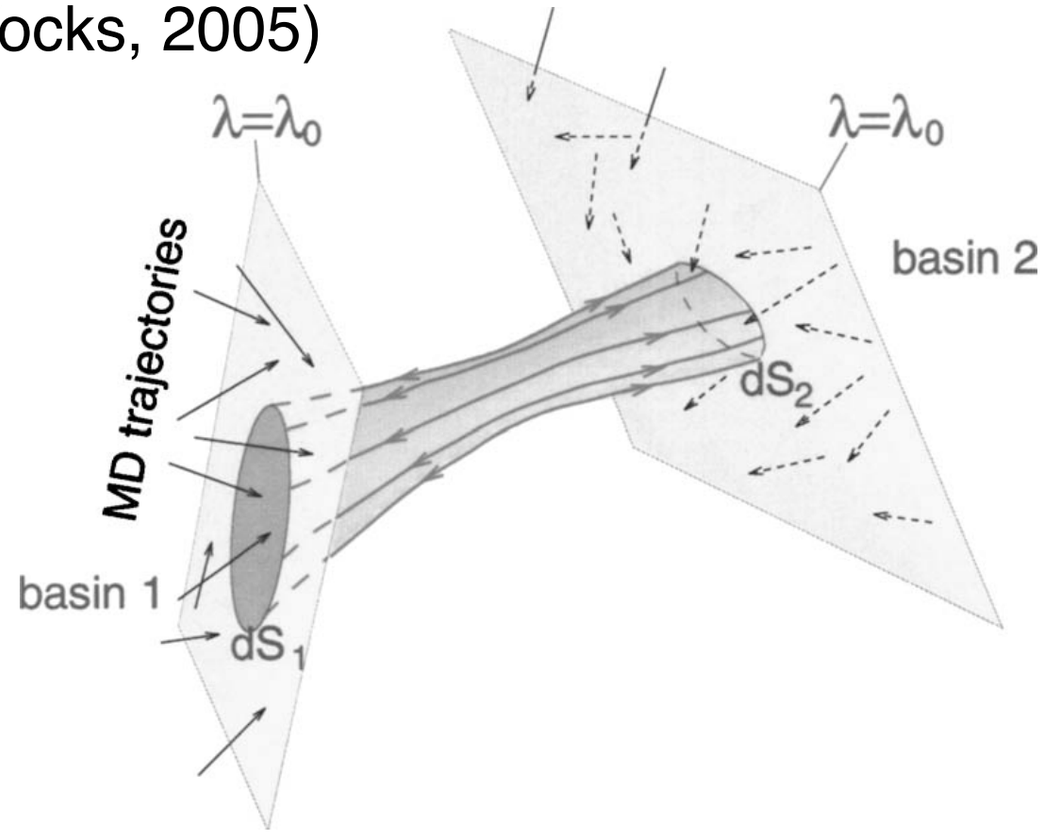


Taken from Voter's presentation

# Parallel Replica Dynamics

In a system dominated by rare events, i.e., with: A.F.Voter PRB (1998)

- infrequent and uncorrelated events
- exponential distribution of first-escape time

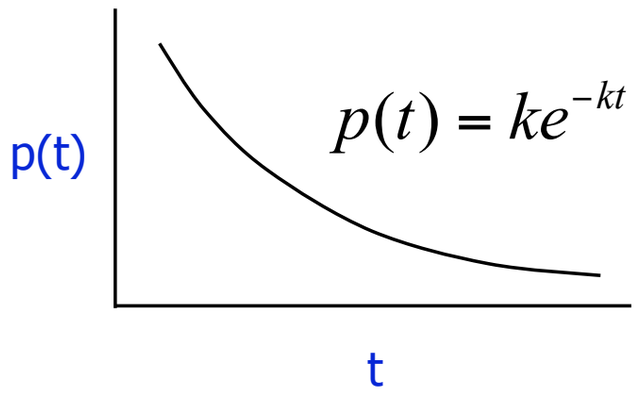


Taken from Voter's presentation, 2007

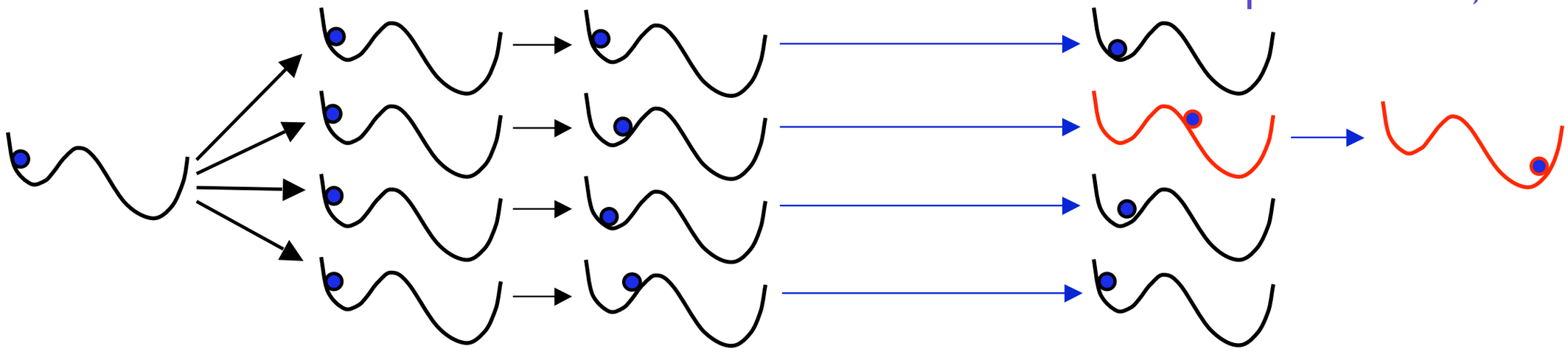

The total run time, over all copies, follows an exponential distribution and leads to the correct state

# Parallel Replica Dynamics: Example

## Simulation of Stick–Slip Friction

Martini et al. Tribol Lett (2009)

Applied rate : M*physical rate

M= number of replicas

Here: up to 256 cores

**Steps:**

1- Dephasing/decorrelation

2. MD

3. Minimisation

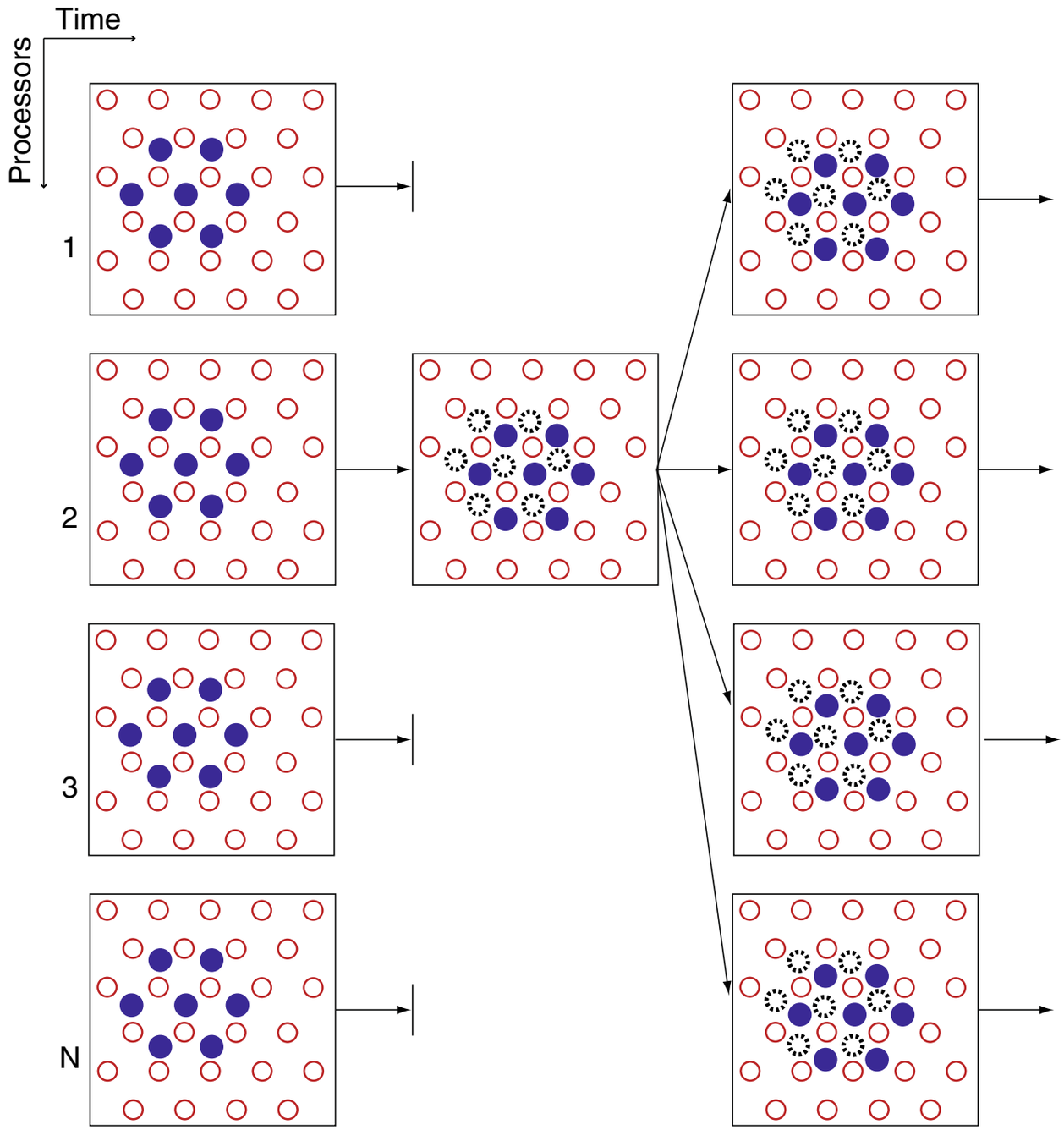

# Parallel Replica Dynamics: Example

## Simulation of Stick–Slip Friction

Martini et al. Tribol Lett (2009)

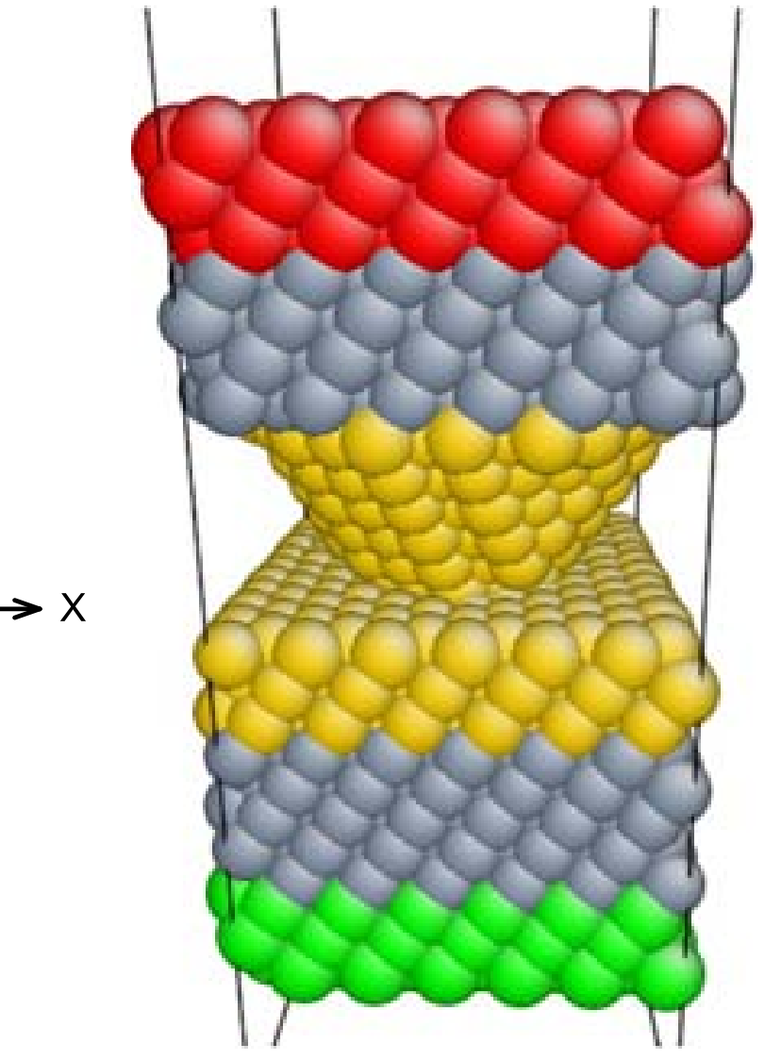


← Y position fixed and velocity applied in x direction

← Thermostat applied

← Transition detection region

← Thermostat applied

← X, y, and z positions fixed

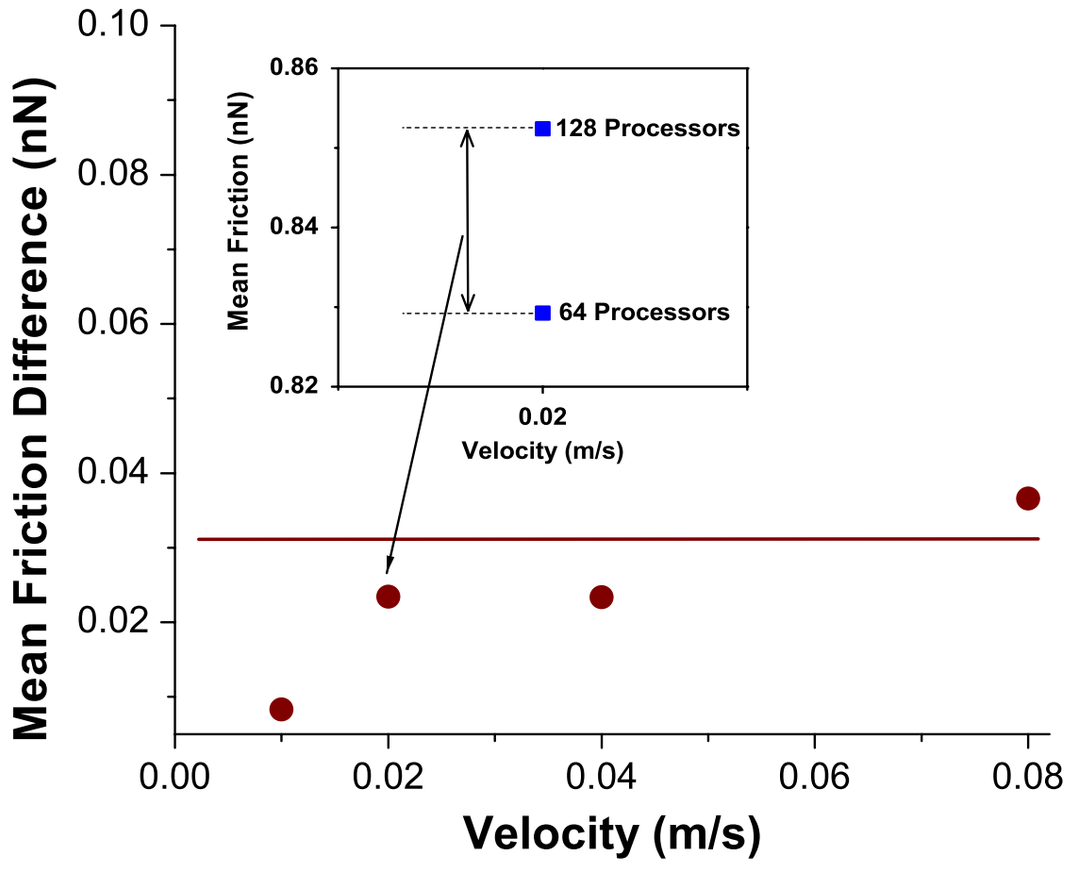

# Temperature-accelerated dynamics

- Run MD at elevated temperature ($T_{high}$) in state A.

- Intercept each attempted escape from basin A

- find saddle point (and hence barrier height)

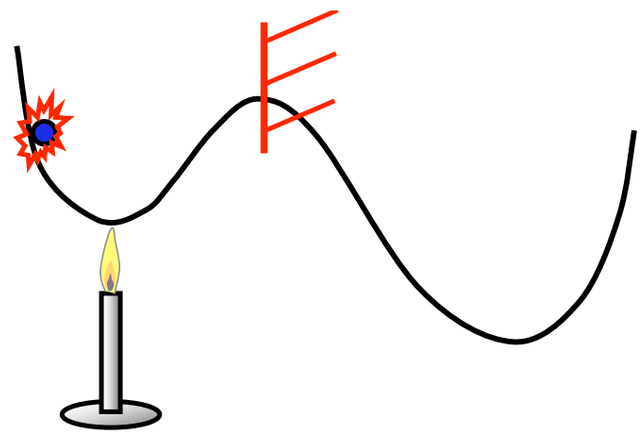

- extrapolate to predict event time at $T_{low}$.

- Reflect system back into basin A and continue.

- When safe, accept transition with shortest time at $T_{low}$.

- Go to new state and repeat.

Taken from Voter's presentation

# Temperature-accelerated dynamics

- If each transition follows the Arhenius law:

  $k = \nu_0 \exp[-\Delta E/kBT]$ ,

- Then it is possible to extrapolate the first-escape time at low temperature from

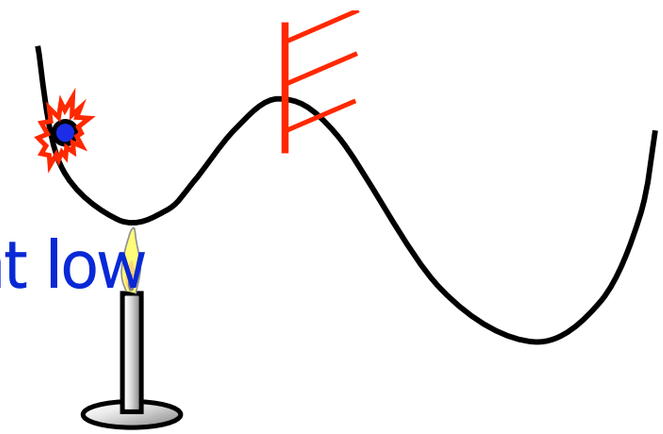

$t_{low} = t_{high} \exp[\Delta E(1/kBT_{low} - 1/kBT_{high})]$

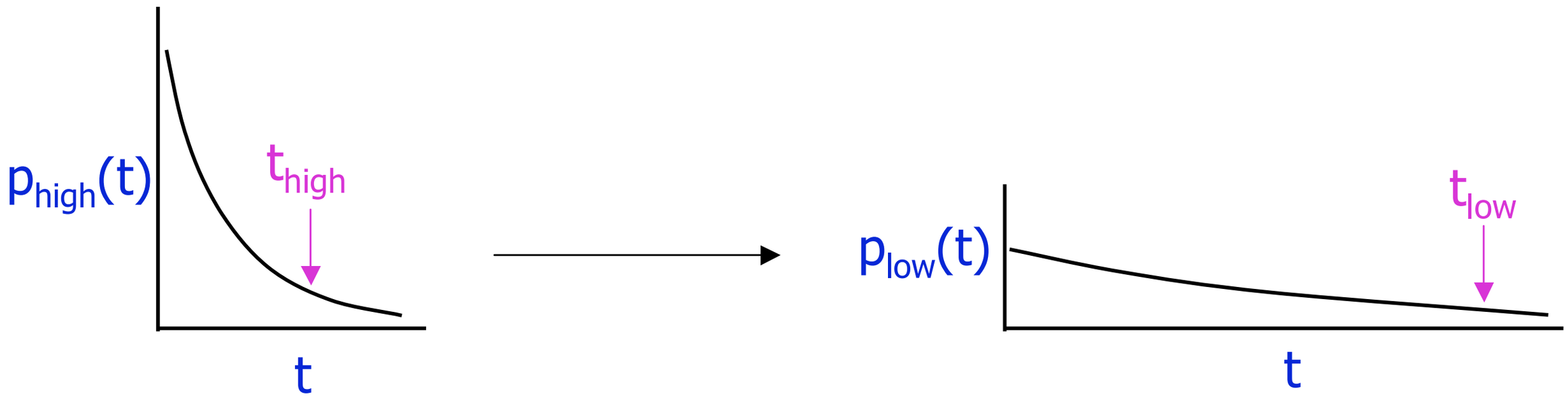


Taken from Voter's presentation

# Temperature-accelerated dynamics

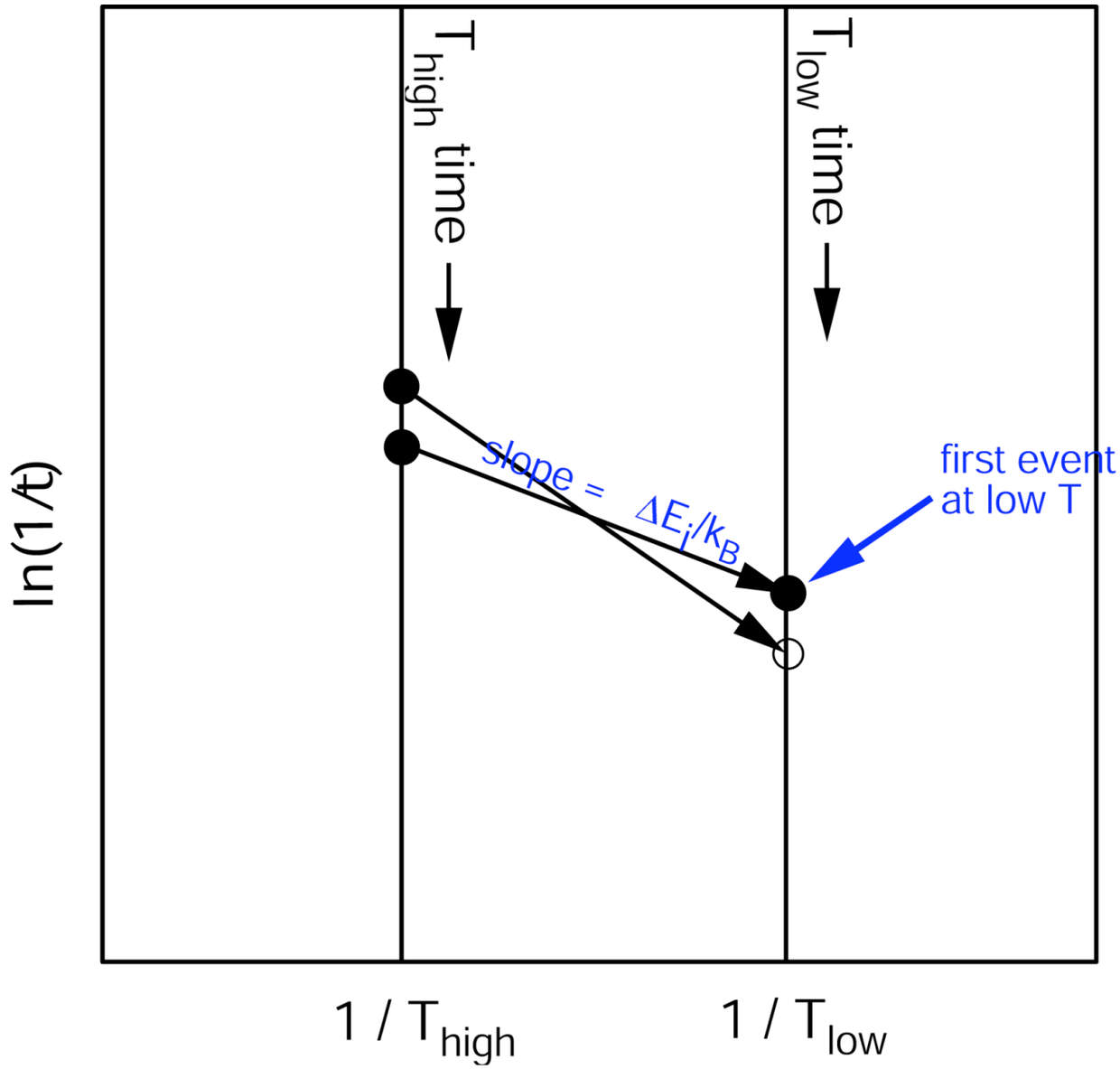


Taken from Voter's presentation

# Temperature-accelerated dynamics : Example

## Vacancy Formation and Strain in Low-Temperature Cu=Cu(100) Growth

Shim *et al. PRL (2008)*

$T_{high}$ = 200-400 K

$T_{low}$ = 40 K

$\nu_{min} = 10^{12} s^{-1}$

Here: up to 256 cores

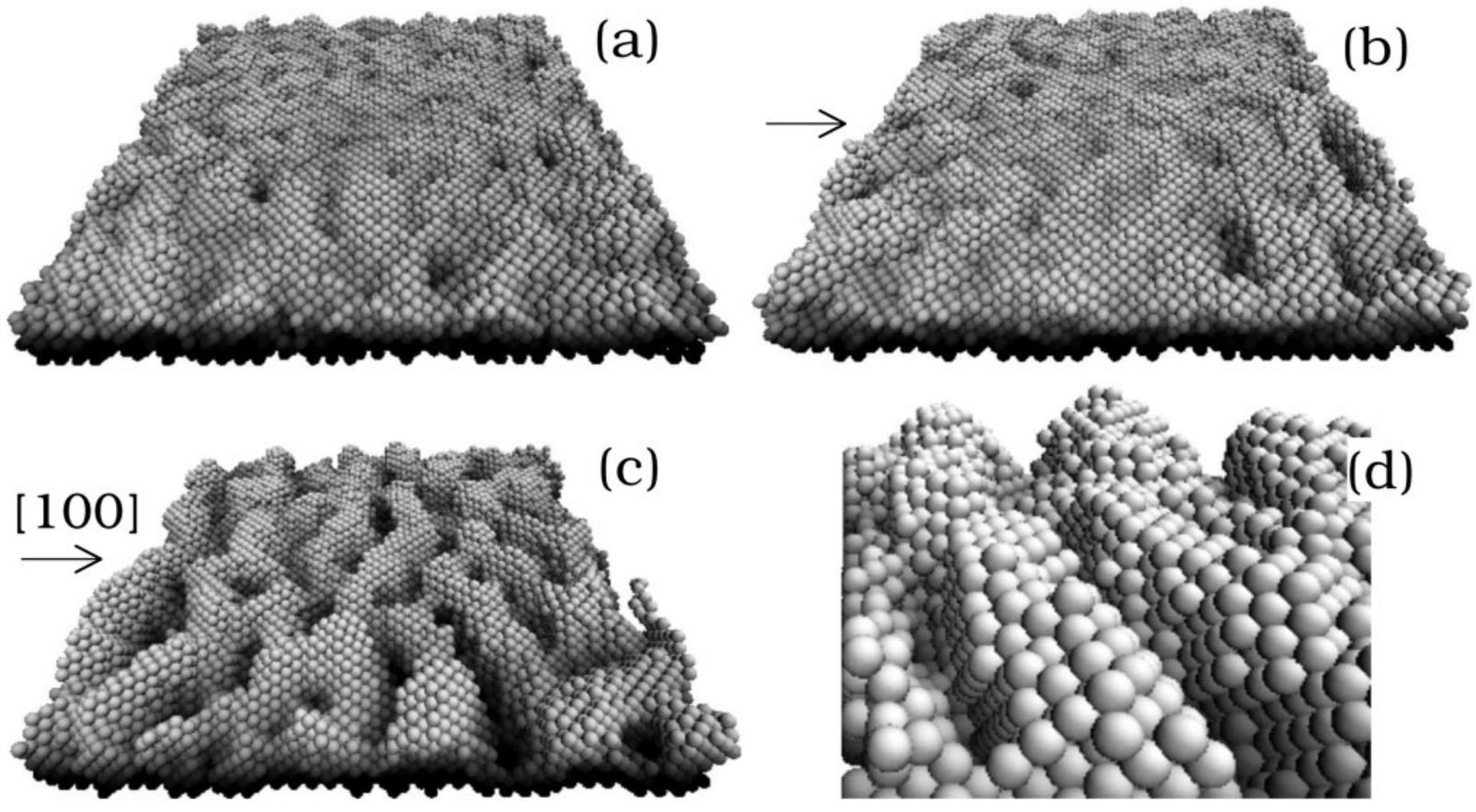


Highest barrier at 40 K : 0.06 eV

# Accelerated molecular dynamics

## Hyperdynamics (1997)

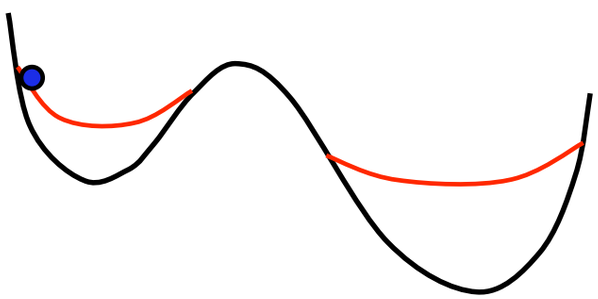

## Parallel Replica Dynamics (1998)

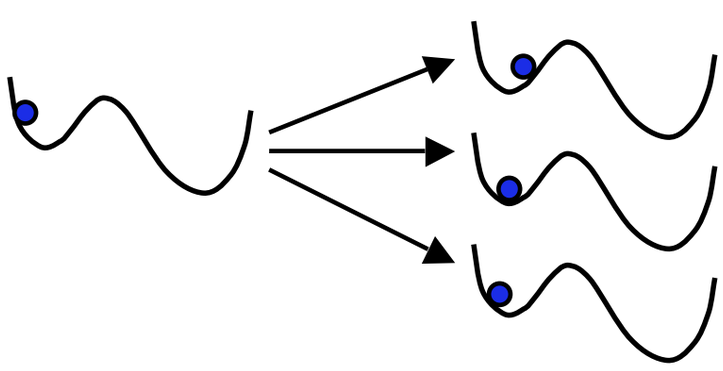

## Temperature Accelerated Dynamics (2000)

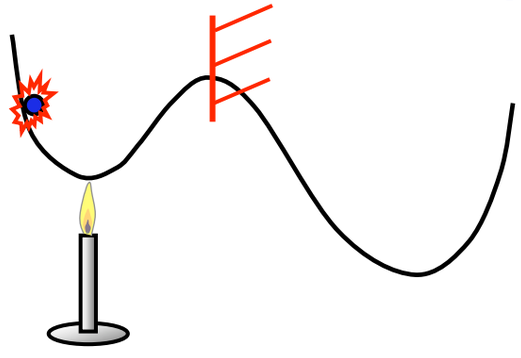

Taken from Voter's presentation

**Properly-obeyed probability**
**Activation-Relaxation Technique**
(Vocks, Mousseau et al, 2005)

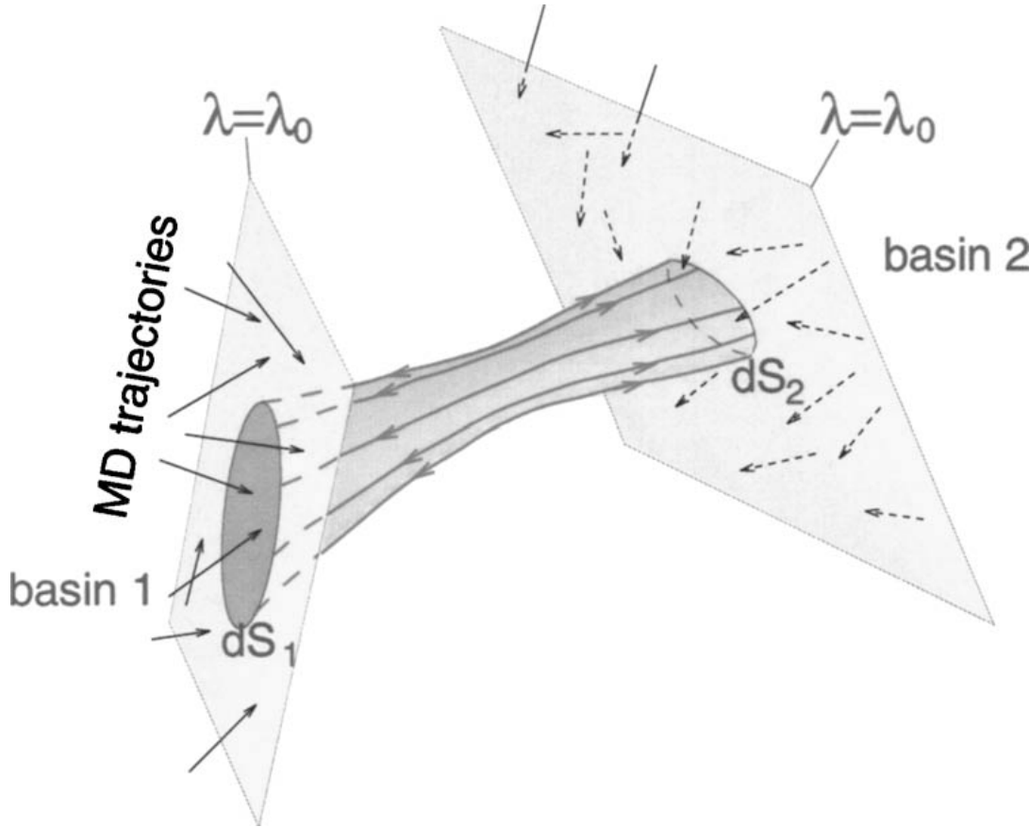

# Hyper molecular dynamics

Concept: Fill the basins with a bias potential to increase the rate of escape and renormalize the time accordingly.

Assumptions:

- transition state theory (no recrossings)

Taken from Danny Perez + AF. Voter presentation, 2008

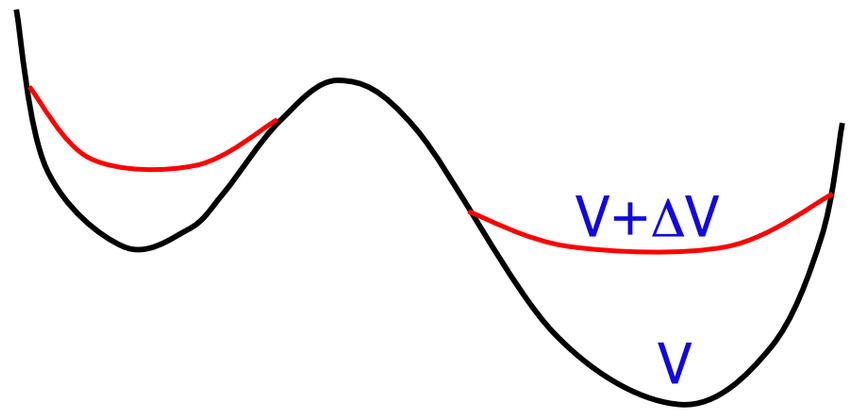


Procedure:

- design bias potential $\Delta V$ which is zero at **all** dividing surfaces so as not to bias rates along different pathways.
- run thermostatted trajectory on the biased surface ($V+\Delta V$)
- accumulate hypertime as

$$t_{hyper} = \Sigma \Delta t_{MD} \exp[\Delta V(R(t))/k_B T]$$

Result:

- state-to-state sequence correct
- time converges on correct value in long-time limit (vanishing relative error)

AFV, J. Chem. Phys. 106, 4665 (1997)

# Hyper molecular dynamics : Example

System coordinate

MD clock

hypertime clock

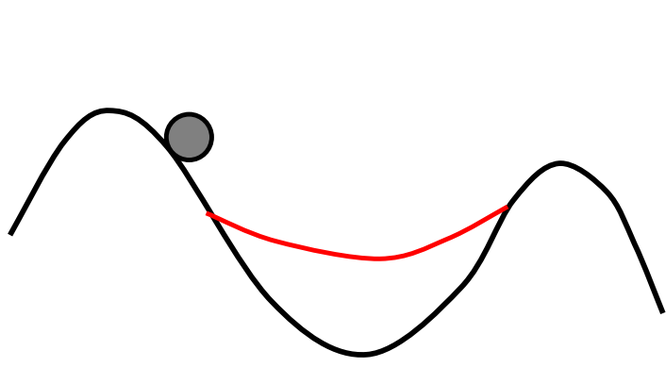


Taken from Danny Perez + AF. Voter presentation, 2008

Boost = hypertime/(MD clock time)

# Hyper molecular dynamics : Example

Key challenge is designing a bias potential that meets the requirements of the derivation and is computationally efficient. This is very difficult since we do not have any a priori information about neighboring states nor about the dividing surfaces in between them. Futher, we have to work in very high dimension.

## An extremely simple form: flat bias potential

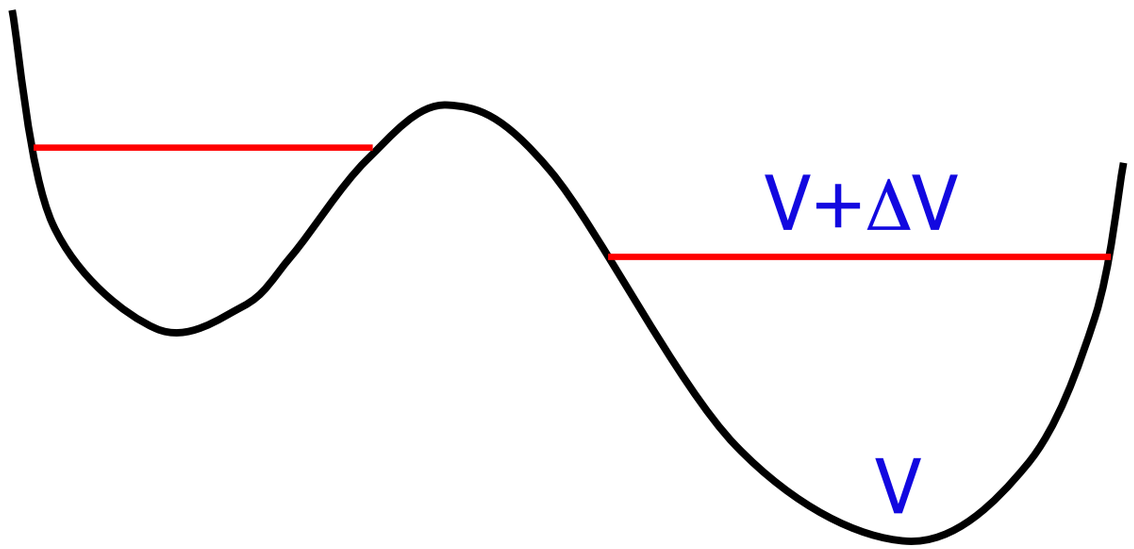


Taken from Danny Perez + AF. Voter presentation, 2008

# Hyper molecular dynamics : Example

Ag monomer on Ag (100) at T=300K: long time behavior

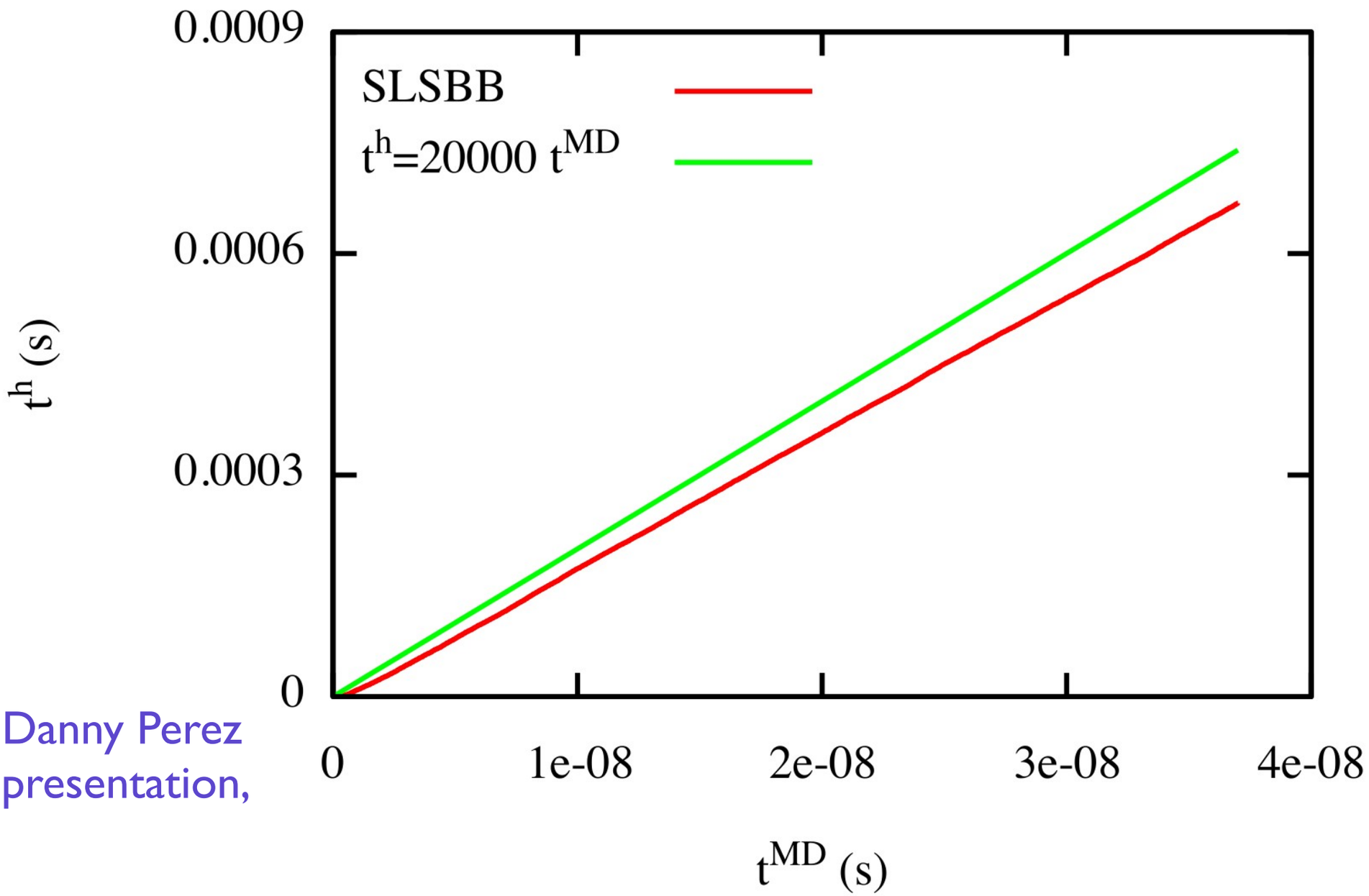


Taken from Danny Perez + AF. Voter presentation, 2008

# Properly-obeying-probability activation-relaxation technique

Can we mix ART with a dynamical method to generate a thermodynamically-weighted version of ART ?

POP-ART POP-ART

POP-ART POP-ART

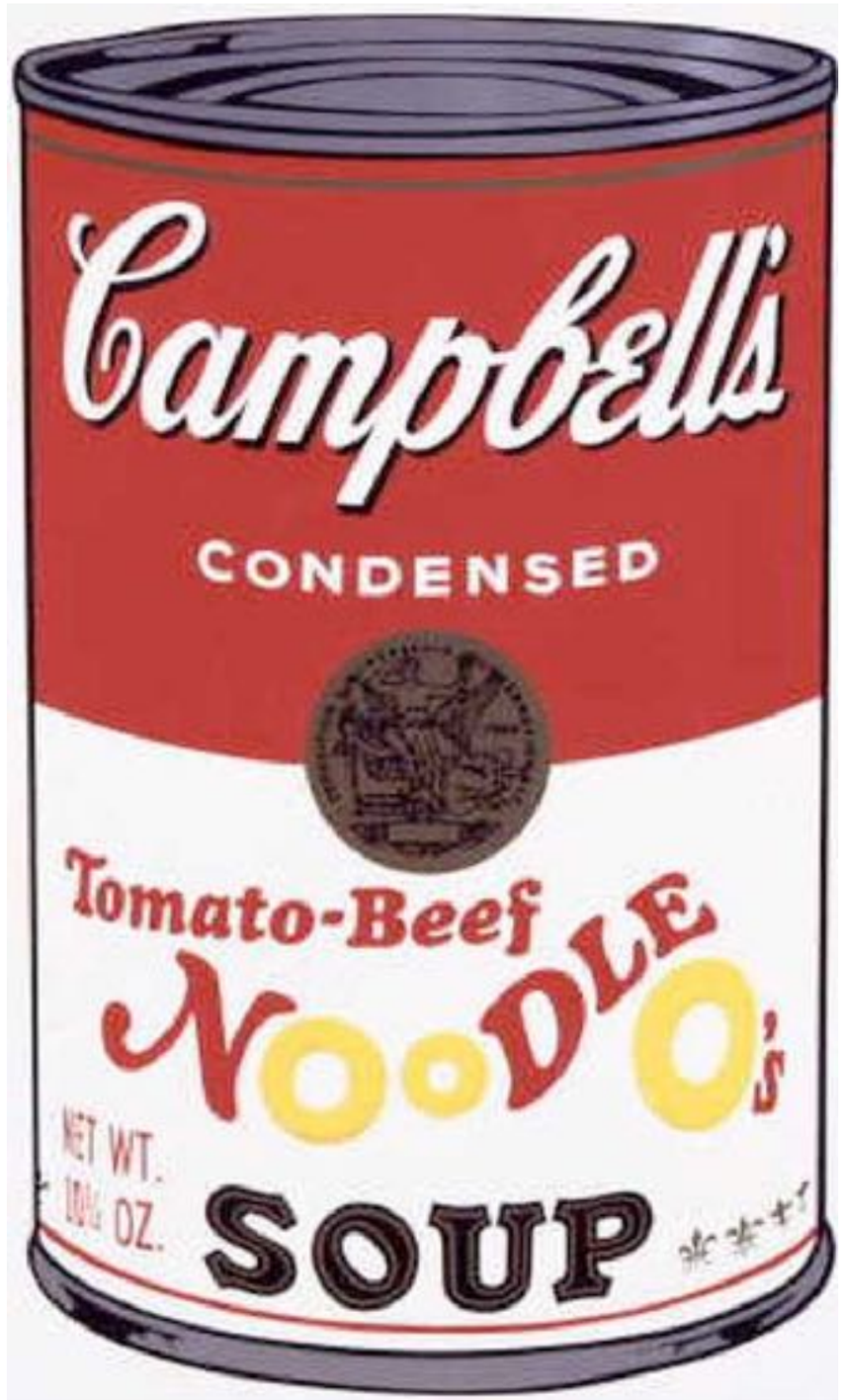

# Basic idea

We divide the landscape into two regions :

**basins:** regions where all the eigenvalues associated with the curvature of the energy landscape are above a give threshold

**saddle regions:** regions where at least one eigenvalue is below the threshold.

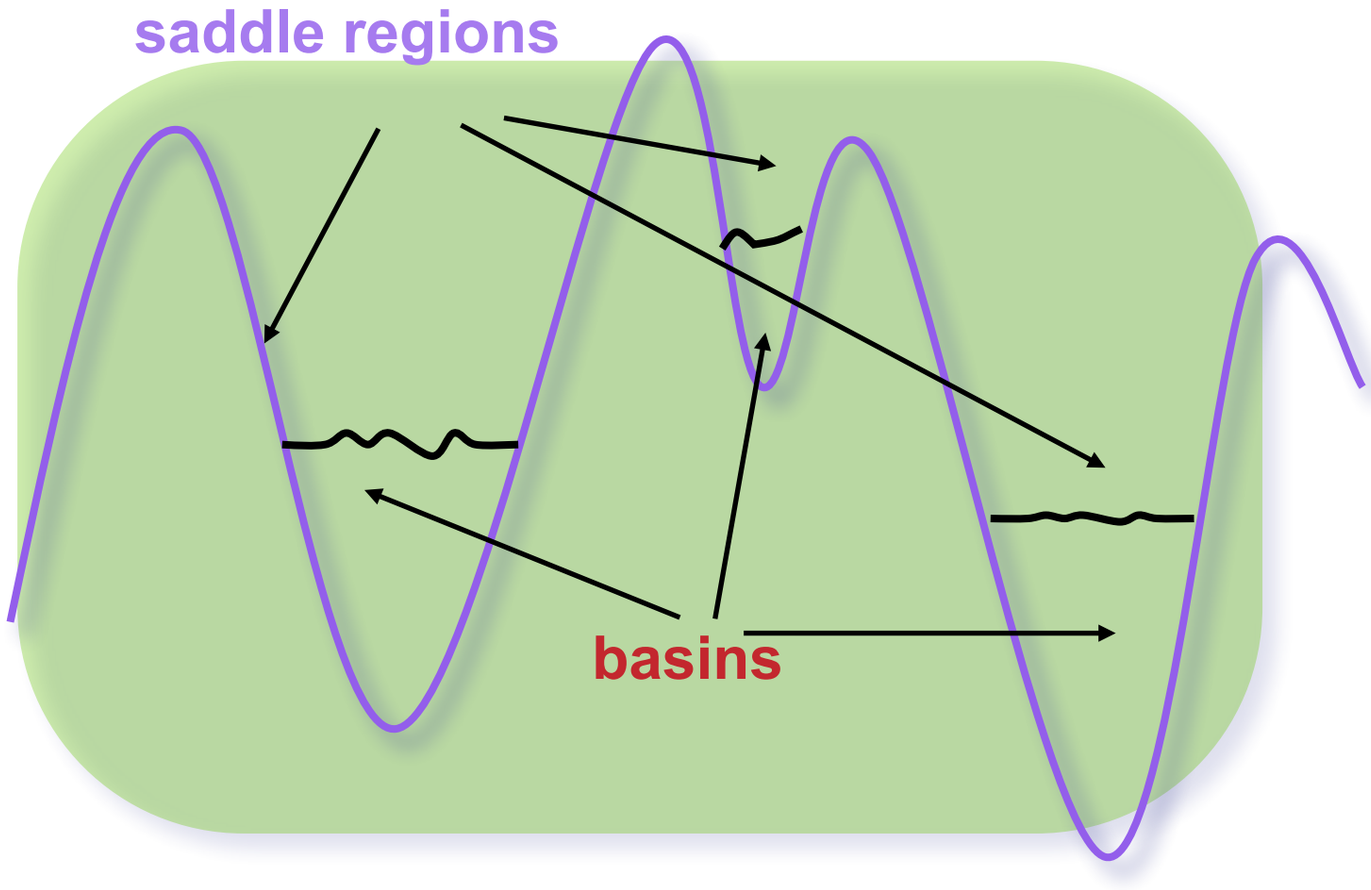


At low temperature, the system samples only the region of phase space associated with the basin regions

The saddle regions are not visited often and do not contribute significantly to the thermodynamics

# Algorithm

Three steps:

1. Standard finite temperature molecular dynamics in a minimum well.

2. As we find a negative eigenvalue, we move on a constant configurational- energy surface following the direction associated with the lowest eigenvalue.

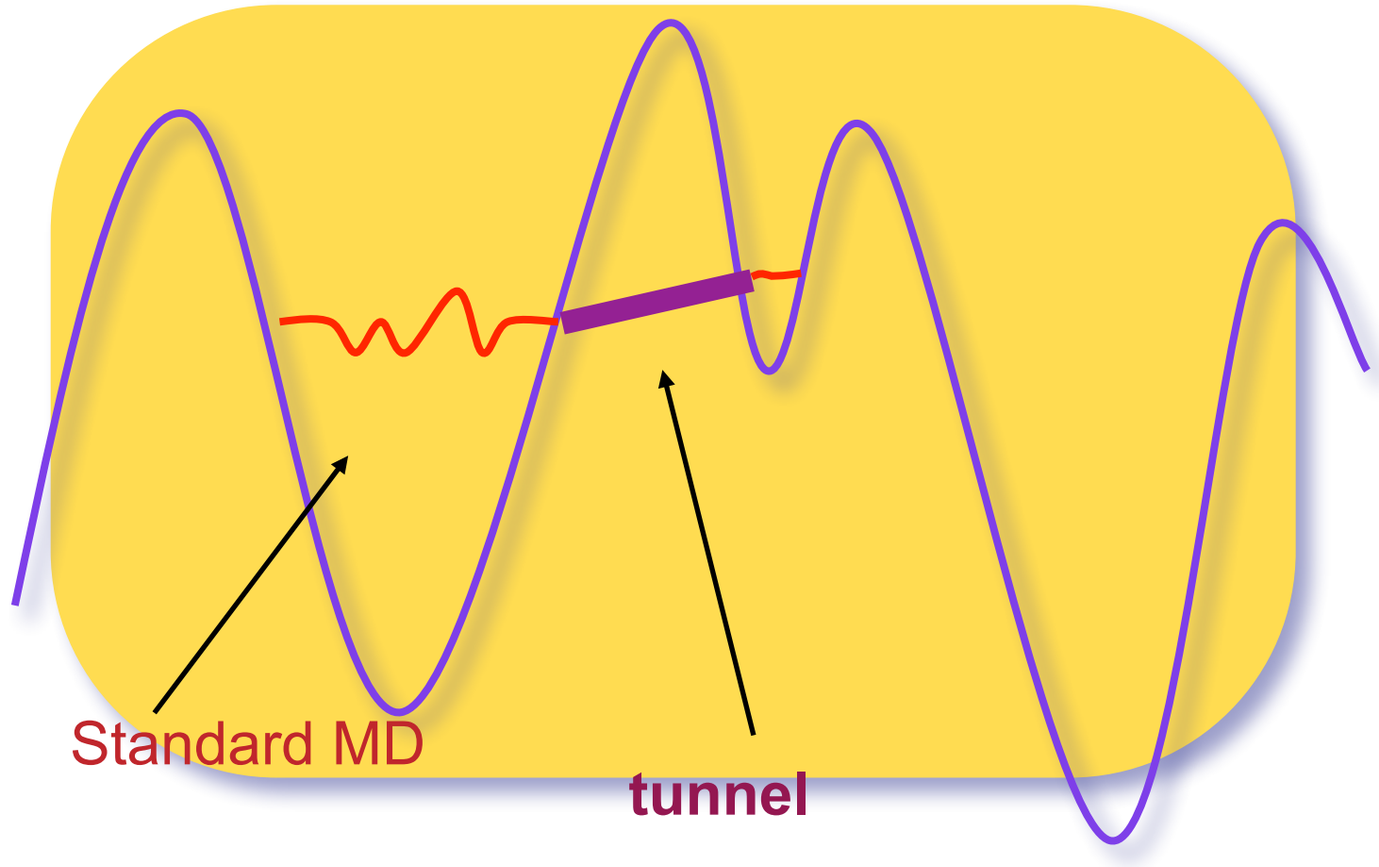


$$\vec{x}_{i+1} = \vec{x}_i + \frac{\Delta\tau}{2}\left(\vec{h}_i + \vec{h}_{i+1}\right) + c\Delta\tau\left(\vec{F}_i + \vec{F}_{i+1}\right)$$

3. We compute the Jacobian of transformation and accept or reject based on this value.

This algorithm respects detailed balance.

# Contributions to the Jacobian of transformation

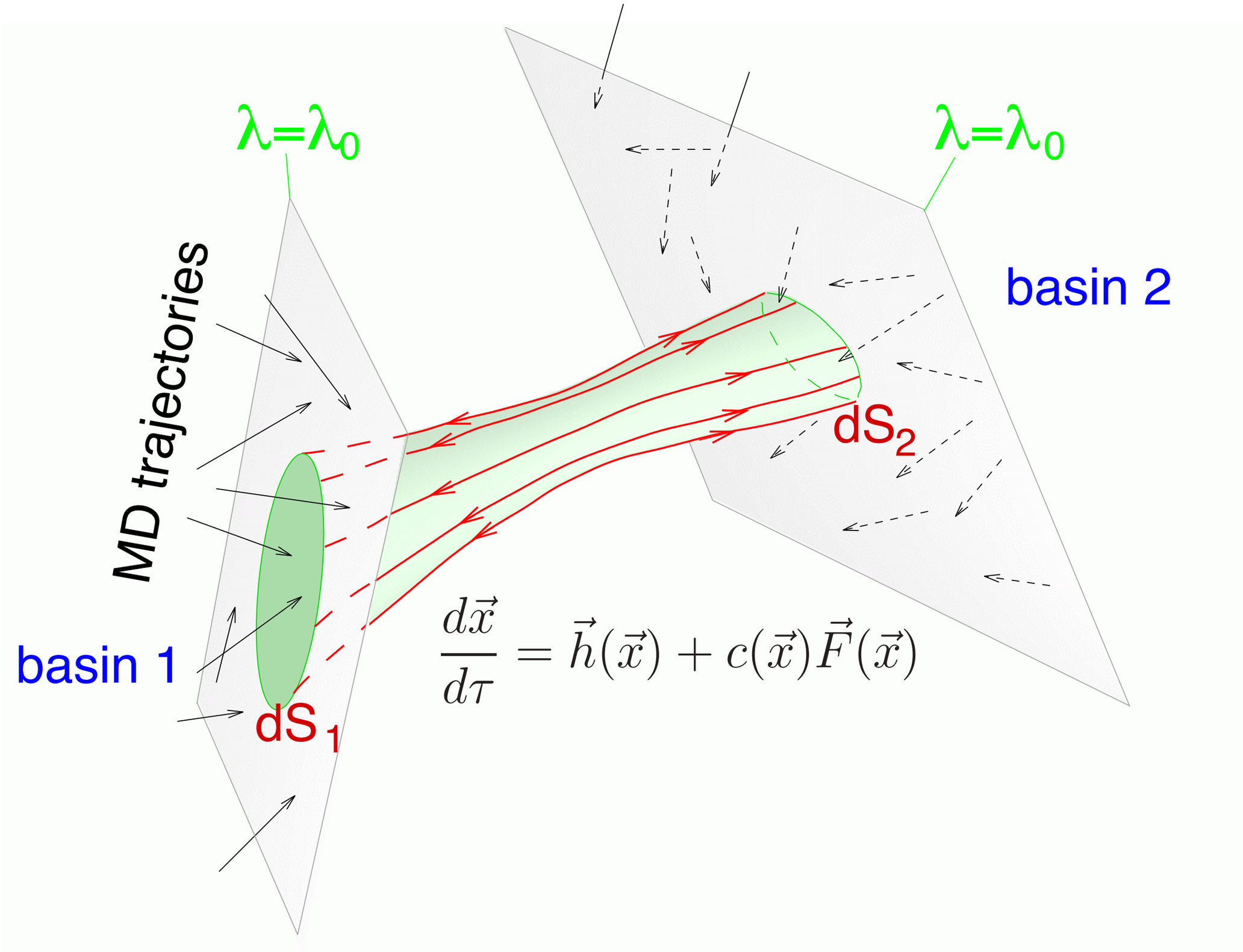

# The boundary Jacobian

The correction on the area (entrance and exit) is simply the ratio of the cosine with respect to the normal

$$J_{\mathrm{b}} = \frac{\cos\alpha_1}{\cos\alpha_2}$$

where

$$\cos\alpha_{1,2} = \frac{\vec{h}\cdot\nabla\lambda}{|\nabla\lambda|}$$

and

$$\nabla\lambda(\vec{x}) = \lim_{\delta\to 0}\frac{2\vec{F}(\vec{x}) - \vec{F}(\vec{x}+\delta\cdot\vec{h}) - \vec{F}(\vec{x}-\delta\cdot\vec{h})}{\delta^2}$$

This last quantity is the gradient of the lowest eigenvalue - the direction perpendicular to the surface of constant value

# The cross-section Jacobian

The displacement along curve is given by

$$\frac{d\vec{x}}{d\tau} = \vec{f}(\vec{x})$$

With $$\vec{f}(\vec{x}) = \vec{h}(\vec{x}) + c(\vec{x})\vec{F}(\vec{x})$$

As $\tau \longrightarrow \tau + d\tau$ then $\vec{x} \longrightarrow \vec{x} + \vec{f}(\vec{x})d\tau$

$$\ln J_{\rm xs} = \int_0^\tau j(\vec{x}(\tau'))d\tau'$$

$$j = \mathrm{div}\,\vec{h} + c\,\mathrm{div}\,\vec{F}$$

$$\begin{aligned} J &= \exp(\textstyle\int j(x_0)dx_0) = \exp\left[-(\Delta U_0 - T\Delta S)/k_BT\right] \\ &= \exp[-\Delta\mathcal{F}/k_BT], \end{aligned}$$

# POP-ART Trajectories

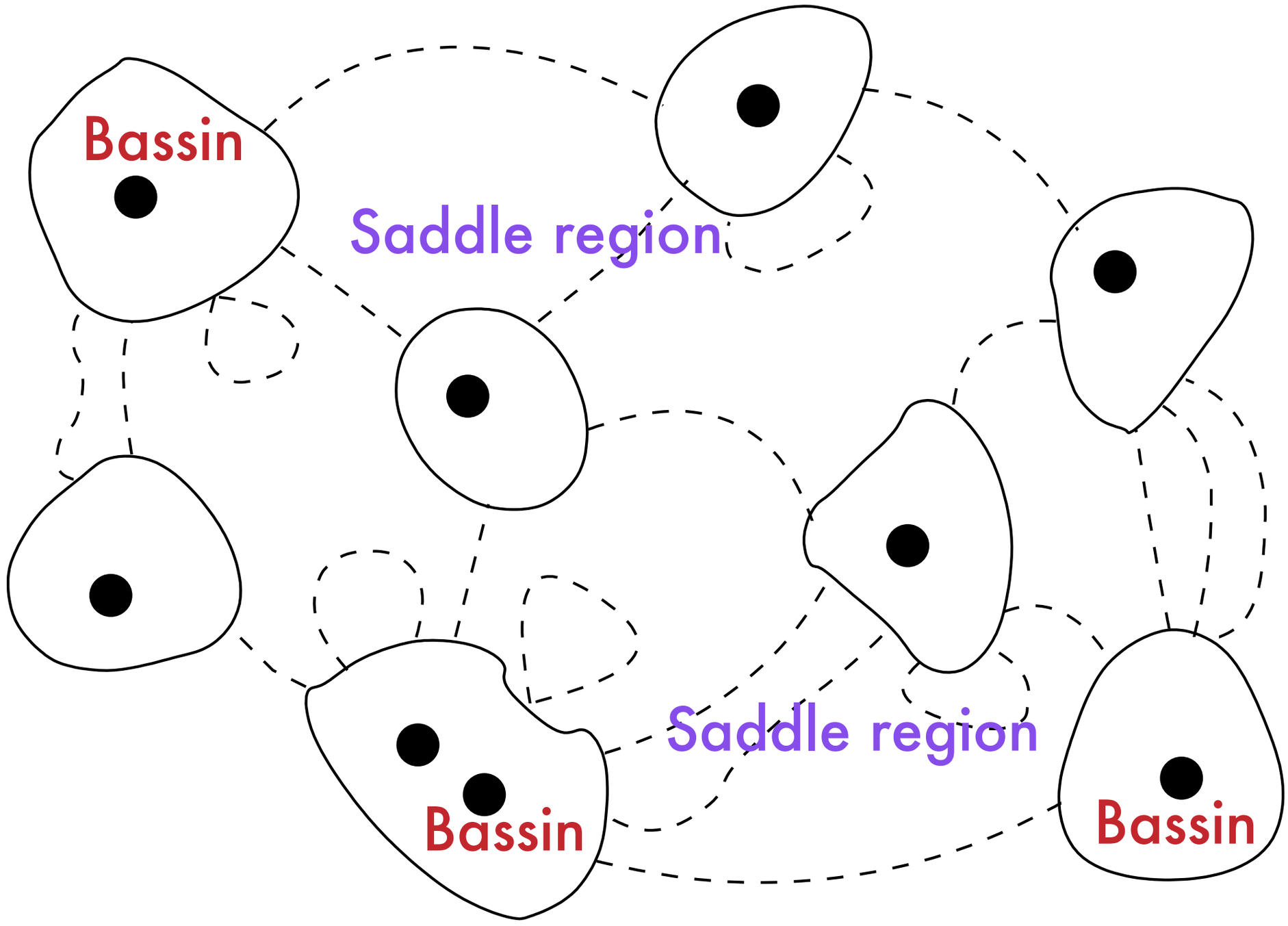

# POP-ART Trajectories

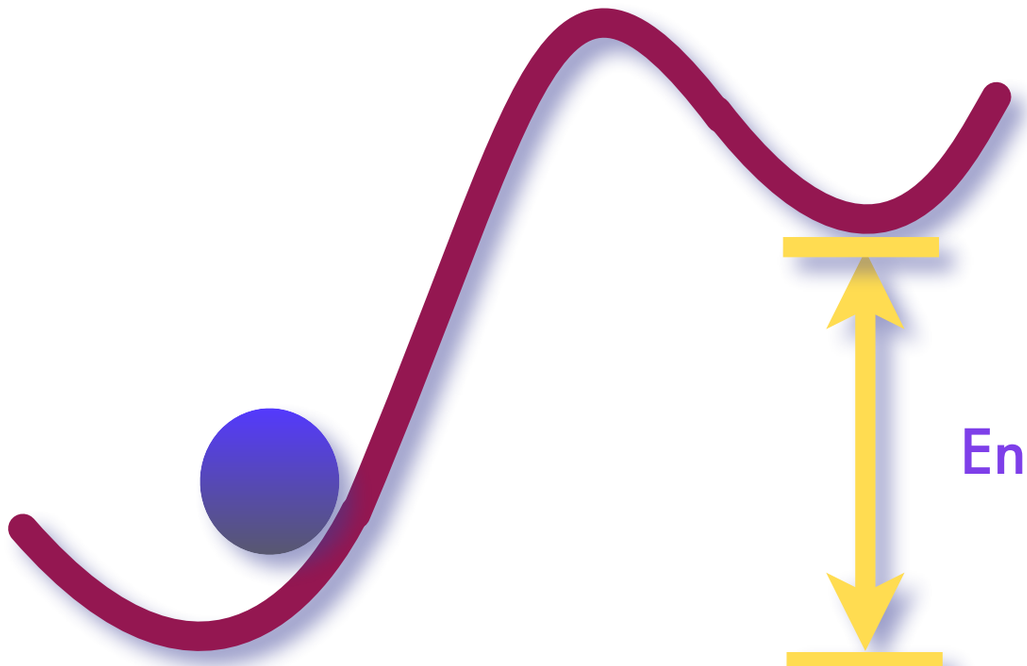

Two energy minima with the same energy (+/- 0.01 eV)

Energy difference: 0.75 eV

To establish the validity of the implementation of POP-ART we compute the probability of  begin in the top states vs. the bottom state at 1000 and 1200 K

| | MD | POP-ART |
|---|---|---|
| Ratio top to bottom at 1000 K | 1.6 +/-0.1 % | 1.3 +/- 0.3% |
| Ratio top to bottom at 1200 K | 3.6 +/-0.1 % | 3.5 +/- 0.3% |

# Sampling the phase space : vacancy in Si

Barrier: 0.43 eV

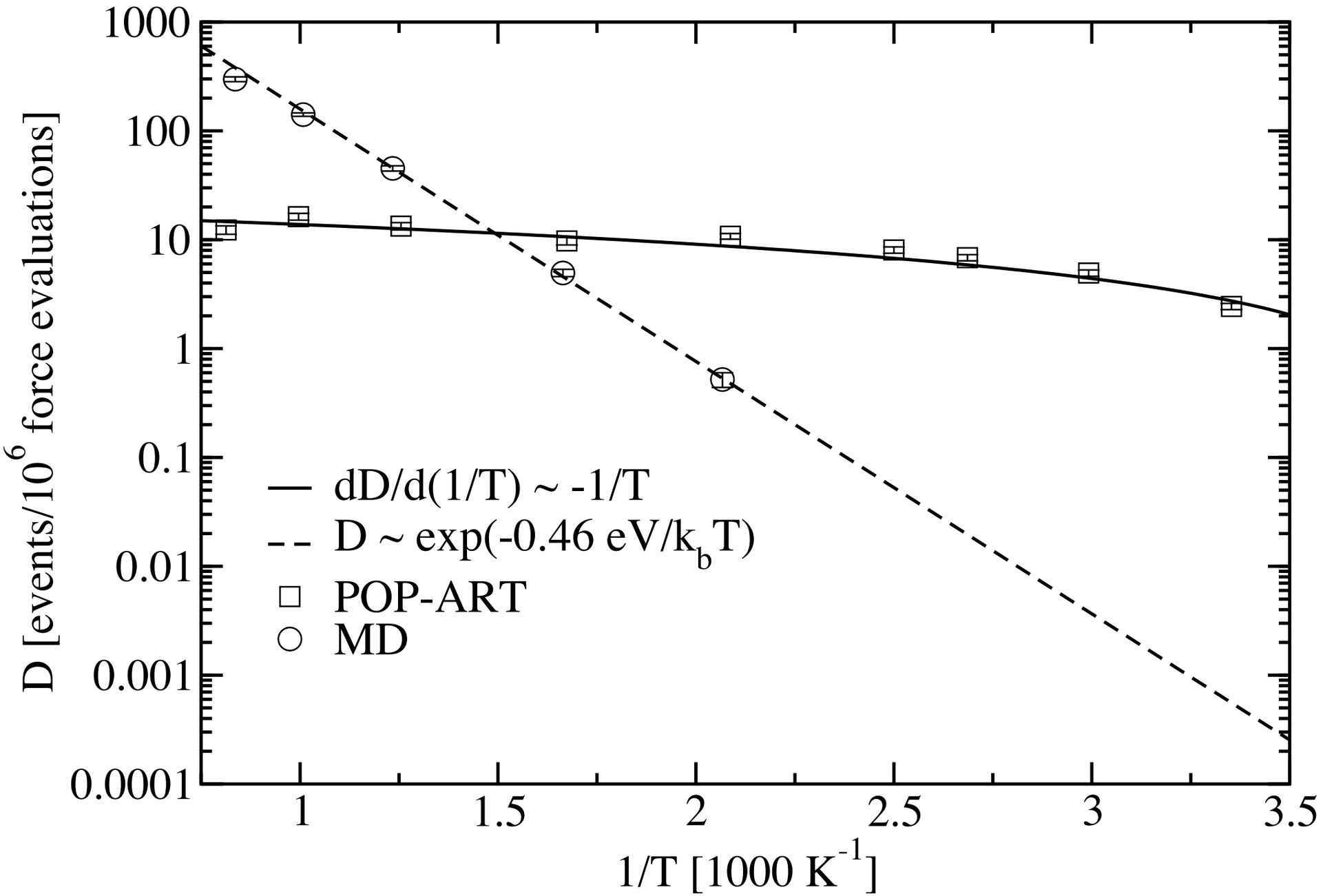


At room temperature: POP-ART samples 10000 faster than MD

# Conclusions

- POP-ART is a promising method to sample thermodynamically the phase space of complex systems
  - it respects detailed balance
  - it requires only local information
  - it computes exactly the free energy difference (no harmonic approximation)
- POP-ART can be up to 10000 faster than MD even at room temperature
- Suffers from low-barrier - a problem that we did not manage to solve

# Standard Kinetic Monte Carlo

We want to solve the evolution of a stochastic system which can be described by the Master's equation:

$$\frac{\partial P_i(t)}{\partial t} = \sum_j \left( P_j(t) R_{j\to i} - P_i(t) R_{i\to j} \right)$$

At any moment, the escape rate from a state is given by :

$$r_e^i = \sum_j R_{i\to j}$$

If the first-passage time is given by a Poisson distribution, then the escape time associated with this rate can be written as

$$t_e = -\frac{\ln \mu}{r_e^i} \qquad \text{with the probability} \qquad \mathcal{P}_{i\to j} = \frac{R_{i\to j}}{r_e^i}.$$

# Standard Kinetic Monte Carlo

In standard KMC, the problem studied must be defined on a lattice

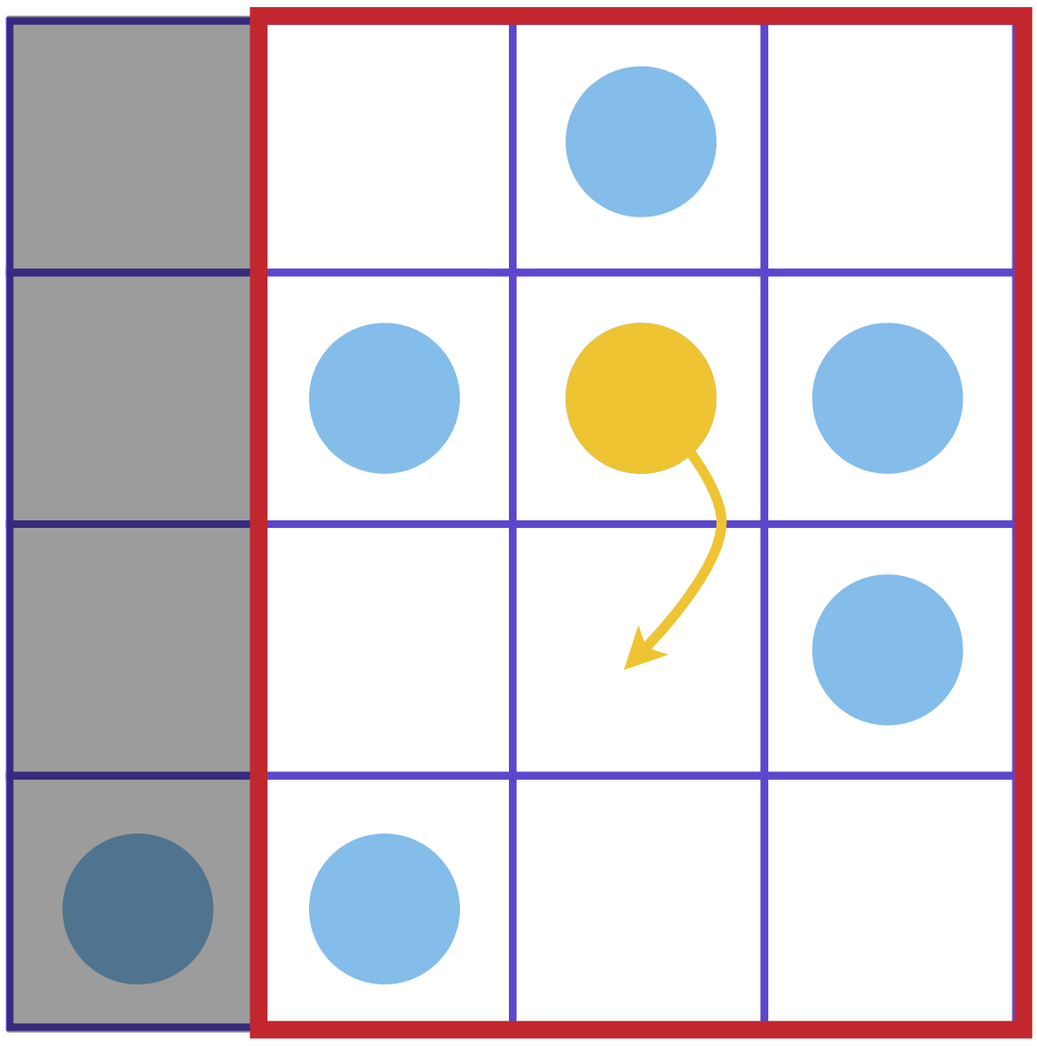

A. B. Bortz, M. H. Kalos, and
J. L. Lebowitz, J. Comput. Phys. (1975).

A list of events must then be constructed.

Including the final sites we get:

$2^{10} = 1024$ different events and barriers and prefactor

At a given moment, we select one of the possible events at random based on their rate *r of occurrence*

and make the move and update the clock according to

$$\Delta t = -\frac{\ln \mu}{\sum r_i}$$

# Kinetic Monte Carlo simulation of the growth of polycrystalline Cu

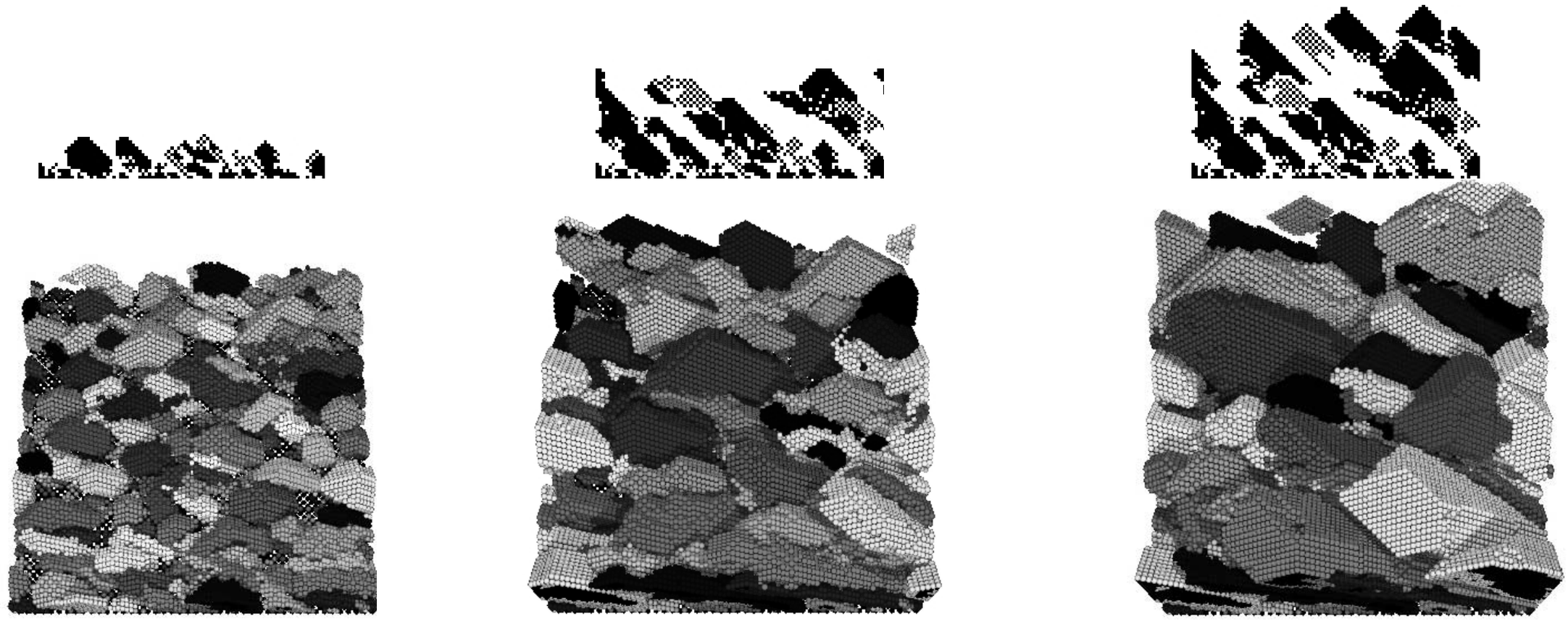

t=0.1 second t=0.2 second t=0.3 second

Fig. 1. Three snapshots showing the time evolution of a poly-Cu thin film. Substrate temperature is 150 K, angle of incidence is 75° from normal. Grains of non-bulk-like atoms are indicated by different shades of grey. Bulk-like atoms are shown in black. Images shown from the top to the bottom are top-down (plan) view, a slice through the film (cutaway view), and a perspective view.

Wang and Clancy, Surface Science 473 (2001) 25

# Co growth on Cu(111)

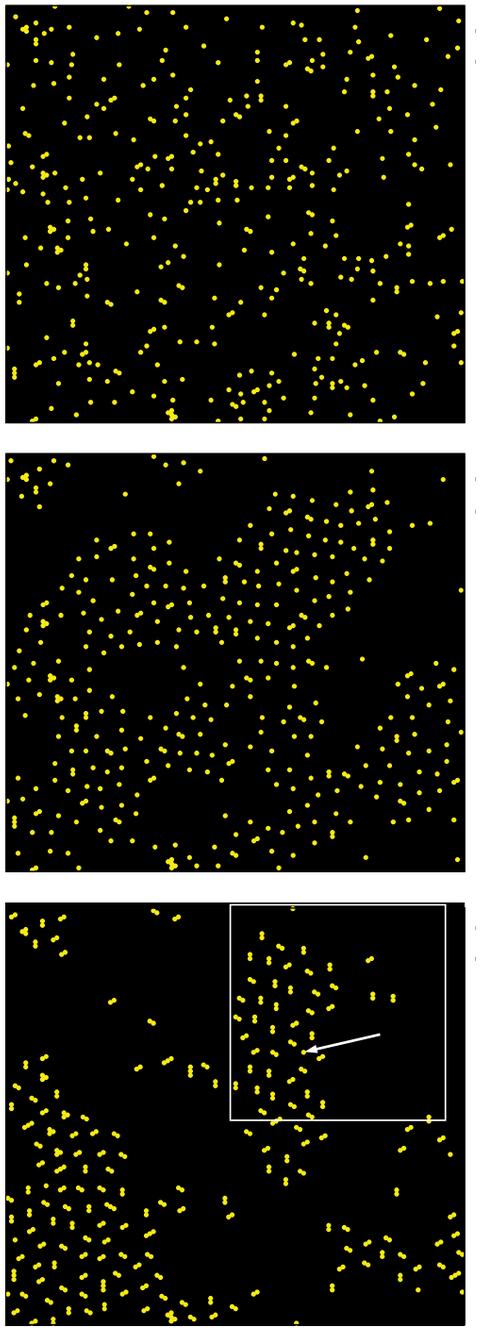

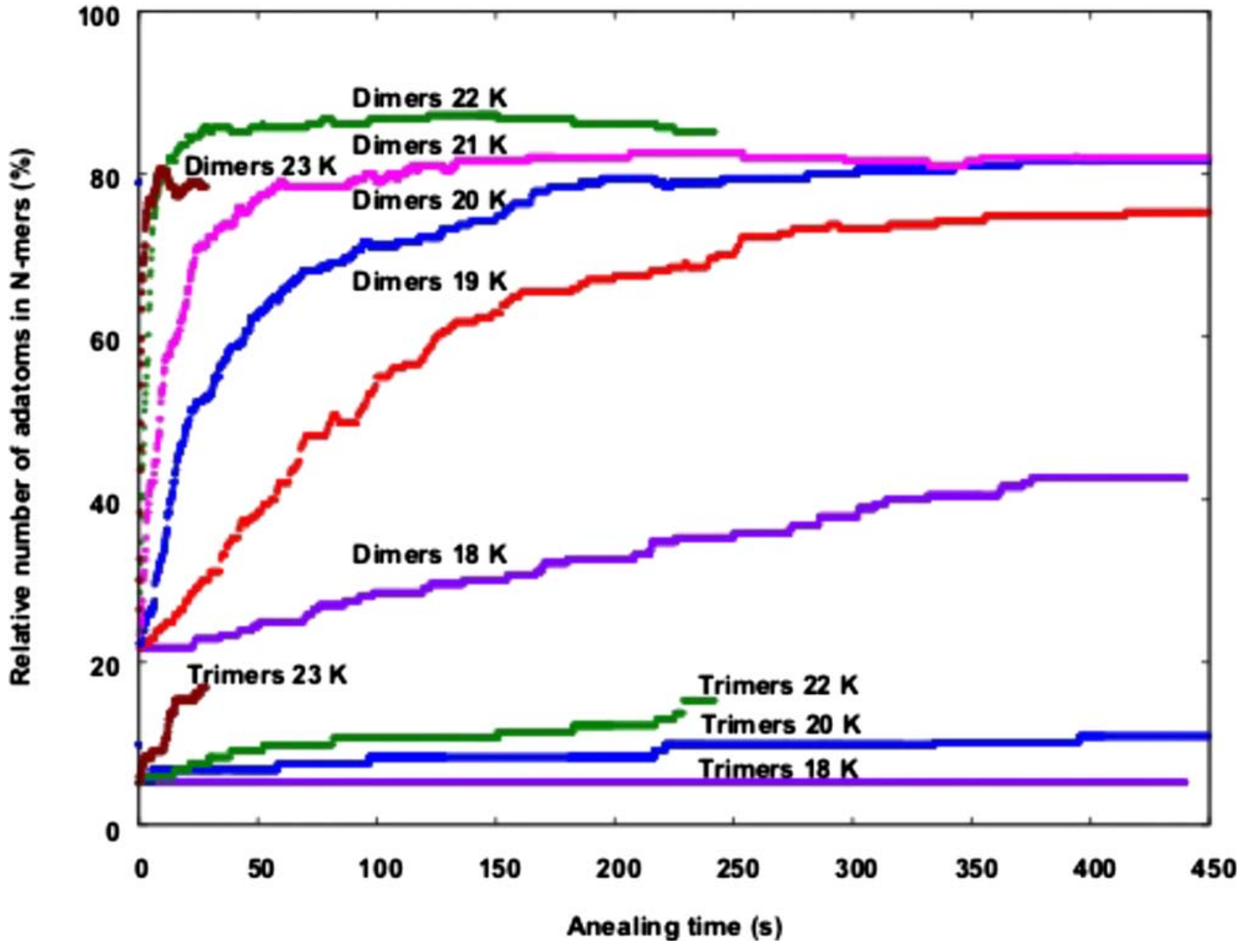


JM Rogowska, PRB (2010)

# Limitations of Standard Kinetic Monte Carlo

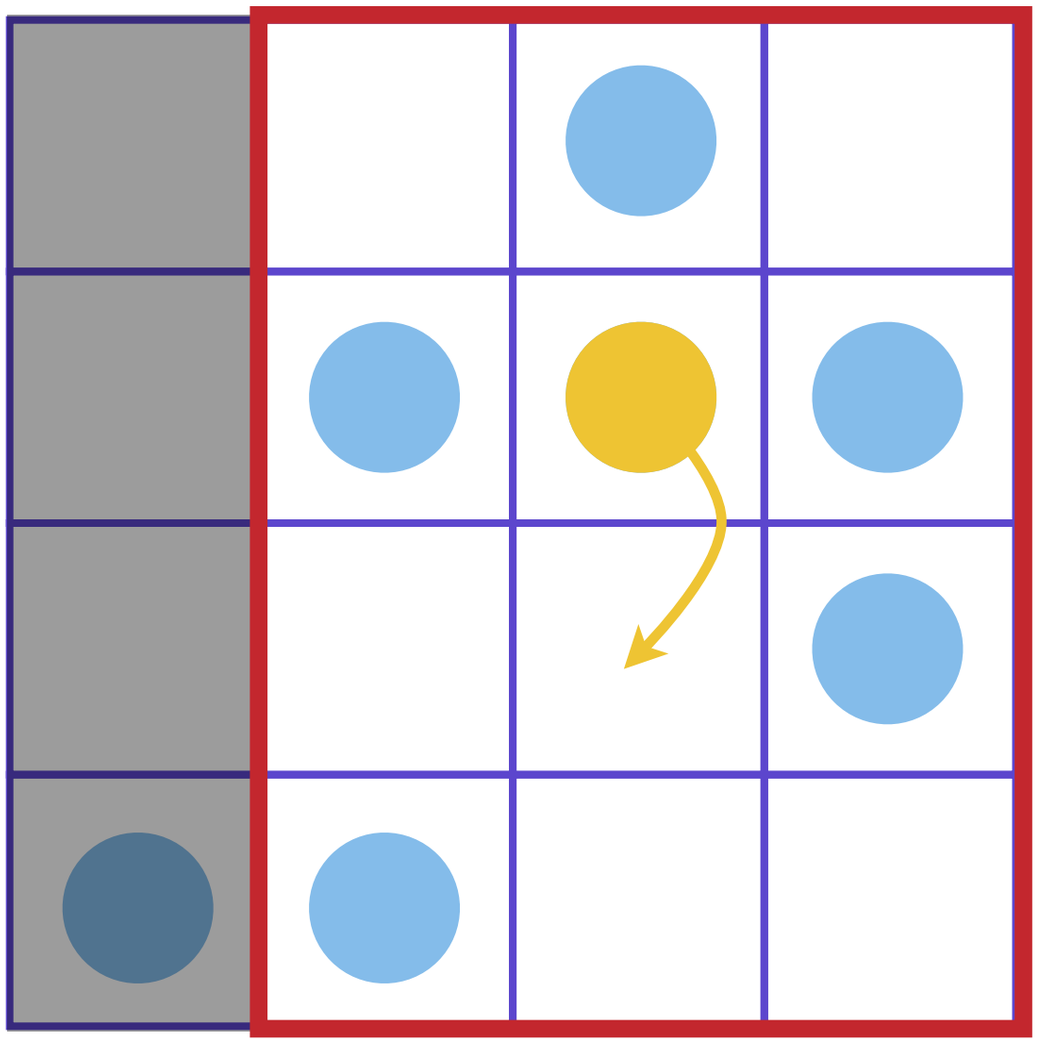

1. Uses a predefined and limited catalogue of known diffusions events and barriers at T=0

   can miss mechanisms

2. Constrains atoms to move only on a predefined lattice which can be real or effective

   atoms are not always on lattice

3. Supposes that there are no long-range interactions between defects

   elastic effects can be important

# But we know that...

1. Diffusion barriers are affected significantly by the **elastic deformation** around the defect and the event catalogue must be enriched as the system evolves

2. For example, vacancy-vacancy interaction is **long range** and so it should be included in the calculations

3. Off-lattice positions are common, especially in semiconductors and **at high temperature**, as observed by molecular dynamics, for example. These cannot all be predicted at the onset of the simulation.

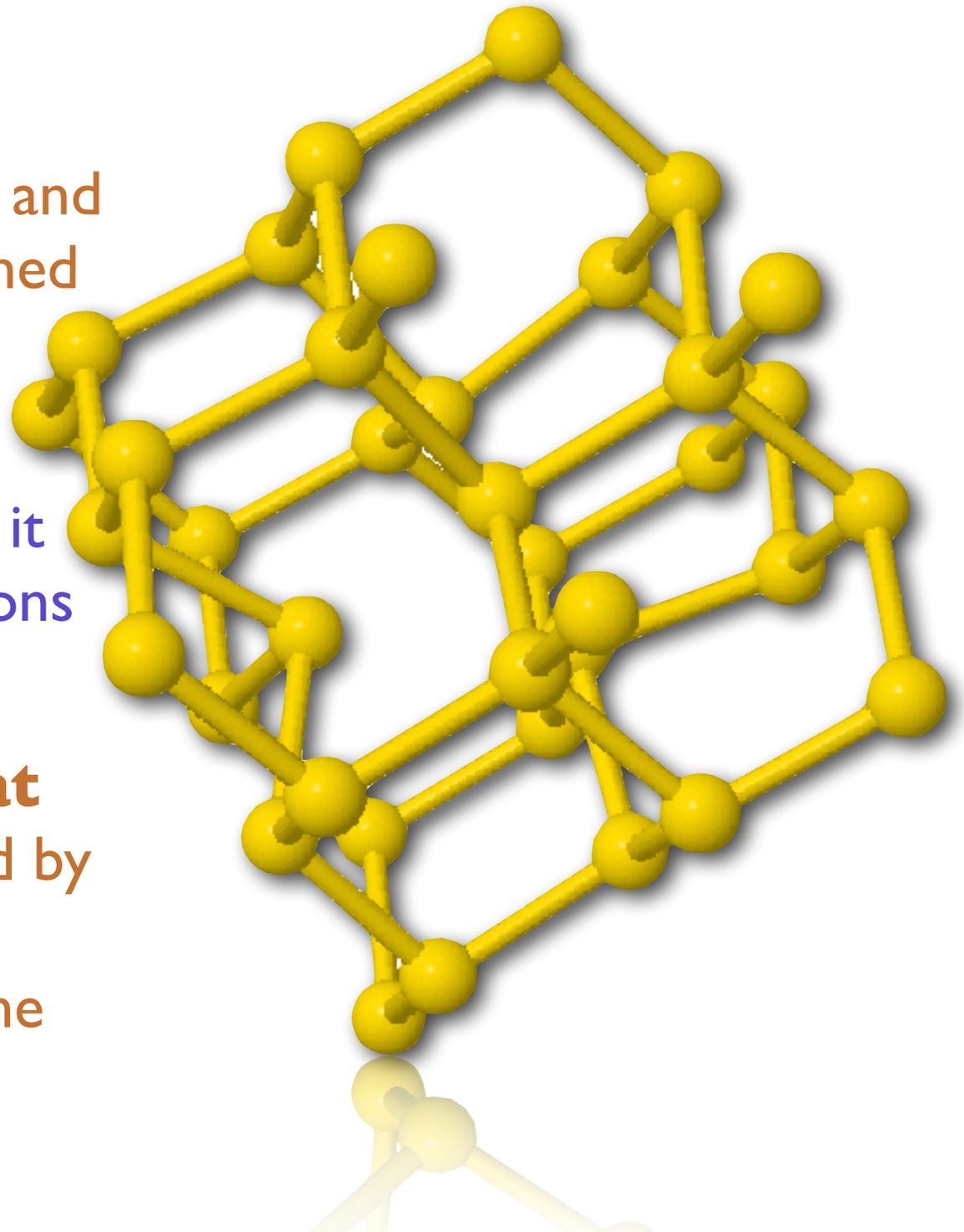

# Overcoming these limitations

**Molecular dynamics:**

Hyperdynamics (Voter, PRL 1997)

Temperature accelerated dynamics (Sørensen and Voter, JCP 2000)

Parallel MD (Voter, PRB, 1998 )

**Master equation:**

Start a connected network of events (DJ Wales, Mol. Phys. 2002)

**kMC on a precalculated trajectory**

Construct a 1D trajectory with autonomous basin climbing method
(Fan, Kushima, Yip and Yildiz, PRL 2011)

# kMC with event list rebuilding at each step

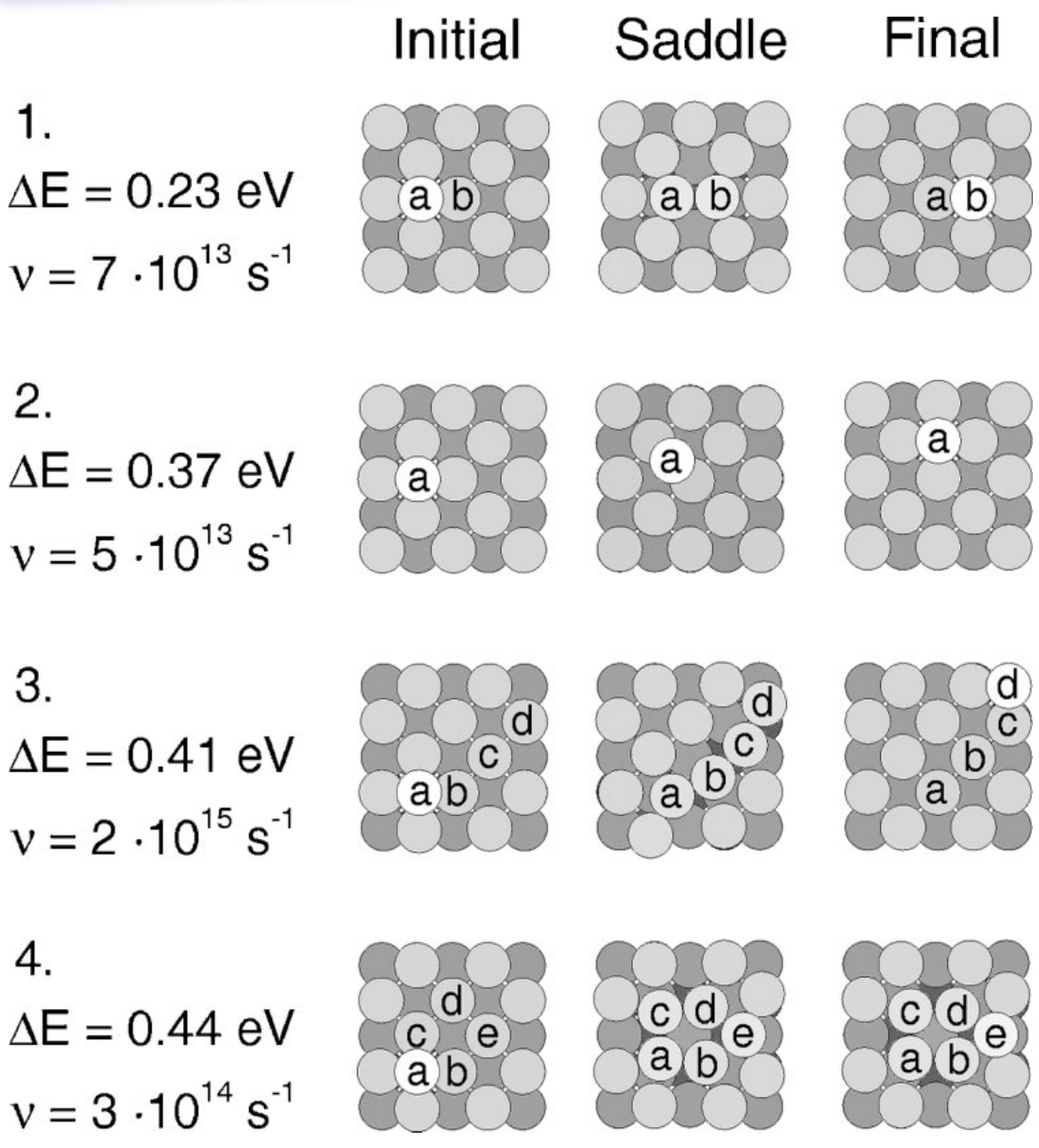


Henkelman and Jonsson, JCP 2001

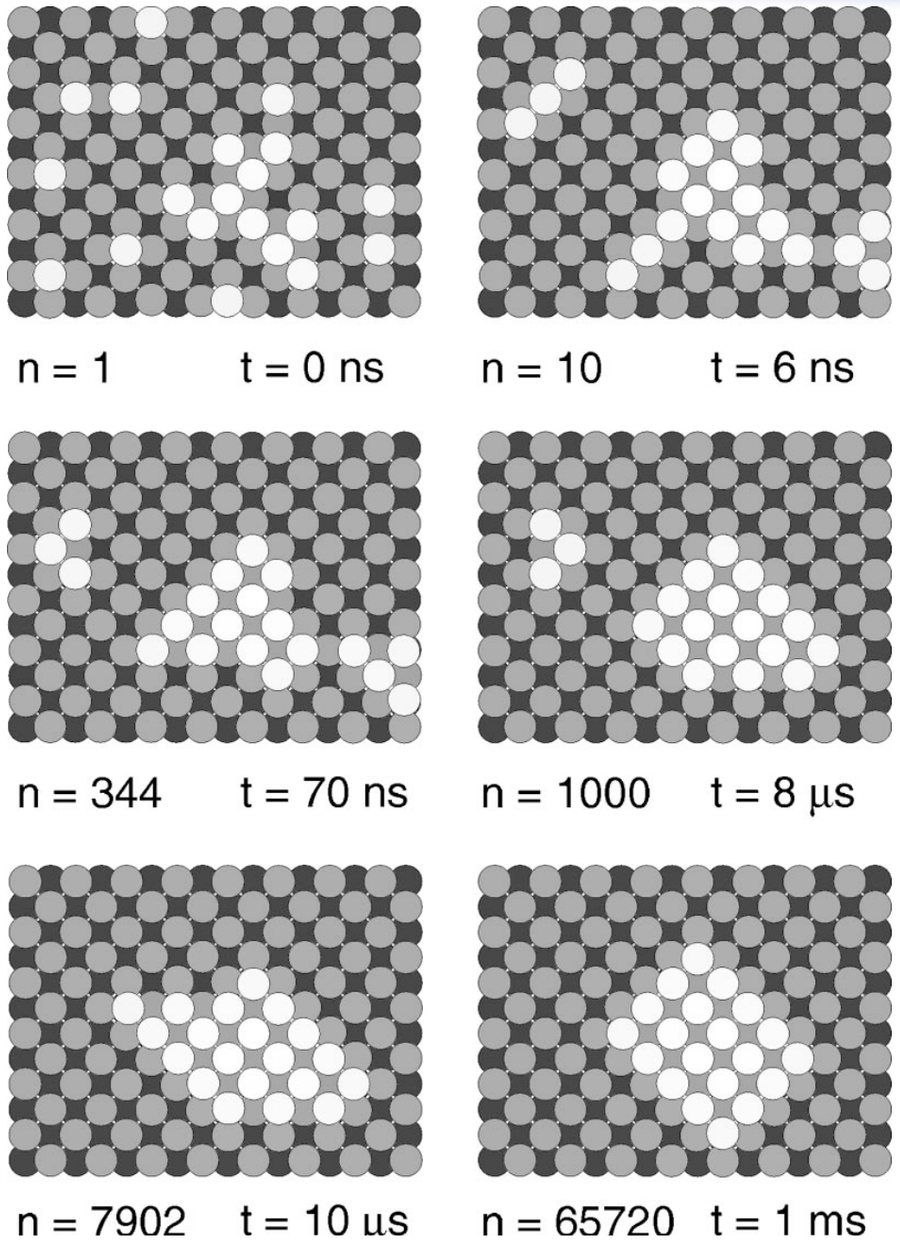


This method works well for small or simple systems. However, the number of barriers at each step much remain low.

# Overcoming these limitations

Over the last few years, many methods have also tried to introduce a catalog with off-lattice configurations

**Kinetic ART** (El-Mellouhi, Lewis and Mousseau, PRB 2008)

- uses ART nouveau (currently, fastest saddle-point search method)
- Topological classification, handles any complexity and full elastic effects

**Self-Learning KMC** (Kara, Trushin, Yildirim and Rahman, JPCM 2009)

- limited saddle point searching capacities (drag + repulsive bias potential)
- pattern recognition based on the existence of a lattice (no elastic effects)

**Self-evolving atomistic KMC** (Xu, Osetsky and Stoller, PRB 2011)

- uses dimer method
- new searches in local environment (no elastic effects)

**Local-environment KMC** (Konwar, Bhute and Chatterjee, JCP 2011)

- NEB for predetermined mechanisms (biased catalog)
- Local geometrical classification (no elastic effects)

# Accelerating time
# Part 4

# Outline

**1.** The challenge of simulating over multiple time scales. Energy landscapes. The transition state theory. Brief overview of various methods for breaching these time scales.

**2.** Basic concepts. Searching for saddle points. Sampling the energy landscape : the activation-relaxation technique (ART nouveau)

**3.** Accelerated MD approaches. Basic concepts kinetic Monte Carlo. Limits.

**4.** Off-lattice kinetic Monte Carlo methods. The kinetic Activation-Relaxation Technique. Topological analysis. Constructing an event catalog. Handling flickers. Limitations of current accelerated methods. Extending to large systems. Coming developments.

# KINETIC ART

Can we recover the dynamics of relatively complex systems dominated by activated diffusion?

# Kinetic ART

1) Generates the catalog and refines events with

**ART nouveau**

2) Classifies and reconstructs events with

**Topological analysis - NAUTY**

3) Evolves the system with

**Kinetic Monte Carlo**

# A topological classification

We suppose that all configurations can be classified in terms of their topology and that the events generated will have the same topological evolution.

1. Using the neighbour list, a graph is generated
2. The graph is analysed at its topology identified
3. All graphs with the same topology belong to the same class

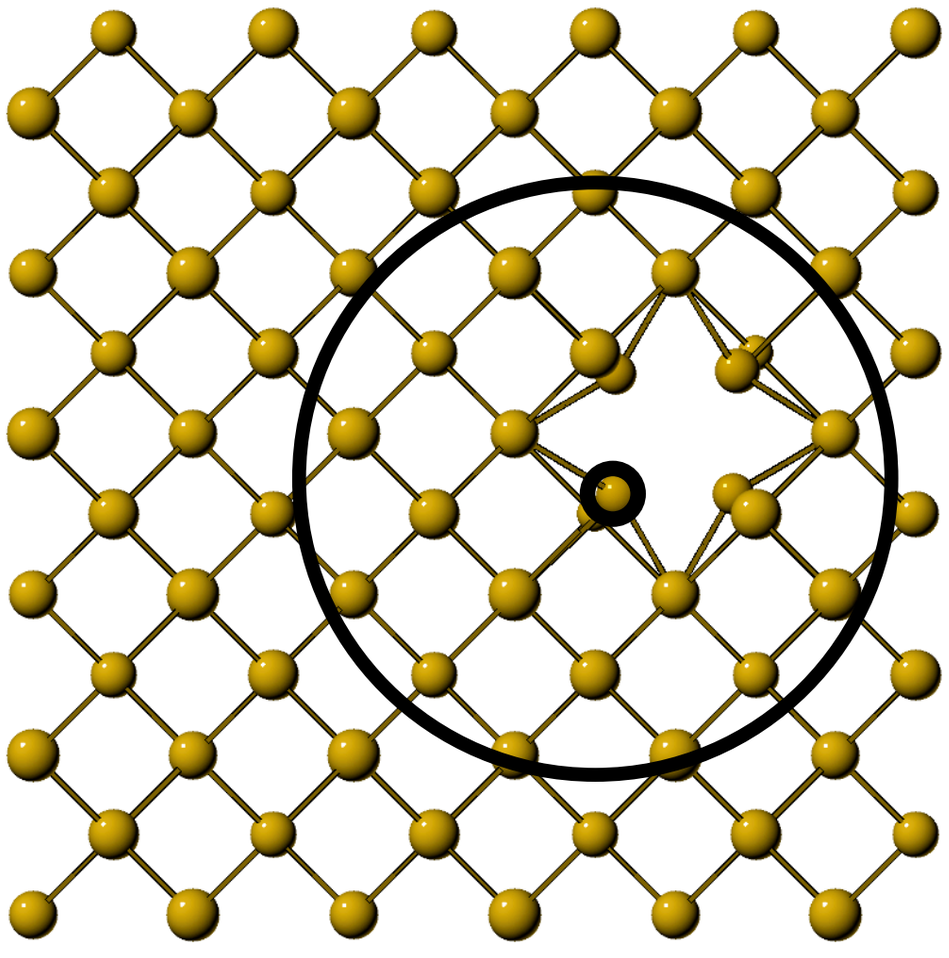

F. El-Mellouhi, NM and L.J. Lewis, PRB **78**, 153202 (2008).

# Topological analysis with NAUTY

Take a sphere around each atom

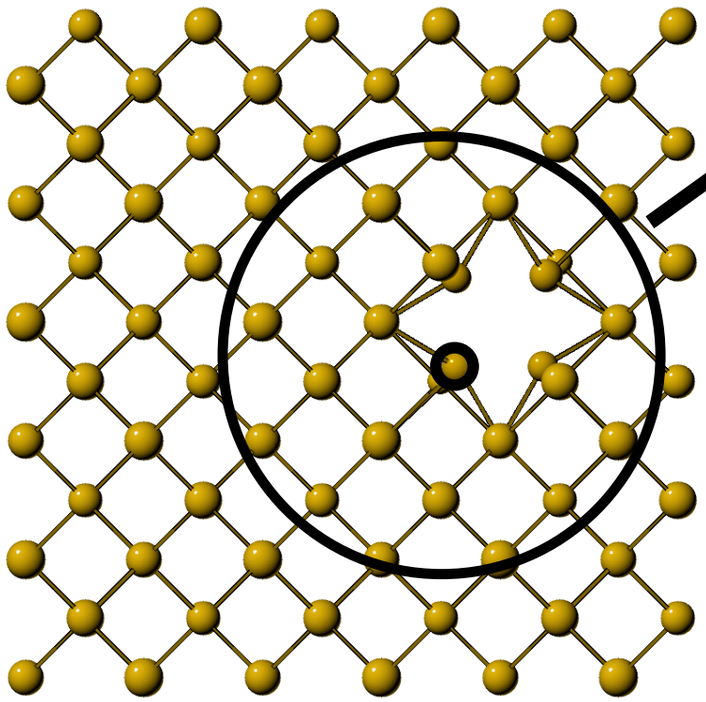

(a)

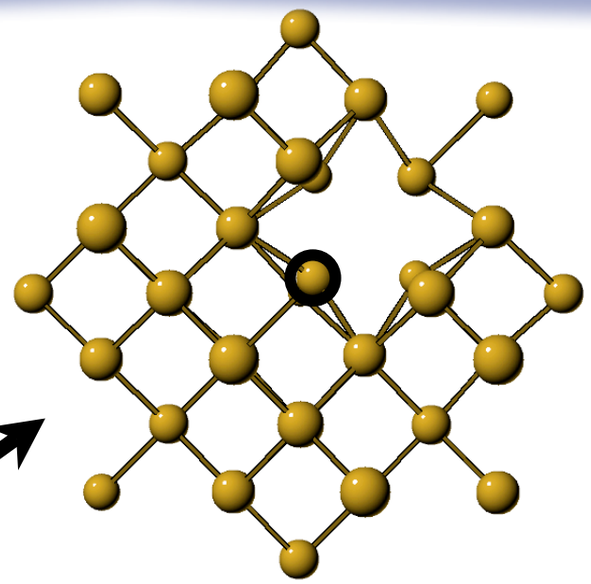

(b)

Prepare the graph of connectivity between atoms and label them

(c)

NAUTY

(d)

[ 912419 ]

1. Store the topology label in a hash table, rehash the label if clustering occurs;
2. Update the occurrence of the topology;
3. If topology is completely new, store it and find the events and rate lists associated with it.

# NAUTY

NAUTY is a program for computing automorphic groups of graphs; it can also produce a canonical labelling taking into account symmetry operations of the graph.

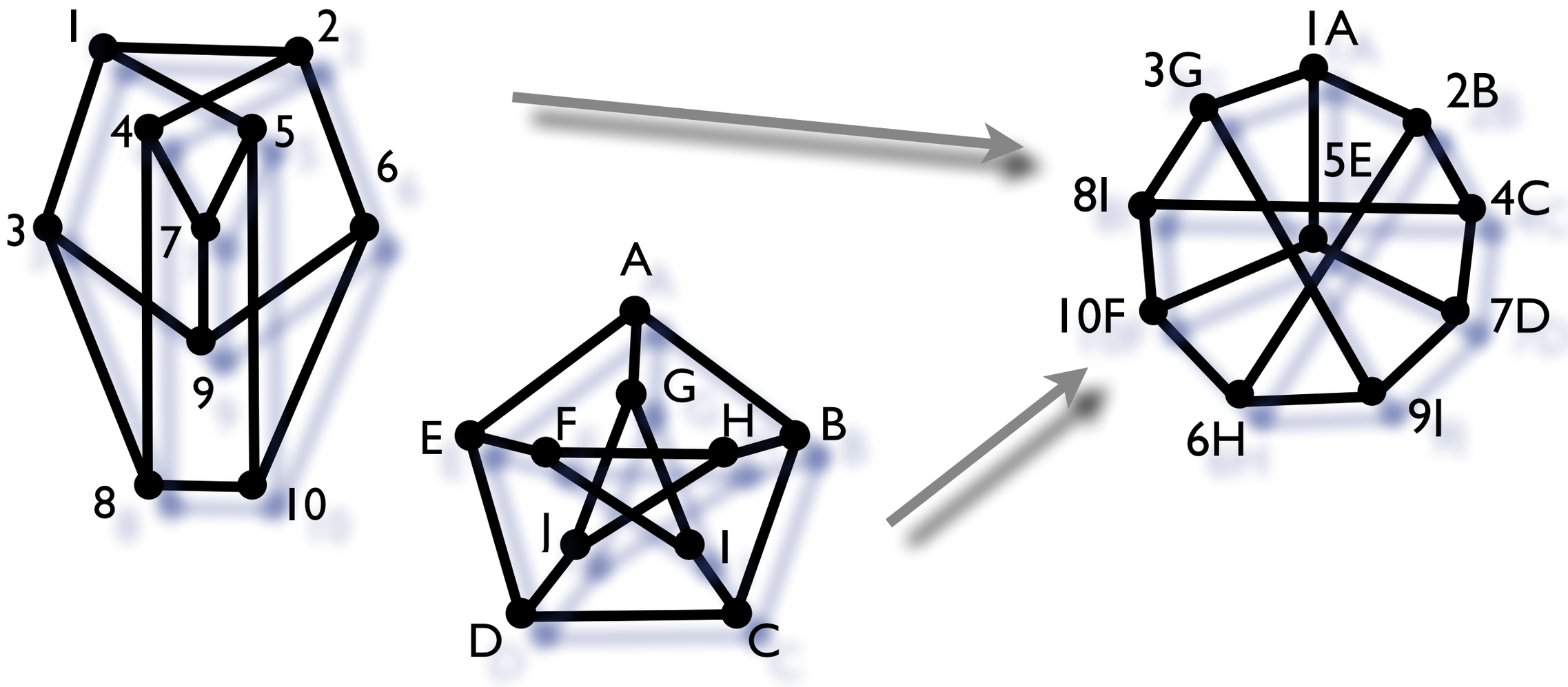


Brendan D. McKay, *Practical Graph Isomorphism*, Congressus Numerantium, **30** (1981) 45-87.
http://cs.anu.edu.au/~bdm/nauty/

# NAUTY

Nauty also handles chemical order and distingues same topology with different chemical distribution

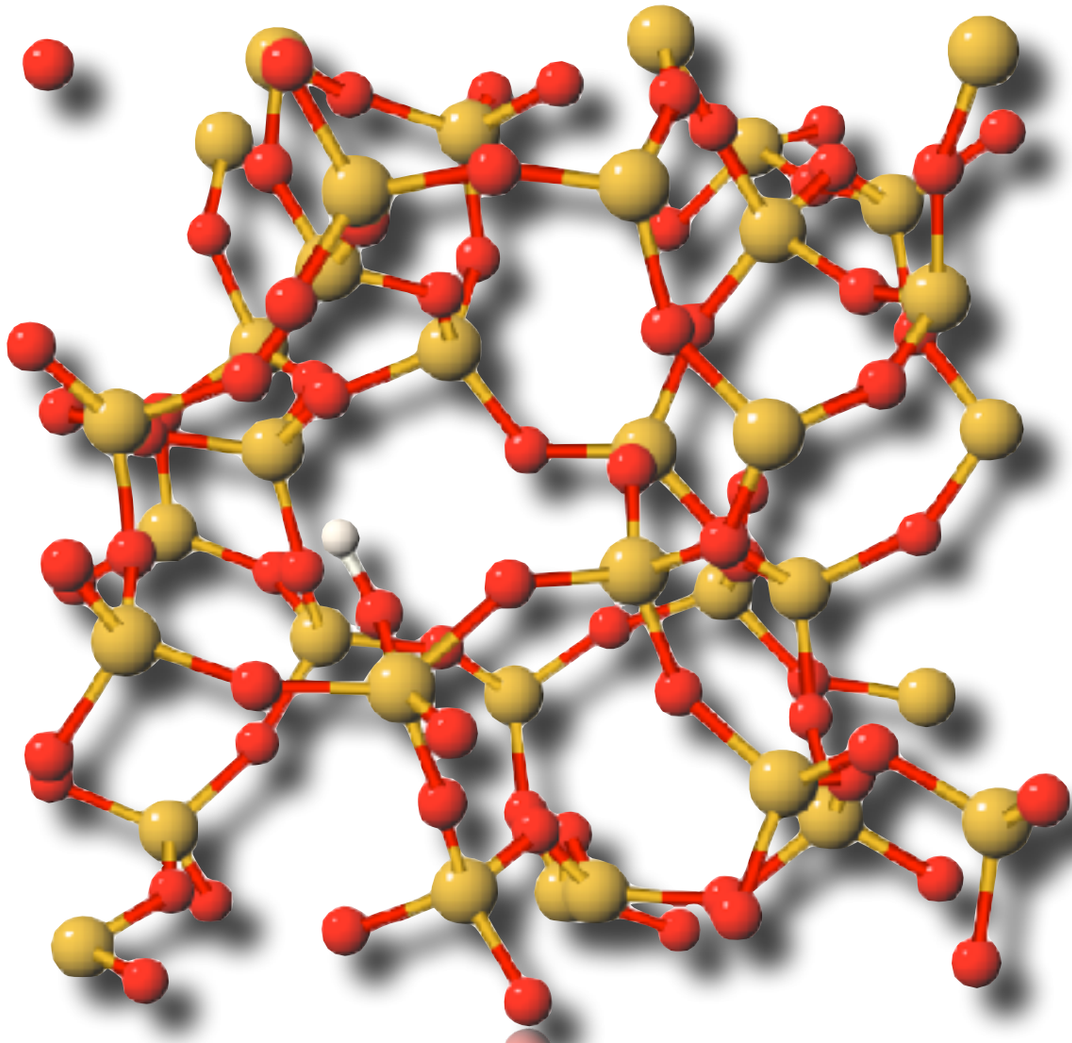

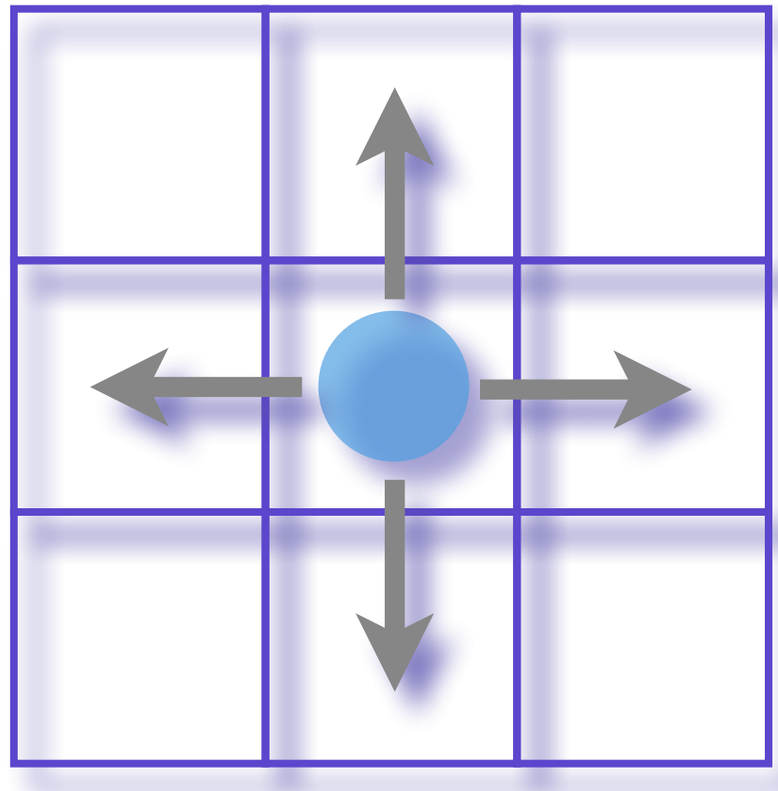

With labels, we can also handle different symmetries with same topology

Brendan D. McKay, *Practical Graph Isomorphism*, Congressus Numerantium, **30** (1981) 45-87.
http://cs.anu.edu.au/~bdm/nauty/

# A few more details of implementation

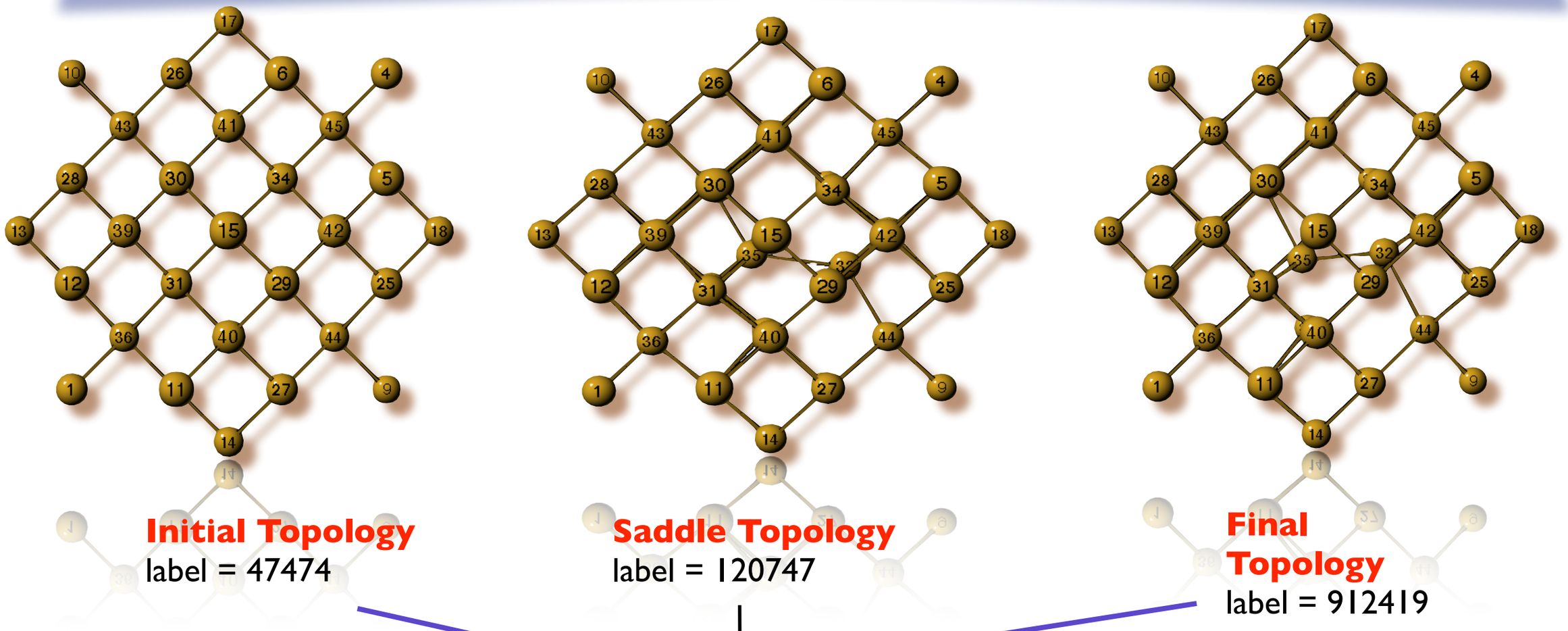

**Initial Topology**
label = 47474

**Saddle Topology**
label = 120747

**Final Topology**
label = 912419

Hash function

event label = 144213

**Event hash table**

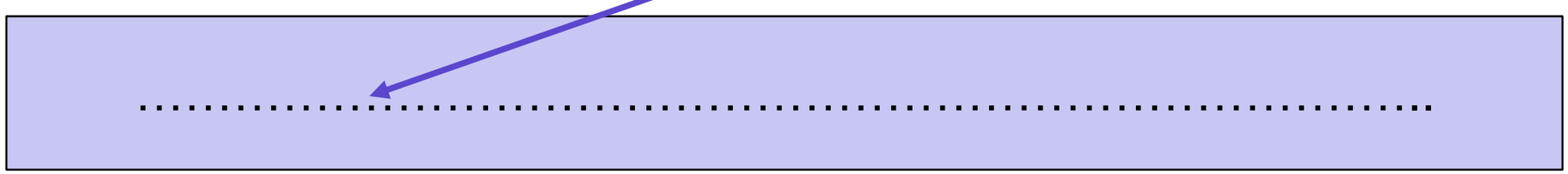

# Storage of events

- Generated events are inserted easily to the binary tree;
- Cumulative rates are updated only along one branch;
- Events can be removed easily without unbalancing the tree;
- Event selection requires O(log n) time in the average case.

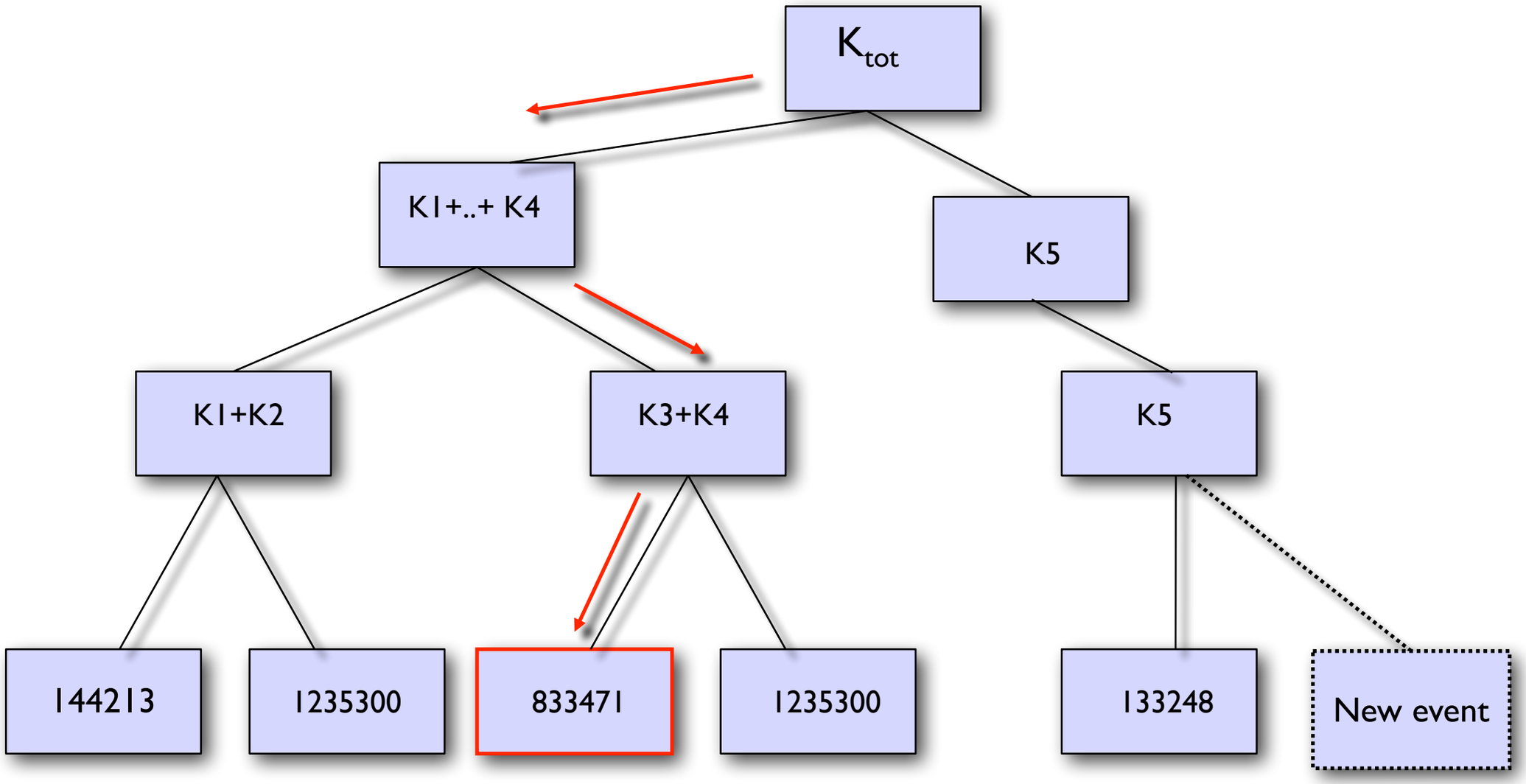


Balanced binary tree with all possible events inserted at the bottom
The upper nodes contain the cumulative rates.

# Reconstructing the events

Initial and final atomic positions for event 833471 are stored in the order that conserves the isomorphism group;
The atom that execute this event is randomly chosen from a list of atoms having the same topology label as Initial.

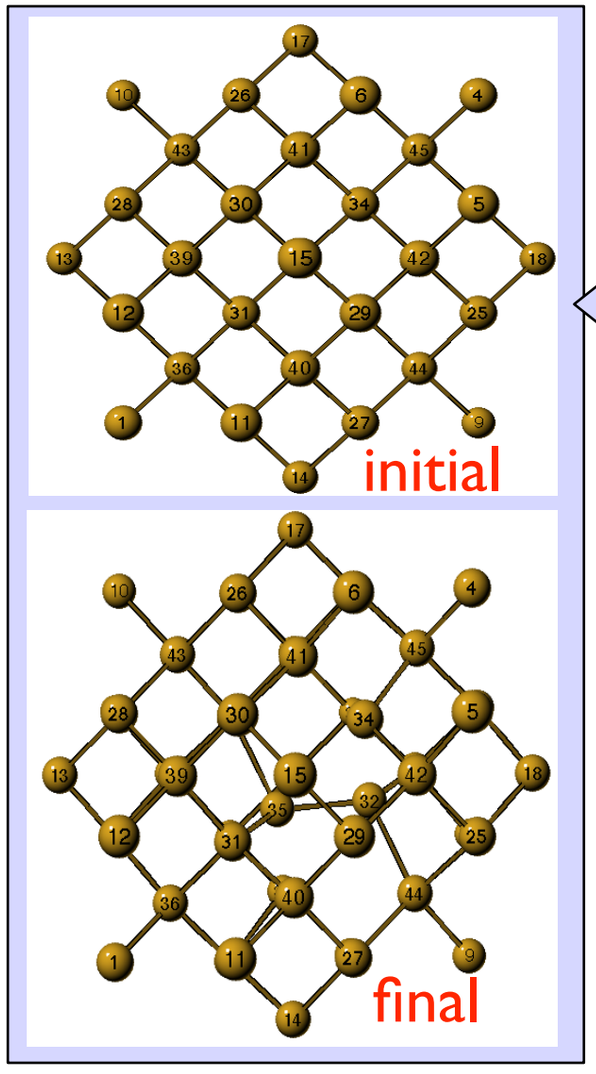


Event 833471

Extract the symmetry operations by comparing atoms order and coordinates

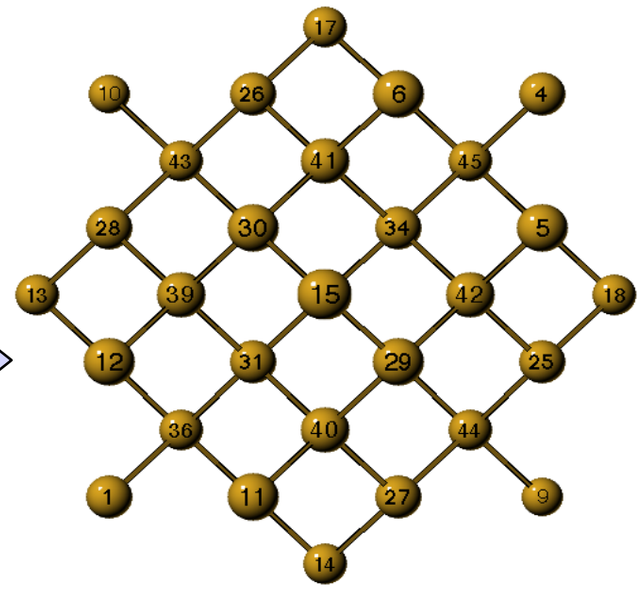

The actual topology around the atom that will execute the move

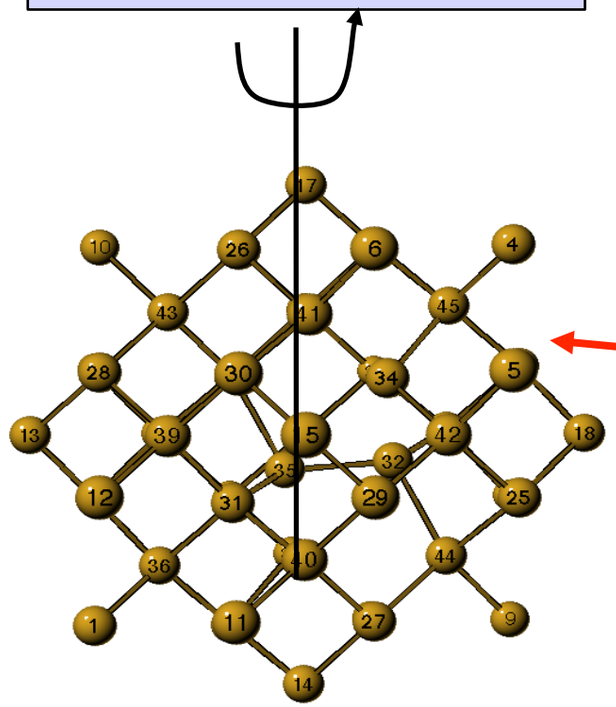

Finally apply the symmetry operation on final to execute the move correctly

# The algorithm

**After an event :**

1. The topology of all the atoms within the active part of the event is evaluated again;
2. If the topology is known, import the list of events; if not, generate ART events;
3. If some of the old topologies do not have enough events, try a few more ART steps;
4. Store these new topologies.
5. Relax all relevant barriers to take into account elastic effects
6. Compute rate and apply KMC

# Taking into account long-range elastic effects

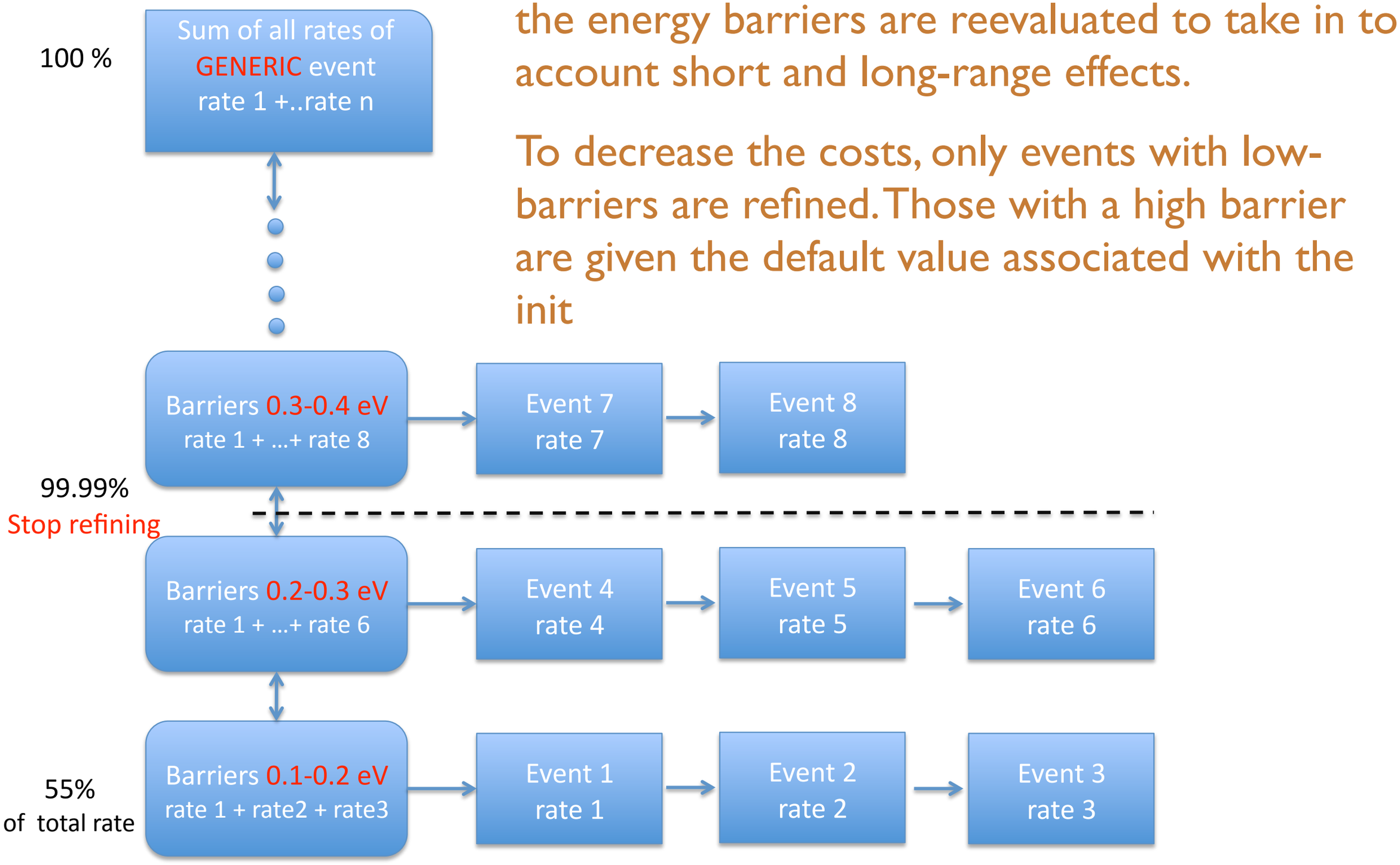


After each event, saddle points are refined and the energy barriers are reevaluated to take in to account short and long-range effects.

To decrease the costs, only events with low-barriers are refined. Those with a high barrier are given the default value associated with the

# A few implementation details

## Economical management of events

All generic events visited **are stored and can be reused**

i. to extend the system's simulation

ii. to use in a new simulation

iii. to use with a different system

This can save a tremendous amount of time for example

study of mono-vacancy, di-vacancy can be used for the 10-vacancy problem.

Specific (relaxed) events **are also stored and relaxation starts from the last points**

# A flow-chart for kinetic ART

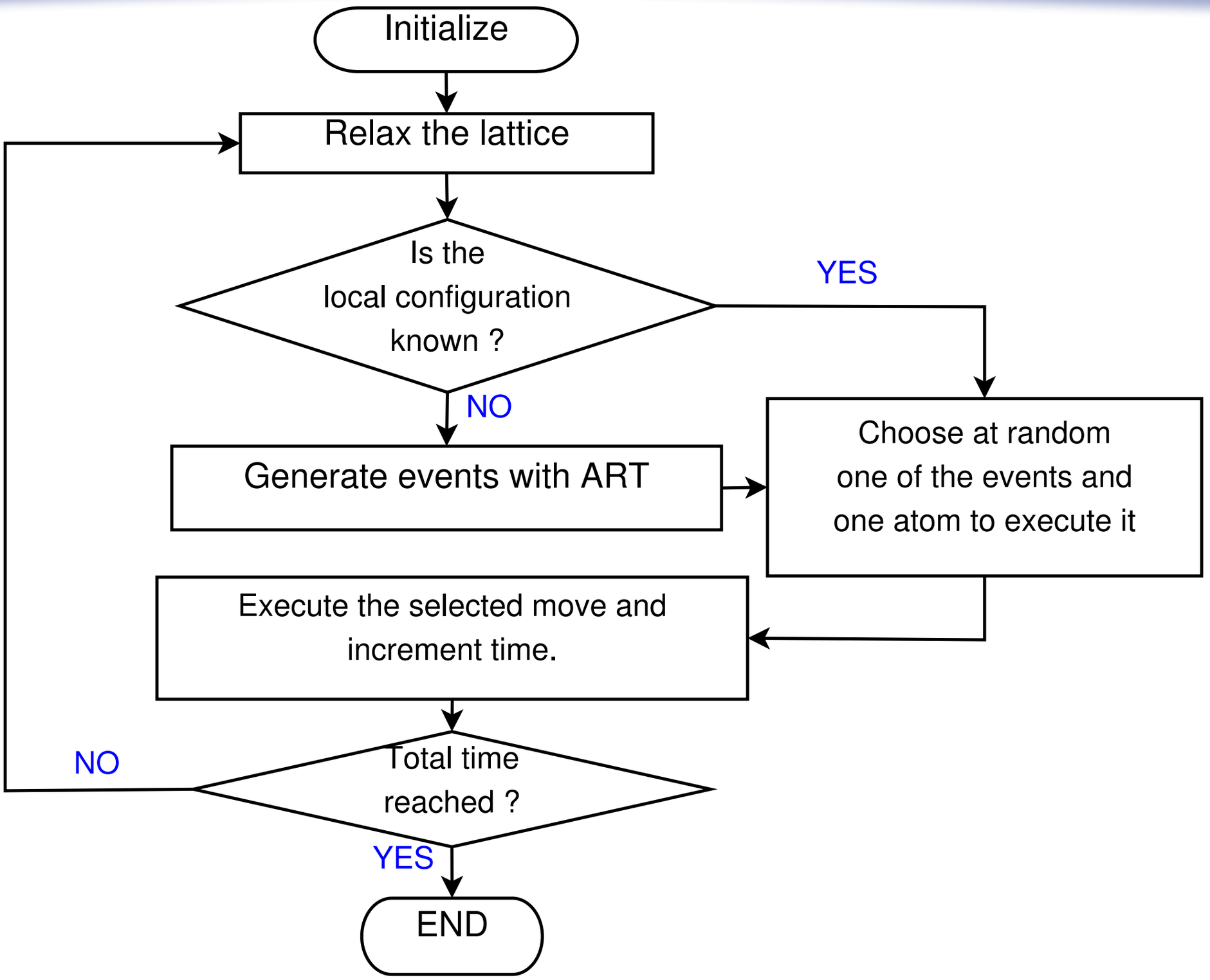

# Diffusion of a single vacancy

The five lowest-energy events are:

| Energy (eV) | Type |
|---|---|
| 0.53 | Vacancy hop |
| 0.65 | Asymmetric hop |
| 0.90 | Asymmetric hop |
| 1.69 | WWW + vacancy |
| 2.79 | WWW near vacancy |
| 3.43 | Isolated WWW |

~1000 atoms
Stillinger-Weber potential
1 vacancy

# 0.53 eV

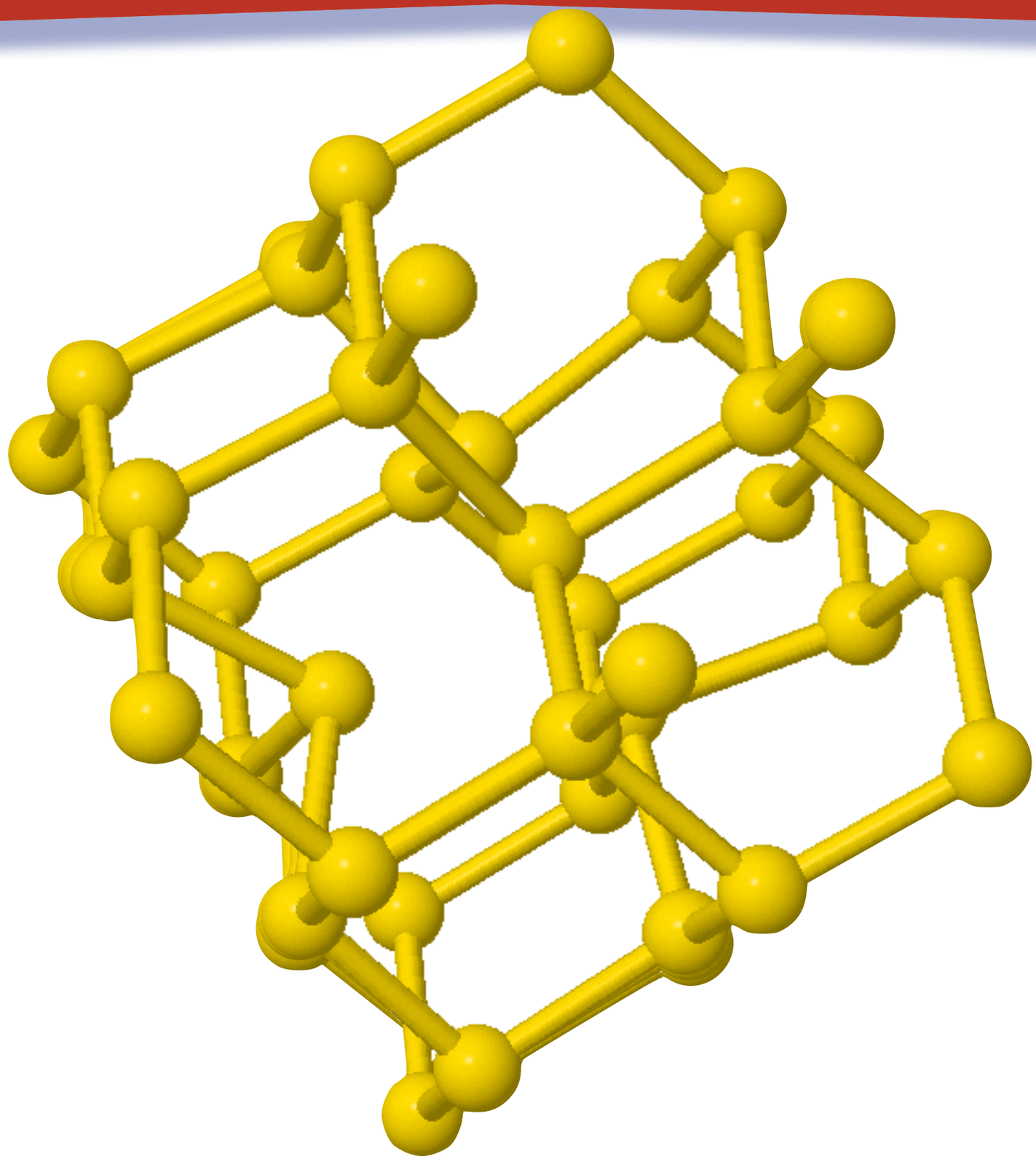

# 0.9 eV

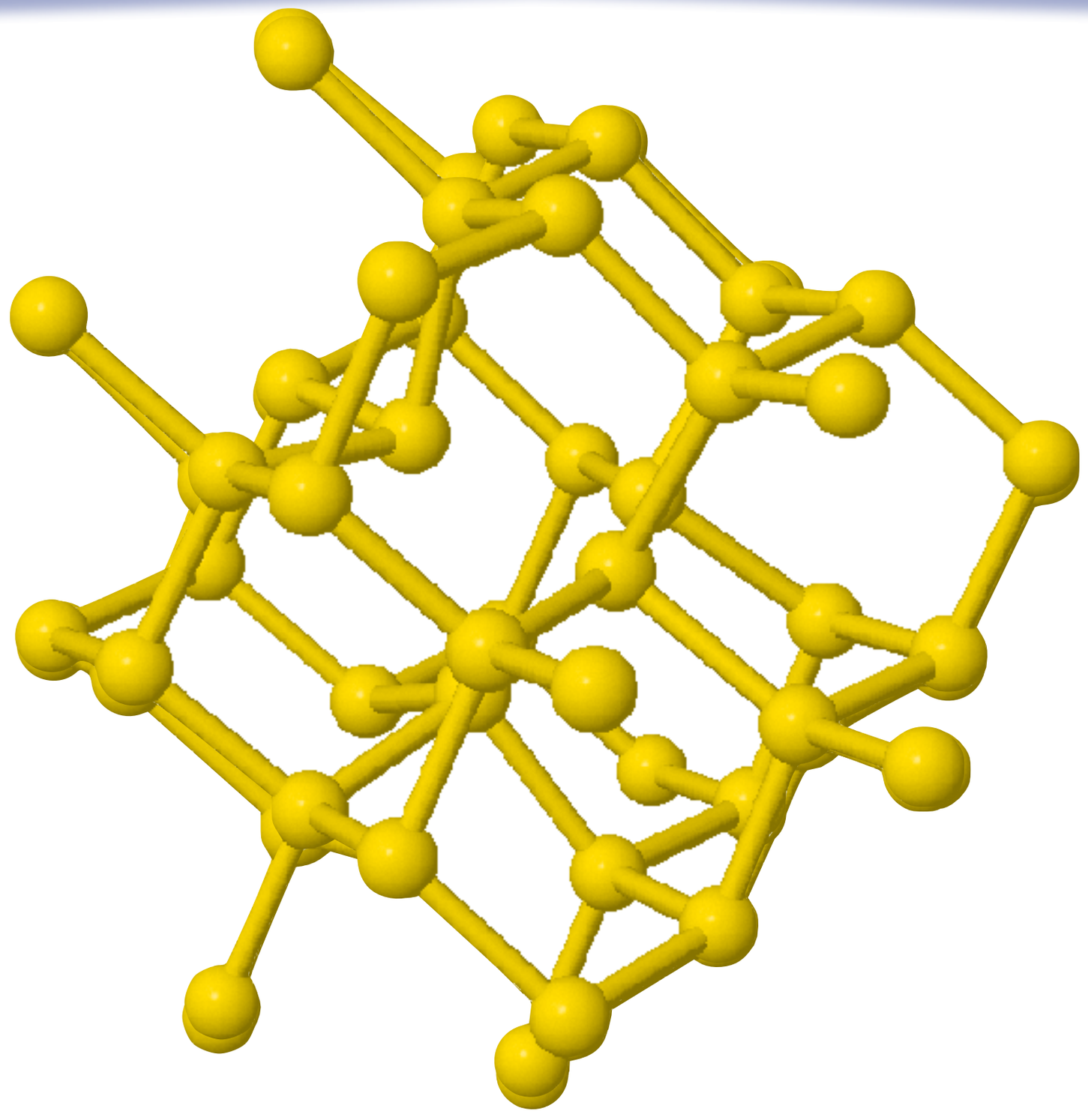

# 3.43 eV — Wooten-Winer-Weaire

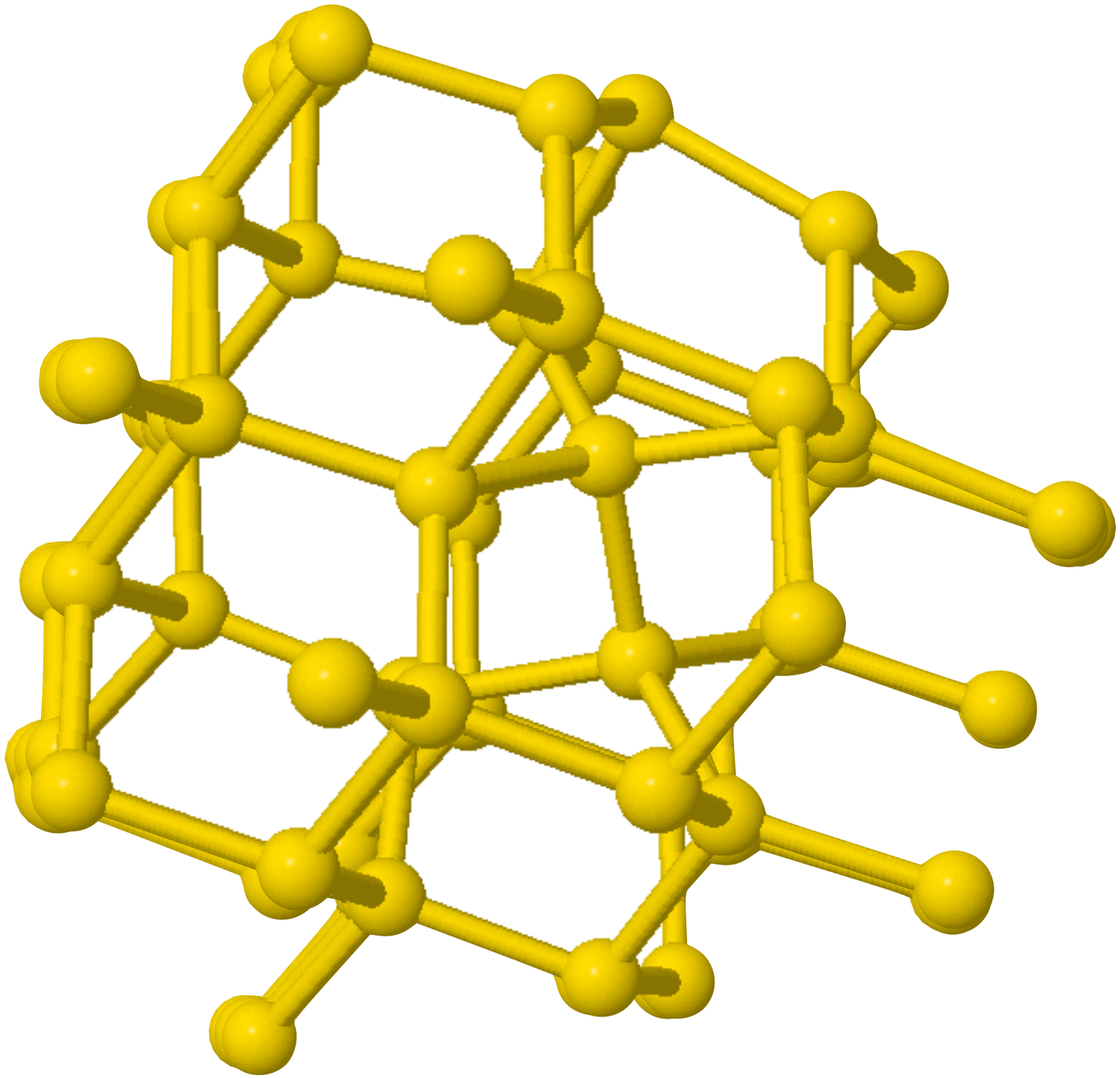

# Diffusion of two vacancies

~1000 atoms
Stillinger-Weber potential
2 vacancies
500 K

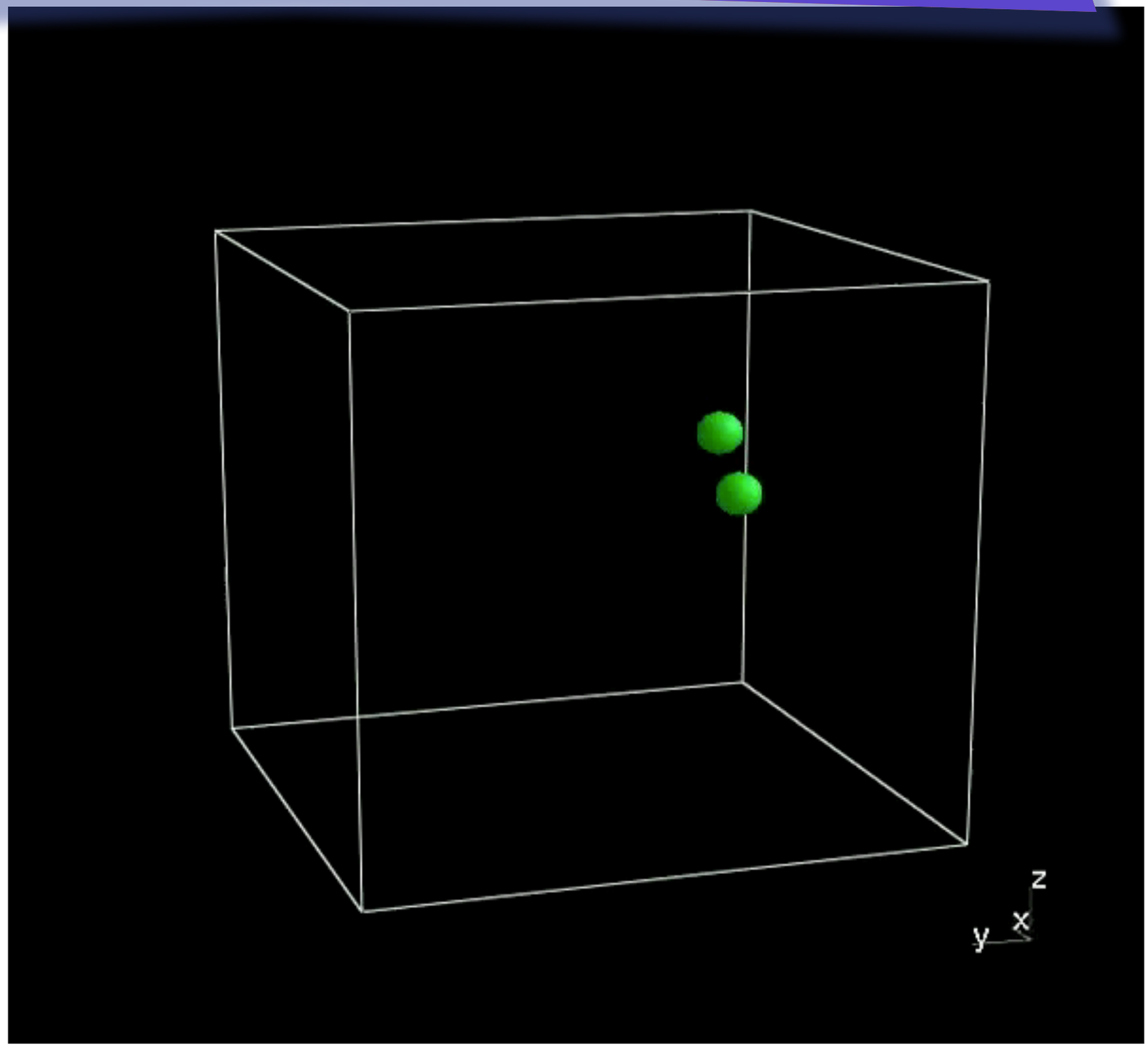


F. El-Mellouhi, NM and L.J. Lewis, PRB 78, 153202 (2008).

# Diffusion of two vacancies — 500 K

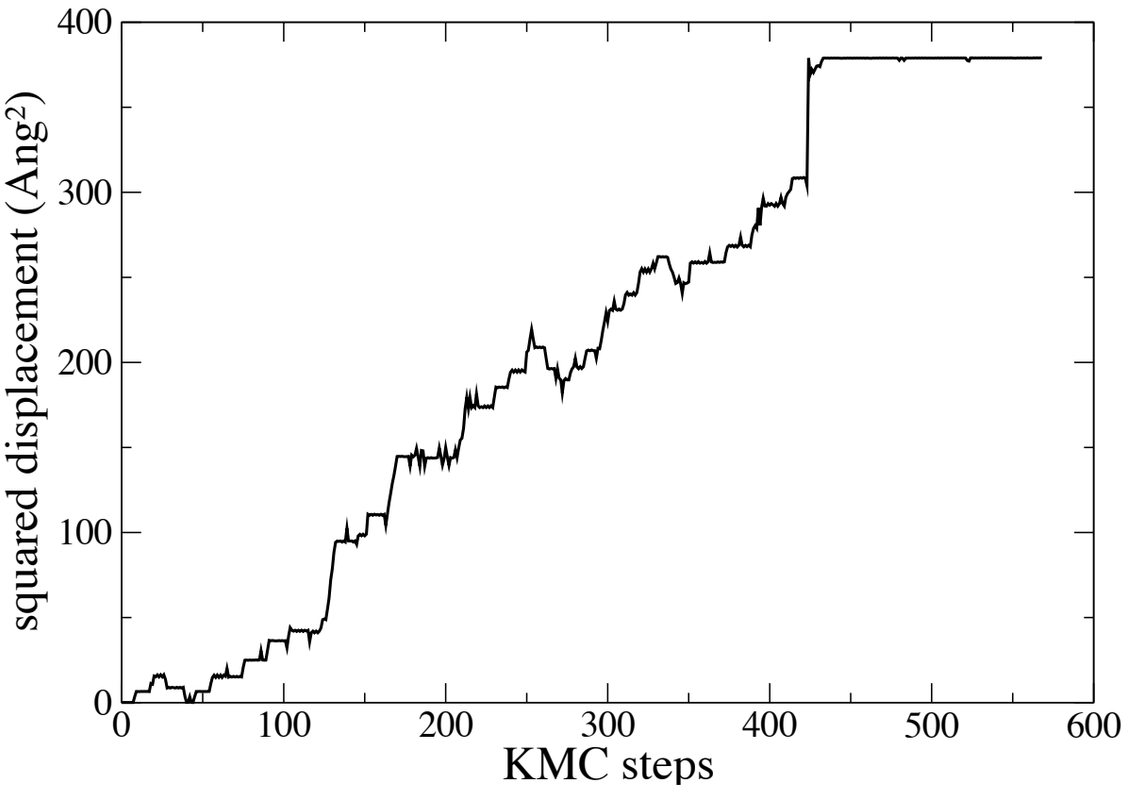


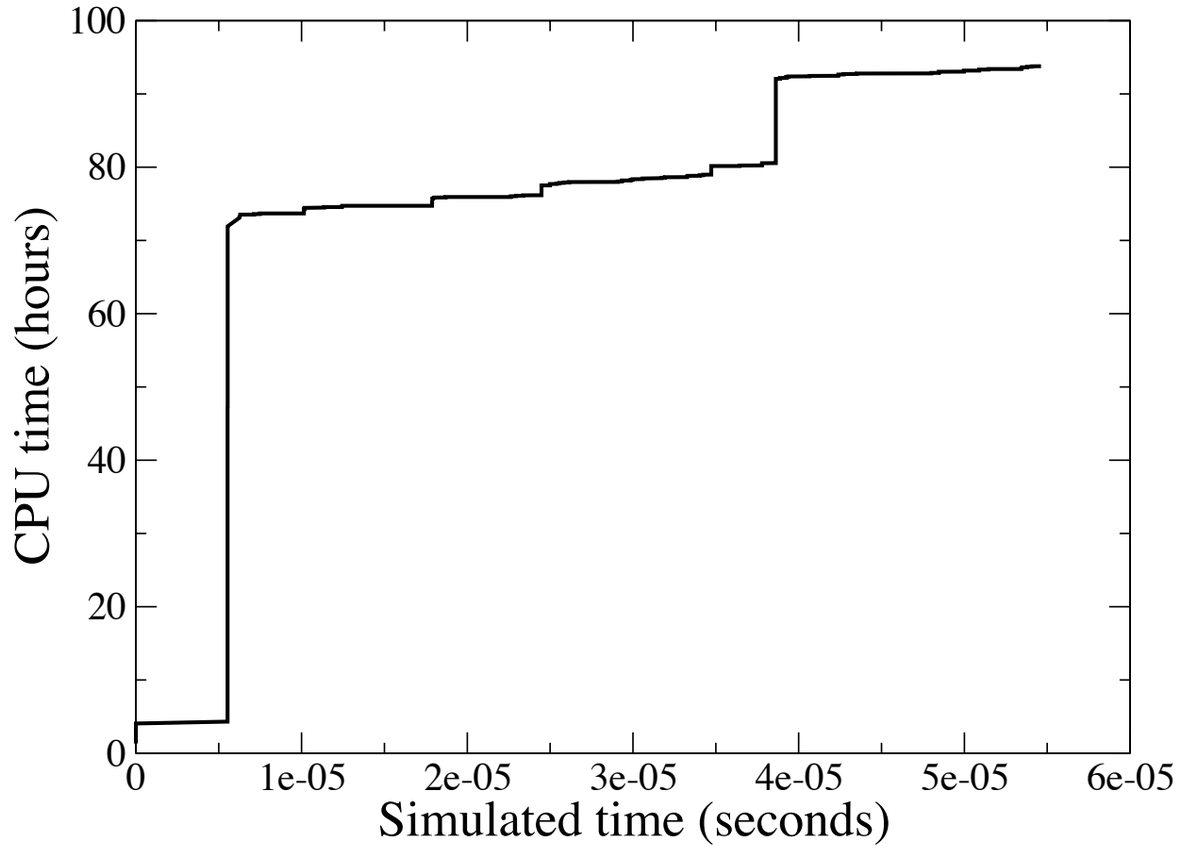


~1000 atoms
Stillinger-Weber potential
2 vacancies
500 K

# Diffusion of two vacancies — 500 K

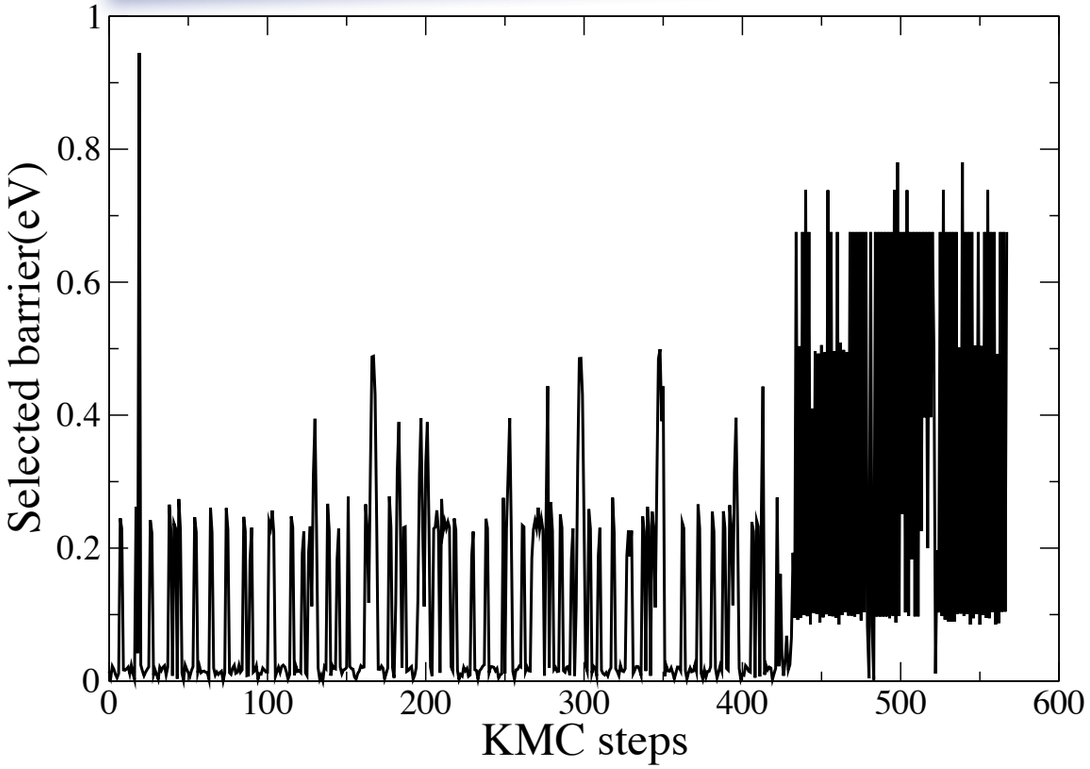


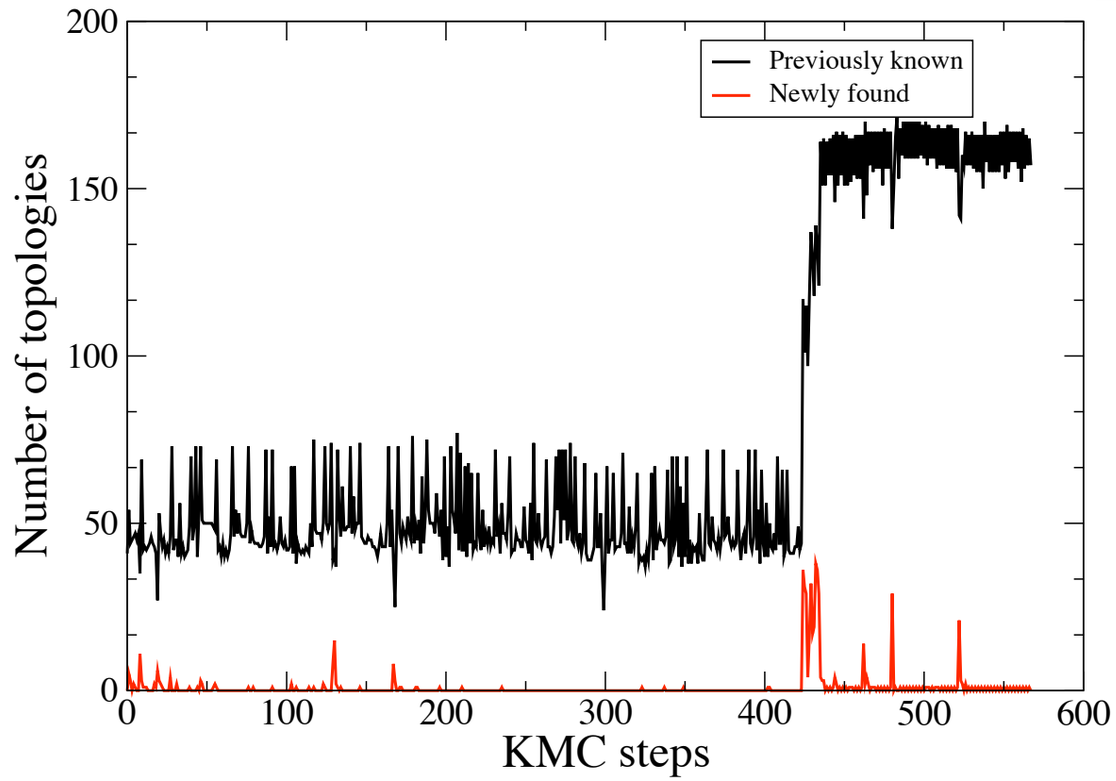


~1000 atoms
Stillinger-Weber potential
2 vacancies
500 K

# Elastic effects - specific barriers

~1000 atoms
Stillinger-Weber potential
6 vacancies
500 K

~1200 events

120 μs

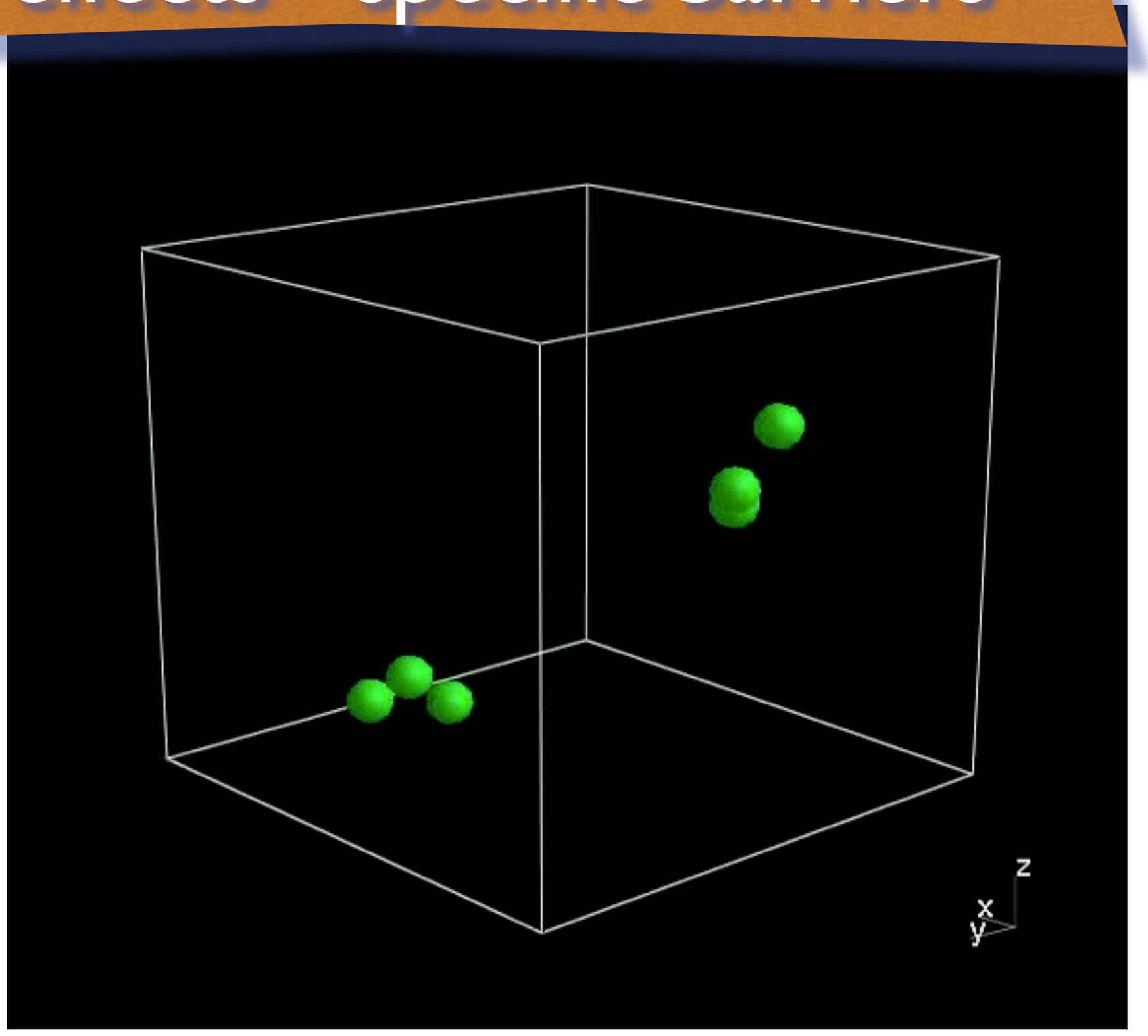

# Only generic events

~1000 atoms
Stillinger-Weber potential
6 vacancies

Only generic events, no relaxation for barriers

500 K

~5000 events

0.001 s

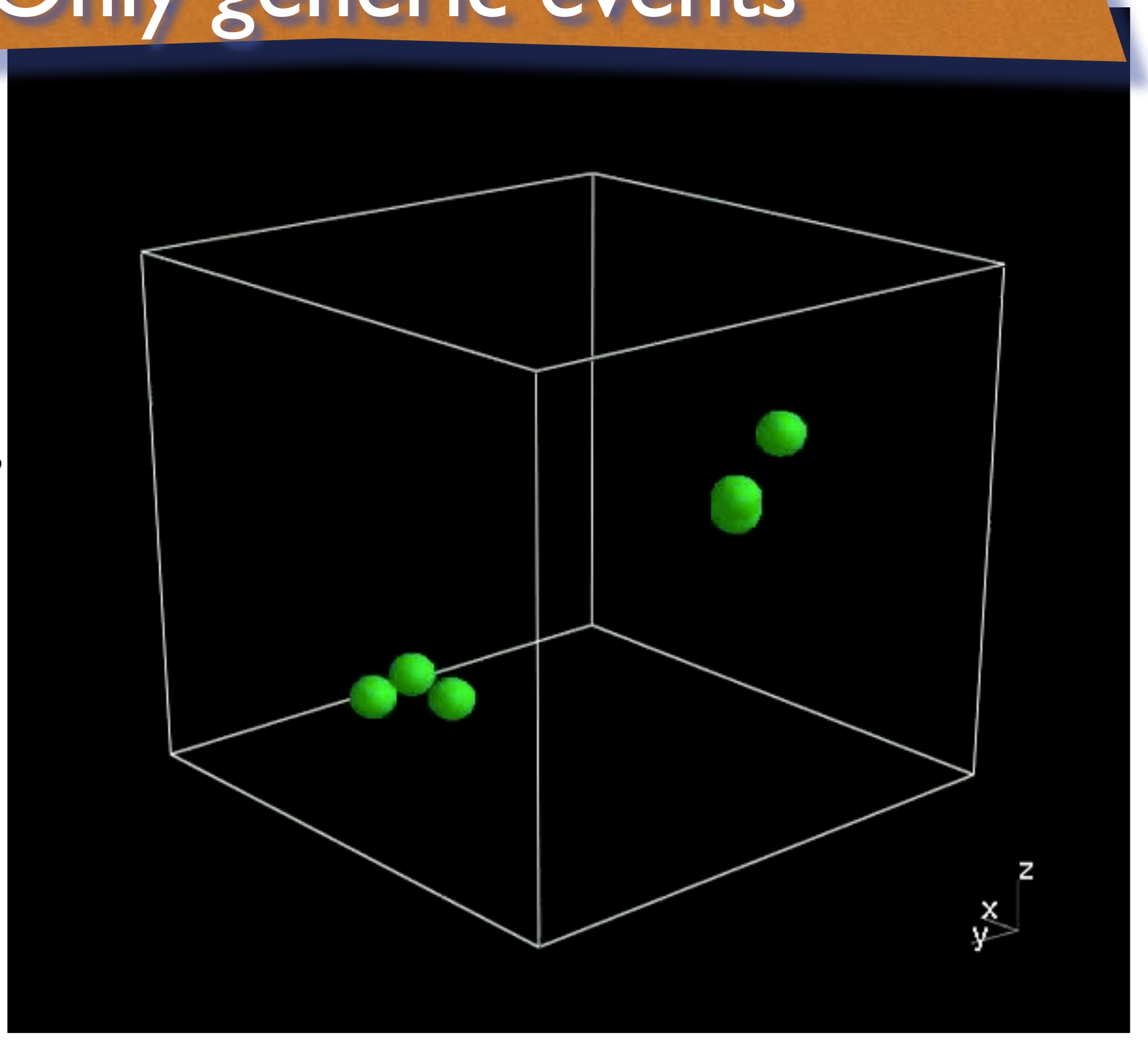

# Example #1: Interstitials and Vacancies

500 K, 8 interstitials and vacancies pairs,

8000 atoms

Stillinger-Weber potential

5-fold coordinated atoms

3-fold coordinated atoms

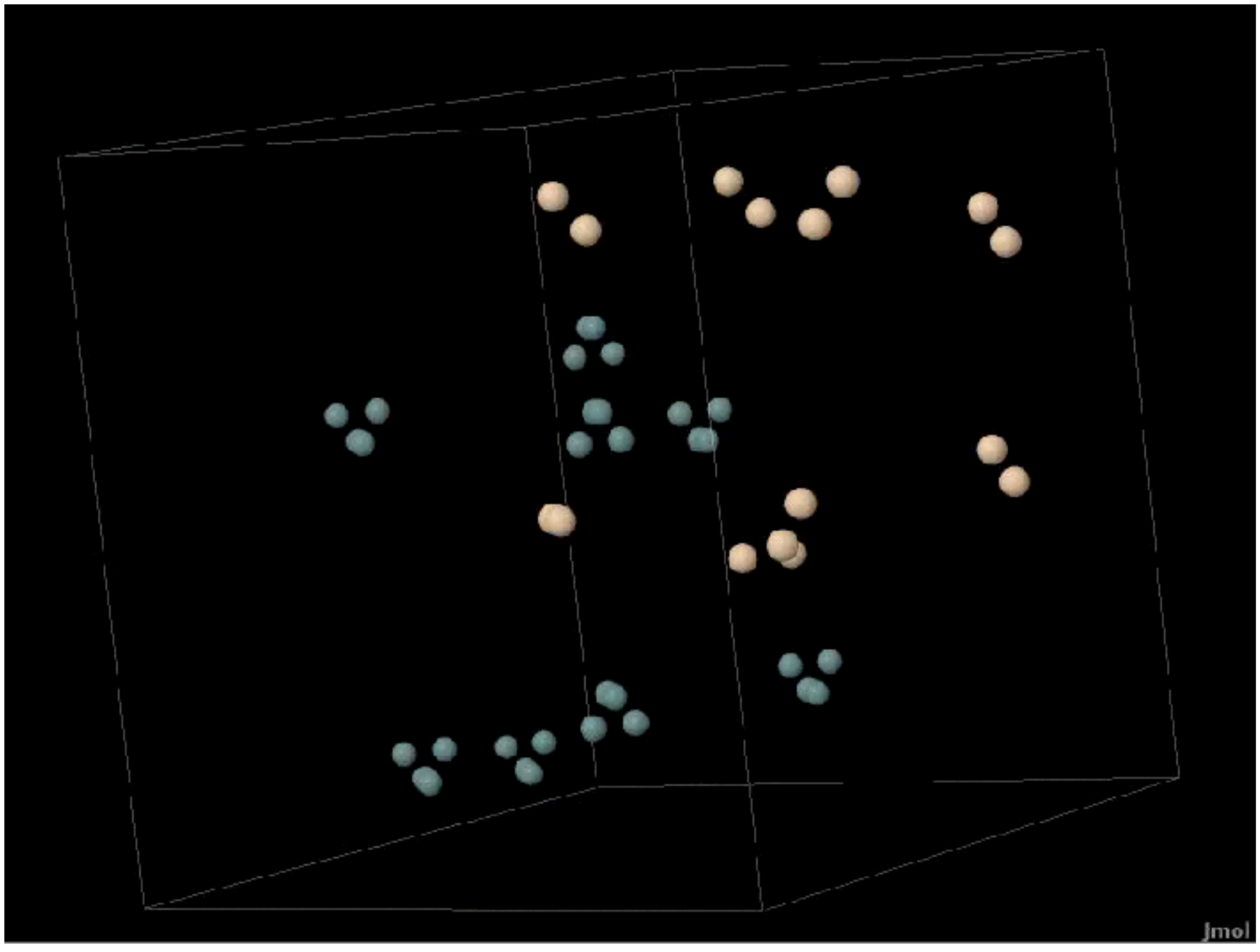

# Interstitials and Vacancies

First arrow : we see a metastable oscillatory state within an IV recombination process. kART spends more time when new topologies appear and spends little time for KMC steps

Second arrow : an orthodox IV recombination.

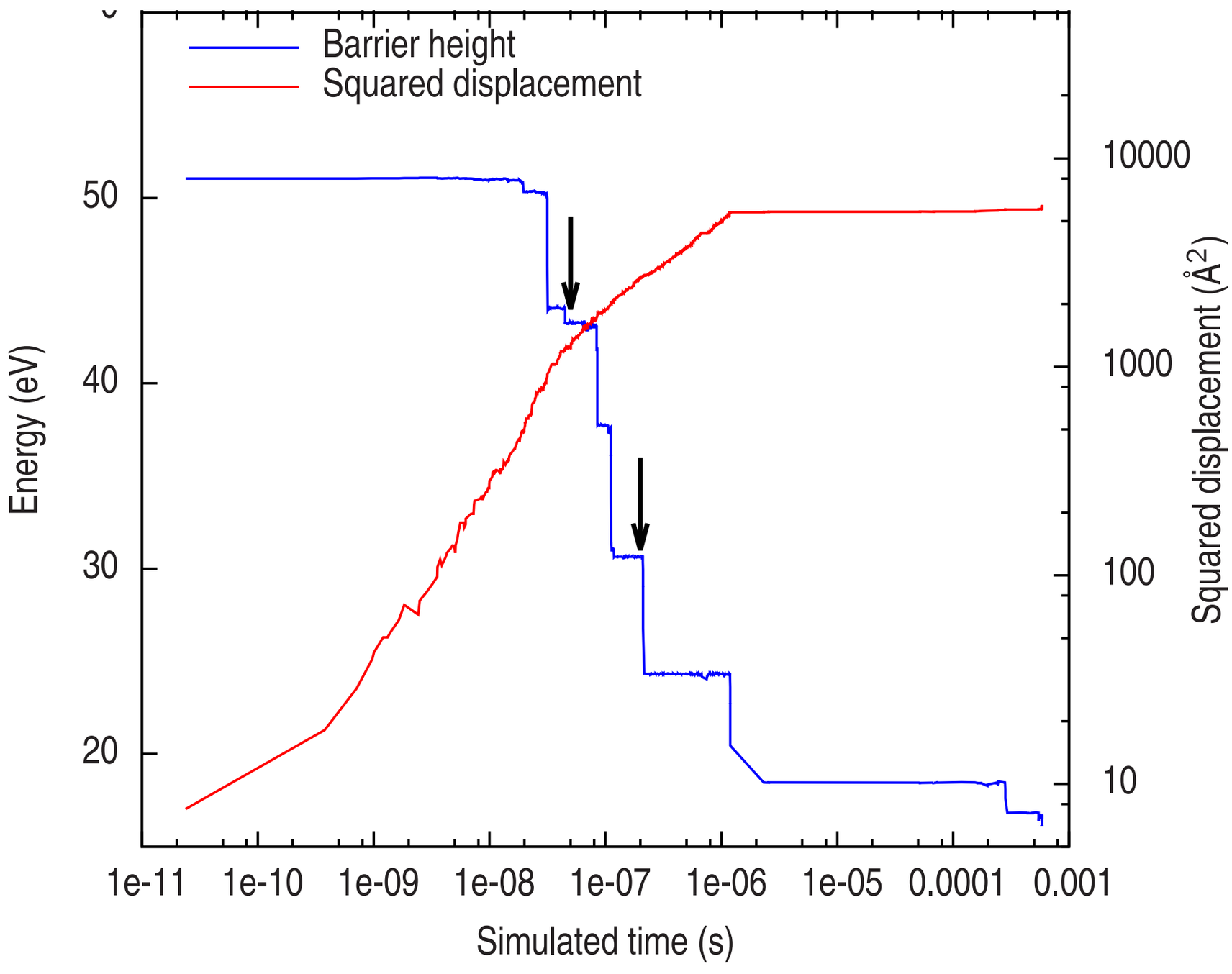

# Interstitials and Vacancies

kART spends more time when new topologies appear and spends little time for KMC steps

We reach long time-scales with a rather large system (8000 atoms) at a temperatures comparable to those of experiments (500K).

k-ART analyzes the transitions between configurations autonomously. This is a big advantage compared to other methods.

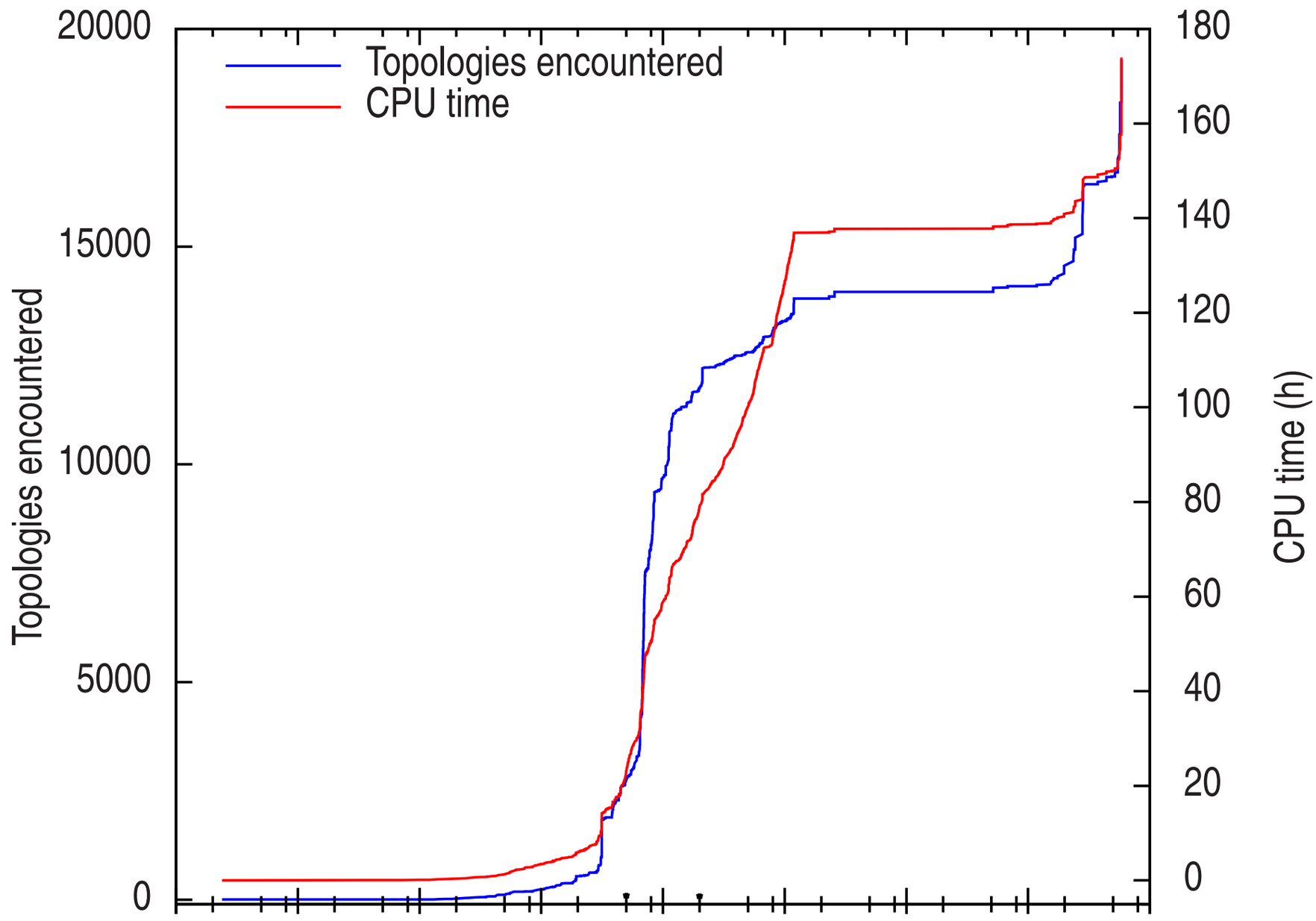

# Taking care of low-energy barriers

Separate states

transient states

- low-energy barriers
- fast transitions between t.s.

absorbing states

- final states: after some time the system will end up in a a.s.

- high-energy barriers

The Mean Rate Method

Puchala et al., JChP **132**, 134104 (2010)
LK Béland, P Brommer, F El-Mellouhi, J-F Joly and NM, PRE **84**,

# Tabu: Taking care of low-energy barriers

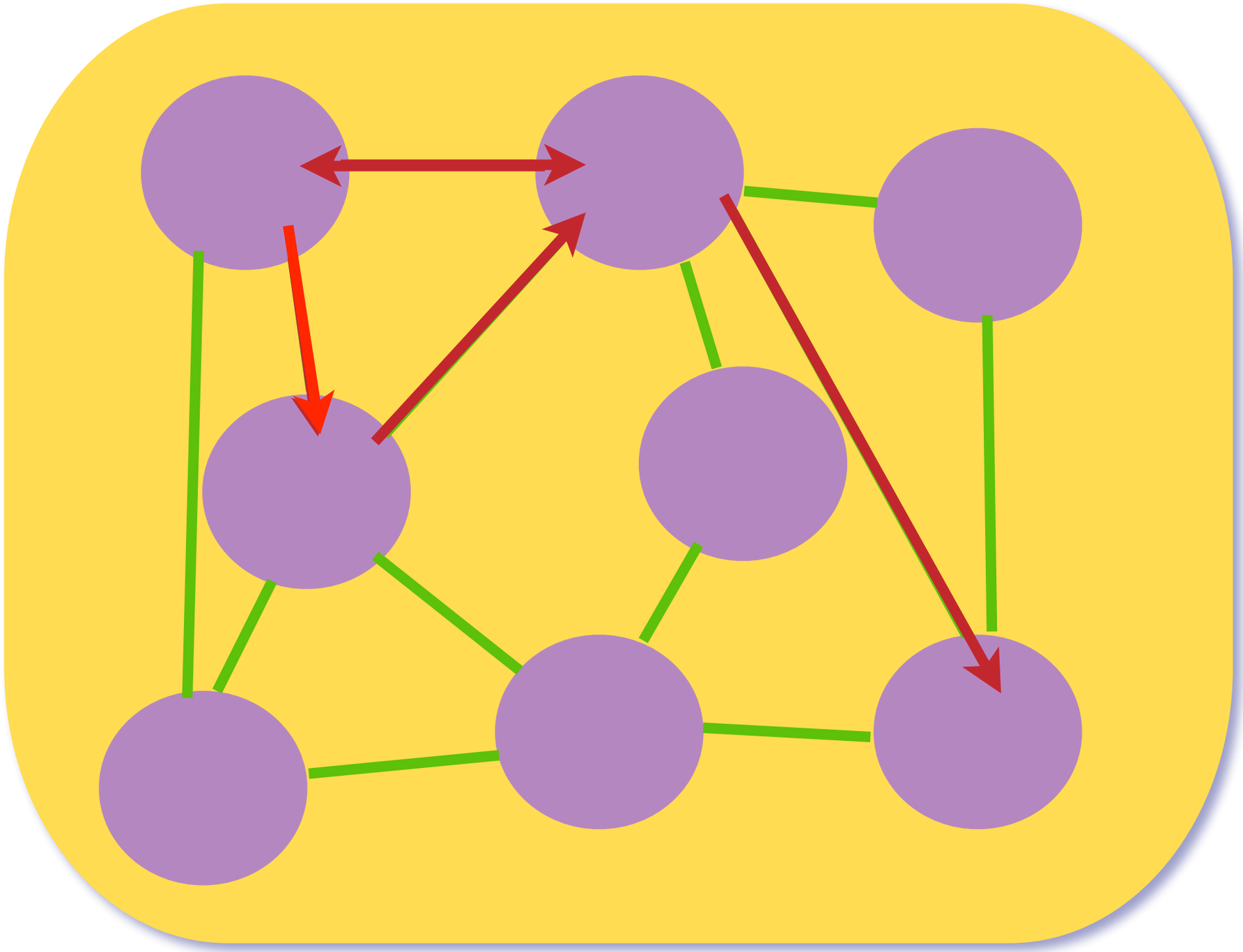

# MRM in kART

- Basin exploration is
  - costly,
  - even unnecessary (early exit to absorbing state).
- Basins are explored and constructed

**on the fly!**

- kART studies transitions (events), classifies:

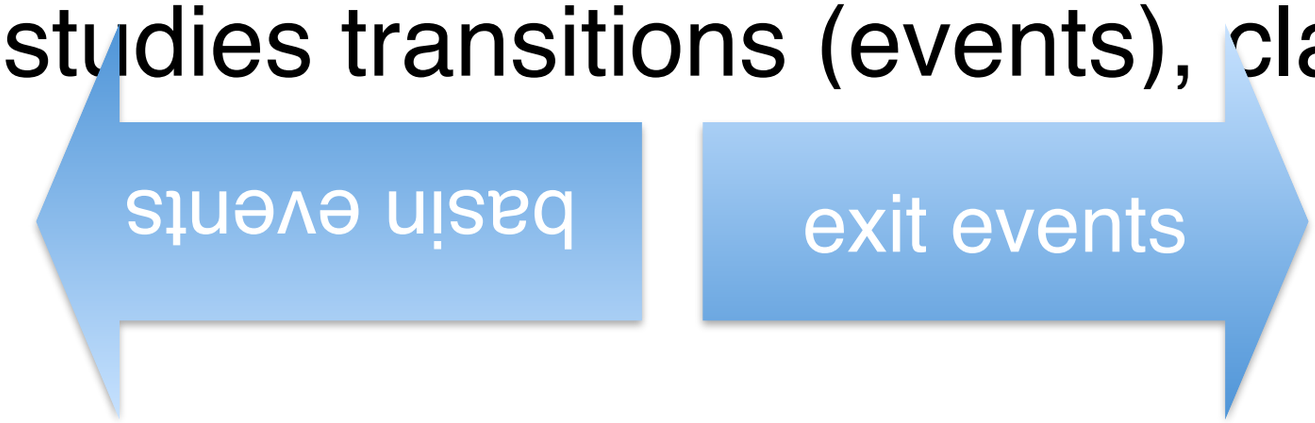


(according to barrier height, reverse barrier height)

# The Basin Mean Rate Method in kART

Starting from state A:

- Identify events.
- If any event could be in basin (low barrier), activate basin search.

blue: potential basin

green: ordinary event

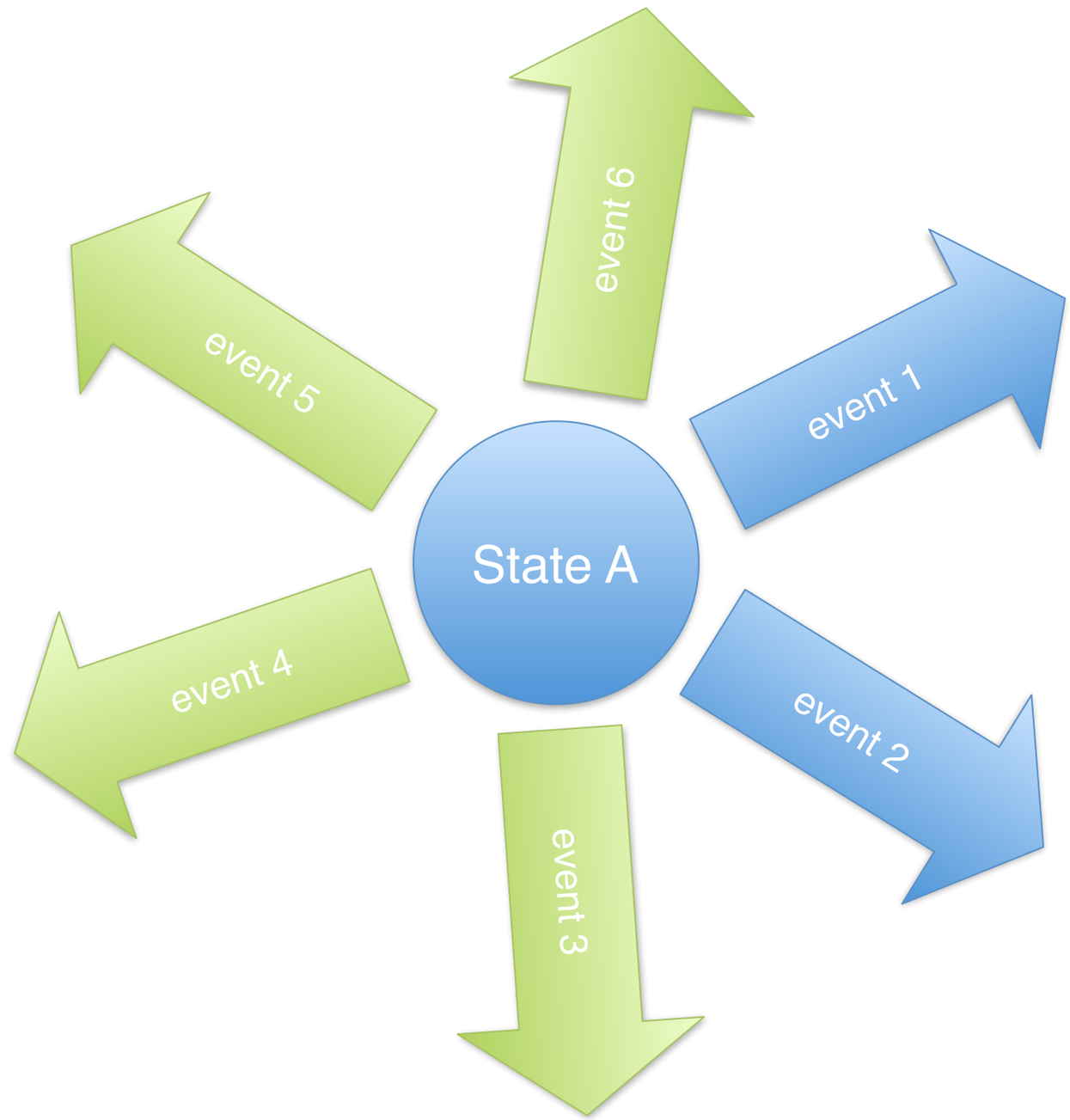

# The Basin Mean Rate Method in kART

Search for new events originating from state B.

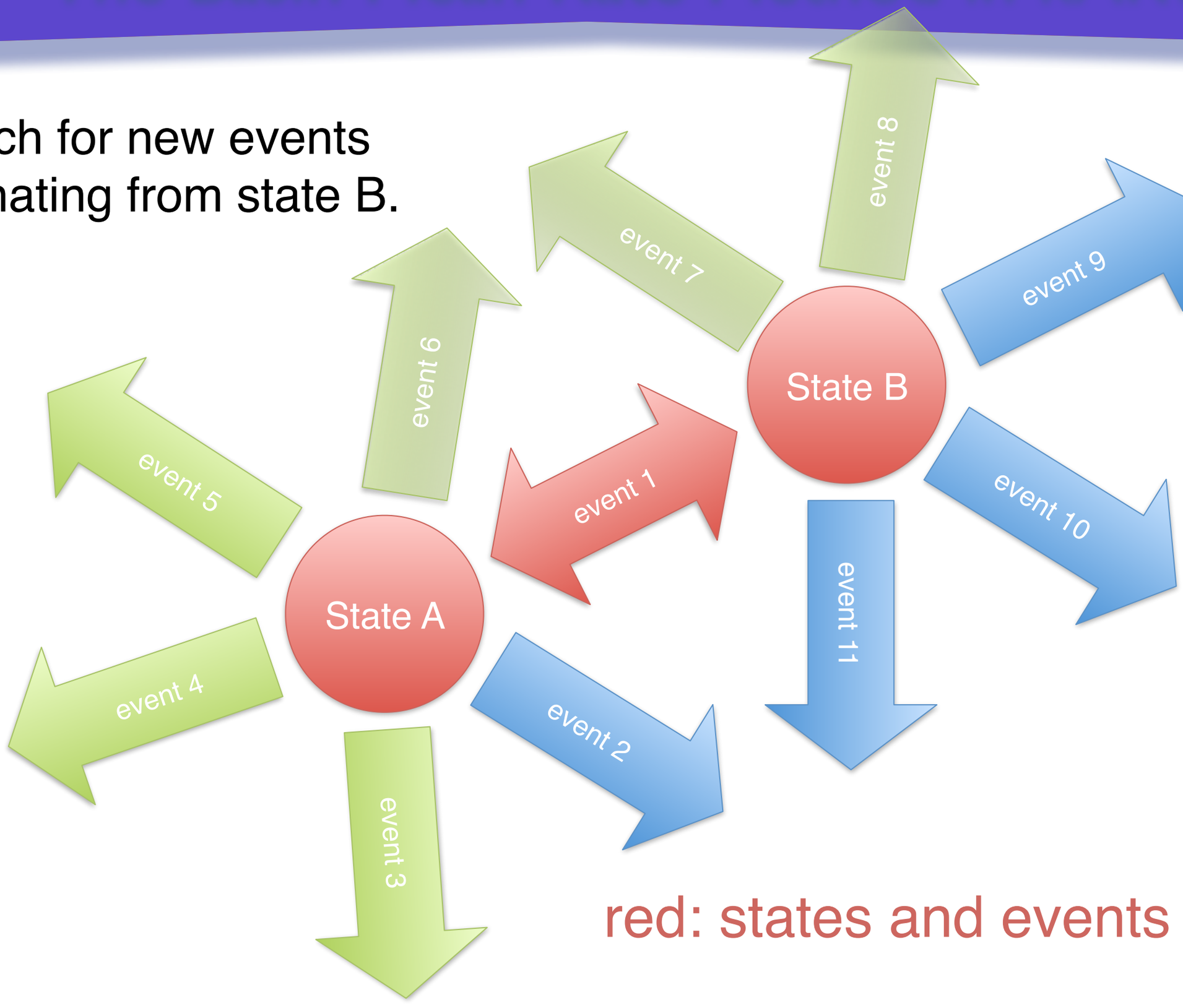


red: states and events in basin

# The Basin Mean Rate Method in kART

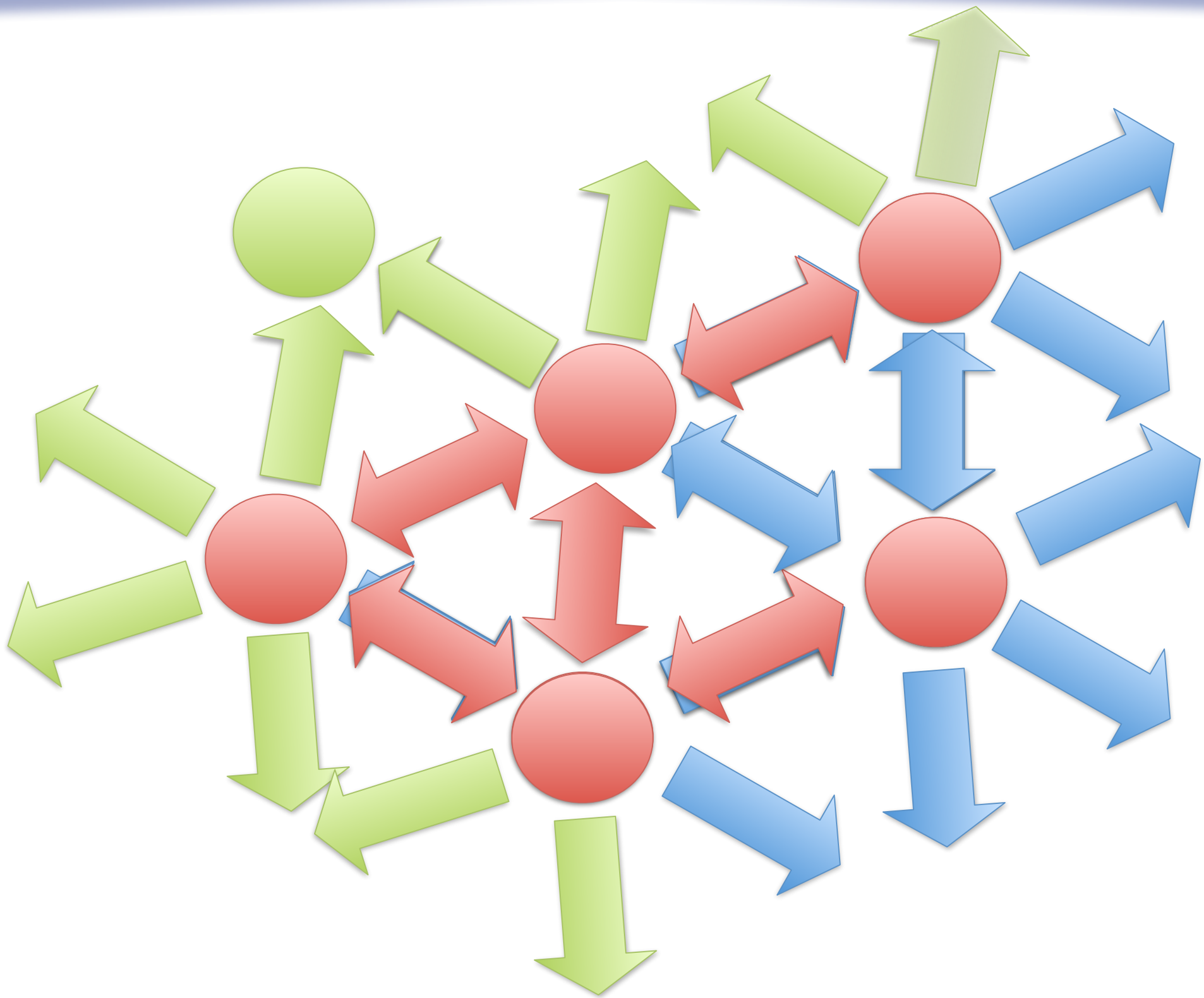

# The Basin Mean Rate Method in kART

- The transition matrix is computed

$$T_{ji} = \frac{R_{i\to j}}{\sum_k R_{i\to k}} = \tau_i^1 R_{i\to j},$$

- Applying this matrix over the initial state of the basin, computing all possible number of jumps

$$\mathbf{\Theta}^{\text{sum}} = \sum_{m=0}^{\infty} \underline{\mathbf{T}}^m \mathbf{\Theta}(0) = (\mathbb{1} - \underline{\mathbf{T}})^{-1} \mathbf{\Theta}(0)$$

we can compute the average residence time in basin

$$\tau_i = \tau_i^1 \Theta_i^{\text{sum}}$$

state *i* before the system exists the basin

- This allows to compute the rate for leaving the basin (*j* here is an exit state)

$$\langle R_{i\to j} \rangle = \frac{\tau_i}{\sum_k \tau_k} R_{i\to j}$$

# The Basin Mean Rate Method in kART

- Basin is constructed “on the fly” – no unnecessary exploration.

- Realistic distribution of final states.

- If selected event does not originate from current state: Trace system back through shortest path to originating state (burning algorithm).

- Ignores correlation between exit state and

# BMRM or Tabu?

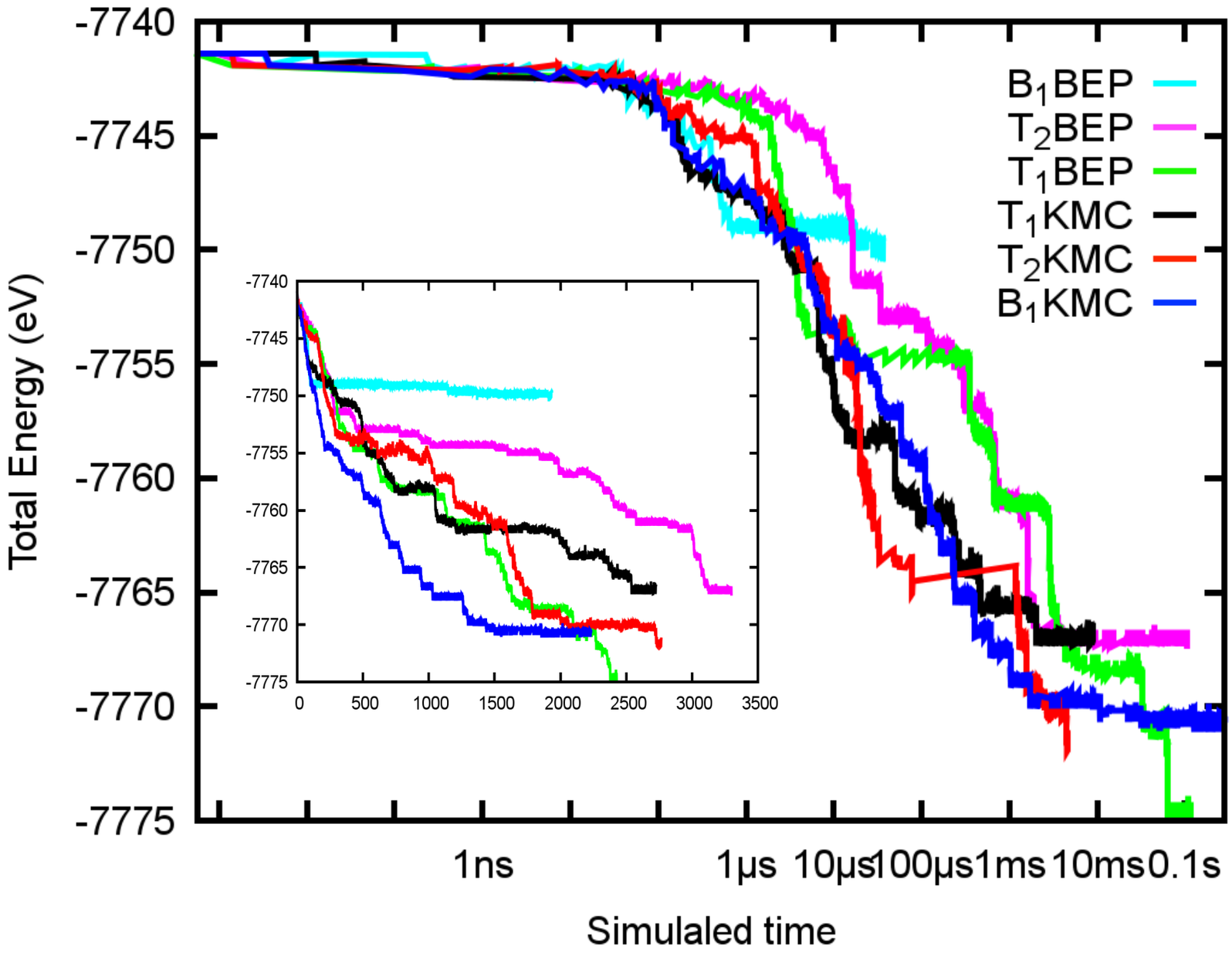
-7740
-7745
-7750
-7755
-7760
-7765
-7770
-7775
Total Energy (eV)
B1BEP
T2BEP
T1BEP
T1KMC
T2KMC
B1KMC
0
500
1000
1500
2000
2500
3000
3500
1ns
1μs
10μs
100μs
1ms
10ms
0.1s
Simulaled time

# KMC or Bell-Evans-Polanyi

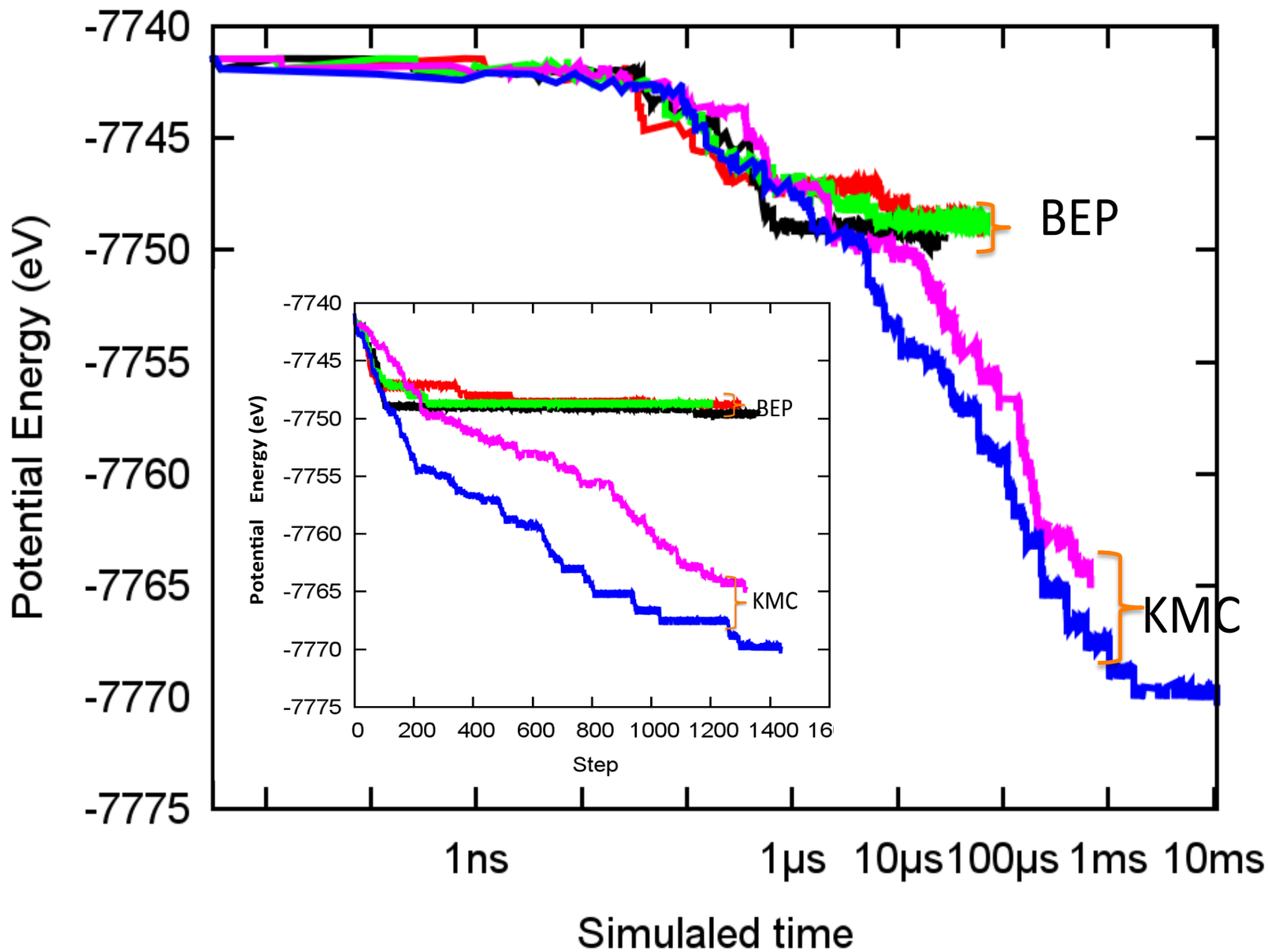

# KMC or Bell-Evans-Polanyi

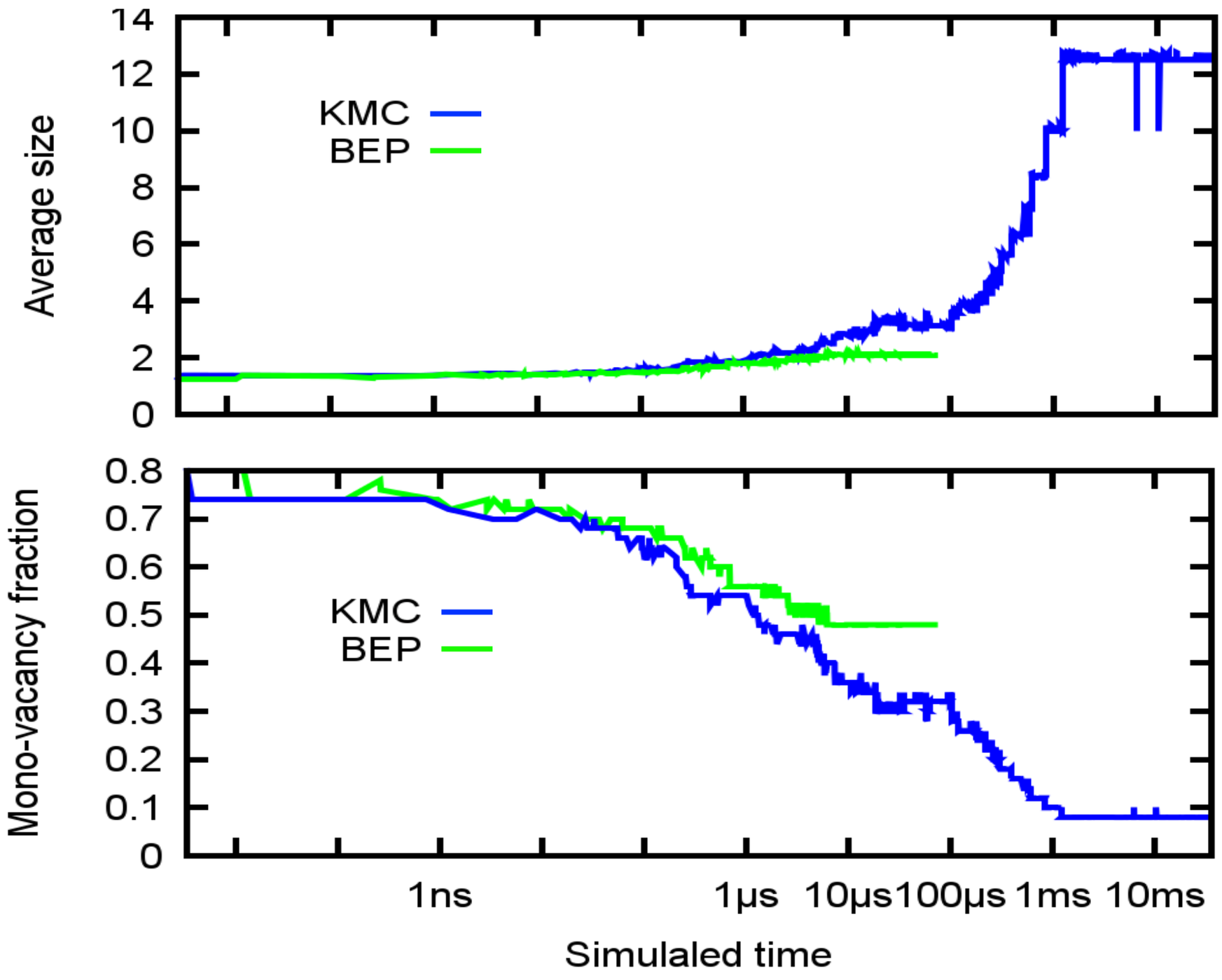

# K-ART : SI ANNEALING AFTER ION-BOMBARDMENT

27000 atoms box, 300 K
1 atom implanted at 3 keV

1 ns simulated with MD, serves as initial configuration for kART run

Comparison with nanocalorimetry experiments is possible

Handling of low-barrier by basin mean-rate method makes these runs even faster

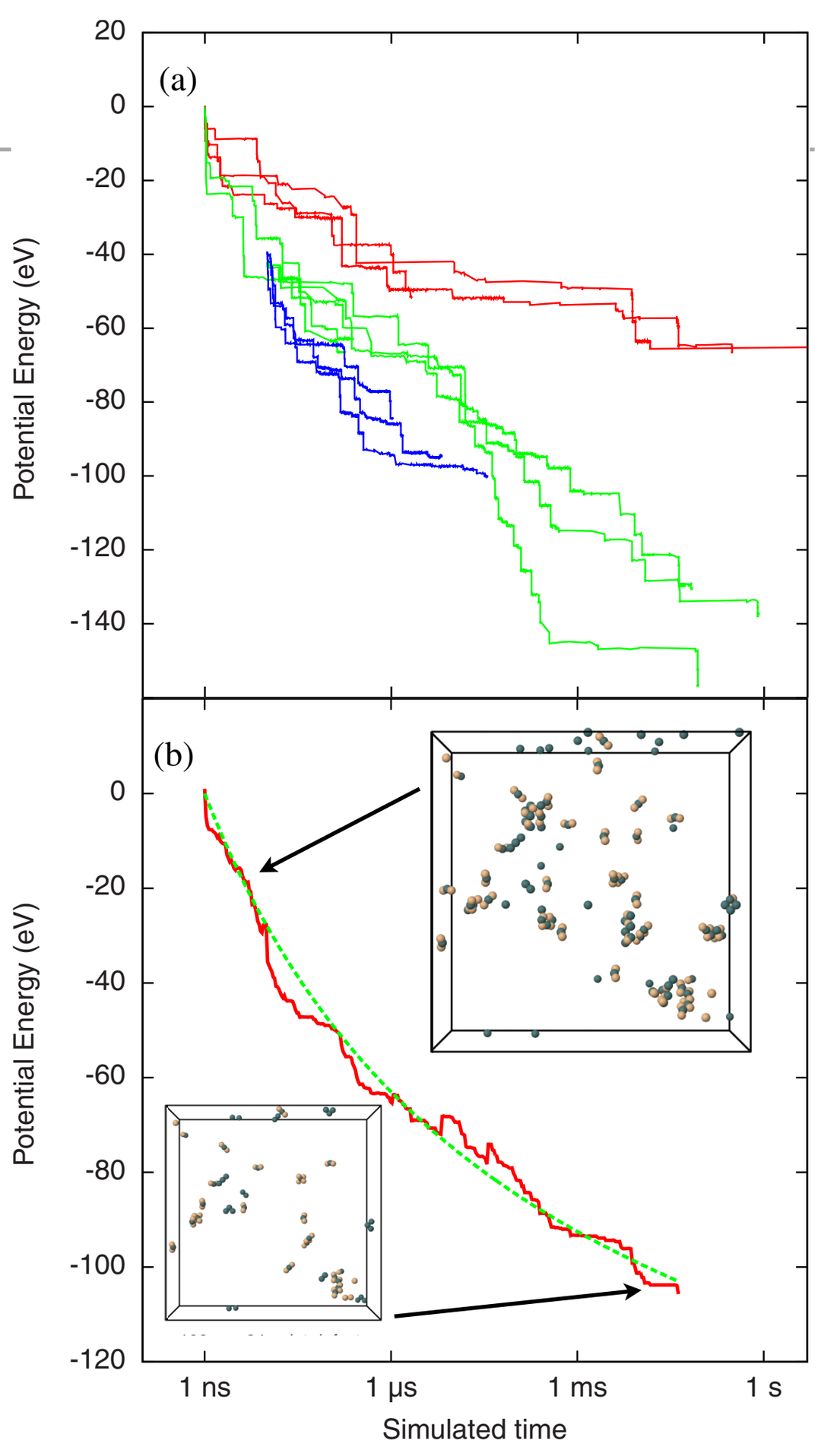


Béland, Mousseau et al, PRL 2013; PRB 2013

# K-ART : SI ANNEALING AFTER ION-BOMBARDMENT

27000 atoms box, 300 K
1 atom implanted at 3 keV

1 ns simulated with MD, serves as initial configuration for kART run

Comparison with nanocalorimetry experiments is possible

Handling of low-barrier by basin mean-rate method makes these runs even faster

Béland, Mousseau et al, PRL 2013; PRB 2013

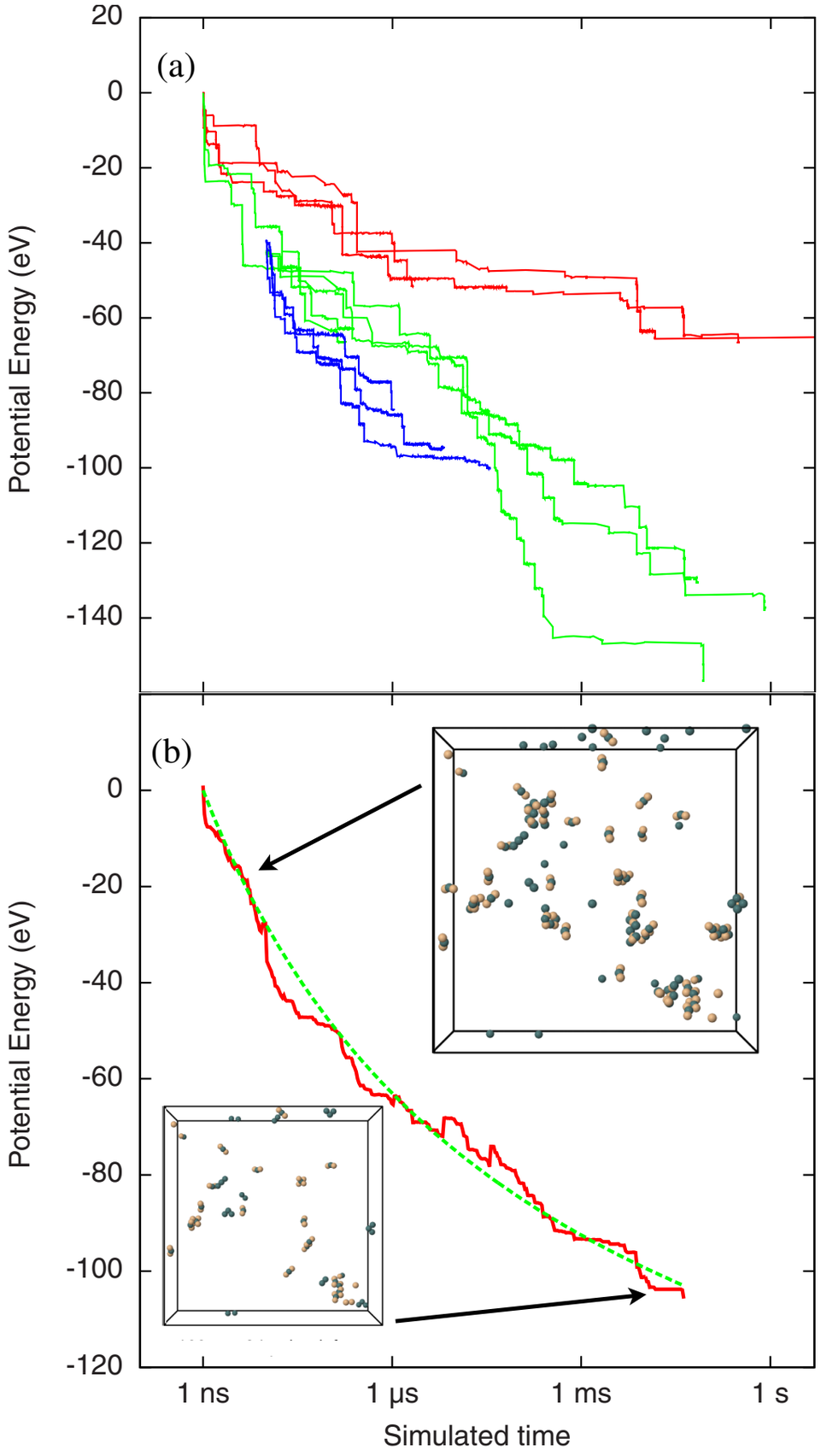

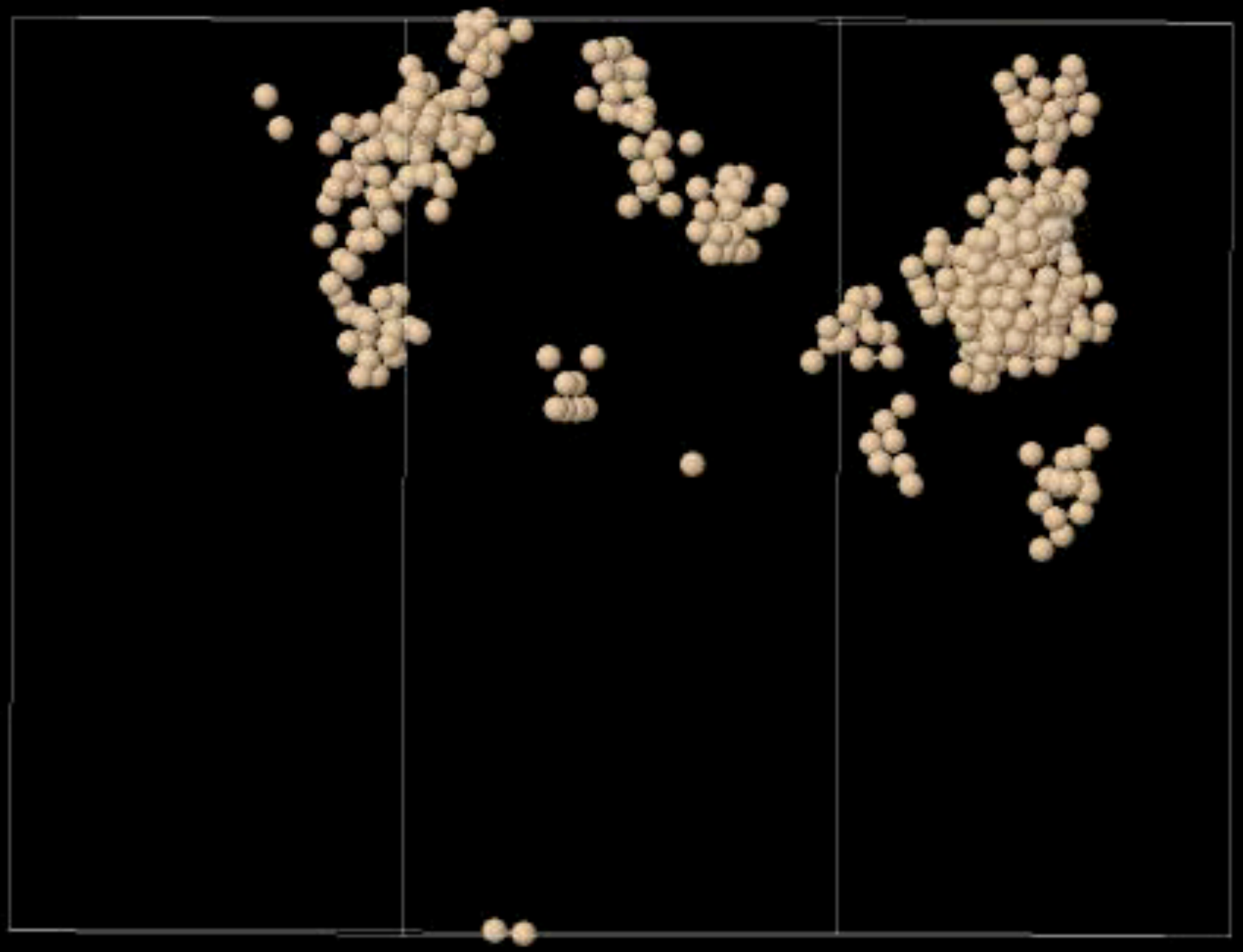

# K-ART : SI ANNEALING AFTER ION-BOMBARDMENT

The jumps in time are caused by the basin method acceleration.

A large number of topologies must be explored to describe the correct PES (potential energy surface) and kinetics.

We show that the damaged system can execute transitions with a quasi-continuum of energy barriers

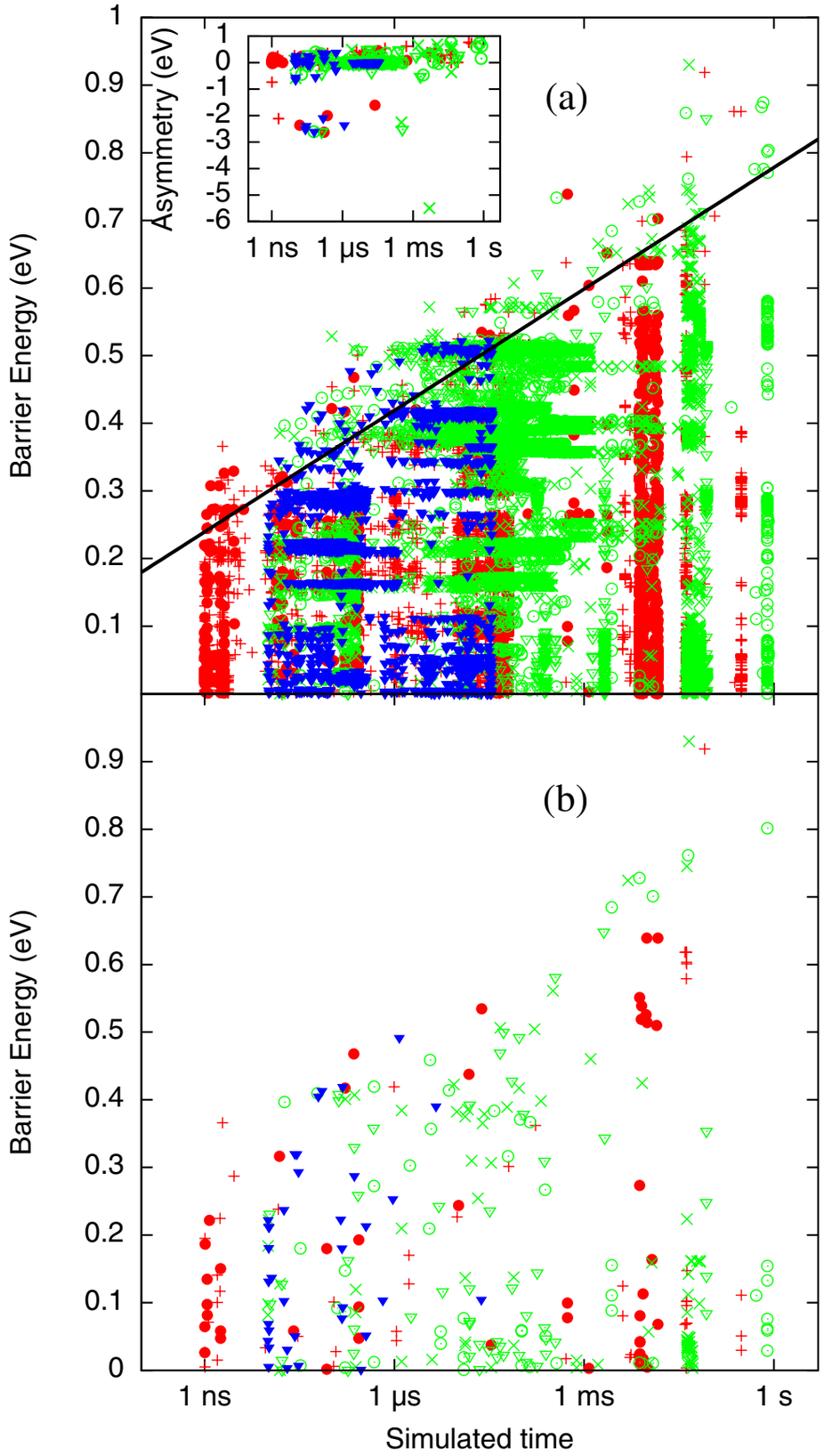


Béland, Mousseau et al, PRL 2013; PRB 2013

# K-ART : SI ANNEALING AFTER ION-BOMBARDMENT

## Comparison with nanocalorimetry measurements

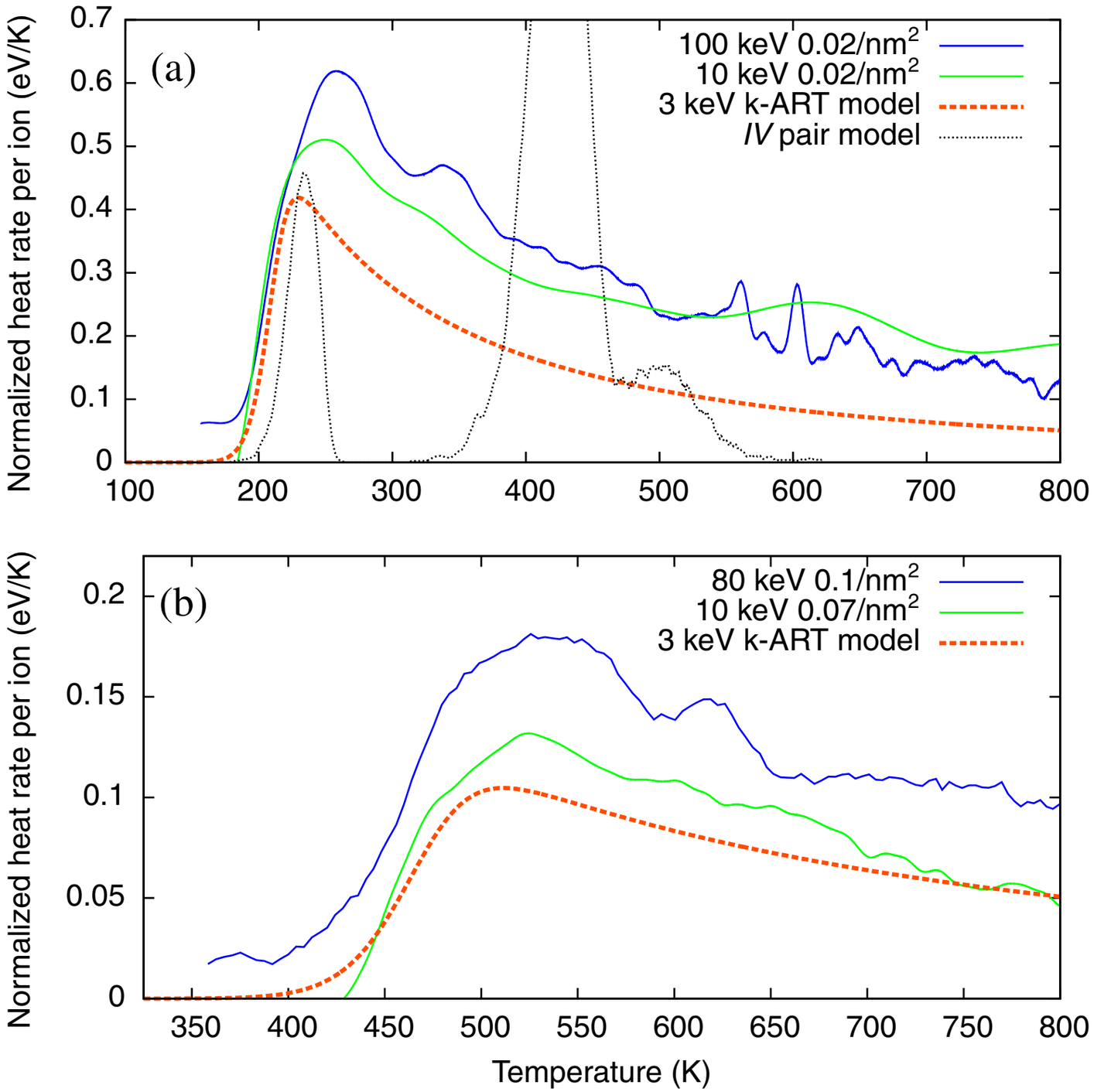


Béland, Mousseau et al, PRL 2013; PRB 2013

# C diffusion in Fe

**What are the fundamental mechanisms responsible for metal dusting ?**

1. Use Becquart's C-Fe EAM potential

2. Start with simple defects :

   1. C interstitials

   2. C subsitutionals

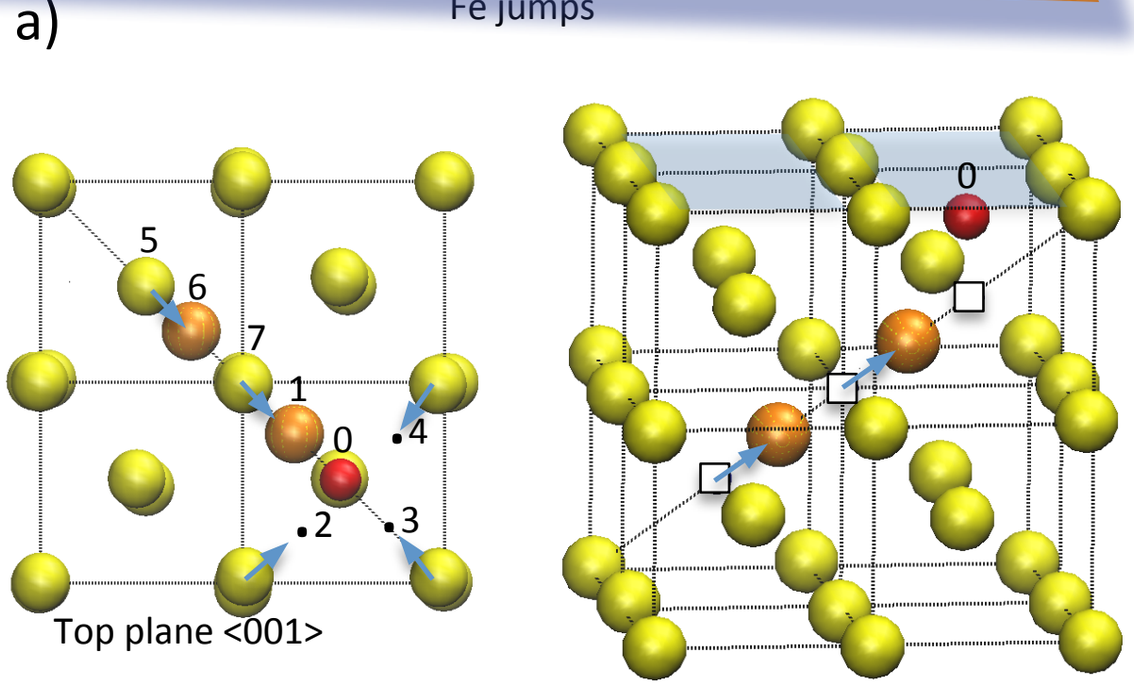


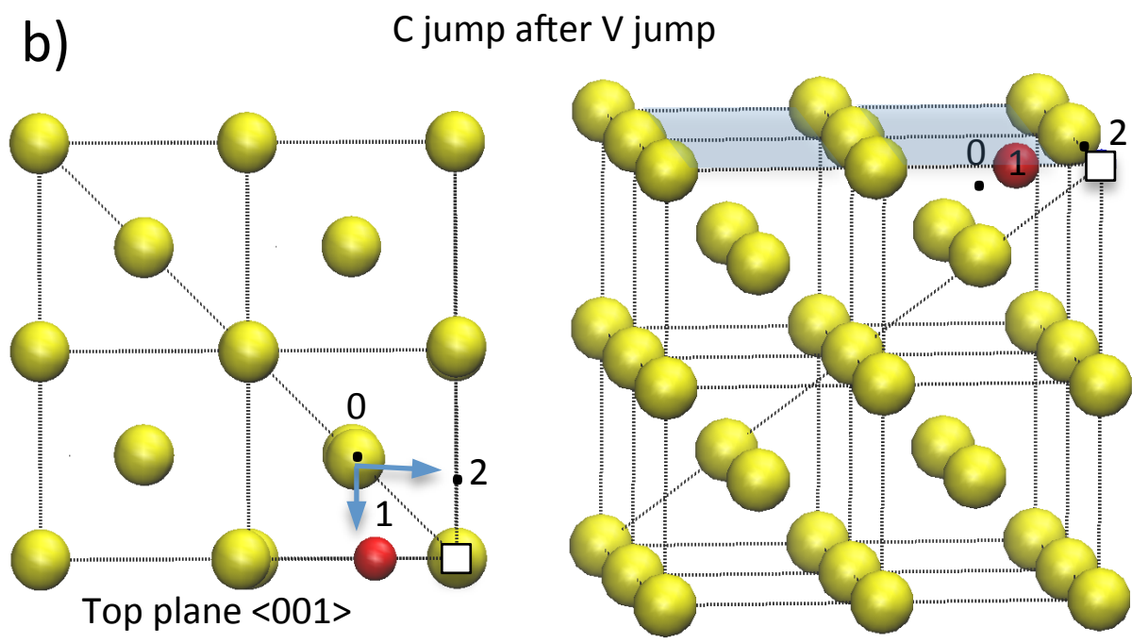


O.A. Restrepo, N. Mousseau, F. El-Mellouhi, O. Bouhali, M. Trochet, C. S. Becquart, Computational Materials Science **112**, Part A, 96-106 (2016).

# C-substitutional in Fe

A complex diffusion:

C-interstitial diffusion barrier: 0.81 eV

The vacancy diffusion barrier: 0.64 eV

Vacancy-C bound state barrier: 1.5 eV

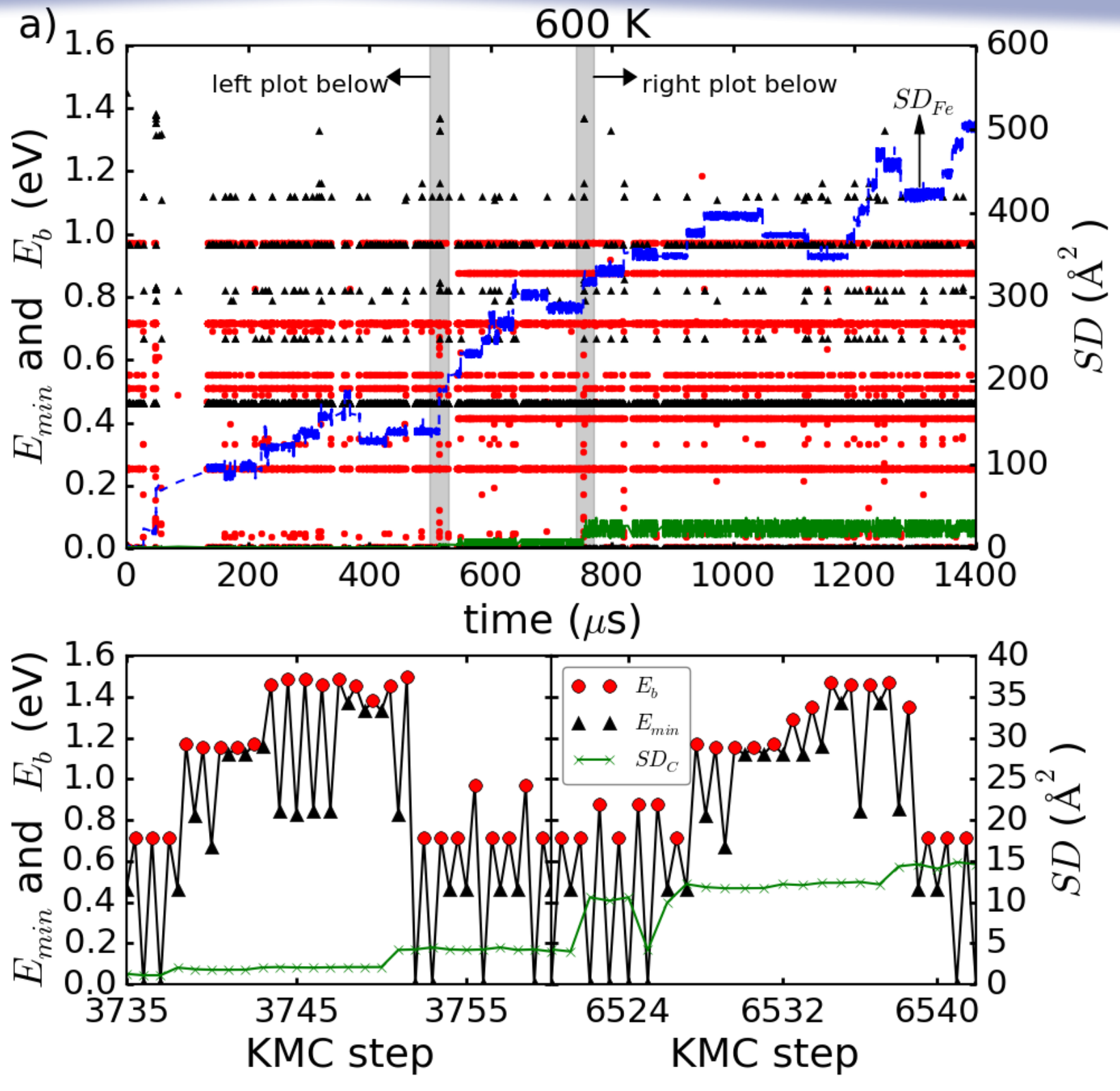

# C diffusion at GB

For a long time, it was believed that GBs provide rapid pathways for impurities, particularly for C in bcc-metals.

This simple image was criticized recently by a number of groups who suggested that diffusion could be enhanced or reduced by the presence of these interfaces, and that their overall behavior was linked to free volume.

A. Oudriss, J. Creus, J. Bouhattate, E. Conforto, C. Berziou, C. Savall, X. Feaugas, Acta Mater, 60, 6814 (2012).

S. M. Teus, V.F. Mazanko, J.-M. Olive, V.G. Gavriljuk, Acta Mater. 69, 105 (2014).

# Effects of Grain Boundaries

- For a long time, it was believed that GBs provide rapid pathways for impurities
- This simple image was criticized recently. It was suggested that diffusion could be enhanced or reduced by the presence of these interfaces, and that their overall behavior was linked to free volume.

See, for example: A. Oudriss et al. , Acta Mater, 60, 6814 (2012); S. M. Teus et al., Acta Mater. 69, 105 (2014).

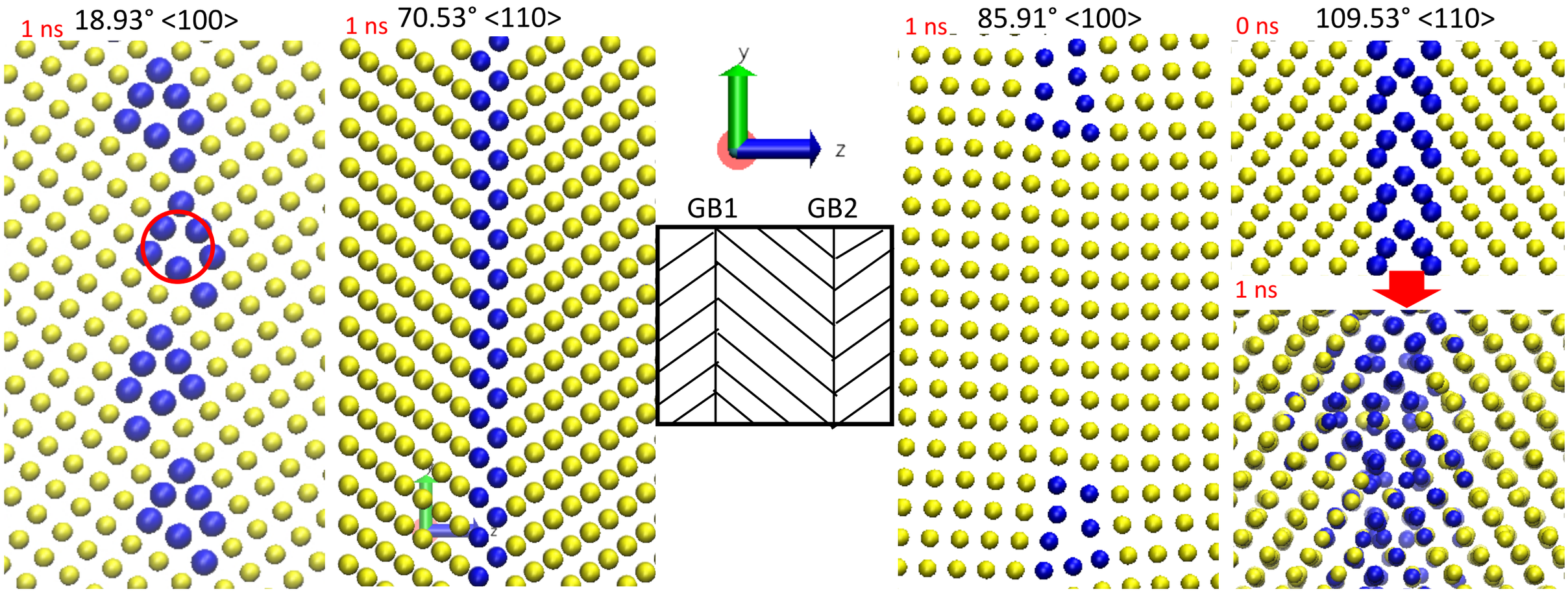


Restrepo, N.M., El-Mellouhi, Bouhali, Becquart, PRB **97**, 054309 (2018).

# Diffusion of Grain Boundaries

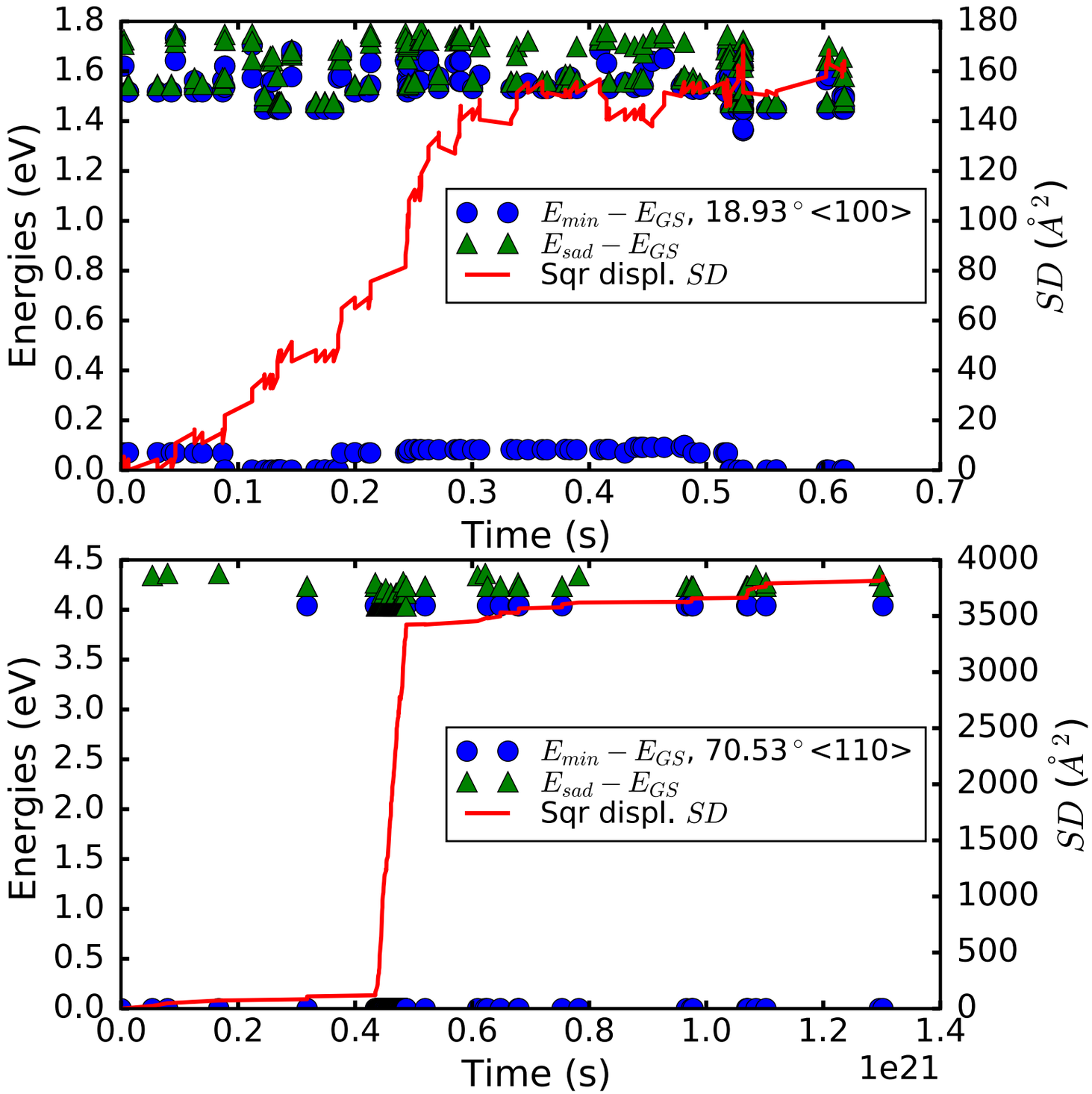

# C diffusion at grain boundaries

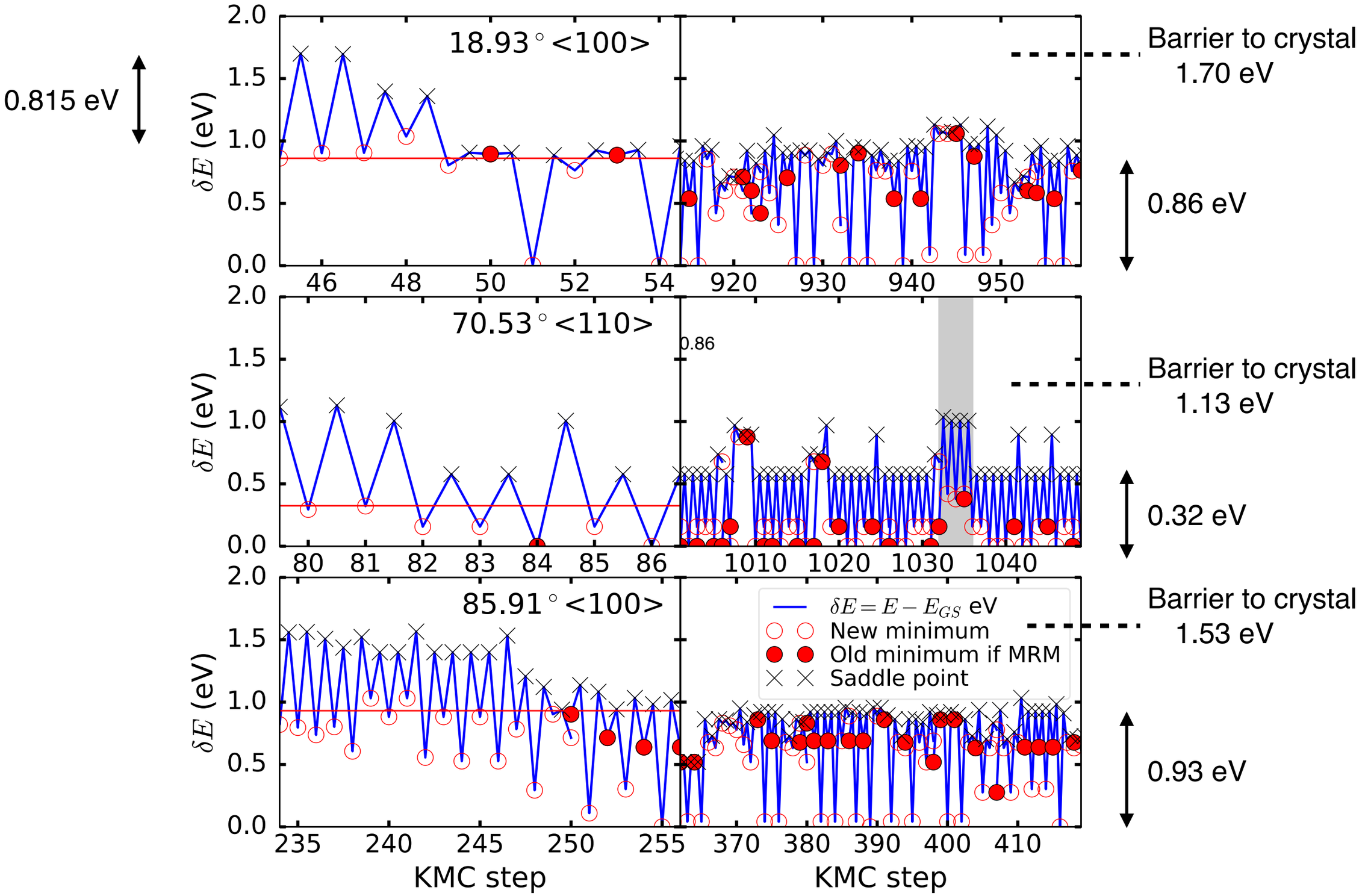

# C diffusion at grain boundaries

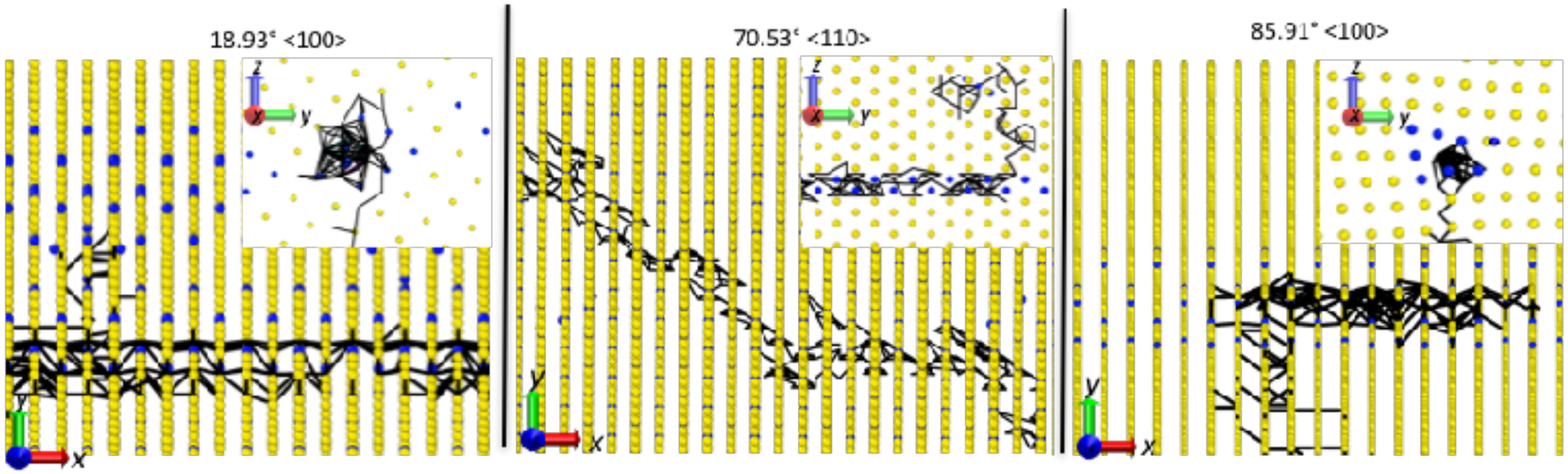


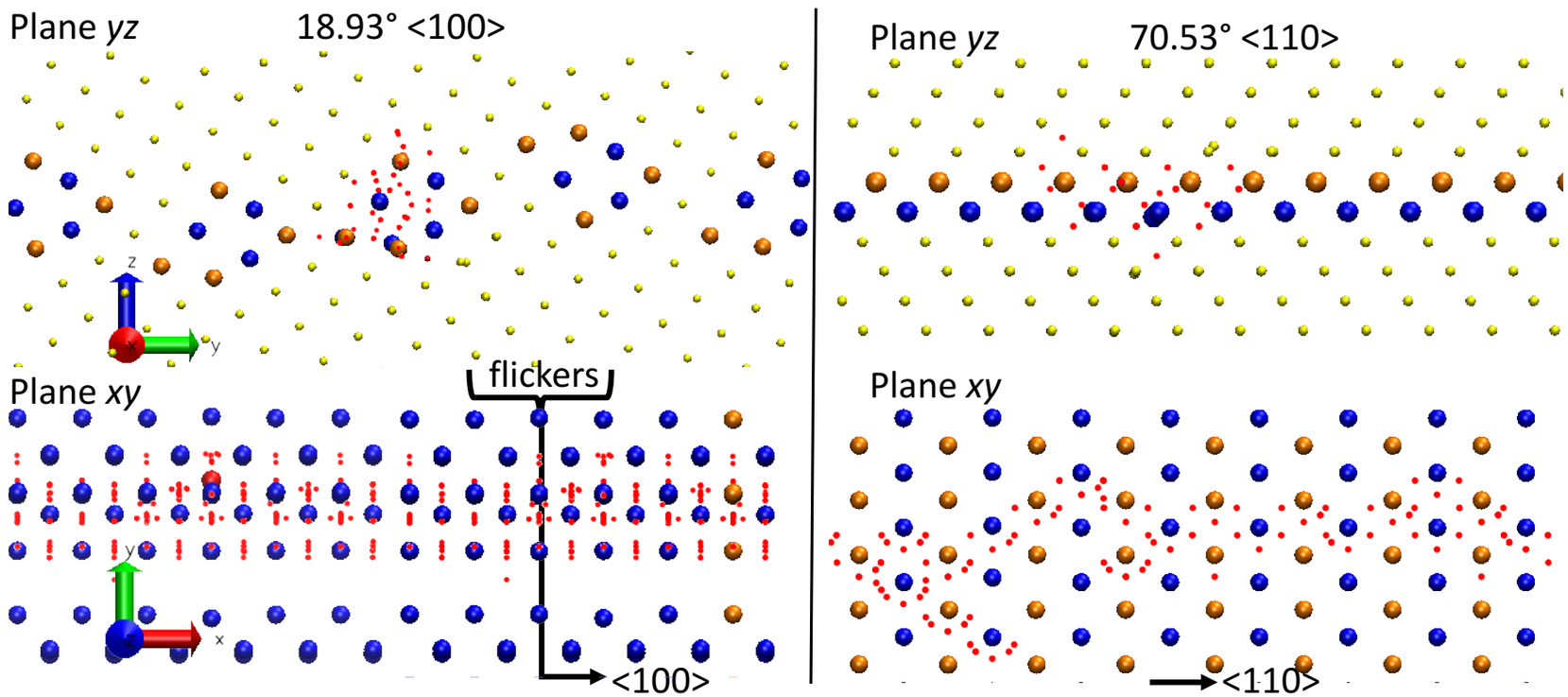

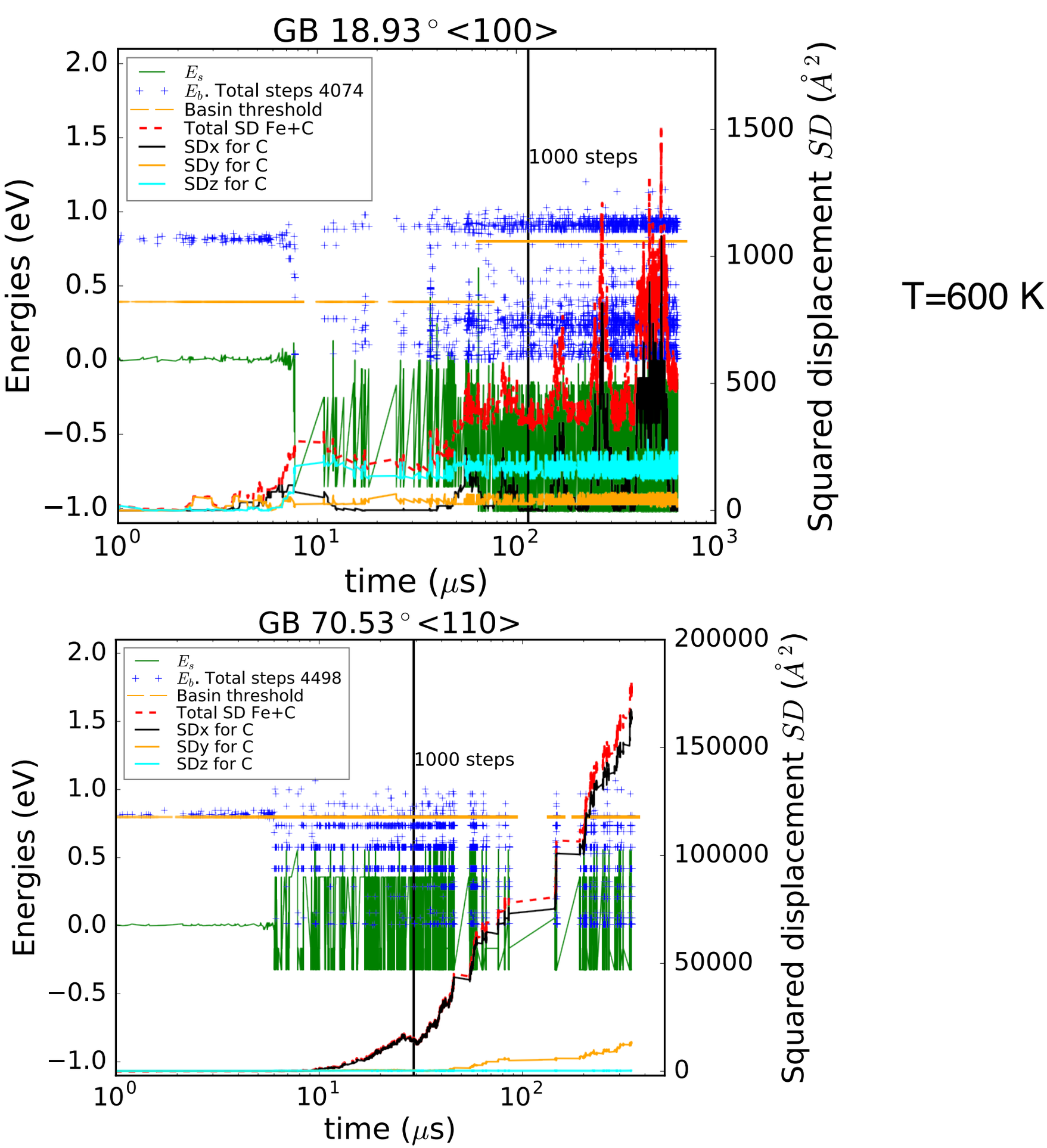
GB 18.93° <100>
$E_s$
$E_b$. Total steps 4074
Basin threshold
Total SD Fe+C
SDx for C
SDy for C
SDz for C
1000 steps
Energies (eV)
Squared displacement $SD$ ($\AA^2$)
time ($\mu$s)
GB 70.53° <110>
$E_s$
$E_b$. Total steps 4498
Basin threshold
Total SD Fe+C
SDx for C
SDy for C
SDz for C
1000 steps
Energies (eV)
Squared displacement $SD$ ($\AA^2$)
time ($\mu$s)

T=600 K

# C diffusion at grain boundaries

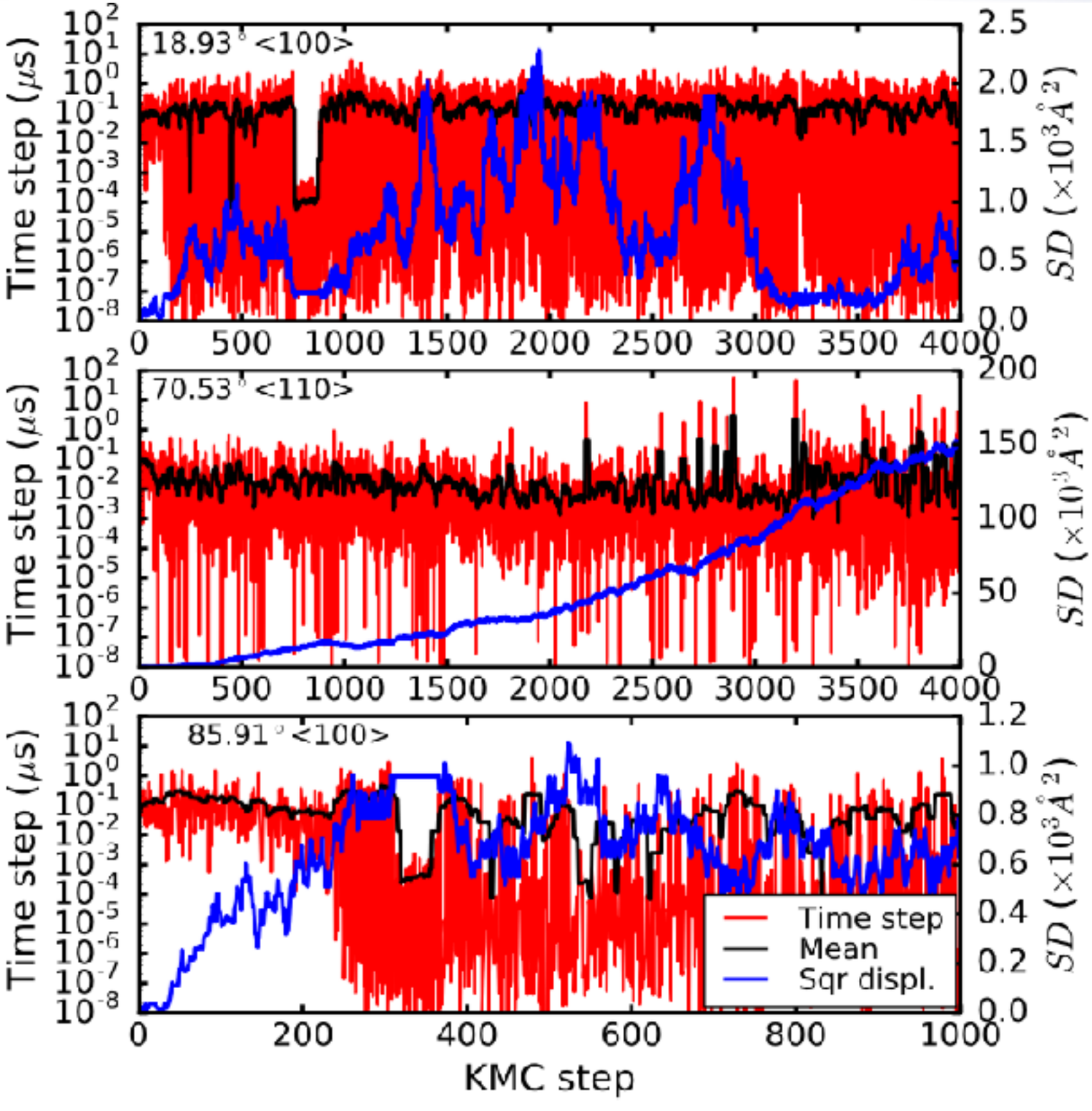

# C diffusion at grain boundaries

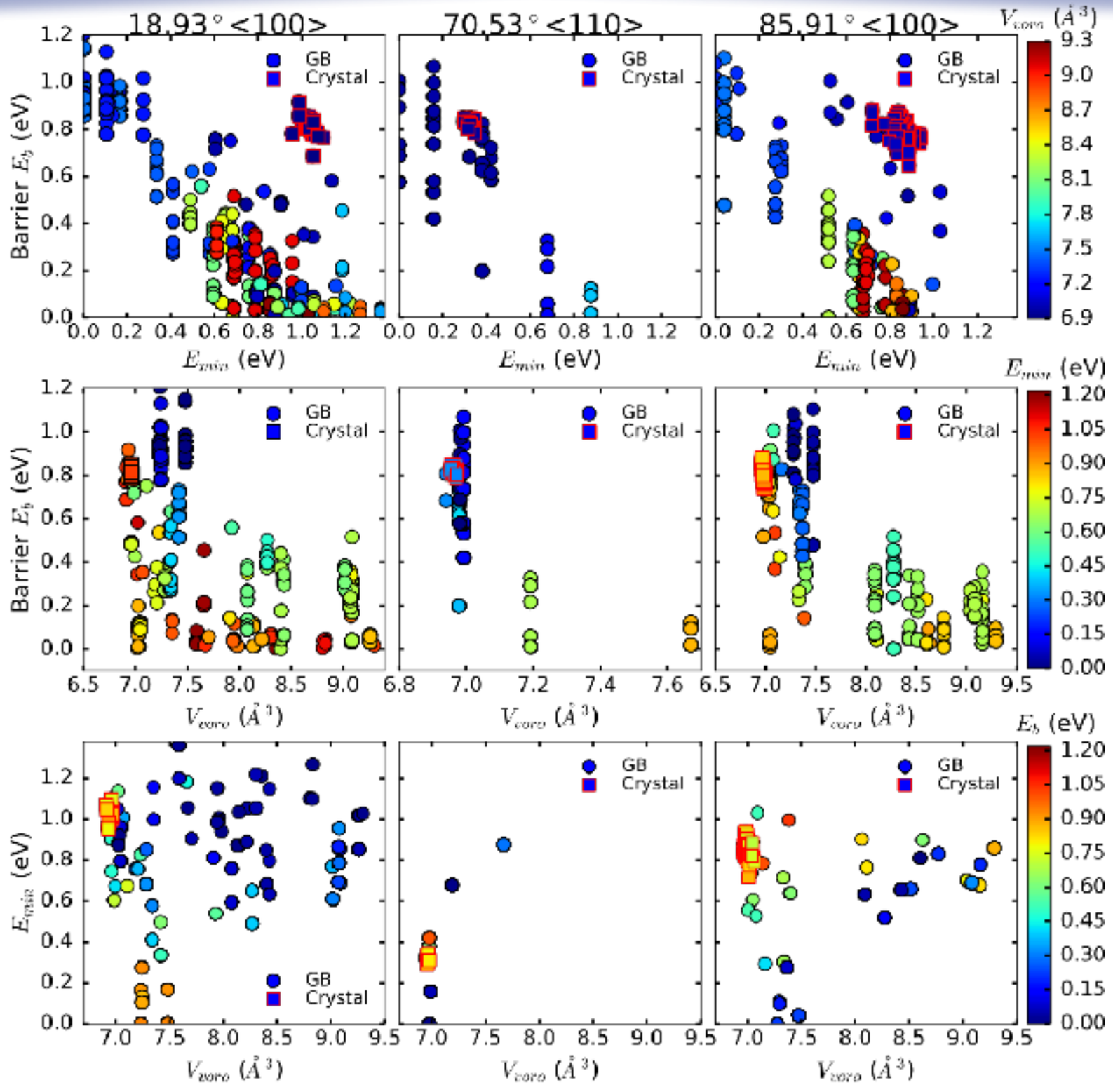

# Conclusions- C diffusion at GB

- For the three stable GBs, C diffuses and remains largely trapped at the GBs, with energy gains ranging between 0.3 and 0.9 eV with respect to the bulk energy.
- Diffusion determined by the effective barriers between the lowest-energy states in the GB.
    - These can be either lower or higher than for bulk C diffusion, ranging from 0.5 to 1.2 eV depending on the GB.
    - Whether slower or faster than in the bulk, impurity diffusion takes place along the GB.
    - C paths can be unidimensional or two dimensional. More precisely diffusion takes place mostly along 1D channels for the 18.93° <100> and 85.91° <100> systems and it can explore the full 2D GB-plane for the 70.53° <110> GB.
- Contrary to what was proposed, the impurity diffusion barriers are not directly correlated with the available free volume.

Restrepo, N.M., El-Mellouhi, Bouhali, Becquart, PRB **97**, 054309 (2018).

# Parallelisation

- Master creates a list of topologies to be searched and distributes the tasks to each node in sequence
- Same approach for refining specific events
  - first a list is constructed
  - tasks are then dispatched to nodes, in sequences
- This ensures maximum flexibility for adapting to the number of available nodes.

# Parallelisation

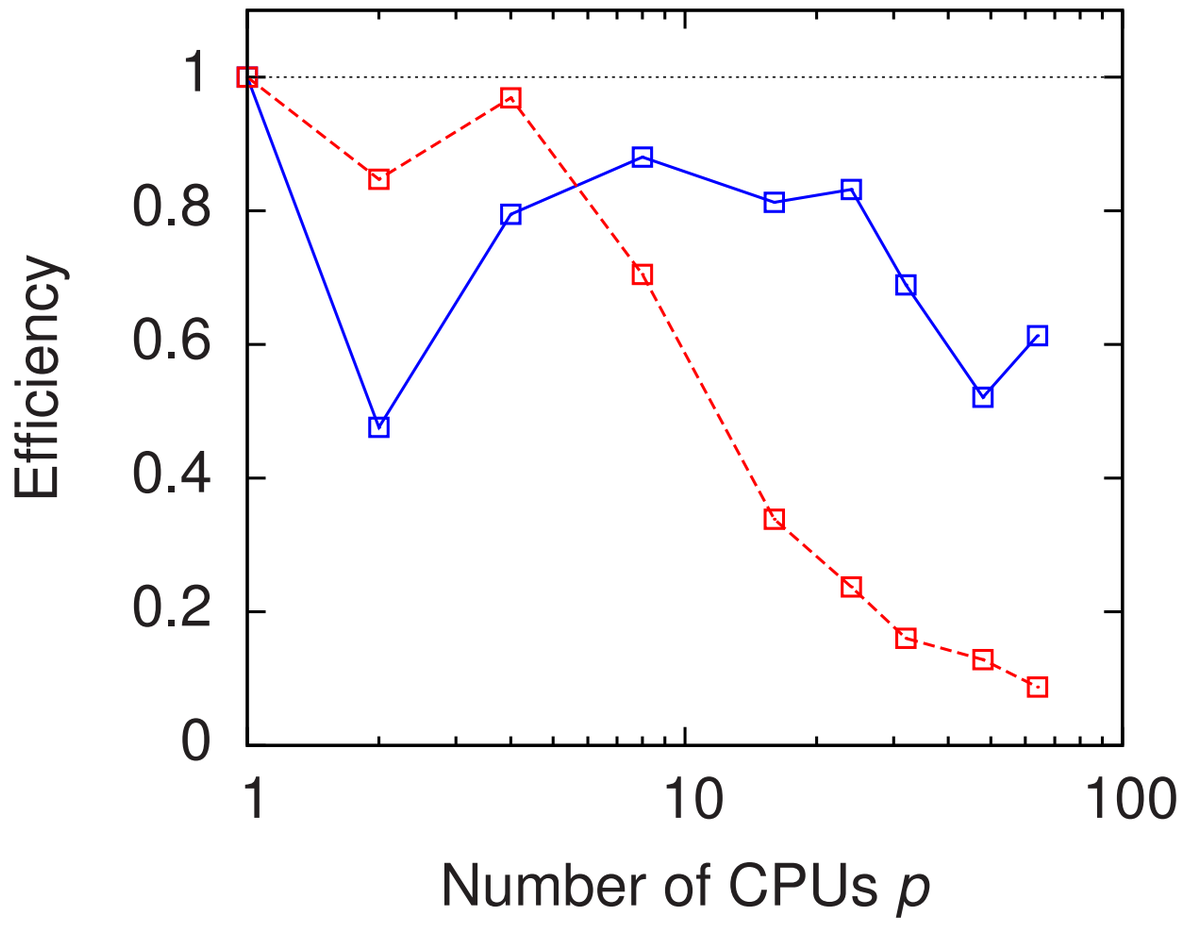


**Figure 5.** Parallel efficiency of event search. —— generic event search; - - - - specific event search; ····· ideal efficiency.

# Parallelisation

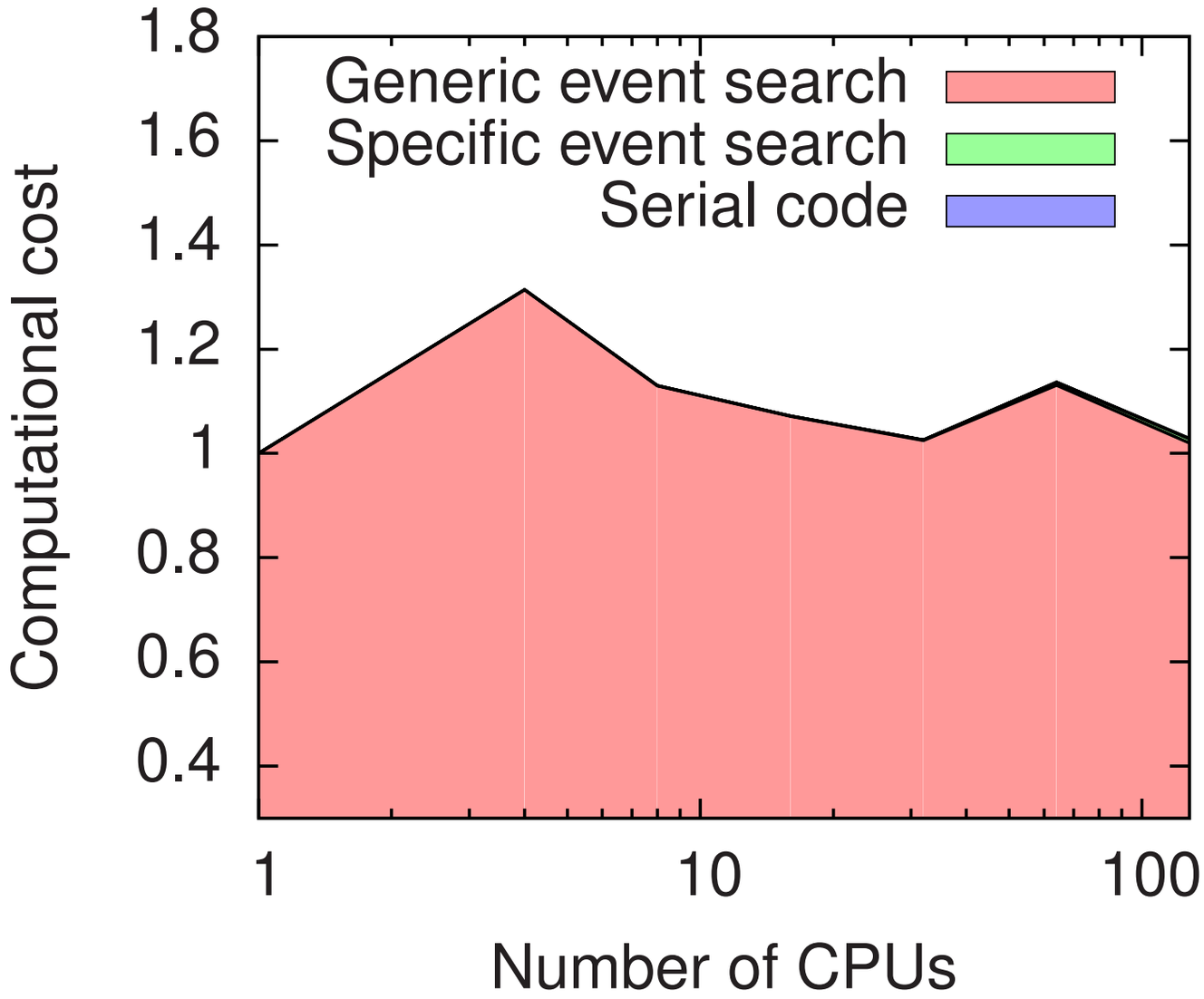


**Figure 8.** Computational cost to simulate the first KMC step in *a*-Si without catalog, relative to serial performance.

# Parallelisation

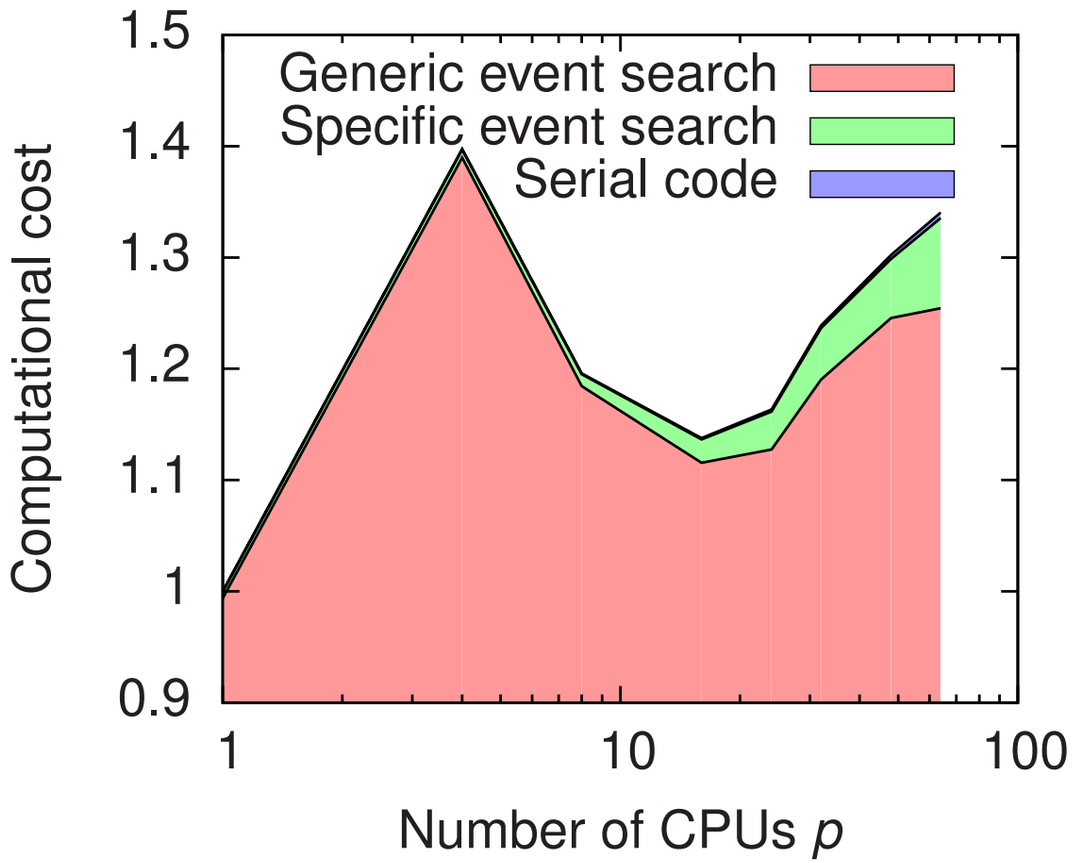


**Figure 6.** Computational cost (number of CPUs × per CPU time) to simulate 40 KMC events, relative to single CPU performance. Lower field: generic event search. Central field: specific event search. Top field: serial code. The relative computational cost displayed here is the inverse of the parallel efficiency.

# Handling large systems

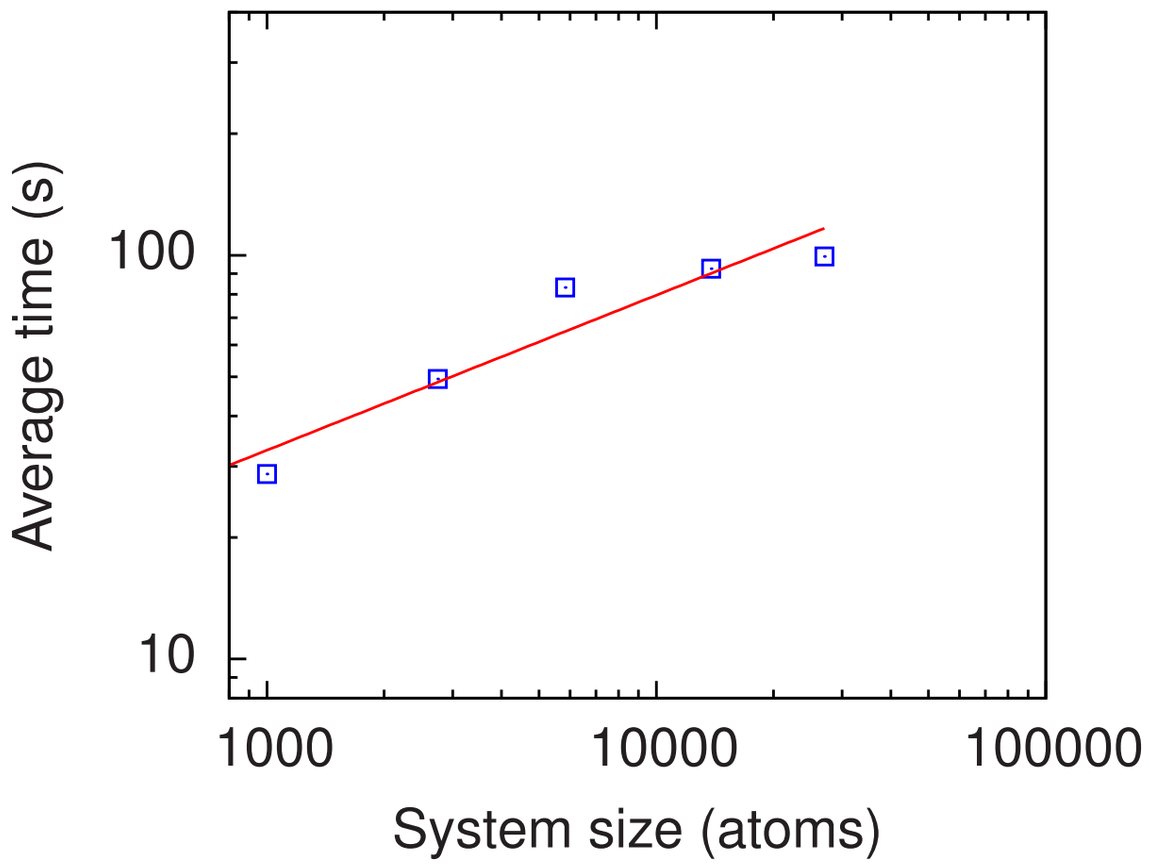


**Figure 4.** The mean time to attempt a generic event search for systems of various sizes. The initial configuration for each simulation was a *c*-Si box containing 1000 to 27000 atoms with four vacancies in each. The simulations were performed at 500 K and run on a 2.66 GHz single core on a quad-core Xeon processor. The blue squares correspond to the data, while the green line is a least-square fit of $f(N) = 2.3\,N^{0.4}$

# Towards large scale systems

- Local force computation
- Verlet neighbor lists
- Cell lists

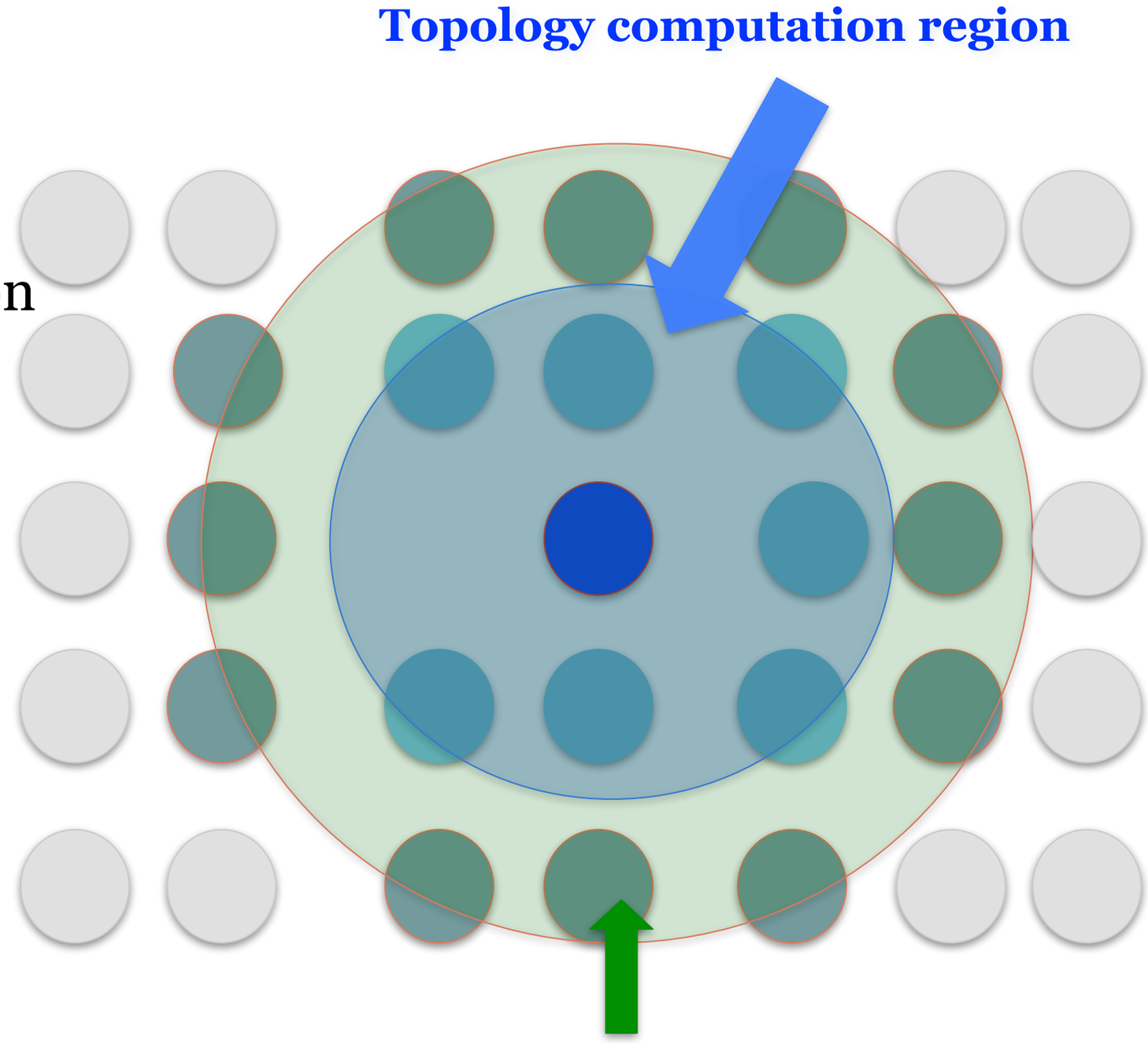

# Reusing specific events

- After each kMC step, keep events specific to atoms that have not changed topology.
- Each atom has its own event list
- If an event is in the top 99.9 % of the CDF, reconverge the saddle.

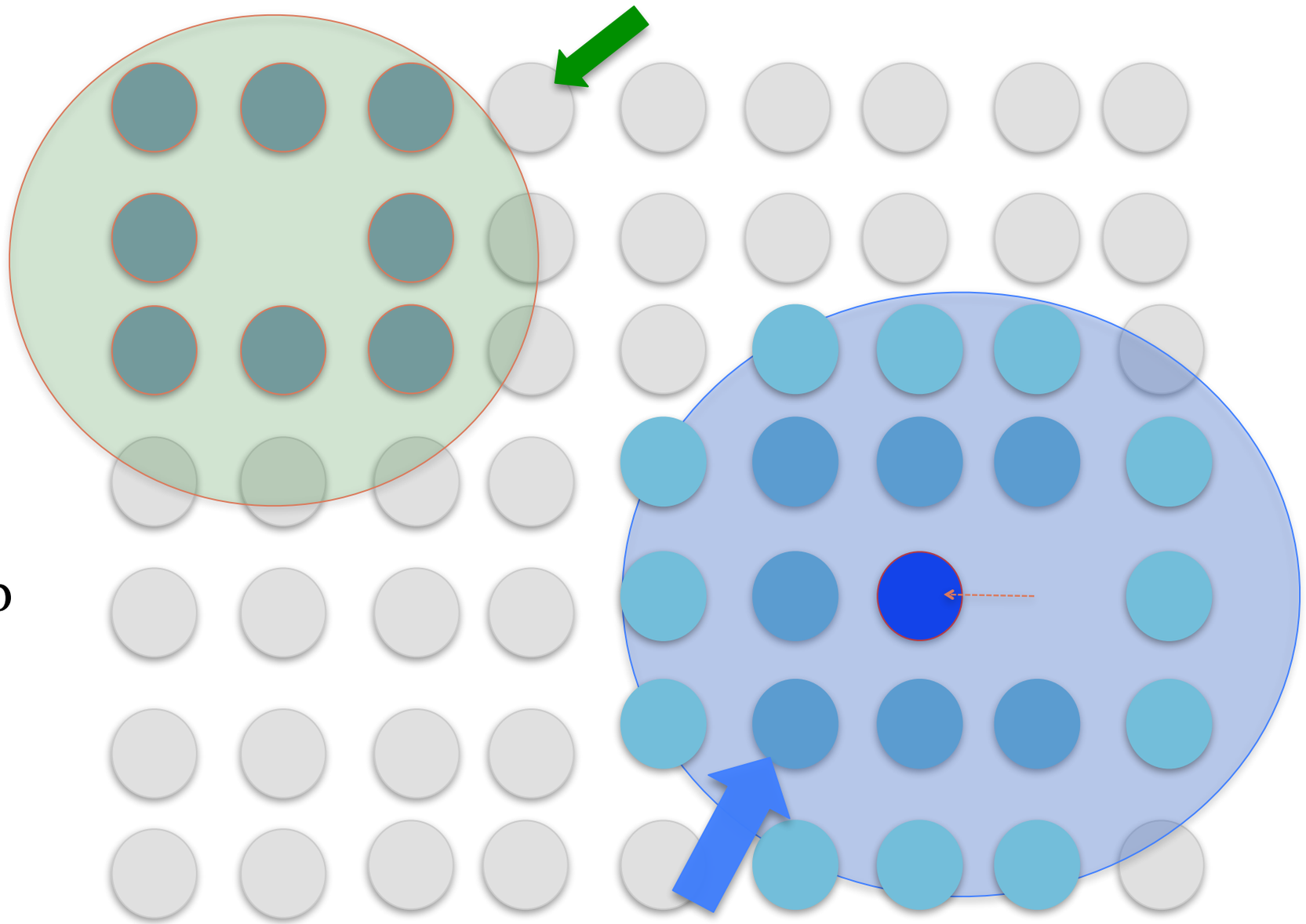

# Benchmarking

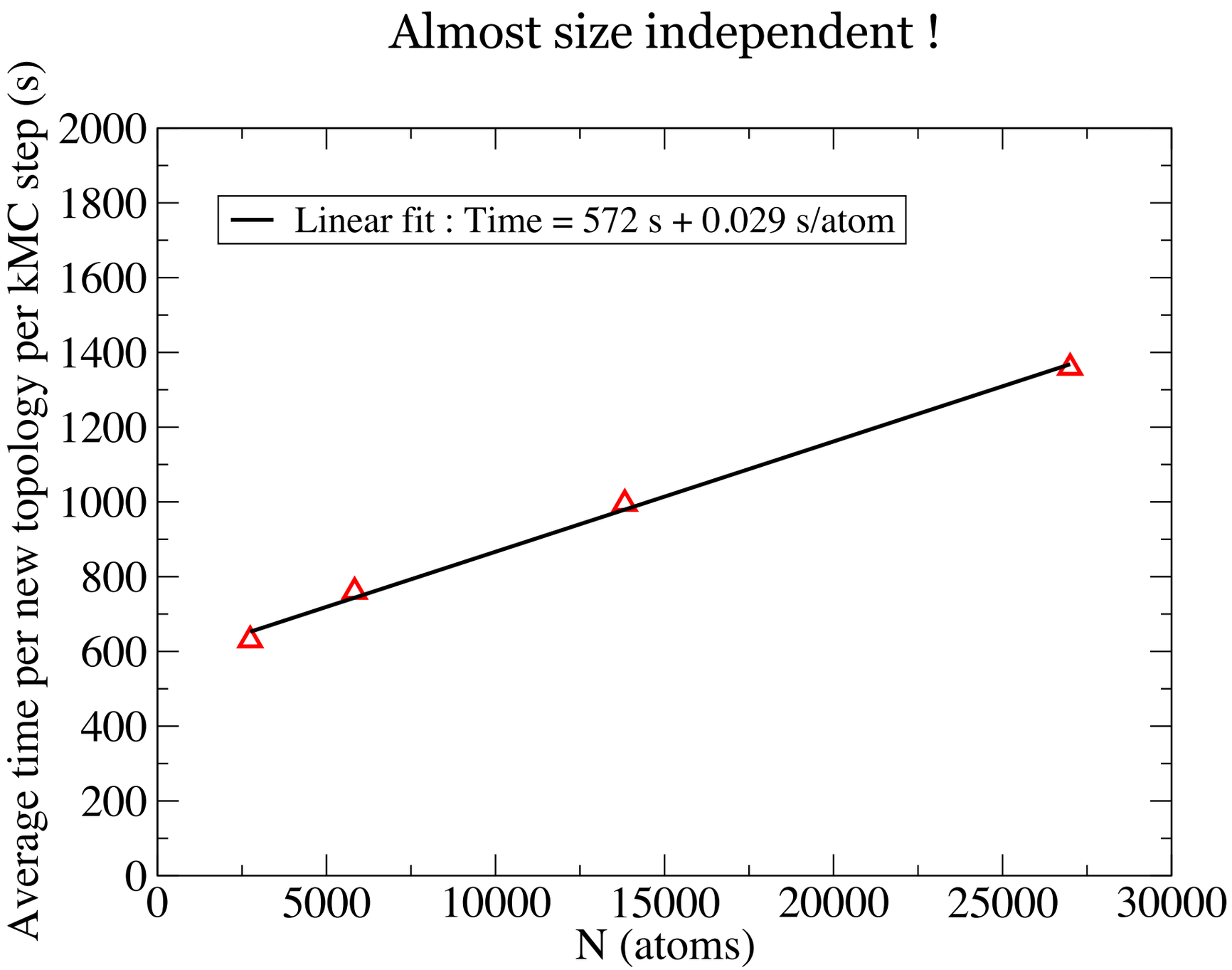

# Simulation

27000 atoms

16 defects

« Interstitials » in blue

« vacancies » in yellow

A dumbell interstitial is represented as two interstitials and a vacancy

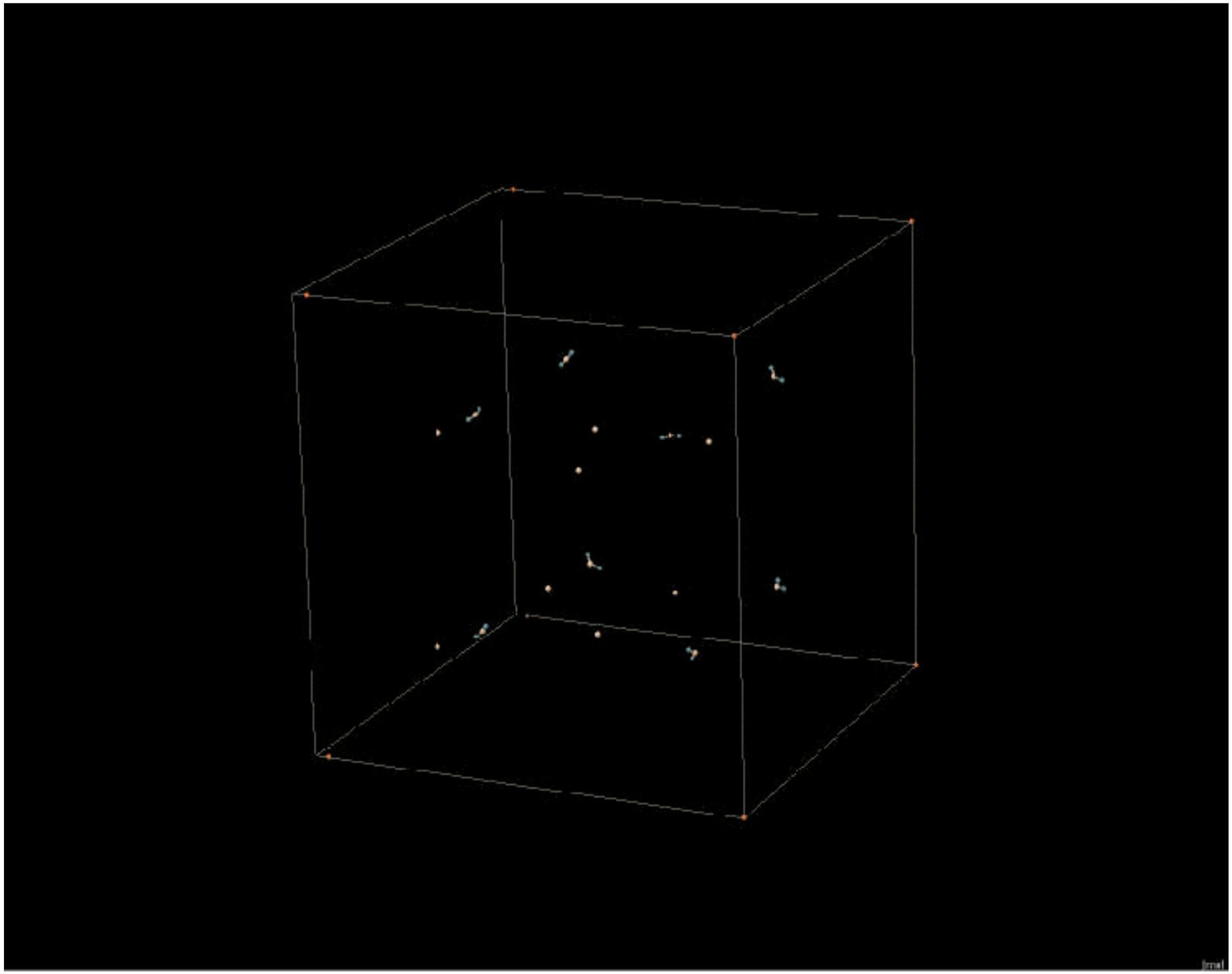

# Application to amorphous silicon

1. What is the relation between average coordination (i.e. defects) and relaxation?

2. How do defects move?

3. No accelerated technique has been applied to these disordered materials

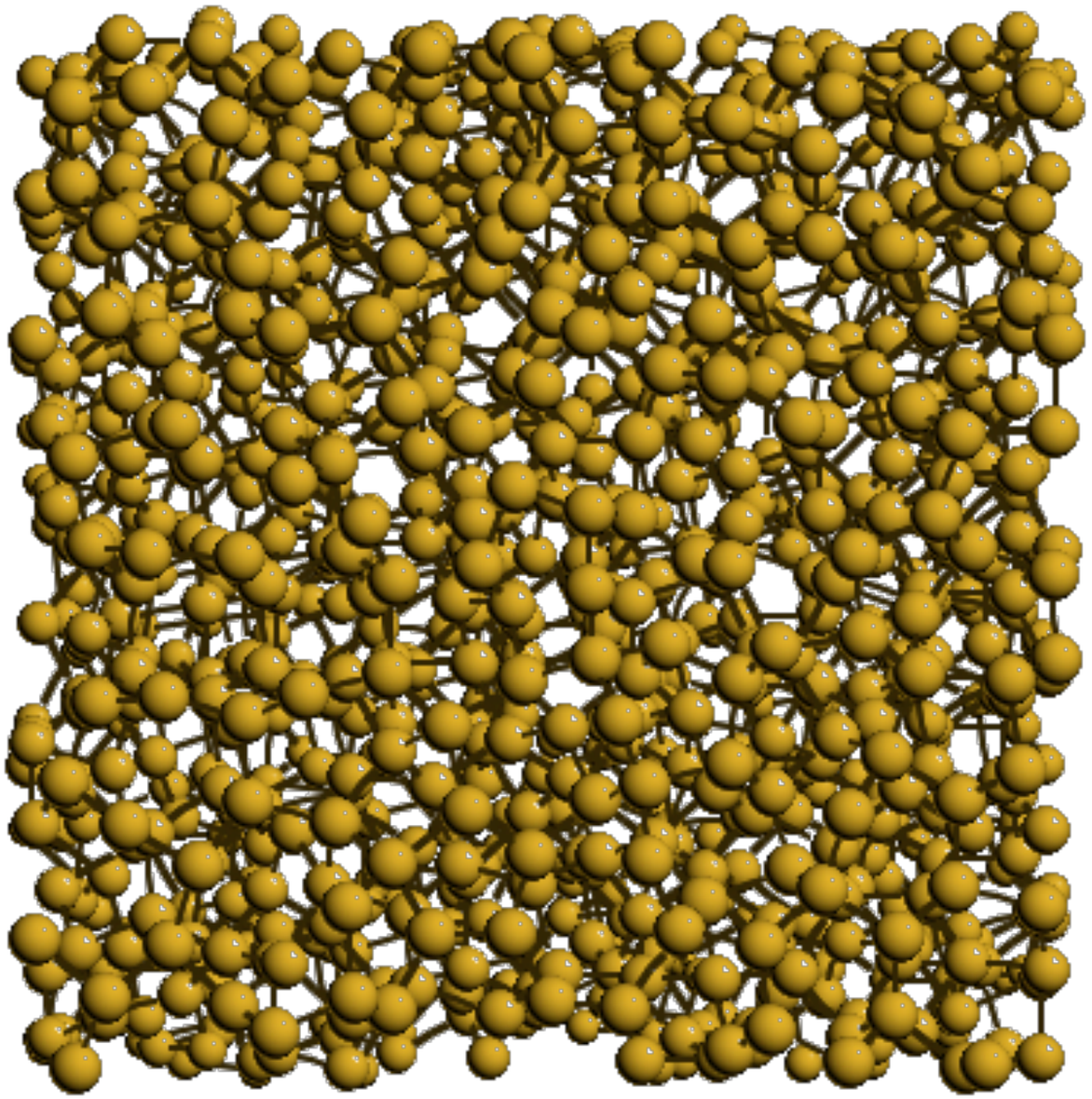

# Application to amorphous silicon

1000-atom box

modified Stillinger-Weber potential

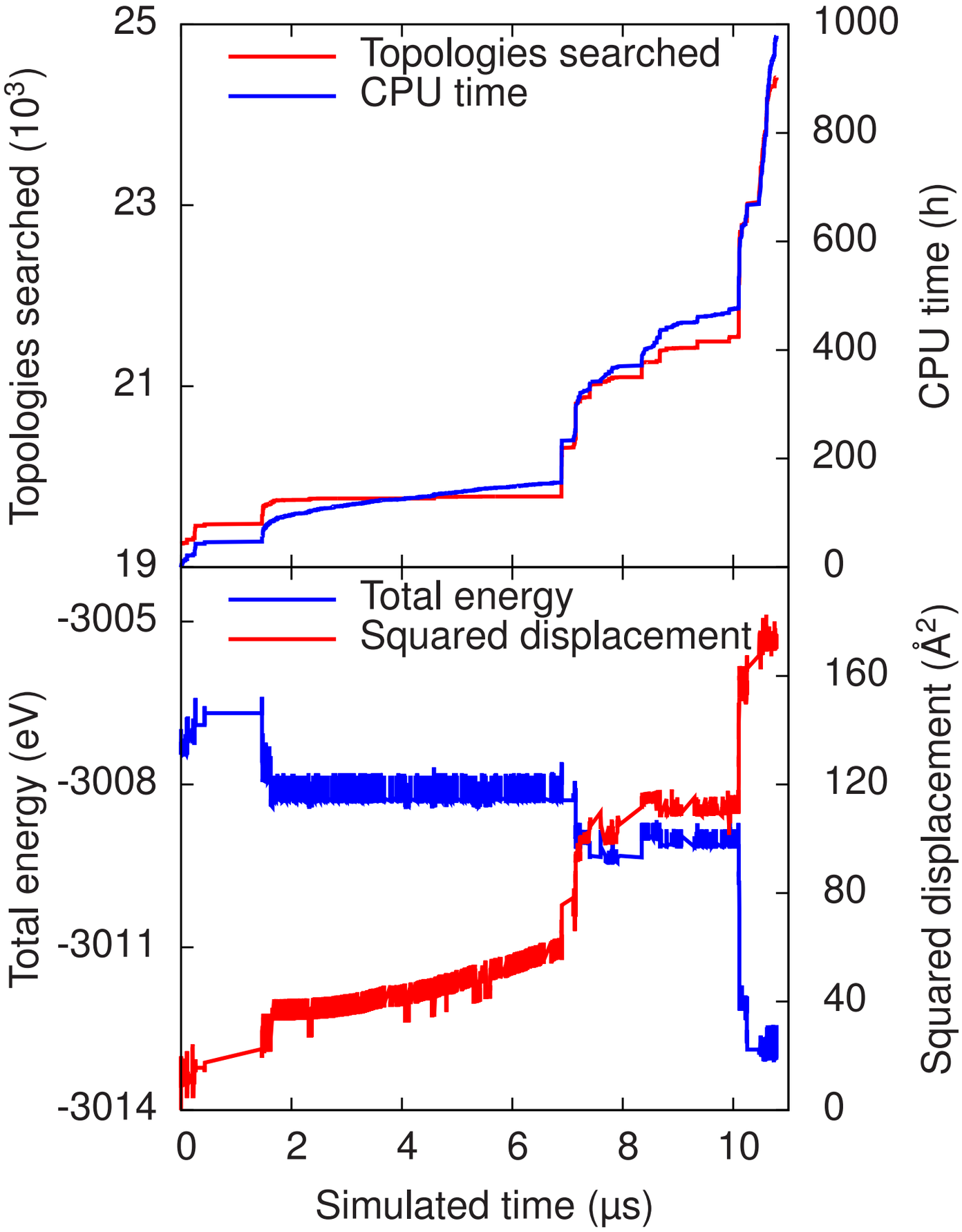

# Stability of vacancies

999-atom box (1 vacancy)

modified Stillinger-Weber potential

T=300 K

Initial catalog: 32 120 events

$E_{basin}$ = 0,45 eV

24 processors (Intel Westmere-EP).

Most vacancies disapear within 1 ns

Here, vacancy survives after 120 µs

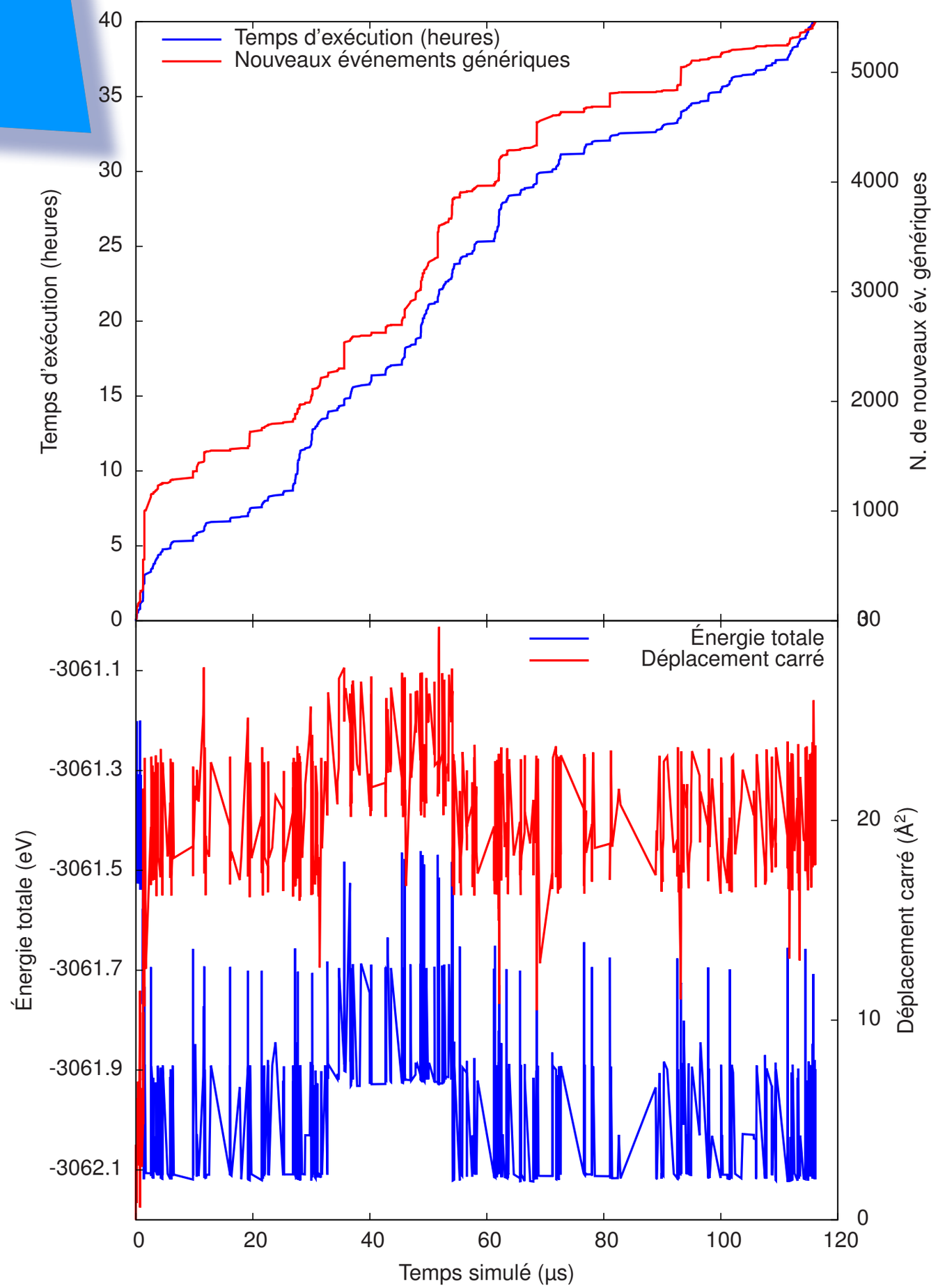

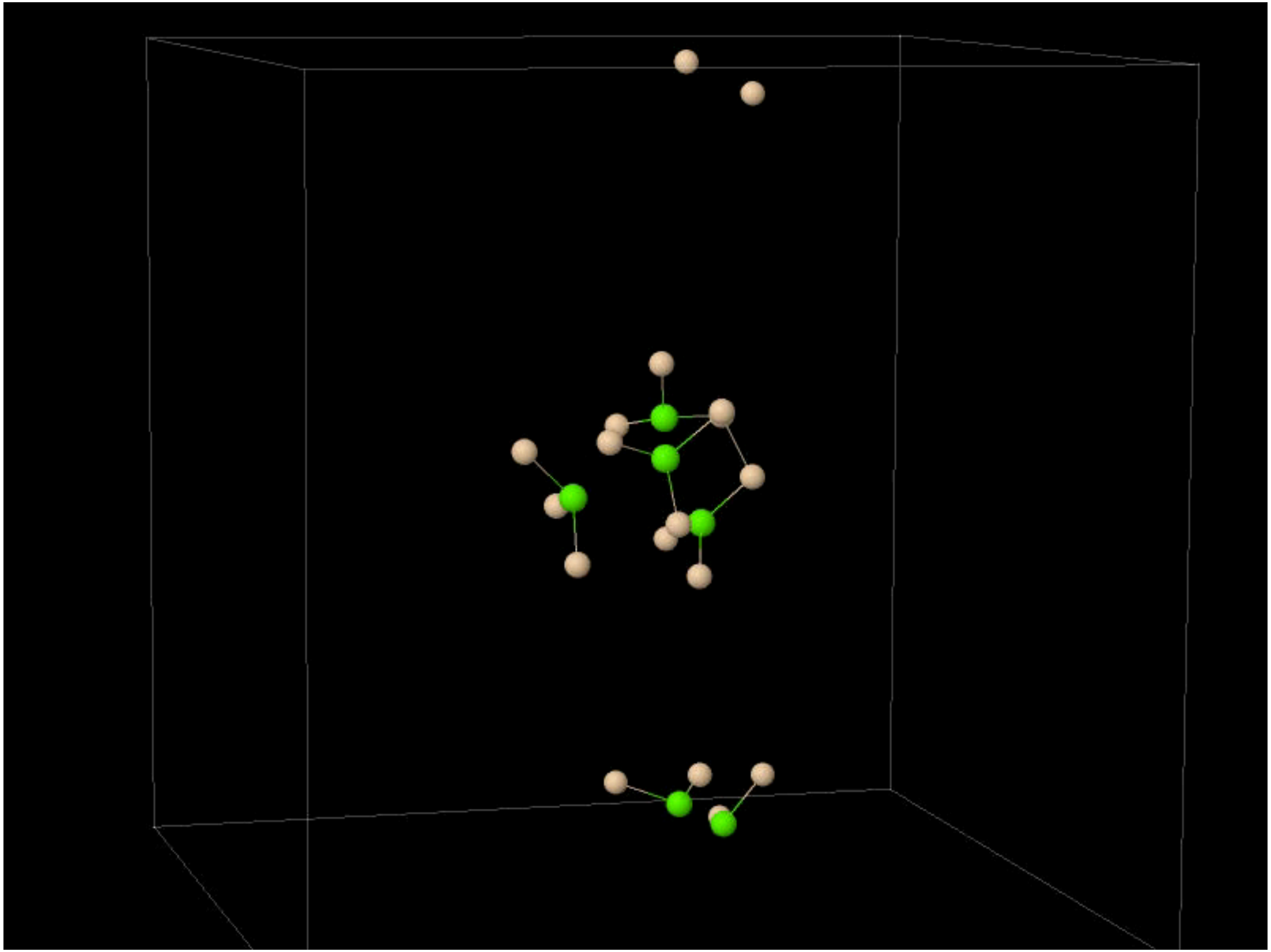

# Vacancies in Iron

Fan, Kushima, Yip and Yildiz

Nanovoid (10-15 vacancies) formation time scale: 20 000 seconds

using KMC + Autonomous climbing basin method

Is it right??

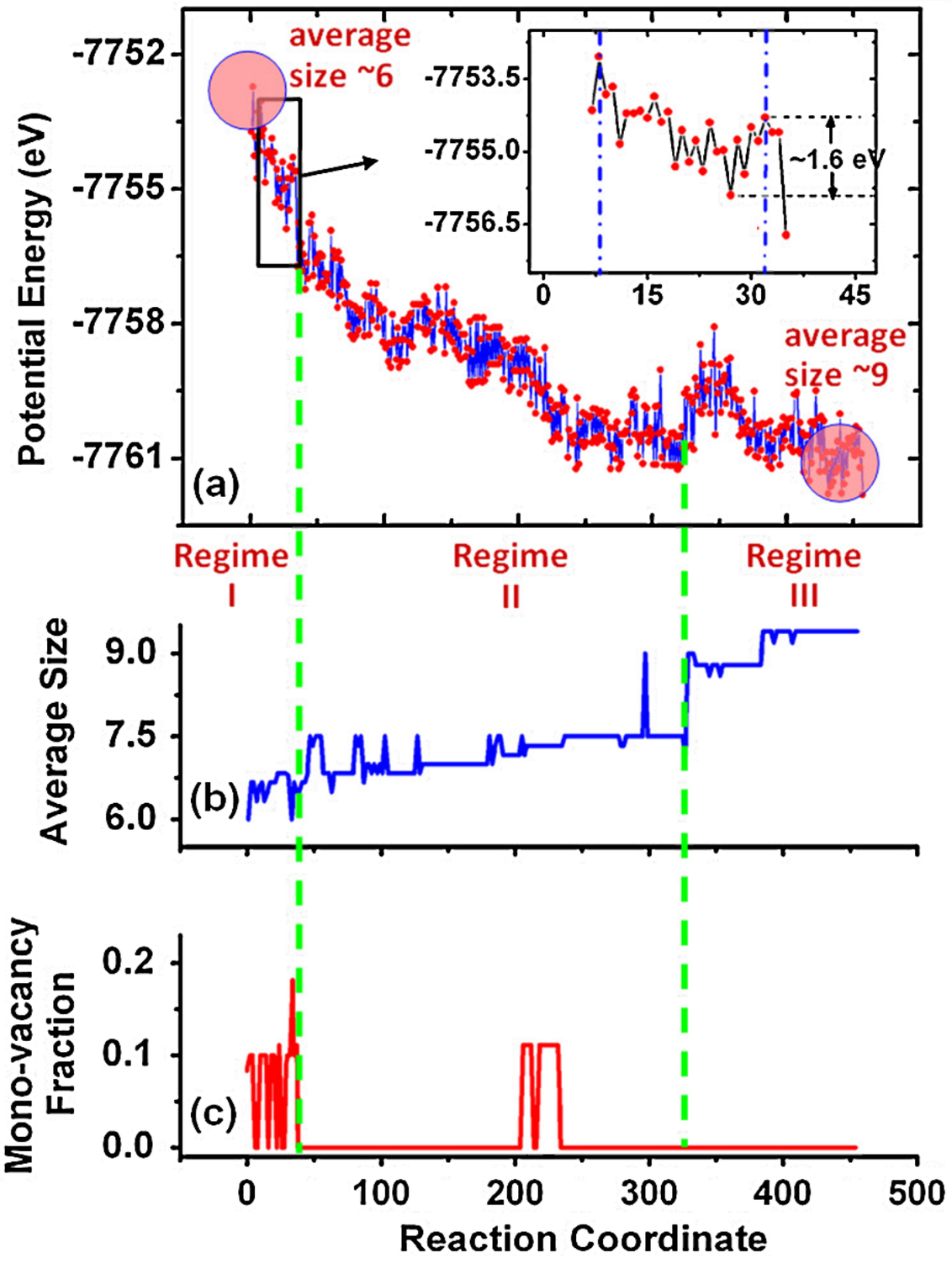

# Vacancies in Iron

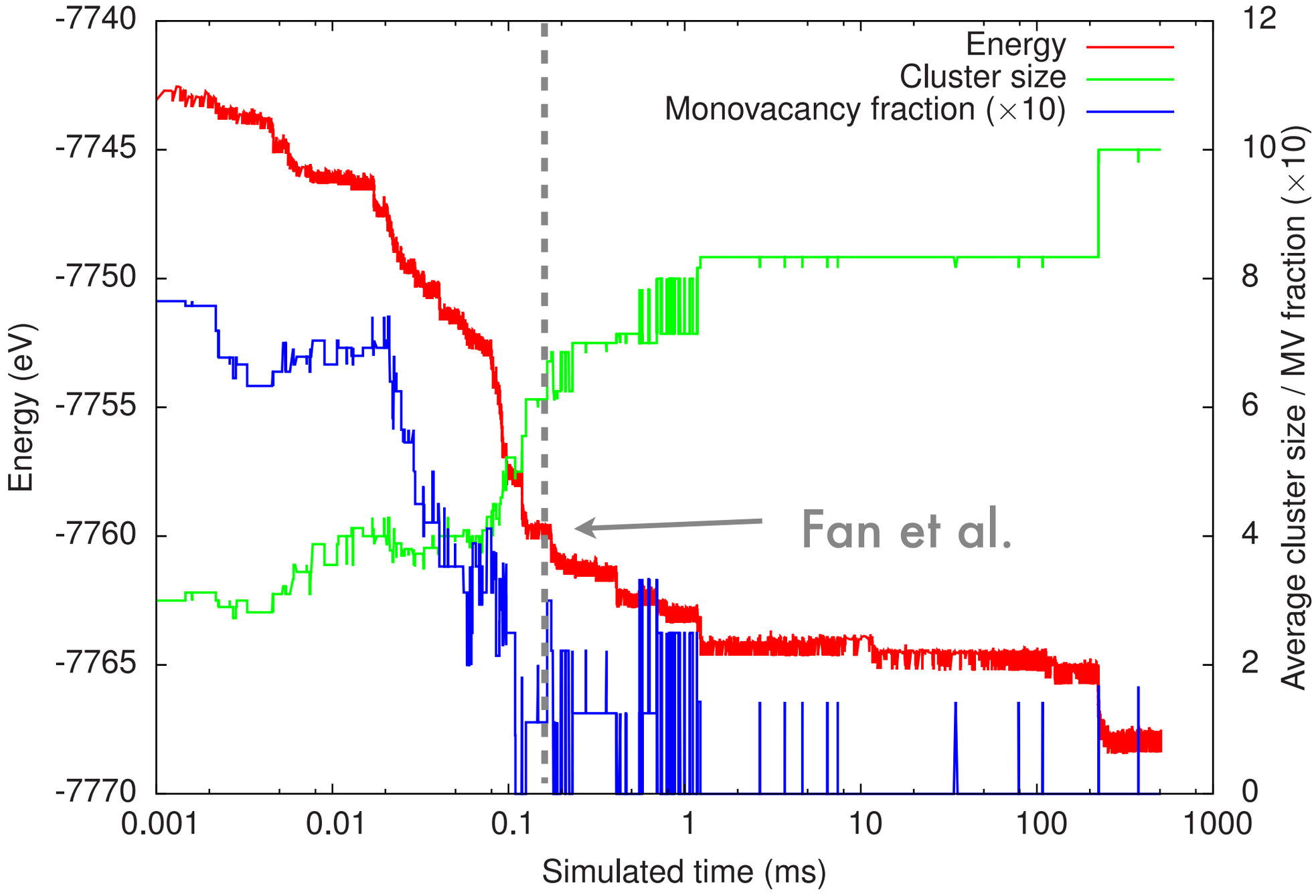


50 randomly placed vacancies in 2000-atom box; Mendeleev Potential.

Peter Brommer and NM

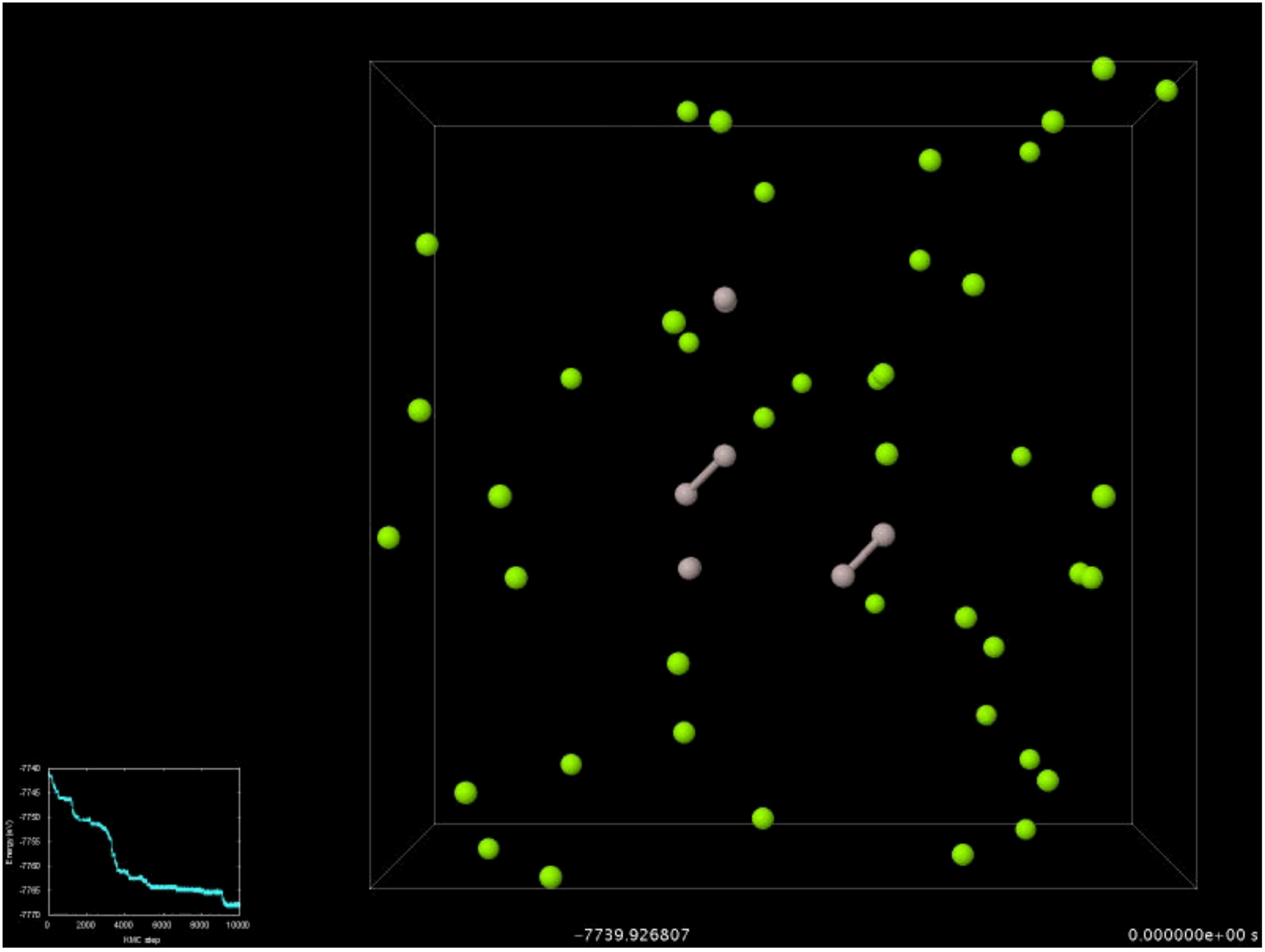
-7740
-7745
-7750
-7755
-7760
-7765
-7770
Energy (eV)
0
2000
4000
6000
8000
10000
KMC step
-7739.926807
0.000000e+00 s

# CONCLUSIONS

- Kinetic ART is an efficient on-the-fly kinetic Monte-Carlo algorithm
- It uses a topological description for the classification of events; the flexibility of nauty allows us to take into account multiple components and more
- It defines two classes of events:
  - low-energy barriers that must be refined after each event
  - high-energy barriers which are treated as

- Kinetic ART should be particularly useful for the study of diffusion in when strain effects are important or asymmetries prevent the use of standard KMC (e.g. presence of defects, interface, etc.).

- It is ideal for problems where the type of barriers evolves with time — self-organisation and aggregation phenomena

- A number of details make the method efficient:
  - parallelization
  - recycling of low-energy barriers
  - handling of highly symmetric events
  - handling of blinkers

# MERCI!